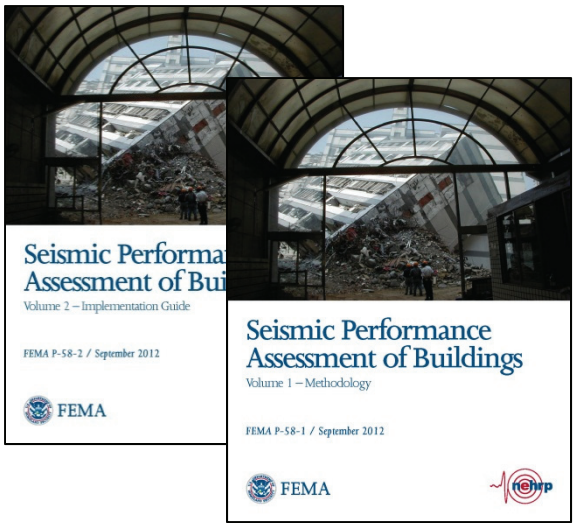

Background Document

FEMA P-58/BD-3.8.4

Fragility Curves for Concentrically Braced Steel Frames with Buckling Braces

Prepared by

Charles W. Roeder, Dawn E. Lehman, and Eric Lumpkin
Department of Civil and Environmental Engineering
University of Washington
Seattle, Washington 98195

Submitted to

APPLIED TECHNOLOGY COUNCIL
201 Redwood Shores Parkway, Suite 240
Redwood City, California 94065
www.ATCouncil.org

Prepared for

FEDERAL EMERGENCY MANAGEMENT AGENCY
U.S. Department of Homeland Security
500 C Street, SW
Washington, D.C. 20472

November 30, 2009

FEMA

nehrp

Background Documentation

FEMA P-58 Background Documents are a series of reports documenting the technical background and source information for key aspects of the FEMA P-58 methodology and its implementation. These reports were developed over the course of the 10-year ATC-58/ATC-58-1 Projects funded under FEMA Contracts EMW-2001-RP-0056 and HSFEHQ-06-D-1105.

Background Documents were developed by consultants, serving at various levels within the project hierarchy, reporting the results of: (1) decisions on technical development protocols; (2) focused studies on the development of key aspects of the methodology; (3) documentation of recommended procedures; and (4) collection of available data for the development of structural and nonstructural fragilities. They were initially intended to serve as a record of the technical state-of-knowledge at the time they were produced, and as resources for the development of the eventual project reports. As such, they represent a snapshot in time, and may, or may not, match the technical content, recommended procedures, or data incorporated into the final methodology and its implementation.

This Background Document is intended for the purpose of providing supplemental knowledge to users of the FEMA P-58 methodology. Information contained herein has not been independently verified for accuracy as a stand-alone document, and may have been superseded in its final implementation within the methodology. Users of information in this document assume all liability arising from such use.

Notice

Cover illustration – Primary resource documents for the FEMA P-58 *Seismic Performance Assessment of Buildings, Methodology and Implementation* series of products: FEMA P-58-1, *Volume 1 – Methodology*, and FEMA P-58-2, *Volume 2 – Implementation Guide*.

Fragility Curves for Concentrically Braced Steel Frames with Buckling Braces

Developed for the ATC-58 Project

Structural Performance Products Team

by

Charles W. Roeder, Dawn E. Lehman
and Eric Lumpkin

Department of Civil and Environmental Engineering

University of Washington

Seattle, WA 98195-2700

Revised November 30, 2009

Table of Contents

Table of Contents i

List of Figures iii

List of Tables iv

CHAPTER 1 - Introduction 1

INTRODUCTION TO REPORT 1

SCOPE OF WORK 2

CHAPTER 2 - Development of the Fragility Curves 4

DAMAGE STATES 4

ENGINEERING DEMAND PARAMETERS 7

FRAGILITY FUNCTION DEVELOPMENT 11

CHAPTER 3 - Issues Effecting Fragility Curve Development 13

DESIGN PROCEDURES 13

BRACE CROSS SECTION AND SLENDERNESS 17

BRACE FRAME CONFIGURATION 19

CONCLUDING CAUTIONARY REMARKS 22

CHAPTER 4 - Fragility Curves 23

S2-BF-1 – STRENGTH DESIGN WITH NO SEISMIC DETAILING 23

S2-CBF-2a and S2-CBF-2b – OCBF DESIGN WITH COMPACT BRACES 27

S2-CBF-2c - OCBF WITH COMPACT BRACES IN K-BRACE CONFIGURATION 29

S2-CBF-3a - SCBF DESIGNS IN GENERAL 30

S2-CBF-3b - SCBF DESIGN WITH HSS BRACING MEMBERS 32

SCBFs WITH OTHER BRACE CROSS SECTIONS 34

S2-CBF-3c - SCBF DESIGN WITH CHEVRON BRACING CONFIGURATION 36

S2-CBF-3d - SCBF DESIGN WITH X-BRACE CONFIGURATION 37

S2-CBF-3e - SCBF DESIGN WITH MOMENT RESISTING BRACE CONNECTION 38

ACCURACY AND RELIABILITY OF FRAGILTY CURVES 39

USING THESE FRAGILITY CURVES 40

CHAPTER 5 - Closing Comments 41

Appendix A - References 42

Appendix B - Summary of Test Data for Brace Tests 48

Appendix C - Summary of Gusset Plate Connection Tests 68

Appendix D - Database of CBF System Behavior 74

List of Figures

Figure 1. Possible Failure Modes for CBF System 8

Figure 2. Illustration of Drift Values 8

Figure 3. Force-Story Drift of SCBF; a) Weld fracture due to welds designed by uniform force method, b) SCBF gusset with added constraints noted above, c) SCBF with very conservative gusset plate design 15

Figure 4. Axial Force Deflection Behavior of Various Braces (from Tremblay et al. 2008) 17

Figure 5. Local Strain Accumulation in Rectangular HSS Tubes 18

Figure 6. Effect of $^{Kl}/_{r}$ on Brace Performance (from Popov et al. 1976) 18

Figure 7. Force Story Drift Behavior of Similar CBF Systems; a) HSS brace, b) Wide Flange Brace 19

Figure 8. Possible Brace Configurations 20

Figure 9. Test Results From Two Chevron Braced Frames; a) Chevron with Beam Designed for Unbalanced Force, b) Chevron with Weak Beam 21

Figure 10. Fragility Curve for CBFs Designed by Strength Design with no Seismic Detailing 27

Figure 11. Fragility Curves for OCBF Frames 29

Figure 12. General Fragility Curves for SCBFs Designed to Minimum Standards 31

Figure 13. General Fragility Curves for SCBFs Designed to Minimum Standards and Having Tapered Gusset Plates 32

Figure 14. General Fragility Curves for SCBFs Having Rectangular Gusset Plates and Designed with Improved Balanced Design Procedure 33

Figure 15. Fragility Curves for SCBFs with Wide Flange Braces 35

Figure 16. Fragility Curves for SCBFs with Double Angle Braces 36

Figure 17. Range of DS1 and DS4 Damage in Chevron Braced Frames Relative to Other HSS Rectangular Braced Frames 37

Figure 18. Fragility Curves for SCBFs with X-Bracing 38

List of Tables

Table 1. Fragility Curves Requested in ATC 35% Report 3

Table 2. Damage States for Braced Frames 5

Table 3. Summarized Fragility Curve Tests 24

Table 4. Parameters for OCBF Fragility Curves 29

Table 5. Parameters for General SCBF Fragility Curves 31

Table 6. Parameters for General SCBF Fragility Curves With Tapered Gusset Plates 32

Table 7. Parameters for General SCBF Fragility Curves With Rectangular Gusset Plates and Improved Balanced Design Procedure 34

Table 8. Parameters for SCBF Fragility Curves With Wide Flange Braces 35

Table 9. Parameters for SCBF Fragility Curves With Double Angle Braces 36

Table 10. Parameters for SCBF Fragility Curves With X-Bracing 38

CHAPTER 1 - Introduction

INTRODUCTION TO REPORT

This report summarizes the background, development, and documentation of fragility curves for concentrically braced frames (CBFs). The work was performed by the authors under subcontract to the Applied Technology Council, and was initiated on August 4, 2008. The primary objectives of the work were:

1. To assemble information on steel braced frames. The experimental data were catalogued according to the type of steel concentrically braced frames and the ductility capacity: limited, low, moderate and high. All existing test data was reviewed and assembled. A detailed bibliography of the relevant data was developed. The latter two items are included as appendices to this report

2. To review existing fragility test data on steel concentrically braced frames. Although this review was conducted, none were found and therefore a summary is not included.

3. To establish damage states and develop related fragility curves using the relevant collected data. The fragility curves were developed using log-normal distributions. Expert judgment was exercised for categories of steel concentrically braced frames where limited or no data were available. In the latter case, the basis for expert-judgment decisions was documented.

To accomplish these objectives, the authors reviewed a wide range of experimental research. Appendix A provides a list of references reviewed. As specified in the scope of work, development of the fragility curves focused on braced frame tests rather than tests on component tests, e.g., individual brace elements or gusset plate connection tests. Since many of the references included in the Appendix are component tests, they were not included in the database of experimental data or fragility curves.

Concentrically braced frames are complex systems that consist of braces, framing elements (beams and columns) and their connections, and the connection between the brace and the frame, typically a gusset plate connection. Therefore a test evaluating a single component evaluates only part of the CBF issue.

Tests on individual brace elements clearly show that different brace cross sections and local and global slenderness ratios have different inelastic performance and deformation capacity. Tests on braced frame gusset plate connections show that the design of the gusset plate has a significant effect on braced frame performance. There is a large amount of test data for individual braces, and there is a significant amount of test data for gusset plate connections. This information is part of our fundamental knowledge base for CBFs and cannot be ignored. However, there are severe limitations for test data from brace or gusset plate connection components. The data for individual brace or gusset plate connection tests do not simulate braced frame performance, since CBF performance depends upon the interaction of these components with one another.

As a result, these component test data were not directly used to develop fragility curves, but they were considered in the broader evaluation of CBF performance and are included in the report. Appendix B provides a brief tabulation of the past test results on individual braces, and Appendix C provides a brief tabulation of the past test results on gusset plate connections. It can be seen from these appendices that there is a large amount of test data available for braces and gusset plate connections, but the data is often incomplete by current standards. The tests were frequently stopped at arbitrary points. Published reports seldom describe all test results and all performance limit states. The reports are often ambiguous or incomplete. In addition, component tests are inherently limited in addressing system performance as noted earlier. As a result, these results help to establish general trends of behavior, but they are of limited value in establishing fragility curves for the CBF system. Appendix B and C are provided for information only, since they were not used in the development of CBF fragility curves developed in this report.

The fragility curves were established primarily with data developed from tests that qualified to be sub-system or system (as opposed to component) braced frame tests. Appendix D provides a database of experimental results that qualified as CBF system tests. That is, these tests approximated at minimum a one-story, one-bay frame with beams, columns, braces as well as brace connections. This appendix provides a much more detailed summary of research results and thereby includes more comprehensive information on the tests than provided in Appendices B and C. Because the behavior from these tests is much more meaningful in evaluating braced frame performance, the data compiled for these tests is much more detailed. The data in Appendix D was used to develop CBF fragility curves in this report, although some data were not employed in development of the fragility curves because the tests were of very small scale or did not relate to CBF construction as practiced in the US. Further, large gaps exist in our current CBF system experimental database, and some brace systems as requested in the ATC58-1 scope of work do not have experimental data to document their performance. In the latter case, professional experience was used to develop appropriate fragility curves.

SCOPE OF WORK

This work was addressed as defined for the Steel Braced Frames, S2, structural system of Table D-1 (reprinted here as Table 1) of the 35% draft of ATC Report 58-1. This table divides the S2 Steel Braced Frame category into multiple sub-categories. In general the S2 category focused on concentrically braced frames (CBFs), but one subcategory (S2-BF-1) included eccentrically braced frames (EBFs) with limited seismic detailing. The CBFs in the S2 category also included subcategory S2-CBF-4, which is focused on buckling restrained braced frames (BRBFs). The work included in this subcontract does not include any work on EBFs and BRBFs, and so subcategories S2-CBF-4 and S2-BF-1 were excluded from this report.

The subcategories of CBFs with buckling braces are S2-CBF-2a, S2-CBF-2b, S2-CBF-2c, S2-CBF-3a, S2-CBF-3b, S2-CBF-3c, S2-CBF-3d, and S2-CBF-3e. These subcategories include a wide range of CBFs with buckling braces, including CBFs which may be classified as Ordinary Concentrically Braced Frames (OCBFs) or Special Concentrically Braced Frames (SCBFs) under the AISC Seismic Design Provisions.

- OCBFs are included under subcategories S2-CBF-2a, S2-CBF-2b, and S2-CBF-2c.

- SCBFs are included under subcategories S2-CBF-3a, S2-CBF-3b, S2-CBF-3c, S2-CBF-3d, and S2-CBF-3e.

In the structural system of Table D-1 (shown in Table 1) of the 35% draft of ATC Report 58-1 document, the subcategories were further separated by brace type, CBF configuration, and variations in the design method. Although the authors attempted attempts to meet these proposed subcategories, there were difficulties with this, as data were not available for all categories. Further discussion is available in Chapter 3.

Table 1. Braced Frame Categories Requested in ATC 58 35% Draft Report

Seismic Ductility Class	**Seismic Behavior Characteristics**	**Numerical Designation**	**Code Equivalency**
Limited	Concentric or eccentrically braced system. Basic strength design w/o special detailing	S2-BF-1	2005 AISC Specification (w/o seismic detailing)
Low	Concentrically braced system. Strength design with capacity design provisions for connections, Chevron configurations, and bracing member compactness.	S2-CBF-2a	2005 AISC – O-CBF
	S2-CBF-2a with braces other than HSS members	S2-CBF-2b	
	S2-CBF-2a with K-brace configuration	S2-CBF-2c	
Medium	Concentrically braced system. Seismically designed and detailed with slenderness/compactness limits on braces and capacity design requirements for connections, beams, and columns.	S2-CBF-3a	2005 AISC – S-CBF
	S2-CBF-3a with braces other than HSS members	S2-CBF-3b	
	S2-CBF-3a with chevron configuration braces	S2-CBF-3c	
	S2-CBF-3a with X-configuration braces	S2-CBF-3d	
	S2-CBF-3a with beam-brace-column connections designed as moment resisting	S2-CBF-3e	
High	Concentrically braced system with buckling restrained braces and capacity design of connections, beams, and columns.	S2-CBF-4	2005 AISC – BRBF

CHAPTER 2 - Development of the Fragility Curves

Development of fragility curves requires definition of a damage states, establishing a engineering demand parameter which is used to define the various damage states, and establishing a method for developing the fragility functions.

DAMAGE STATES

The damage states for braced frames were developed with an eye toward the required repair and the important component damage states. Four damage states are proposed for CBFs as described in Table 2. Damage state DS1 consists of initial seismic damage, but damage of such limited extent that no repair or other actions are required. Damage states, DS2 and DS3, consists of extensive inelastic damage to the brace, connections and/or framing members that necessitates significant repair or replacement, but does not adversely affect the integrity of the structural system. This may include one or more of:

- significant inelastic buckling and local deformation of brace,
- significant inelastic deformation of the gusset plate but limited gusset plate out-of-plane movement such that the resistance and deformation capacity of the brace is intact,
- crack initiation and limited crack growth for welds joining the gusset plate to the framing members but of sufficiently limited extent to assure stability against ultimate fracture,
- inelastic deformation of beams and columns in the structural system due to bending action of the frame, and
- fracture of one or more bolts in the beam-column or gusset plate connections.

The separation between DS2 and DS3 is based on the extent of the damage levels and therefore the required level of repair. In general, it is expected that repair requirements for DS2 may well be driven by engineering judgment as well as architectural and nonstructural damage associated with CBF deformation and performance. While DS3 represents similar damage to DS2, it is more severe and repair requirements are more strongly driven by structural concerns. It should also be noted that some relatively brittle CBF failures may not experience these more ductile response modes and thus effectively step over these intermediate damage states to DS4.

Damage state DS4 is a more severe damage state and requires more extensive component replacement. It must be recognized that DS4 does not imply collapse of the frame. Braced frame test data in Appendix D that continued cyclic deformations beyond the point of attaining the DS4 damage state typically retained 25% to 40% of their lateral stiffness and resistance at these larger deformation levels. Hence the damage states and fragility curves described in this report do not address structural collapse. It is a damage state that reflects very severe structural damage, but the damage is short of life safety and collapse prevention limit states. The damage corresponding to DS4 may include one or more of the following:

Table 2. Damage States for Braced Frames

NOTE: Fragility curves are normally used to predict expected seismic damage and estimate future losses for given seismic events. As such, the engineering demand parameters should be compared to maximum computed response of the structure when subject to the seismic hazard under consideration. In the table, these noted damage levels are listed as MAXIMUM SEISMIC RESPONSE damage levels. The residual damage or the actual condition of a structure after an earthquake depends on many factors including the specific characteristics of ground motion as well as the structural performance. As a result, the residual damage cannot be precisely related to the maximum response levels. A structure that has been recentered may show significantly less apparent damage than a structure with significant residual deformation or story drift. The actual damage to the structure depends upon the MAXIMUM SEISMIC RESPONSE, however, estimated residual deformation estimates have been requested as part of this report. As a result, these residual damage estimates must be viewed as approximate and are identified as OBSERVABLE RESIDUAL DAMAGE in the table below.

Damage State	**Component**	**Braced Frame Damage**	**Repair Measure**
DS1	Brace	MAXIMUM SEISMIC RESPONSE. Buckling of the brace has begun but does not exceed the depth of the brace. OBSERVABLE RESIDUAL DAMAGE. Slight residual buckling of the brace has occurred but is barely noticeable to the naked eye and does not exceed half of the brace depth. Initial yielding of the brace has occurred and may be observable.	Replacement not to develop full stiffness, resistance and deformation capacity.
	Gusset Plates	MAXIMUM SEISMIC RESPONSE. Initial yielding has begun but it has not progressed to a point where it concentrates around a hinge line. OBSERVABLE RESIDUAL DAMAGE. There is no visible residual rotation of the gusset plate and weld or base metal tearing has not begun.	Replacement or repair of the gusset plate not warranted.
	Frame and Framing Elements	MAXIMUM SEISMIC RESPONSE. Initial yielding has occurred especially on the flanges at the reentrant gusset plate corners but does not extend beyond this area. No local buckling of the webs or flanges has occurred. OBSERVABLE RESIDUAL DAMAGE. There is no residual drift in the frame.	None

DS2	Brace	MAXIMUM SEISMIC RESPONSE. Buckling deformation does not exceed twice the depth of the brace. OBSERVABLE RESIDUAL DAMAGE. Residual buckling is visible to the naked eye but permanent buckling deformation does not exceed the brace depth.	Permanent brace damage is largely an aesthetic concern. Heat straightening may be desirable for aesthetic reasons. Estimated 40% probability that replacement is required
	Gusset Plates	MAXIMUM SEISMIC RESPONSE. Yielding around the buckling clearance fold line but is not widespread over the entire gusset. Crack initiation may occur in welds and base metal, but crack length well below critical limit for unstable crack growth. OBSERVABLE RESIDUAL DAMAGE. Slight residual rotation visible to the naked eye. Locations of yielding can be noted because of Luder's lines on the steel.	Insignificant loss of strength and stiffness of the gusset. Replacement not needed. Estimated 20% probability rewelding of gusset at cracks is required. Heat straightening may be desirable to reduce gusset deformation for aesthetic reasons.
	Frame and Framing Elements	MAXIMUM SEISMIC RESPONSE. Yielding has progressed beyond the reentrant corners and spread to the web and outer flange, but does not yet cover the entire depth of the member. Local buckling of webs and flanges may have initiated. OBSERVABLE RESIDUAL DAMAGE. Local buckling of the flanges and webs are not visible to the naked eye.	None

DS3	Brace	MAXIMUM SEISMIC RESPONSE. Maximum bucking deformation of the braced exceeds 3 times the brace depth. Local buckling of the brace that preceeds brace fracture has occurred. OBSERVABLE RESIDUAL DAMAGE. Local buckling of the brace is visible however complete fracture has not occurred. Residual buckling of the brace does not exceed two times the depth of the brace.	Significant axial capacity has been lost, replacement is probably necessary. Estimated 70% probability that replacement of brace is required. With HSS tubes the probability that replacement of the brace will be required approaches 100%
	Gusset Plates	MAXIMUM SEISMIC RESPONSE. The entire surface of the gusset is yielded. Tears and crack growth of the welds and gusset are relatively large and approaching the critical crack length. OBSERVABLE RESIDUAL DAMAGE. The residual rotation of the gusset plate is very noticeable to the naked eye. Because the yielding has spread throughout the thickness and the residual rotation is beyond a point that it could be safely heat straightened, replacement is necessary.	Estimated 50% probability that replacement of gusset is required.
	Frame and Framing Elements	MAXIMUM SEISMIC RESPONSE. Yielding has occurred over the depth of the members and has spread to areas outside gusset corner. Local buckling of the flanges and webs have occurred. OBSERVABLE RESIDUAL DAMAGE. Luder's lines indicating past yielding are very visible. Local buckles may be visible, but amplitude of residual buckles do not exceed the thickness of the buckled web or flange..	Beam and column yielding are in isolated area, and the axial and flexural capacity of the members are only slightly affected. Heat straightening of damaged elements or added stiffeners may be desirable for aesthetic reasons.

DS4	Brace	MAXIMUM SEISMIC RESPONSE. The brace has lost all ability to transfer compressive or tensile forces and has most likely fractured. If the brace is not fractured it has buckled over three times the brace depth with significant localization of damage. OBSERVABLE RESIDUAL DAMAGE. The brace has fractured or has a residual displacement greater than two times the brace depth.	The brace has either fractured or lost the vast majority of its compressive resistance. Replacement is required.
	Gusset Plates	MAXIMUM SEISMIC RESPONSE. Significant inelastic deformation of the gusset plate has occurred. Base metal and weld tearing has extended to a point that the gusset plate or gusset plate welds have torn from one of the framing elements for more than 50% of their length. OBSERVABLE RESIDUAL DAMAGE. Gusset plate will have large visible residual deformations. These deformations exceed several times the gusset thickness. Cracks or tears of the gusset plate or welds joining the gusset have completely fractured or have progressed over one half the interface length.	The gusset offers little to no rotational stiffness or resistance. Estimated 90% probability of replacement.
	Frame and Framing Elements	MAXIMUM SEISMIC RESPONSE. Local buckling of the flange and web exceed 3 times their respective thicknesses, yielding has extended to a point that a plastic hinge is visible, complete or partial fracture of the flanges may have occurred. OBSERVABLE RESIDUAL DAMAGE. Visible flange and web buckles will be noted. Cracks or tears may have initiated at these yield locations, and complete fractures are possible. Damage to this extent would not be repairable and complete replacement would be necessary.	Yielding and local buckling may be repaired by heat straightening, stiffeners or reinforcement, if cracking or tearing has not initiated. If cracking or tearing has initiated replacement will be needed. This is likely to occur only when very thick and heavy gussets are employed.
	Global Frame Performance	MAXIMUM SEISMIC RESPONSE. Loss of frame resistance due to global aspects of frame behavior at extreme drift levels. OBSERVABLE RESIDUAL DAMAGE. Bolt fracture has occurred for beam-column or gusset plate connections resulting in significant loss of frame resistance. Tensile resistance of the brace, which is less than 80% of the nominal yield resistance of the brace, also meets this deterioration criteria.	Bolt replacement required. Combinations of above.

- fracture of the brace,
- fracture of gusset plate welds or severe buckling or inelastic deformation of the gusset plate so as to limit the load capacity of the brace,
- severe inelastic deformation of the beams or columns so as to initiate cracking (or fracture) of these structural members, and
- significant, permanent loss of total frame resistance.

Appendix D contains detailed information of CBF system tests used to establish the fragility curves developed for and presented in this report. This data presented in the appendix typically includes a description of the test specimen, hysteresis curves of the test results, and definitions of the frame deformation when key damage states were achieved. When available, photographs are included in these descriptions to aid in the evaluation of the damage state. As noted earlier, test results from component (e.g. isolated brace) tests are not used in development of these fragility curves, but brace and component behavior clearly influence the performance of the CBF system. Appendices B and C summarize this available data, but CBF system performance depends upon the combination of the various components rather than the performance of a single element. As a result, brace and connection test results were used to evaluate the impact of the design parameters on the damage states and this information was used to support the development and evaluation of the damage states. This evaluation is further discussed in Chapter 3. In addition, the secondary information was combined with the primary information of Appendix D to establish the appropriate engineering demand parameters for use in the damage evaluation, as presented in the next section.

ENGINEERING DEMAND PARAMETERS

Engineering demand parameters (EDPs) are used by structural engineers to quantify performance of the structural system. Therefore the parameter must be (1) quantifiable using structural analysis software, and (2) reliably predict the structural performance (or damage) state. Within the context of this document, several engineering demand parameters were considered for use to predict the structural performance, all of which focus on the maximum system drift, Δ_{max}. Since a normalized EDP eliminates the dependency on the structural units, the maximum story drift ratio, Δ_{max}/h was the logical engineering demand parameter for this evaluation, where Δ_{max} is the max drift and h is the story height. CBFs commonly sustain greater inelastic deformation in a single story, because of issues such as discussed in Chapter 3. Hence this EDP must be considered in a story-by-story basis. It is important to note that non-symmetrically braced CBFs typically demonstrate significantly different behavior when the brace is in tension than it is when the brace is in compression. Therefore, for those CBF categories, experiments may show very different maximum drift limits for tension and compression, e.g. $\Delta_{tens,max}$ and $\Delta_{comp,max}$. To develop an EDP which is consistent among all experiments and all categories of CBFs, these differences must be taken into account.

The failure modes of the braced frame are illustrated in Fig. 1, and these failure modes are less dependent on these maximum deformations than on the range of story drift deformation ($\Delta_{range,max} = \Delta_{tens,max} - \Delta_{comp,max}$). This drift range is then converted to average maximum normalized story drift by $\Delta_{range,max}/2h$. It should be noted that all of the failure modes shown in Fig. 1 have been

noted in one or more component tests, but some have very limited data regarding their occurrence and some have not been observed in system (as opposed to individual component) braced frame tests. The maximum drift-range ratio provides a better measure of both the deformability and the performance of the CBF system, because it provides not only a measure the total brace elongation and the total brace post-buckling deformation as well as the total demands on the gusset plate connections and the framing members. In addition, it also permits relatively consistent use and comparison of different cyclic load protocols to better compare different test results. Figure 2 provides a graphical demonstration of the various drift values. For all of these reasons the maximum drift-range ratio was the EDP of choice for CBF systems and was used herein.

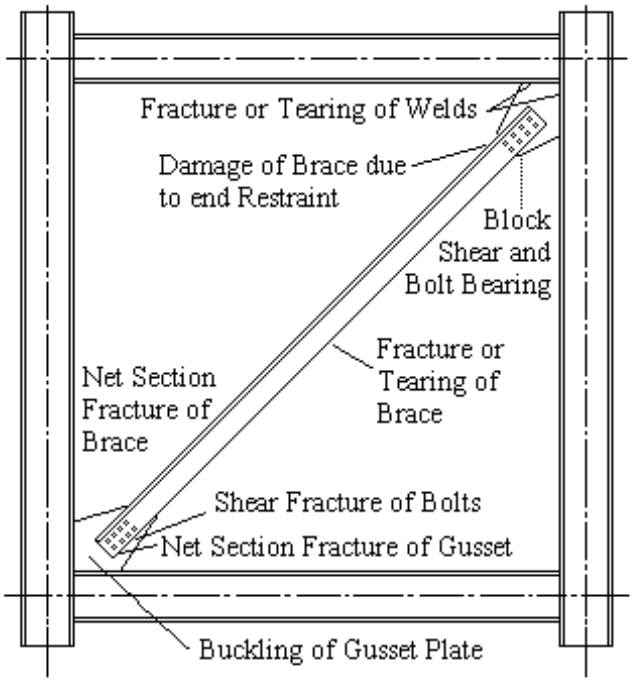

Figure 1. Possible Failure Modes for CBF System

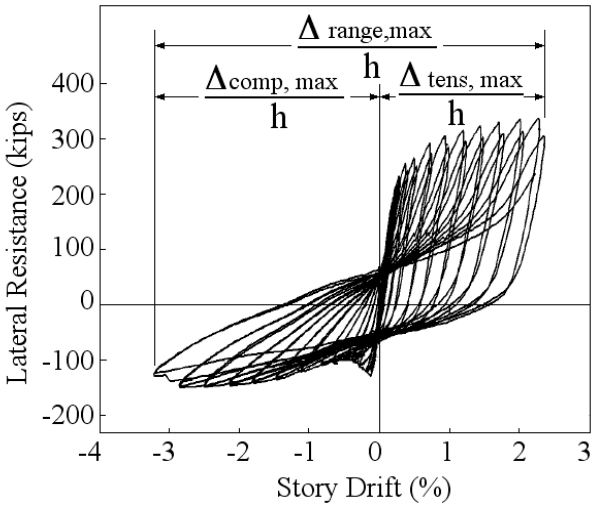

Figure 2. Illustration of Drift Values

FRAGILITY FUNCTION DEVELOPMENT

The fragility curves were developed based on procedures defined by Porter (Porter et al. 2006, 2008) and the guidance provided in Appendix C of the ATC58 35% draft report. In general, the fragility curves are to be developed in the form of a lognormal cumulative distribution function, $F_i(D)$,

$$F_i(D)=\Phi\left(\frac{\ln(D/\theta_i}{\beta_i}\right)$$

where D is the demand parameter ($\Delta_{range,max}/(2h)$), Φ is the normal cumulative distribution function, θ_i is the median value of the probability distribution, and β_i is the logarithmic standard deviation of the behavior. The parameters θ_i and β_i can be established by evaluation of actual experimental data, analytical derivation of expected behavior, or expert opinion. In general, the experimental data described in Appendix D was used to establish these fragility curves except for special cases where no experimental data was available. With experimental data, the statistical parameters are:

$$\theta_i = e^{\left(\frac{1}{M}\sum_{i-1}^{M}\ln di\right)} \quad \text{Eq. 1}$$

and

$$\beta_r = \sqrt{\left(\frac{1}{M-1}\sum_{i-1}^{M}\left(\ln\left(di/\theta\right)\right)^2\right)^2} \quad \text{Eq. 2}$$

where β_r is the logarithmic standard deviation obtained from the experimental data and M is the number of tests with this observed behavior. It is of note that M does not necessarily coincide with the number of specimens used in the given fragility-curve category. This does imply that the given damage state did not or would not occur for this test specimen. Instead a smaller value of M indicates that test was stopped at a deformation before this damage could be noted or the written documentation of the test results did not provide adequate information to determine the engineering demand parameter value at which the damage state was noted.

This procedure establishes the logarithmic standard deviation obtained from the experimental data, β_r, however, a further correction was made to adjust for uncertainty in the evaluation. This was done by the recommended equation:

$$\beta = \sqrt{\beta_r^2 + \beta_u^2} \quad \text{Eq. 3}$$

where β_u is intended to account for the uncertainty in the data. Following Porter et al. 2006, the value of β_u was taken to be equal to 0.1 if M was greater than 5, and it was taken to be equal to 0.25 for curves with fewer experimental results. CBF response is largely in-plane, and experimental test with transverse (out-of-plane) loading is not available. However, due to the in-plane stiffness and resistance of CBFs, out-of-plane deformation is not expected to have significant impact on their structural performance. Hence, the 3-dimensional stipulation by Porter is not employed. Second, there is limited variation in the test protocol within the research outlined in Appendix D, but this

variation suggests that CBFs are primarily controlled by their design details and the total inelastic deformation range. As a result, the larger value of β_u was not considered appropriate if a significant test database was available.

Appendix D shows that there are numerous CBF frame test results. In some cases, individual categories of the CBF system have a significant experimental database that can be used to develop a high-quality fragility function. However, many of the categories listed in Table 1 have limited data or very inconsistent data and may not be appropriate for developing fragility curves.

The development methods outlined by Porter and others permit the use of expert opinion, analytical derivation and bounding data to develop fragility curves, but every effort was made to avoid insertion of opinion in the fragility curves developed here. Nevertheless, opinion was used in some cases, because there is little or no data to support development of fragility curves for the given brace cross section and configuration combination. When opinion was inserted it is discussed in some detail, when the fragility curve is presented. This is true in one case for which no experimental data are available. In this case it is the writers' opinion that some aspects of the performance of this systems is quite clear based upon experimental observations of braces, connections and other CBF system tests. As a result, a fragility curves based upon opinion is presented for this specific category of behavior. The rationale of this is clearly explained. However, the fragility curves for this special case is drawn as a very simple curve rather than the formalized procedure proposed for fragility curves developed by expert opinion. This was done, because the refinement suggested by the formalized procedure was not warranted for these specific conditions. In other cases where the data was not sufficient for development of a fragility curve, the existing data was compared to other documented curves to establish its relative position compared to other behaviors. However, no fragility curves were developed in these cases.

CHAPTER 3 - Issues Affecting Fragility of CBFs

A number of factors affect the seismic performance and deformation capacity of CBFs with buckling braces. These include:

- the design procedures for the brace, gusset plate and the braced frame,
- the cross section and slenderness of the brace, and
- the configuration and geometry of the braced frame system.

All of these issues are important to the data in Appendix D, which includes data from braced frame tests. However, each of these categories has a wide range of variables that can potentially affect the behavior of the CBF systems. In addition, multiple test results are needed to develop reliable fragility curves, and this further complicates the development of and uncertainty in the fragility curves as they are not widely available. These aspects to the design and testing procedures deserve careful understanding prior to presenting the fragility curves that were developed for the CFB systems. As a result, some discussion of these major issues is presented below. Further discussion is available in Lumpkin (2009).

DESIGN PROCEDURES

Design procedures affect the performance of braced frames on several levels. On the first level, the decision to design a braced frame as an OCBF or an SCBF controls the required resistance of the braced frame, however the resistance of past test specimens is not the critical issue in developing fragility curves. The resistance of the frame will influence the deformation expected from a given seismic excitation, but the resulting deformation is the key to defining the expected damage level. Fragility curves are primarily based upon the relationship between damage and deformation level. These issues are largely related to the detailing requirements for the brace and connections and the relative strength of the brace to other framing members. OCBFs and SCBFs are distinguished from one another by their expected ductility and inelastic deformation capacity, and the differences in the detailing requirements for the two design methods. Unfortunately, there is great difficulty in separating past research results as belonging to the OCBF or SCBF systems. First, individual test specimens seldom fully satisfy or were designed to simulate the OCBF or SCBF detailing requirements of their day. Second, the specific detailing requirements for OCBFs and SCBFs have changed over the years. The concept of ductile design of CBFs is relatively new, since ductile CBF design was first proposed in seismic design specifications in the 1988 Uniform Building Code. Since that date, there have been numerous changes to design requirements for CBFs. The actual OCBF and SCBF concepts were introduced in the 1990s with the introduction of the AISC Seismic Design Provisions (AISC 1997). Since that time both the SCBF and OCBF design requirements have experienced continued evolution, and today the separation between the design requirements of OCBFs and SCBFs is smaller than it has been in the past. These changes are reflected in CBF test specimens and test data, because the design of test specimens approximate or reflect the design requirements of that time. Hence, it is difficult to combine and use test data from different periods, and it is seldom possible to find extensive test data to support OCBF and SCBF design criteria for specific frame types or specific periods of history.

The design details for SCBF connections have been relatively stable for approximately 10 years, since the connection is designed for the expected tensile (R_y,F_yA_g) and compressive (R_y,$F_{cr}A_g$) forces, and the connection must either be designed to achieve the end rotation or plastic moment capacity of the brace. However, recent research (Lehman et al. 2008) has shown that current

connection design procedures may be deficient in achieving the ductility and deformation capacity needed to achieve the target SCBF behavior. First, recent experiments show that the welds joining the gusset plate to the beam and column must be designed to achieve the plastic capacity of the gusset plate rather than the expected resistance of the brace as required by the current SCBF provisions (AISC 2005b) and as established by the uniform force method. This required weld resistance can be achieved by either using CJP welds of matching metal or by fillet welds on both sides of the gusset equal to (or slightly greater than) the thickness of the gusset. Second, experiments show that the strength and stiffness of the gusset plate connection should be adequate to develop the expected resistance of the brace, but they should not be excessively large, because a stiff, strong connection concentrates the inelastic deformation into a short length of the center of the brace and causes early brace fracture. Third, SCBF design provisions require that the gusset plate connection design either develop either 110% of the expected bending capacity of brace or have clear rotational capacity needed to readily permit brace rotation required for brace buckling. This connection rotation is typically achieved with the $2t_p$ linear clearance zone perpendicular to the axis of the brace. This clearance model results in larger gusset plates, and recent research has shown that this adversely affects SCBF system performance (Lehman et al. 2008). An elliptical clearance model has been proposed to alleviate this problem. Finally, gusset plate connections that sustain some yielding significantly increase the deformation capacity of braced frames.

These observations are illustrated in Fig. 3. This figure shows three force deflection plots of three different braced frames. All three frames have the same brace and column, but different gusset plate connections and all connections would meet (or exceed) today's SCBF connection design criteria. However, the behavior of the connection is quite different for the three frames, thereby effecting the failure mode and system deformation capacity. Figure 3a shows a SCBF with gusset plate connection welds meeting current SCBF criteria with welds designed by the uniform force method to the expected tensile resistance of the brace. The gusset plate was relatively large because the $2t_p$-linear clearance zone was employed. This connection results in early weld fracture with limited ductility. Figure 3c is an SCBF frame with a gusset plate connection, which is designed to have a greater strength and stiffness than the minimum required, that is the ratio of the strength of the gusset plate to the tensile strength of the brace is much greater than 1.0. The additional strength and stiffness in the gusset plate results in limited ductility and deformation capacity, as shown in the figure, although the desired failure mode of brace fracture is achieved. Figure 3b is a connection that meets current SCBF requirements, but it has some additional design constraints designed to maximize the system response. First, the resistance of the gusset is design to develop the expected tensile force of the brace with little reserve capacity, that is the capacity ratio of the gusset-to-brace is approximately 1.1. In addition, the connection was designed using the proposed elliptical clearance model which produced a compact gusset, and the gusset plate welds are sized to develop the expected plastic capacity of the gusset rather than the expected tensile force in the brace. This connection design results in improved SCBF system performance and greater frame ductility.

As noted earlier, the brace size and shape was identical for all three tests. The actual frame failure mode was identical (brace fracture for the rectangular HSS brace) for the frames in Figure 3b and 3c, but the changes in connection design significantly influence the ductility, deformation capacity, and failure mode of the SCBF system. This comparison shows that considerable variation in performance must be expected with frames meeting the basic SCBF (or OCBF) design criteria. This variation can result in great variation within a fragility curve, increasing the uncertainty related to predicting the performance of the system. At the same time, this suggests that additional constraints upon the SCBF design criteria may significantly improve and reduce the variation in system performance.

Connection Details	Lateral Force-Story Drift Behavior	Ultimate Failure Mode
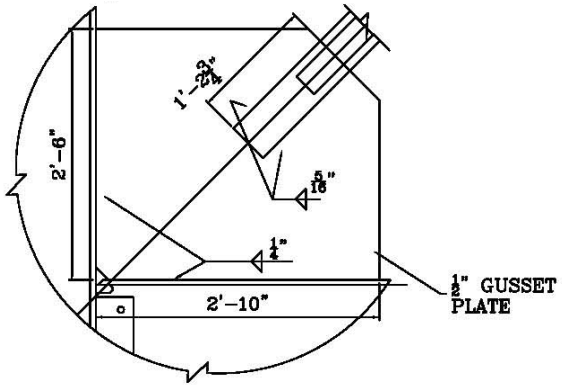 a) 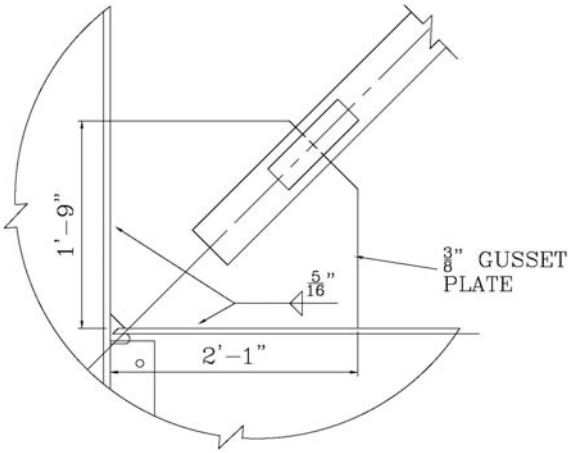 b)	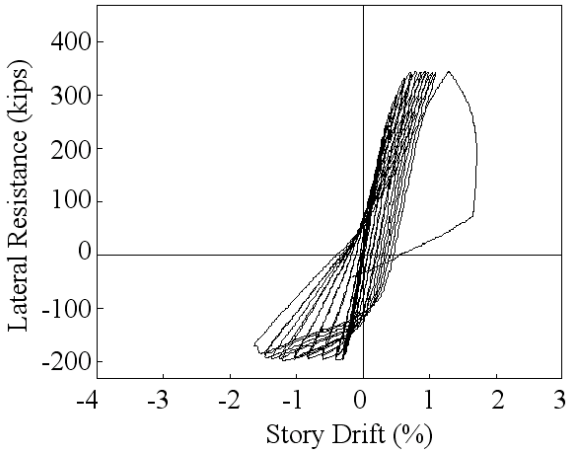 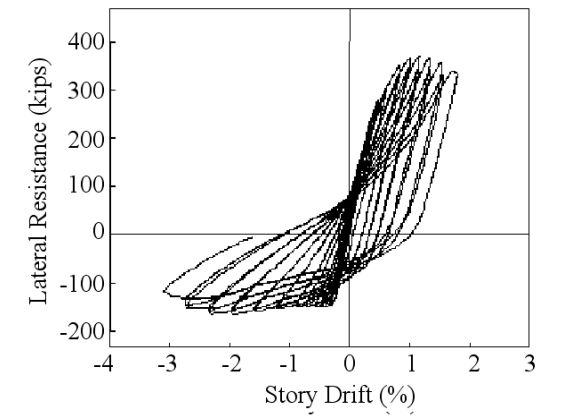	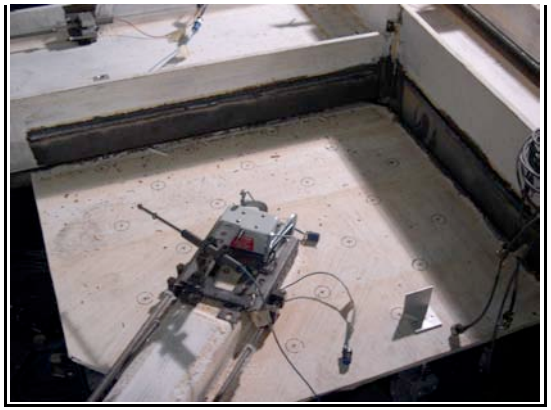 

Figure 3. Force-Story Drift of SCBF; a) Weld fracture due to welds designed by uniform force method, b) SCBF gusset with added constraints noted above, c) SCBF with very conservative gusset plate design.

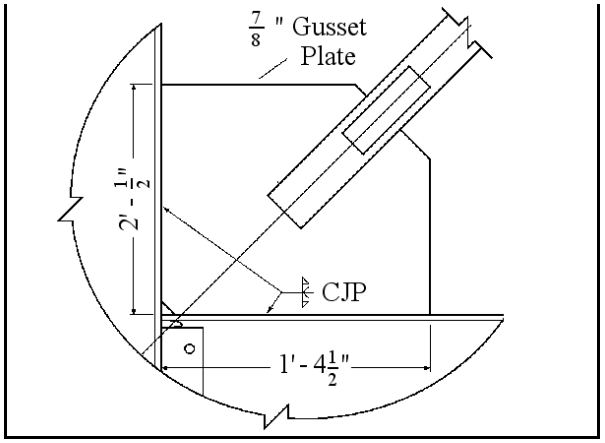

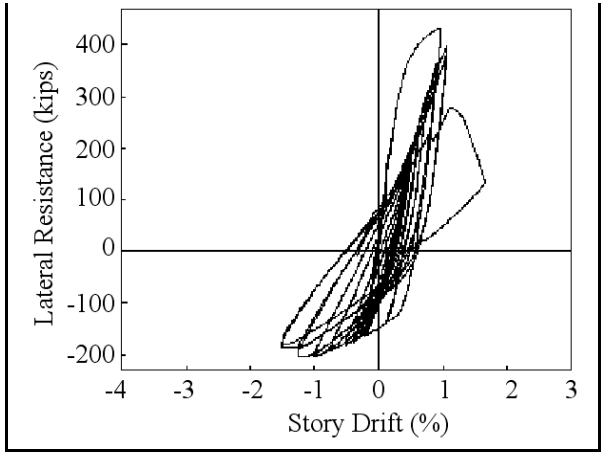

Figure 3. Force-Story Drift of SCBF (Continued); a) Weld fracture due to welds designed by uniform force method, b) SCBF gusset with added constraints noted above, c) SCBF with very conservative gusset plate design

BRACE CROSS SECTION AND SLENDERNESS

The brace cross section and slenderness have considerable impact upon the inelastic performance of braces as indicated by the experiments by (Tremblay et al. 2008, Tremblay 2002) and in turn influence the system response. Figure 4 illustrates this observation. This plot shows the results of 6 recent large scale cyclic tests of single braces. Three of the plots (RHS-4, RHS-2 and RHS-19) show the results from tests on rectangular HSS tubes, two plots show the results from tests on circular HSS tubes (CHS-1 and CHS2) and one plot shows the results from a test of a wide flange section (W-6). Comparing the curves provides considerable insight into the effect of cross section and slenderness on the cyclic performance braces.

Rectangular HSS tubes are known to be strongly influence by the local strain deformation accumulated in the buckled region of the brace, as shown in Fig. 5. Rectangular HSS tubes develop local crimping at the corners and this result in local strain concentrations, crack formation and tearing of the cross section, as shown in the figure. This local damage occurs at smaller deformations and progresses to earlier brace fracture at a smaller frame deformation than braces with larger local slenderness ratios as shown by comparing the deformation capacity achieved with RHS-4 with RHS-2 in Fig. 4. Although both specimens meet current AISC slenderness limits, RHS-4 is at the limit of the current design specification and has less deformation capacity that RHS-2, which is well under the current design limit.

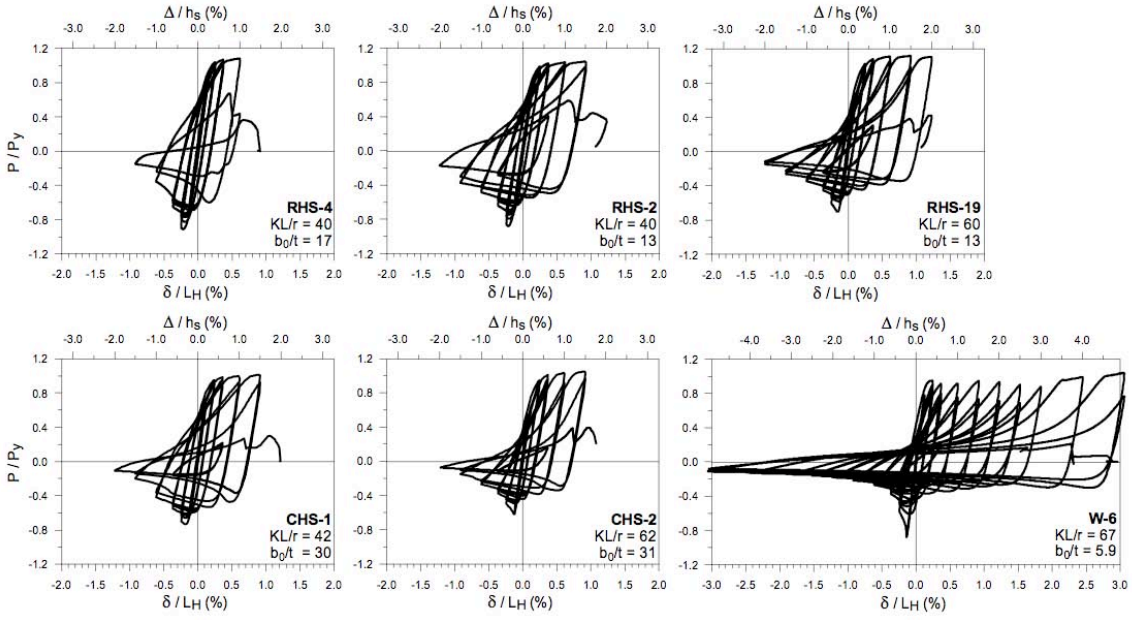

Figure 4. Axial Force Deflection Behavior of Various Braces (from Tremblay et al. 2008)

Braces with large global brace slenderness ratios (i.e., large Kl/r ratios) behave somewhat differently than braces with small slenderness ratio (Kl/r) values. This can be seen by comparing the behavior of RHS-2 with RHS-19 and CHS-1 with CHS-2 in Fig. 4. In both cases, the brace cross section and local slenderness are the same, but the global slenderness varies between tests. As shown in these comparisons, the braces with larger Kl/r values have greater variation between the tensile yield capacity and the compressive buckling capacity. Slender braces often provide somewhat greater inelastic deformation capacity as can be seen by comparing RhS-2 to RHS-19, but

there is considerable variability in CBF behavior and this observation is not consistently noted in all test results. Slender braces may have more rapid loss of compressive capacity after brace buckling as shown in Fig. 6, but slender braces have also demonstrated larger inelastic deformation capacity than stocky braces in some past test programs.

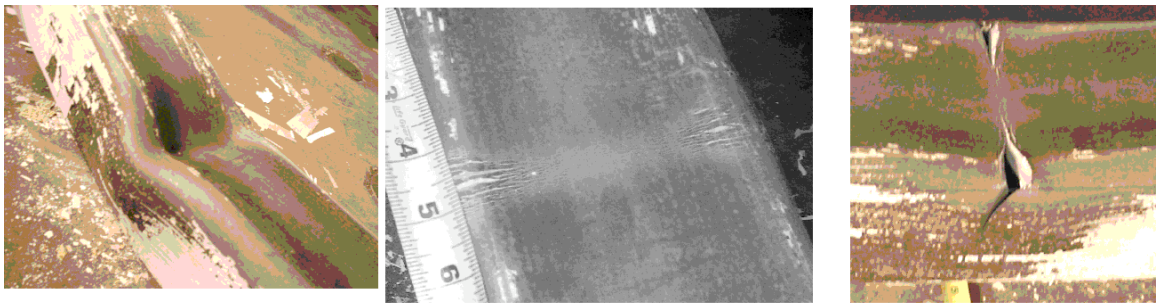

Figure 5. Local Strain Accumulation in Rectangular HSS Tubes (Johnson 2006)

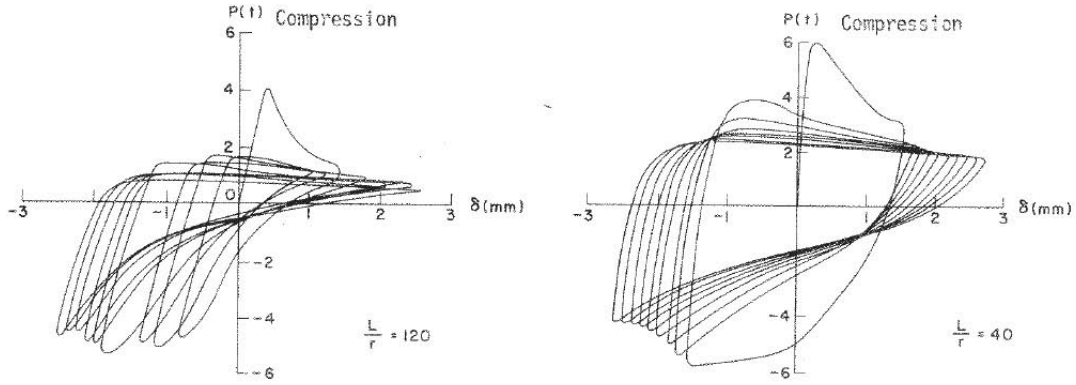

Figure 6. Effect of $^{Kl}/_{r}$ on Brace Performance (from Popov et al. 1976)

Finally, the brace cross section may impact on the seismic performance of the brace. As note earlier and demonstrated in Fig. 5, rectangular HSS tubes have localization of damage, which often leads to early fracture of the brace. This cross sectional effect can be illustrated by comparison of the measured force-deflection behavior of RHS-19, CHS-2, and W-6 in Fig. 4. These three specimens have similar global slenderness values, but very different brace cross-section slenderness values. The rectangular and circular HSS tubular braces have significantly smaller inelastic deformation capacities than the wide flange brace. It is commonly observed that open steel sections such as wide flanges, angles and channels often achieve larger inelastic deformation capacities prior to brace fracture than rectangular tubes of comparable slenderness ratio. Further, it is often postulated that rectangular tubes frequently provide less inelastic deformation capacity than circular tubes (Oliveira and Packer, Modern Steel Construction June 2009). This beneficial effect of circular tubes is clearly not shown in comparing CHS-2 to RHS-19, which indicates larger deformation range in the rectangular tubular brace with similar global slenderness properties. However, it must be recognized that the circular tube has a larger local slender, and comparing local slenderness between brace cross sections is not a particularly valid comparison. Open steel sections typically show more dramatic reduction in compressive resistance and reduced energy dissipation at given deformation levels when compared to tubular sections. This difference can be seen in Fig. 4 where the post-buckling compressive resistance of W-6 shows a sharper and more

dramatic reduction in resistance than CHS-2 and RhS-19 with similar global slenderness levels. It should also be emphasized that recent research shows that the ductility achieved with a given brace cross-section shape is strongly influenced by the connection design (Lehman et al. 2008).

To close this discussion, it must be recognized that there is great variability in the performance of CBF components, and system performance is often different from that noted with component tests because of competing behaviors within the system (for example, connection detailing and bracing configuration). This is illustrated in Fig. 7. Figure 7 shows the force-story drift behavior of braced bays with HSS tube braces and wide flange braces with similar slenderness and member sizing. The wide flange brace provides greater ductility than the HSS rectangular tube, but the beneficial effect of the wide flange section is much smaller than the component tests of Fig. 4 would suggest. Further, there is insufficient test data to develop fragility curves for narrow definitions of CBF systems. As a consequence of these variables, it must be recognized that fragility curves are not likely to provide a clear precise picture of braced frame performance unless the curves are defined for the brace cross section shape, local and global slenderness, braced frame configuration as well as connection and frame design method and detailing. The wide range of experimental data needed to accomplish this is not available, and the fragility curves derived here must be used with some caution.

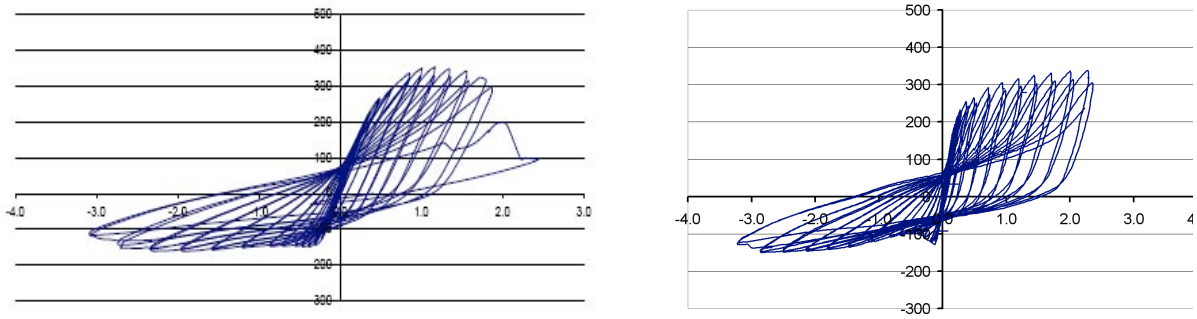

Figure 7. Force Story Drift Behavior of Similar CBF Systems; a) HSS brace, b) Wide Flange Brace

BRACED FRAME CONFIGURATION

A third important design issue is the CBF frame geometry and configuration. Figure 8 shows several CBF brace configurations that have been used in practice. X-bracing historically was used with very slender braces that were designed as tension only bracing or with limited compressive buckling capacity. The resulting braces had high $\frac{K l}{r}$ ratios. A few early tests of braced frames considered tension only bracing, and the seismic performance was often poor. Tension only bracing is not permitted for SCBFs today, because a balance between tensile and compressive brace resistance is required. Further, slenderness limits on the brace prevent the compressive resistance from being too small. Current SCBF design provisions require that no more than 70% of the lateral resistance of a CBF may be resisted by braces in tension. Hence, some older X-braced experiments with minimum tension only bracing are not suitable for SCBF construction and are excluded from the Appendix D database. Other older X-braced test frames were built to very small scale. It is well known that small-scale test specimens consistently achieve greater ductility than full scale frames, because deformations scale quite directly with specimen size. However, strain levels are significantly smaller for small scale specimens at a given deformation level than for large scale specimens at the same dimensionless deformation, and ultimate failure is more commonly related to strain level than to global deformation.

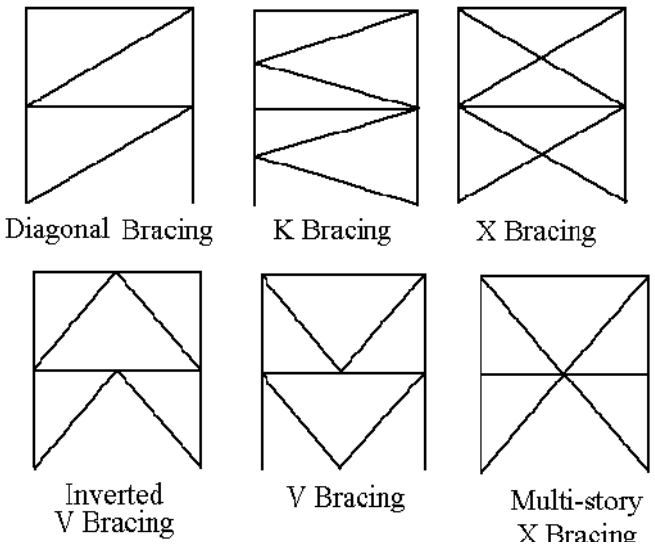

Figure 8. Possible Brace Configurations

V-braced or inverted V-bracing are also known as inverted-chevron and chevron bracing and are also shown in Fig. 8. These configurations result in bracing connections at midspan of the beam. Under lateral load, one brace acts in compression while the other acts in tension. The capacity of the tensile brace is significantly larger then the capacity of the compression brace, and this results in an unbalanced force at the brace-beam intersection during severe seismic excitation. The may cause beam yielding invariably pulls the beam downward during inelastic deformation for the inverted V-braces. This beam flexural yielding may provide a significant increase in energy dissipation, but it also causes architectural damage to the building through the resulting floor deflections. This flexural yielding has a substantial impact on the braced frame behavior, and changes to the SCBF provisions today require that the beam be designed to resist this unbalanced brace forces. Some existing test data is available for the inverted V- or Chevron brace configuration, but the number of tests is limited. Two full-scale tests evaluate the system are all performance levels, and other tests provide information more limited performance range. Figure 9 shows test results for the critical stories of these two frames. The two frames were tested under different conditions, and so the tests are not totally comparable, since the frame in Fig. 9a was tested with a prescribed displacement history (Uriz and Mahin (2004)) and Fig. 9b was a pseudo dynamic test (Foutch et al. (1987)). When comparing these results, there are some differences and similarities. The test lighter floor beam (Fig. 9b) appeared to mask the brace buckling effects when compared to Fig. 9a, because of the large amount of flexural yielding noted within the beam. As a result, the hysteresis curves are more pinched with indications of lost resistance after brace buckling with the heavy newer construction detail in Fig. 9a. On the other hand, the story drift at brace fracture was similar for both tests. The specimen of Fig. 9a gives the appearance of having greater deformation capacity, but this added deformation capacity was achieved at the cost of ultimate column fracture after initial CBF failure, while the test of Fig. 9b was stopped immediately after initial brace fracture to permit use of the specimen in subsequent testing. With this single comparison, it is logical to ask if the requirement to design the floor beam for the full unbalanced load is achieving a useful function. The available experimental research data to evaluate the performance of chevron or V-braced frames are limited, and this clearly affects the reliability of fragility curves for this case.

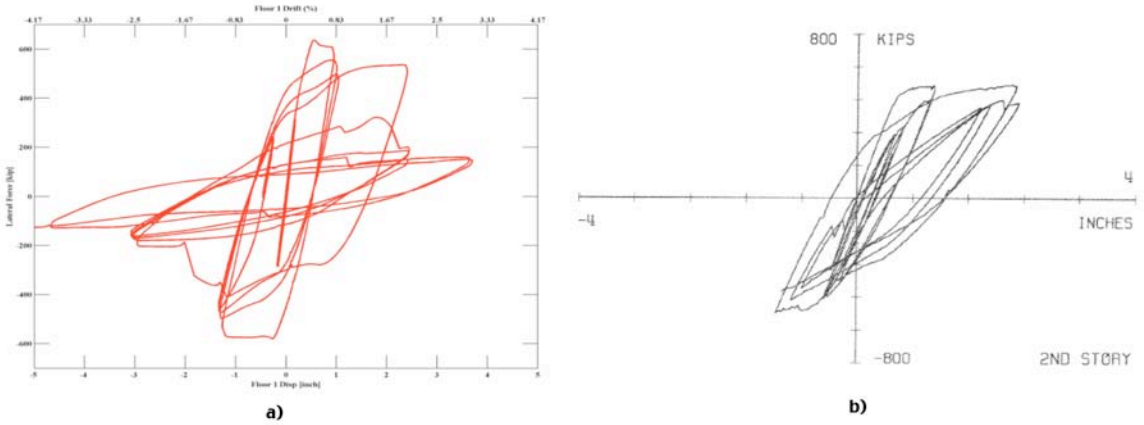

Figure 9. Test Results From Two Chevron Braced Frames; a) Chevron with Beam Designed for Unbalanced Force, b) Chevron with Weak Beam

Chevron and inverted-chevron bracing shown in Fig. 7 may be combined to form the multi-story bracing system. The multi-story X bracing prevents the unbalanced brace force after brace buckling as noted with the V- and chevron-braced systems. This prevents the extensive flexural yielding in the floor beam and potentially reduces the concentration of floor damage within a given story of the structural system. This configuration is used with increasing frequency, and limited test data is available to form fragility curves for this braced frame system.

K-bracing (sometimes known as knee bracing) as shown in Fig. 7 has an intersection of a tensile and compressive brace at midheight of the column. This application has the same unbalanced force problem as described with the V-bracing systems, but the inelastic flexural deformation resulting from this unbalanced force occurs within the column rather than the beam. The columns support the gravity loads of the structure, and so this inelastic deformation of the column cannot be tolerated in a ductile system. As a result, K-bracing is expressly prohibited for special concentrically braced frames, but is a possible application as an OCBF. This bending action of the column is likely to a significant impact on the structural performance and stability, and they may affect the fragility curves of the structural system. Appendix D shows that there is no available experimental data available for the seismic behavior of the K-braced structural system. As a result, fragility curves for this system can only be developed based upon expert opinion developed through examination of other test results.

Diagonal bracing is shown in Fig. 7. It is quite common in seismic design, and results from these tests can often be used to gain insight into the behavior of other brace configurations. The bracing acts in tension for lateral loads in one direction and in compression for lateral loads in the other direction. The tensile capacity of the brace is significantly larger than the compressive capacity of the brace. As with other bracing systems, the AISC seismic provisions for concentrically braced frames requires that the direction of inclination of bracing be balanced to assure appropriate resistance in both directions at all times for SCBF frames. There is considerable research data for this brace configuration, and so much of the experimental data that can be used to develop reliable fragility curves are included in this brace configuration.

Other similarities and differences were noted with other brace configuration. One major issue noted with CBF testing is that multi-story CBFs frequently concentrate damage into a single story, and this concentration of damage also appears to be influenced by the CBF configuration. The multi-story X-braced configuration shown in Fig. 7 is one configuration that has been proposed

as a possible configuration to reduce this story drift concentration, because the midspan brace-beam connection offers a direct path for the story shear to be transmitted between floors by braces in tension. Fragility curves developed in this report are based upon individual story drift, and as a result, the concentration of damage issue becomes an analytical concern, since the ability of the analytical procedure to predict this concentration is the issue of concern. Nevertheless, the potential for concentration of damage into a given story level raises concerns about the influence of that concentration on the reported system behavior.

CONCLUDING CAUTIONARY REMARKS

In view of these comments, the reader is cautioned that the fragility curves developed in this report have limited applicability. Specifically, each curve is applicable to a specific category of CBF brace cross section, CBF design methods, and brace configurations. Local and global slenderness are important, but there is insufficient data to define fragility curves for narrow ranges of these slenderness values. As a result, the fragility curves provided here, cover a fairly wide range of slenderness limits as defined by SCBF, OCBF and other design methods. The limitations of the fragility curves are clearly noted on the curve developed here. While it is very tempting to extrapolate these results to other apparently similar systems, there is considerable risk in doing this, because the fragility curves may vary significantly with changes in one or more important system parameters, specifically:

- Connection geometry, strength, and connecting weld properties
- Brace geometry and cross section
- Brace global and local slenderness ratio
- Braced frame configuration

These parameters may not be specifically considered or have adequate variability in the experimental research to effectively understand their influence on the performance of the braced frame. Therefore, further study and updating of the fragility curves is warranted as additional data become available.

CHAPTER 4 - Fragility Curves

Fragility curves were developed for a number of different brace cross section shapes and brace configuration combinations. The 69 braced frame system tests documented in Appendix D were used for this curve development. The damage state results for the 69 tests are more briefly summarized in Table 3. The tests are grouped by authors and test programs but characteristics of each test as well as the average maximum drift level at each of the four damage states are noted. It must be noted that average maximum drift levels are not included for some damage states for some individual specimens, for one of two reasons. First, some specimens did not display certain damage levels. Second, and more commonly, the written test description did not include adequate information to accurately define the drift range at which the specified damage state was observed. For either of these cases, the drift level was noted as a dash in the table, and these specimens were not included in the statistical evaluation needed to develop the fragility curve for that damage state.

As noted in prior discussion, Table D-1 of Appendix D of the 35% draft ATC-58 report specifies the development of fragility curves for different categories of braced frames covering a wide range of performance levels, as indicated in Table 1. As discussed previously, these categories include a number of special cases, and some of these special cases have no experimental data or rational basis for developing a fragility curve. Others have significant data, and in some cases multiple curves can be developed based upon specific data for subdivisions of that category. Nevertheless, each category will be discussed in some detail, and where possible fragility curves will be presented.

S2-BF-1 - STRENGTH DESIGN WITH NO SEISMIC DETAILING

The concept of strength design of braced frames with no seismic detailing does not fit the research database, and no test data was available to support development of fragility curves for this concept. In general, every test included in the data base was designed to examine some issue of CBF performance. The concept of strength design is that members are designed to achieve a factored design load, and connections are designed to these same factored loads. If the factored design loads are large enough that the structure can remain fully elastic with no brace buckling and yielding, the connections and other elements may provide adequate seismic performance under these conditions. However, there are many uncertainties in behavior that are not addressed. In particular, most problems for steel structures are related to connection performance. Connections may be designed for the same factored loads as the structural members, however the actual state of stress and strain are far less certain for connections than for structural members. In particular, design rules such as Whitmore width and Uniform Force Method are only approximate indicators of connection strength and performance. Thus, yielding and inelastic deformation is likely to occur in the connections, before the expected resistance of the brace is developed. Once brace buckling and yielding have occurred the connections experience significantly larger stress and strain demands that are not considered in the connection design. Connections are unlikely to tolerate these demands without any seismic detailing. As a result, rapid deterioration and failure of the connection must be expected once brace buckling and yielding have occurred. These problems with improperly designed connections are documented in numerous experiments. Further, with this design concept these problems must be expected.

Table 3. Summarized Fragility Curve Tests

Test Program	Specimen ID	Brace Configuration	Brace Shape	Brace End Restraint	Brace Compactness	Design Procedure	Damage State Drift Levels (%)			
							DS1	DS2	DS3	DS4
Charles Roeder, Dawn Lehman, UW Test Program Johnson 2005 Herman 2006 Kotulka 2007 Powell 2009 Clark 2009 Lumpkin 2009	HSS01	Single Diag.	HSS5x5x3/8	Gusset Plate	Seismic	AISC SCBF	0.30	0.89	1.46	1.37
	HSS02	Single Diag.	HSS5x5x3/8	Gusset Plate	Seismic	UW Mod. SCBF	0.35	1.03	1.72	2.01
	HSS03	Single Diag.	HSS5x5x3/8	Gusset Plate	Seismic	UW Mod. SCBF	0.41	0.96	1.46	2.47
	HSS04	Single Diag.	HSS5x5x3/8	Gusset Plate	Seismic	UW Mod. SCBF	0.41	0.67	1.38	2.42
	HSS05	Single Diag.	HSS5x5x3/8	Gusset Plate	Seismic	UW Mod. SCBF	0.46	1.85	1.85	2.66
	HSS06	Single Diag.	HSS5x5x3/8	Gusset Plate	Seismic	UW Mod. SCBF	0.49	1.05	1.62	2.37
	HSS07	Single Diag.	HSS5x5x3/8	Gusset Plate	Seismic	AISC SCBF	0.40	0.73	1.58	2.02
	HSS08	Single Diag.	HSS5x5x3/8	Gusset Plate	Seismic	UW Mod. SCBF	0.30	0.89	1.71	2.30
	HSS09	Single Diag.	HSS5x5x3/8	Gusset Plate	Seismic	AISC SCBF	0.36	0.77	1.40	1.85
	HSS10	Single Diag.	HSS5x5x3/8	Gusset Plate	Seismic	AISC SCBF	0.40	0.64	1.68	2.24
	HSS11	Single Diag.	HSS5x5x3/8	Gusset Plate	Seismic	AISC SCBF	0.19	0.42	1.08	1.29
	HSS12	Single Diag.	HSS5x5x3/8	Gusset Plate	Seismic	AISC SCBF	0.55	0.92	1.48	1.75
	HSS13	Single Diag.	HSS5x5x3/8	Gusset Plate	Seismic	AISC SCBF	0.43	0.93	1.81	2.04
	HSS14	Single Diag.	HSS5x5x3/8	Gusset Plate	Seismic	UW Mod. SCBF	0.31	1.49	1.81	1.97
	HSS15	Single Diag.	HSS5x5x3/8	Gusset Plate	Seismic	UW Mod. SCBF	0.39	0.87	1.98	2.05
	HSS17	Single Diag.	HSS5x5x3/8	Gusset Plate	Seismic	UW Mod. SCBF	0.41	0.93	1.58	2.47
	HSS18	Single Diag.	HSS5x5x3/8	Gusset Plate	Seismic	UW Mod. SCBF	0.28	0.70	1.75	2.09
	HSS20	Single Diag.	HSS5x5x3/8	Gusset Plate	Seismic	AISC SCBF	0.36	0.66	1.31	1.98
	HSS21	Single Diag.	HSS5x5x3/8	Gusset Plate	Seismic	AISC SCBF	0.35	0.72	1.66	1.87
	HSS22	Single Diag.	HSS5x5x3/8	Gusset Plate	Seismic	UW Mod. SCBF	0.30	0.51	1.54	1.99
	HSS23	Single Diag.	WF6x25	Gusset Plate	Seismic	UW Mod. SCBF	0.24	0.39	1.51	2.78
	HSS24	Single Diag.	HSS5x5x3/8	Gusset Plate	Seismic	UW Mod. SCBF	0.49	0.89	1.77	2.22
	HSS25	Single Diag.	HSS5x5x3/8	Gusset Plate	Seismic	AISC SCBF	0.39	0.73	1.31	1.65
	TCBF1-1	Double Story X	HSS125x125x9 (mm)	Gusset Plate	Seismic	UW Mod. SCBF	0.44	0.85	1.70	2.19
	TCBF1-2	Double Story X	WF 175x175x9.5x11 (mm)	Gusset Plate	Seismic	UW Mod. SCBF	0.52	0.88	2.09	2.99
	TCBF1-3	Double Story X	HSS125x125x9 (mm)	Gusset Plate	Seismic	AISC SCBF	0.52	0.85	1.27	2.77
	TCBF2-1	3 Story X, Chevron	HSS5x5x3/8	Gusset Plate	Seismic	UW Mod. SCBF	0.37	0.78	1.60	2.19

	TCBF2-2	3 Story X, Chevron	WF 175x175x9.5x11 (mm)	Gusset Plate	Seismic	UW Mod. SCBF	0.34	-	0.90	2.73
Wakabayshi,Nakamura,Yoshida, 1979	SPC 3	Single Diag.	Circ. Tube 4.29x0.345 (cm)	Gusset Plate	Seismic	-	0.13	-	1.11	1.73
	DPC 1	Single Story X	Circ. Tube 4.3x0.346 (cm)	Gusset Plate	Seismic	-	0.22	-	0.81	1.00
	SAC 3	Single Diag.	2L5x5x0.381 (cm)	Gusset Plate	Compact	-	0.07	-	1.01	2.71
	DAC 2	Single Story X	2L5x5x0.381 (cm)	Gusset Plate	Compact	-	0.32	0.33	1.10	2.13
El-Tayem, Goel, X-Bracing, 1985	AW0	Single Story X	L2.5x2.5x1.4	Gusset Plate	Compact	AISC OCBF	0.18	0.70	1.44	1.48
	AW1	Single Story X	L4x4x1/4	Gusset Plate	Compact	AISC OCBF	-	0.93	1.34	2.78
	AW2	Single Story X	L4x4x3.8	Gusset Plate	Compact	AISC OCBF	-	-	1.57	2.20
	AW3	Single Story X	L2.5x2.5x5/16	Gusset Plate	Compact	AISC OCBF	0.14	1.15	-	1.75
	AW4	Single Story X	L2.5x2.5x3.16	Gusset Plate	Compact	AISC OCBF	0.32	0.95	-	1.38
Aslani and Goel, Double Angles, 1989	AB1	Single Diag	2L3.5x2.5x1/4	Gusset Plate	Compact	AISC OCBF	0.18	0.32	-	1.36
	AB2	Single Diag	2L3.5x2.5x1/4	Gusset Plate	Compact	AISC OCBF	0.18	0.49	-	1.50
	AB3	Single Diag	2L3.5x2.5x1/4	Gusset Plate	Compact	AISC OCBF	0.19	0.49	-	1.20
	AB4	Single Diag	2L3.5x2.5x3/8	Gusset Plate	Compact	AISC OCBF	0.32	0.81	-	1.58
	AB5	Single Diag	2L3.5x2.5x3/8	Gusset Plate	Compact	AISC OCBF	0.31	0.47	-	1.40
	AB6	Single Diag	2L3.5x2.5x3/8	Gusset Plate	Compact	AISC OCBF	0.31	0.46	-	1.53
	ABS7	Single Diag	2L3.5x2.5x1/4	Gusset Plate	Compact	AISC OCBF	0.32	-	-	0.73
	ABS8	Single Diag	2L3.5x2.5x1/4	Gusset Plate	Compact	AISC OCBF	-	-	-	0.36
	AB9	Single Diag	2L3x3x3/8	Gusset Plate	Compact	AISC OCBF	0.31	-	-	1.34
	AXH10	Single Diag	2L3x3x3/8 (Bulit up Box)	Gusset Plate	Compact	AISC OCBF	0.32	-	1.50	2.01
	AXH11	Single Diag	2L3x3x3/8 (Bulit up Box)	Gusset Plate	Compact	AISC OCBF	0.32	-	1.58	2.06
	AXH12	Single Diag	2L3x3x3/8 (Bulit up Box)	Gusset Plate	Compact	AISC OCBF	0.32	-	-	2.39
	AXH13	Single Diag	2L3x3x3/8 (Bulit up Box)	Gusset Plate	Compact	AISC OCBF	0.30	-	0.45	1.43
	AXH14	Single Diag	2L3x3x3/8 (Bulit up Box)	Gusset Plate	Compact	AISC OCBF	0.30	-	0.75	1.92
	AXH15	Single Diag	2L3x3x3/8 (Bulit up Box)	Gusset Plate	Compact	AISC OCBF	0.33	-	-	1.23
	AXH16	Single Diag	2L3x3x3/8 (Bulit up Box)	Gusset Plate	Compact	AISC OCBF	0.32	-	-	1.51

	AXH17	Single Diag	2L3x3x3/8 (Bulit up Box)	Gusset Plate	Compact	AISC OCBF	0.32	-	1.60	2.08
Wakabayshi,Nakamura,Yoshida, 1977	SIC 1	Single Diag	WF 5x5x0.6x0.6 (cm)	Moment	Seismic	-	0.29	-	3.00	3.69
	DIC 1	Single Story X	WF 5x5x0.6x0.6 (cm)	Moment	Seismic	-	0.25	-	2.00	3.12
	DOC 1	Single Story X	WF 5x5x0.6x0.6 (cm)	Moment	Seismic	-	0.20	-	2.00	4.25
	DOC2	Single Story X	WF 5x5x0.6x0.6 (cm)	Moment	Seismic	-	0.42	-	-	4.25
	SIC 2	Single Diag	WF 5x5x0.6x0.6 (cm)	Moment	Seismic	-	0.18	-	3.00	3.69
	SIC 3	Single Diag	WF 5x5x0.6x0.6 (cm)	Moment	Seismic	-	0.07	-	-	4.07
	SOC 1	Single Diag	WF 5x5x0.6x0.6 (cm)	Moment	Seismic	-	0.37	-	2.00	4.11
	SOC 2	Single Diag	WF 5x5x0.6x0.6 (cm)	Moment	Seismic	-	0.18	-	-	4.11
	SOC 3	Single Diag	WF 5x5x0.6x0.6 (cm)	Moment	Seismic	-	0.05	-	-	2.02
	DIC 2	Single Story X	WF 5x5x0.6x0.6 (cm)	Moment	Seismic	-	0.28	-	2.00	3.12
	DIC 3	Single Story X	WF 5x5x0.6x0.6 (cm)	Moment	Seismic	-	0.26	-	3.00	3.15
	DOC 3	Single Story X	WF 5x5x0.6x0.6 (cm)	Moment	Seismic	-	0.36	-	-	3.15
Mahin and Uriz, 2004	SCBF-1	2 Story Chevron	HSS 6x6x3/8	Gusset Plate	Seismic	AISC SCBF	0.25	-	1.00	1.00
Foutch, Goel, Roeder, 1986	6 Story SCBF	6 Story Chevron	Varying HSS Shapes	Moment	Seismic	AISC SCBF	0.41	-	-	1.64

Table 3. Summarized Fragility Curve Tests

Test Program	Specimen ID	Brace Configuration	Brace Shape	Brace End Restraint	Brace Compactness	Design Procedure	Damage State Drift Levels (%)			
							DS1	DS2	DS3	DS4
Charles Roeder, Dawn Lehman, UW Test Program Johnson 2005 Herman 2006 Kotulka 2007 Powell 2009 Clark 2009 Lumpkin 2009	HSS01	Single Diag.	HSS5x5x3/8	Gusset Plate	Seismic	AISC SCBF	0.30	0.89	1.46	1.37
	HSS02	Single Diag.	HSS5x5x3/8	Gusset Plate	Seismic	UW Mod. SCBF	0.35	1.03	1.72	2.01
	HSS03	Single Diag.	HSS5x5x3/8	Gusset Plate	Seismic	UW Mod. SCBF	0.41	0.96	1.46	2.47
	HSS04	Single Diag.	HSS5x5x3/8	Gusset Plate	Seismic	UW Mod. SCBF	0.41	0.67	1.38	2.42
	HSS05	Single Diag.	HSS5x5x3/8	Gusset Plate	Seismic	UW Mod. SCBF	0.46	1.85	1.85	2.66
	HSS06	Single Diag.	HSS5x5x3/8	Gusset Plate	Seismic	UW Mod. SCBF	0.49	1.05	1.62	2.37
	HSS07	Single Diag.	HSS5x5x3/8	Gusset Plate	Seismic	AISC SCBF	0.40	0.73	1.58	2.02
	HSS08	Single Diag.	HSS5x5x3/8	Gusset Plate	Seismic	UW Mod. SCBF	0.30	0.89	1.71	2.30
	HSS09	Single Diag.	HSS5x5x3/8	Gusset Plate	Seismic	AISC SCBF	0.36	0.77	1.40	1.85
	HSS10	Single Diag.	HSS5x5x3/8	Gusset Plate	Seismic	AISC SCBF	0.40	0.64	1.68	2.24
	HSS11	Single Diag.	HSS5x5x3/8	Gusset Plate	Seismic	AISC SCBF	0.19	0.42	1.08	1.29
	HSS12	Single Diag.	HSS5x5x3/8	Gusset Plate	Seismic	AISC SCBF	0.55	0.92	1.48	1.75
	HSS13	Single Diag.	HSS5x5x3/8	Gusset Plate	Seismic	AISC SCBF	0.43	0.93	1.81	2.04
	HSS14	Single Diag.	HSS5x5x3/8	Gusset Plate	Seismic	UW Mod. SCBF	0.31	1.49	1.81	1.97
	HSS15	Single Diag.	HSS5x5x3/8	Gusset Plate	Seismic	UW Mod. SCBF	0.39	0.87	1.98	2.05
	HSS17	Single Diag.	HSS5x5x3/8	Gusset Plate	Seismic	UW Mod. SCBF	0.41	0.93	1.58	2.47
	HSS18	Single Diag.	HSS5x5x3/8	Gusset Plate	Seismic	UW Mod. SCBF	0.28	0.70	1.75	2.09
	HSS20	Single Diag.	HSS5x5x3/8	Gusset Plate	Seismic	AISC SCBF	0.36	0.66	1.31	1.98
	HSS21	Single Diag.	HSS5x5x3/8	Gusset Plate	Seismic	AISC SCBF	0.35	0.72	1.66	1.87
	HSS22	Single Diag.	HSS5x5x3/8	Gusset Plate	Seismic	UW Mod. SCBF	0.30	0.51	1.54	1.99
	HSS23	Single Diag.	WF6x25	Gusset Plate	Seismic	UW Mod. SCBF	0.24	0.39	1.51	2.78
	HSS24	Single Diag.	HSS5x5x3/8	Gusset Plate	Seismic	UW Mod. SCBF	0.49	0.89	1.77	2.22
	HSS25	Single Diag.	HSS5x5x3/8	Gusset Plate	Seismic	AISC SCBF	0.39	0.73	1.31	1.65
	TCBF1-1	Double Story X	HSS125x125x9 (mm)	Gusset Plate	Seismic	UW Mod. SCBF	0.44	0.85	1.70	2.19
	TCBF1-2	Double Story X	WF 175x175x9.5x11 (mm)	Gusset Plate	Seismic	UW Mod. SCBF	0.52	0.88	2.09	2.99
	TCBF1-3	Double Story X	HSS125x125x9 (mm)	Gusset Plate	Seismic	AISC SCBF	0.52	0.85	1.27	2.77
	TCBF2-1	3 Story X, Chevron	HSS5x5x3/8	Gusset Plate	Seismic	UW Mod. SCBF	0.37	0.78	1.60	2.19

	TCBF2-2	3 Story X, Chevron	WF 175x175x9.5x11 (mm)	Gusset Plate	Seismic	UW Mod. SCBF	0.34	-	0.90	2.73
Wakabayshi,Nakamura,Yoshida, 1979	SPC 3	Single Diag.	Circ. Tube 4.29x0.345 (cm)	Gusset Plate	Seismic	-	0.13	-	1.11	1.73
	DPC 1	Single Story X	Circ. Tube 4.3x0.346 (cm)	Gusset Plate	Seismic	-	0.22	-	0.81	1.00
	SAC 3	Single Diag.	2L5x5x0.381 (cm)	Gusset Plate	Compact	-	0.07	-	1.01	2.71
	DAC 2	Single Story X	2L5x5x0.381 (cm)	Gusset Plate	Compact	-	0.32	0.33	1.10	2.13
El-Tayem, Goel, X-Bracing, 1985	AW0	Single Story X	L2.5x2.5x1.4	Gusset Plate	Compact	AISC OCBF	0.18	0.70	1.44	1.48
	AW1	Single Story X	L4x4x1/4	Gusset Plate	Compact	AISC OCBF	-	0.93	1.34	2.78
	AW2	Single Story X	L4x4x3.8	Gusset Plate	Compact	AISC OCBF	-	-	1.57	2.20
	AW3	Single Story X	L2.5x2.5x5/16	Gusset Plate	Compact	AISC OCBF	0.14	1.15	-	1.75
	AW4	Single Story X	L2.5x2.5x3.16	Gusset Plate	Compact	AISC OCBF	0.32	0.95	-	1.38
Aslani and Goel, Double Angles, 1989	AB1	Single Diag	2L3.5x2.5x1/4	Gusset Plate	Compact	AISC OCBF	0.18	0.32	-	1.36
	AB2	Single Diag	2L3.5x2.5x1/4	Gusset Plate	Compact	AISC OCBF	0.18	0.49	-	1.50
	AB3	Single Diag	2L3.5x2.5x1/4	Gusset Plate	Compact	AISC OCBF	0.19	0.49	-	1.20
	AB4	Single Diag	2L3.5x2.5x3/8	Gusset Plate	Compact	AISC OCBF	0.32	0.81	-	1.58
	AB5	Single Diag	2L3.5x2.5x3/8	Gusset Plate	Compact	AISC OCBF	0.31	0.47	-	1.40
	AB6	Single Diag	2L3.5x2.5x3/8	Gusset Plate	Compact	AISC OCBF	0.31	0.46	-	1.53
	ABS7	Single Diag	2L3.5x2.5x1/4	Gusset Plate	Compact	AISC OCBF	0.32	-	-	0.73
	ABS8	Single Diag	2L3.5x2.5x1/4	Gusset Plate	Compact	AISC OCBF	-	-	-	0.36
	AB9	Single Diag	2L3x3x3/8	Gusset Plate	Compact	AISC OCBF	0.31	-	-	1.34
	AXH10	Single Diag	2L3x3x3/8 (Bulit up Box)	Gusset Plate	Compact	AISC OCBF	0.32	-	1.50	2.01
	AXH11	Single Diag	2L3x3x3/8 (Bulit up Box)	Gusset Plate	Compact	AISC OCBF	0.32	-	1.58	2.06
	AXH12	Single Diag	2L3x3x3/8 (Bulit up Box)	Gusset Plate	Compact	AISC OCBF	0.32	-	-	2.39
	AXH13	Single Diag	2L3x3x3/8 (Bulit up Box)	Gusset Plate	Compact	AISC OCBF	0.30	-	0.45	1.43
	AXH14	Single Diag	2L3x3x3/8 (Bulit up Box)	Gusset Plate	Compact	AISC OCBF	0.30	-	0.75	1.92
	AXH15	Single Diag	2L3x3x3/8 (Bulit up Box)	Gusset Plate	Compact	AISC OCBF	0.33	-	-	1.23
	AXH16	Single Diag	2L3x3x3/8 (Bulit up Box)	Gusset Plate	Compact	AISC OCBF	0.32	-	-	1.51

	AXH17	Single Diag	2L3x3x3/8 (Bulit up Box)	Gusset Plate	Compact	AISC OCBF	0.32	-	1.60	2.08
Wakabayshi,Nakamura,Yoshida, 1977	SIC 1	Single Diag	WF 5x5x0.6x0.6 (cm)	Moment	Seismic	-	0.29	-	3.00	3.69
	DIC 1	Single Story X	WF 5x5x0.6x0.6 (cm)	Moment	Seismic	-	0.25	-	2.00	3.12
	DOC 1	Single Story X	WF 5x5x0.6x0.6 (cm)	Moment	Seismic	-	0.20	-	2.00	4.25
	DOC2	Single Story X	WF 5x5x0.6x0.6 (cm)	Moment	Seismic	-	0.42	-	-	4.25
	SIC 2	Single Diag	WF 5x5x0.6x0.6 (cm)	Moment	Seismic	-	0.18	-	3.00	3.69
	SIC 3	Single Diag	WF 5x5x0.6x0.6 (cm)	Moment	Seismic	-	0.07	-	-	4.07
	SOC 1	Single Diag	WF 5x5x0.6x0.6 (cm)	Moment	Seismic	-	0.37	-	2.00	4.11
	SOC 2	Single Diag	WF 5x5x0.6x0.6 (cm)	Moment	Seismic	-	0.18	-	-	4.11
	SOC 3	Single Diag	WF 5x5x0.6x0.6 (cm)	Moment	Seismic	-	0.05	-	-	2.02
	DIC 2	Single Story X	WF 5x5x0.6x0.6 (cm)	Moment	Seismic	-	0.28	-	2.00	3.12
	DIC 3	Single Story X	WF 5x5x0.6x0.6 (cm)	Moment	Seismic	-	0.26	-	3.00	3.15
	DOC 3	Single Story X	WF 5x5x0.6x0.6 (cm)	Moment	Seismic	-	0.36	-	-	3.15
Mahin and Uriz, 2004	SCBF-1	2 Story Chevron	HSS 6x6x3/8	Gusset Plate	Seismic	AISC SCBF	0.25	-	1.00	1.00
Foutch, Goel, Roeder, 1986	6 Story SCBF	6 Story Chevron	Varying HSS Shapes	Moment	Seismic	AISC SCBF	0.41	-	-	1.64

Brace frame system tests such as illustrated in Appendix D show that CBF brace buckling and tensile yielding invariably occur at drift levels between 0.25% and 0.45%. Once brace buckling or tensile yielding occurs increased demands are placed upon the connections, and the performance of the connection is likely to be poor unless a reasonable level of seismic detailing is employed. As a result, Fig. 10 provides a fragility curve proposed for the S2-BF-1 category. This curve is based entirely upon judgment, and it is conditioned upon the requirement that the connections and all structural members are designed to the seismic strength design forces with no seismic detailing. It is also assumed that local slenderness limits are evaluated to assure that local buckling will not occur prior to developing the required design strength of the brace. No distinction is made between damage levels DS1 through DS4 in this fragility curve, because all damage levels must be expected at very similar, small deformation levels. This figure suggests that damage initiates at approximately 0.25% drift, because brace buckling is commonly noted at that drift level, and the probability of damage is approaches 100% by 0.5% story drift.

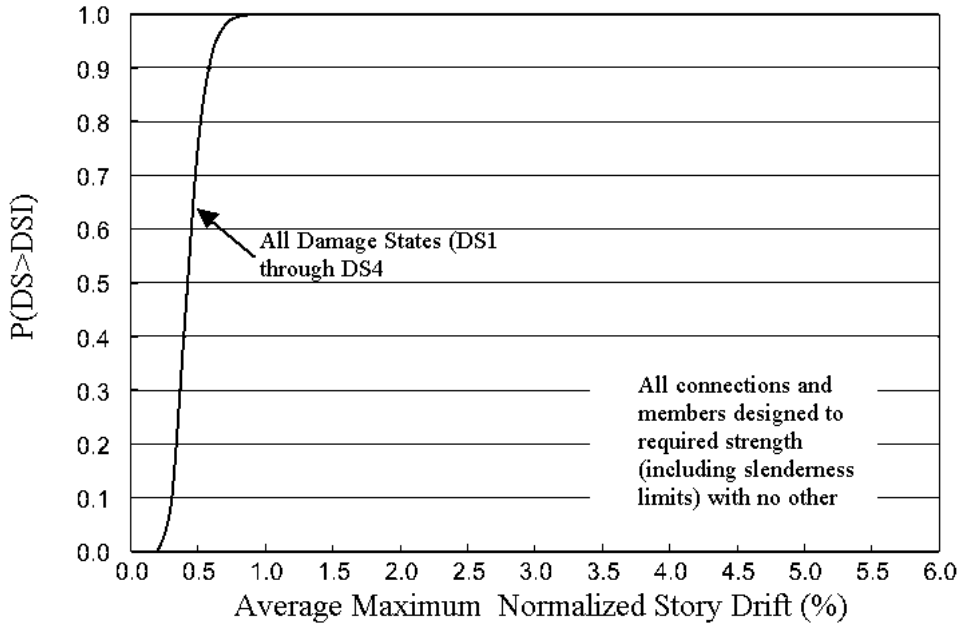

Figure 10. Fragility Curve for CBFs Designed by Strength Design with no Seismic Detailing

S2-CBF-2a and S2-CBF-2b - OCBF DESIGN WITH COMPACT BRACES

OCBF design is a relatively new concept, and it has changed significantly over its short history. Prior to approximately 1988, detailing requirements for braced frames were often illogical and counter productive. For example, braced frame design provisions prior to 1988 assumed that inelastic post-buckling and tensile yielding of the brace was the controlling yield mechanism of the frame, but these same design provisions required increased resistance of the brace beyond the seismic design forces for fear of brace buckling. As a consequence of provisions such as these, it is not possible to define the expected seismic behavior of these earlier braced frames. In 1988, this was changed somewhat when the concept of ductile behavior was more formally introduced for the CBF system. The first SCBF design requirements further advanced the concept of ductile braced

frame behavior, and OCBFs were introduced during that same period (AISC 1997). The SCBF provisions have evolved since the first AISC Seismic Design Provisions, but the OCBF design provisions have gone through a much greater evolution since that initial specification. The earliest version of the OCBF provisions were not dissimilar to the pre-1988 CBF design provisions in the Uniform Building Code (ICBO 1988), however today the OCBF provisions have evolved to something quite similar to the SCBF provisions (AISC 2005b). Today, the OCBF provisions require that connections be designed to develop the expected tensile resistance of the brace, and there are constraints on the slenderness of the brace. Nevertheless, current OCBFs are clearly less restrictive than SCBFs in that OCBFs permits:

- K-brace and several other restricted brace configurations,
- Greater latitude in balancing the resistance of braces in tension and compression so that tension only bracing is not prevented,
- Fewer restrictions on the connection design with respect to brace end rotation, connection moment resistance and connection resistance for compressive load in the brace,
- Permits the use of inverted V-brace or Chevron braced frames without considering the unbalanced force on the beam, and
- Fewer restrictions on the protected zones of braced frames.

As a consequence of the evolutionary process for OCBFs and the fundamental differences between OCBFs and SCBFs, it must be expected that the seismic performance of OCBF frames is approaching the performance of SCBF frames with recent changes in the AISC Seismic Provisions. However, it is also clear that the seismic performance of OCBFs must be inferior to that of comparable SCBF frames, but the expected performance should be quite variable, since OCBFs will approach SCBF behavior in some cases and provide little or no ductility in other cases. However, there is insufficient experimental evidence to support this observation, and there is little rational basis for developing fragility curves that reflect this broad variation possible with the OCBF system.

Figure 11 shows fragility curves that were developed from 4 test specimens in Appendix D that approximate OCBF conditions. Table 4 shows the statistical parameters for these curves. It can be seen that deformation capacity is quite variable. The test results where also extremely variable with story drifts associated with brace fracture varying between 1% and 2.7% story drift.

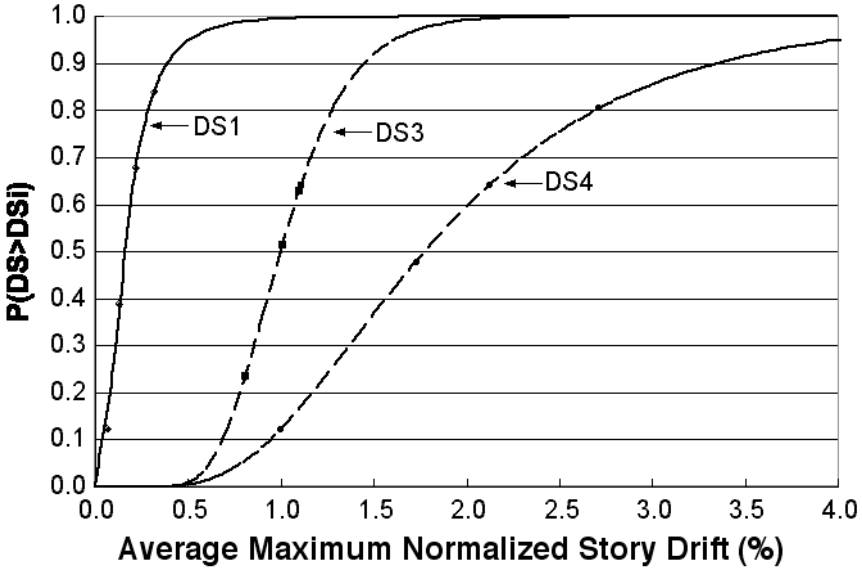

Figure 11. Fragility Curve for OCBF Frames

Table 4. Parameters for OCBF Fragility Curves

Damage State	M	β_r	β_u	θ
DS1	4	0.6604	0.25	0.159
DS3	4	0.1466	0.25	1.000
DS4	4	0.4248	0.25	1.776

S2-CBF-2c - OCBF WITH COMPACT BRACES IN K-BRACE CONFIGURATION

There are no test data for CBFs with braces in the K-brace configuration, and there is no sound basis for developing precise fragility curves for this application. However, there is a clear basis for understanding the behavior that will occur with this bracing configuration. Inverted V- or chevron-bracing has been evaluated in 4 of the 69 test frames. Inverted V- or chevron-bracing develops a very large unbalanced force in the beam after brace buckling occurs. This occurs because the tensile yield capacity of the brace is significantly larger than the compressive buckling capacity of the brace. In current SCBF design provisions, the beam must be designed to have the flexural capacity to resist this unbalanced load. K-braced frames will have similar problem, but the unbalanced brace forces will be acting on the column of the frame. One of the 4 inverted V-braced frames included in Appendix D database had beams, which were not designed to resist this unbalanced force. This one test frame developed beam deflections in the order of several inches with a maximum story drift of 1.9%. Similar deflections must be expected in the

columns of K-braced frames. The beam deflection is somewhat beneficial for inverted V-braced frames, because flexural yielding of the beam provides substantial energy dissipation, and causes no loss of stability of the structure. However, yield deflections in the columns of K-braced frames will result in a dramatic reduction in the stability of the column because of the large axial forces and the P-δ moments induced by column deflection. Column failure is clearly a potentially disastrous failure mode, which has consequences that are much more severe than the normal brace fracture noted with other brace systems.

As a result, the seismic performance of an OCBF frame with K-braced configuration must have a significant reduction in the deformation capacity associated with DS2, DS3, and DS4 damage states. Figure 11 represents the seismic performance for OCBF frames. The performance is quite variable, but OCBF frames with K-bracing will clearly have significantly less deformation capacity than most other OCBF systems. Figure 10 is regarded as a possible fragility curve for a frame that is designed by strength design with no ductile detailing, and it offers a lower bound to expected K-brace performance. It is logical to expect that K-braced OCBFs will be closer to Fig. 10 than Fig. 11, but more accurate assessment of this performance is not possible without experimental data to better establish system performance.

S2-CBF-3a - SCBF DESIGNS IN GENERAL

Significantly more data exists for SCBFs than OCBFs. However, there is still wide variability in the parameters of the test data. Fragility curves for SCBF frames with rectangular HSS braces which were designed to minimum SCBF standards with no additional design constraints are shown in Fig. 12. The data supporting this fragility curve includes 12 SCBF frames and all of those frames were designed with HSS rectangular tube braces. While 12 specimens are included in this data set, a slightly smaller number of tests were used to develop the fragility curves for damage states DS2 and DS3, because the initiation of these intermediate damage states were not clearly identified in some research studies. Table 5 defines the parameters for these general fragility curves. The quality of the curves is good, and they easily passed the goodness of fit test with the experimental data. It should be noted that much wide scatter results if all brace cross sections are included in this figure, and so other brace cross sections are discussed separately in this report.

While Fig. 12 provides information regarding the general seismic performance of SCBF frames, a subset of the data shows that improved performance can be achieved with additional design constraints. The above data includes SCBFs with HSS rectangular tube braces that are designed to minimum SCBF standards with both rectangular and taper gusset plates. Figure 13 and Table 6 provide a subset of the data including only gusset plates designed with tapered gusset plate connections. These tapered gussets are designed to achieve a greater level of connection deformability and flexibility, since the are somewhat more restrictive than the current SCBF criteria, while still being consistent with current procedures. A total of 6 tests are included in this data set.

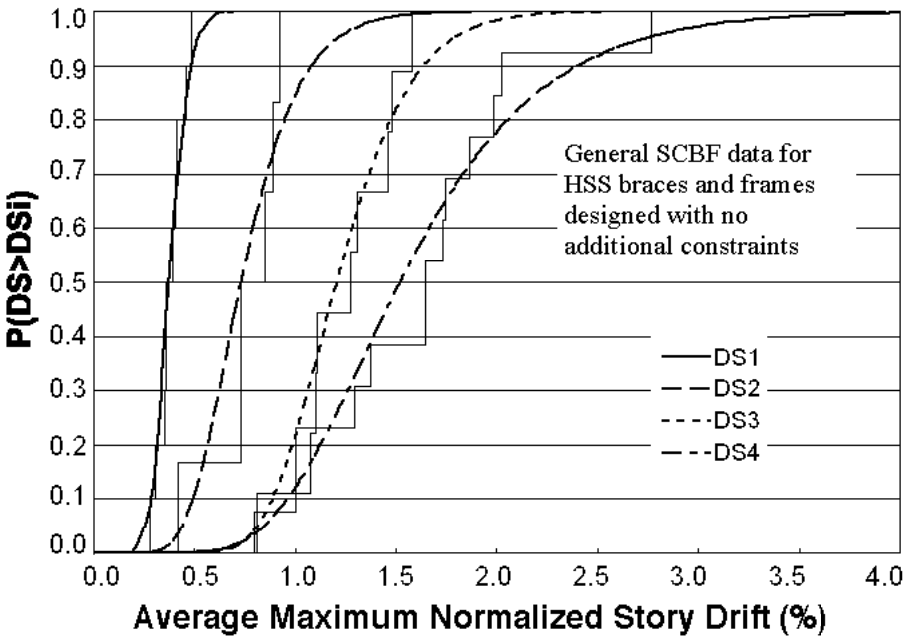

Figure 12. General Fragility Curves for SCBFs Designed to Minimum Standards

Table 5. Parameters for General Fragility Curves

Damage State	M	β_r	β_u	θ
DS1	10	0.1694	0.1	0.377
DS2	6	0.2880	0.1	0.735
DS3	9	0.2383	0.1	1.209
DS4	13	0.3417	0.1	1.524

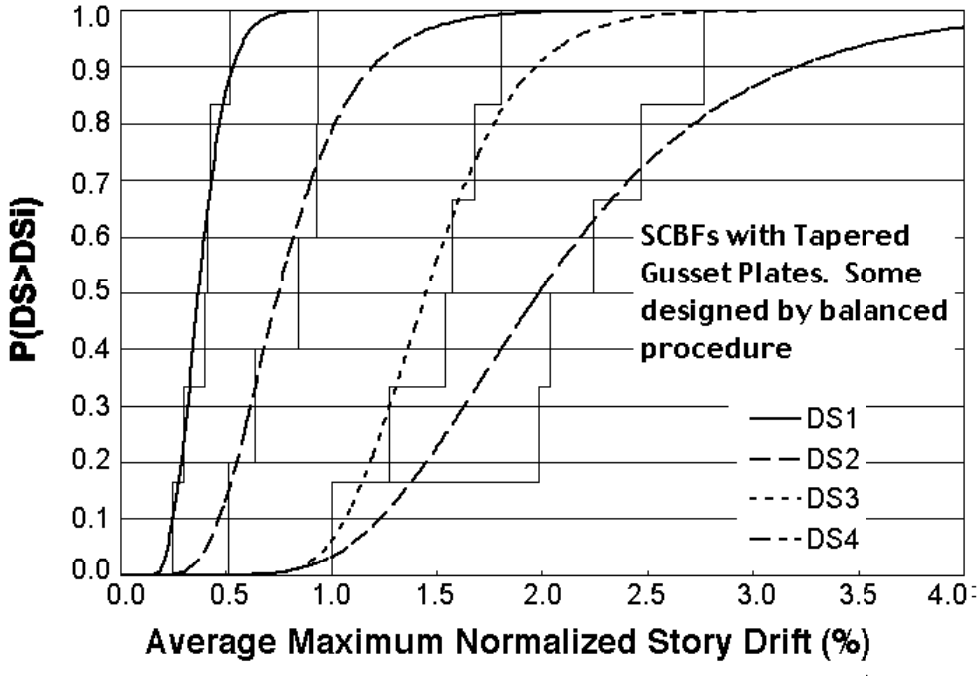

Figure 13. General Fragility Curves for SCBFs Designed to Minimum Standards and Having Tapered Gusset Plates

Table 6. Parameters for General SCBF Fragility Curves With Tapered Gusset Plates

Damage State	M	β_r	β_u	θ
DS1	6	0.2637	0.1	0.373
DS2	5	0.2642	0.1	0.753
DS3	6	0.216	0.1	1.452
DS4	6	0.358	0.1	1.989

Comparison of Figs. 12 and 13 show that improved performance is possible with changes in the connection design, since the SCBR HSS braces provide somewhat greater inelastic deformation capacity with tapered gussets than with general SCBF design.

S2-CBF-3b - SCBF DESIGN WITH HSS BRACING MEMBERS

Since Figs. 12 and 13 include only test data for tests with HSS rectangular tubes, the data from these figures and Tables 5 and 6 also applies to the S2-CBF-3b subcategory, when the frames are designed to minimum SCBF design requirements. However, recent research has shown that improved performance can be achieved from SCBF frames when additional constraints are applied to the gusset plate connection design (Lehman et al. 2008). These

benefits are particularly apparent for frames with rectangular gusset plate connections, because the improved design procedures bring the connection behaviors for tapered and rectangular gusset plates closer together. These additional requirements include:

- Use of a balanced design procedure to assure that the gusset plate has adequate strength and stiffness to develop the expected capacity of the brace but little excess capacity (Lehman et al. 2008, Roeder et al. 2009b). This assures that assures that the gusset plate is not overly stiff and strong, because excess gusset plate stiffness and resistance forces early fracture of the brace.

- Welds joining the gusset plate to the bean column framing members are designed to achieve the plastic capacity of the gusset plate rather than the expected capacity of the brace.

- Use of the elliptical clearance model to assure that the gusset plate is as compact and thin as possible, because thinner, more compact gussets reduce the inelastic deformation to structural framing members and enhance the ductility of the brace.

Fourteen braced frame tests with rectangular gusset plates, HSS rectangular tube braces, and this modified design procedure have been completed. There is still considerable variation within these acceptable design criteria since some both bolted and welded connections and variations in the beam-column connection are employed. Figure 14 shows the resulting fragility curves from this data, and Table 7 provides the parameters for these curves.

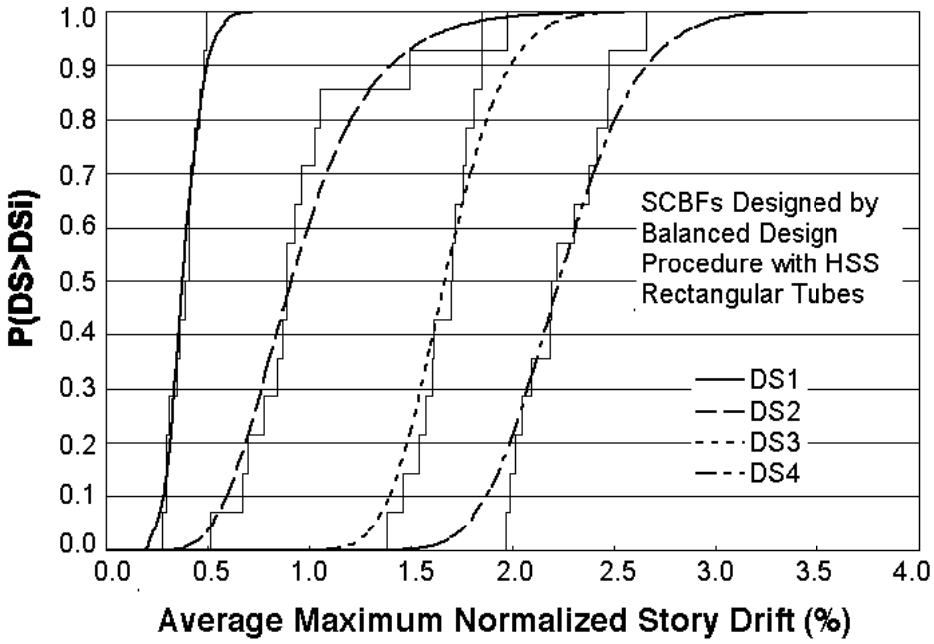

Figure 14. General Fragility Curves for SCBFs Having Rectangular Gusset Plates and Designed with Improved Balanced Design Procedure

Table 7. Parameters for General SCBF Fragility Curves With Rectangular Gusset Plates and Improved Balanced Design Procedure

Damage State	M	β_r	β_u	θ
DS1	14	0.1878	0.1	0.3804
DS2	14	0.3174	0.1	0.9152
DS3	14	0.0962	0.1	1.668
DS4	14	0.0939	0.1	2.2331

Comparison of Fig. 14 with Fig. 12 shows that the improved design procedure results in a significant improvement in the seismic performance of rectangular gusset plates. Initial buckling and yielding of the brace occurs at very similar deformation levels, but higher damage states and ultimate brace fracture occur at significantly larger drift levels with the modified design procedure. Comparison of Figs. 14 and 13 is not a completely valid comparison, because tapered and rectangular gussets have been shown to be fundamentally different, however, the comparison shows that rectangular gussets designed by the balanced design procedure develop slightly better performance that achieved with tapered gussets. The mean deformation capacity is larger and the statistical variation is smaller for the improved design procedure with rectangular gusset plates than the basic SCBF design with tapered gusset plates.

SCBFs WITH OTHER BRACE CROSS SECTIONS

It is well known that HSS rectangular tube braces fracture are susceptible to early brace fracture because of the localization of damage as discussed earlier and illustrated in Fig. 5 . This is known from cyclic load tests of braces as well as braced frame system tests. Subcategory S2-CBF-2b was to address different brace cross sections, but the target was OCBF frames. Limited test data is available on CBF systems with different brace cross sections, but all of the test specimens are to standards closer to SCBF design requirements than OCBF standards. As a result, they are discussed here as SCBF systems.

Three system tests address the seismic performance of SCBFs with wide flange braces. Cyclic brace testing as summarized in Appendix B show that wide flange braces can develop larger cyclic inelastic deformations than HSS rectangular tube braces, and the 3 wide frame system tests support this observation. However, CBF system tests may show smaller benefits than brace tests, because the greater ductility of the brace places greater demands on the connections and other elements of the structural system. Comparison of Fig. 15 to Figs. 12 through 14 document this increased deformation capacity, but the benefit is not as great as suggested by brace component tests as can be observed by comparing RHS19 and W4 in Fig. 4. Table 8 provides the statistical parameters of the curve. However, the limited number of tests result in a large deviation and flat slope of the fragility curve.

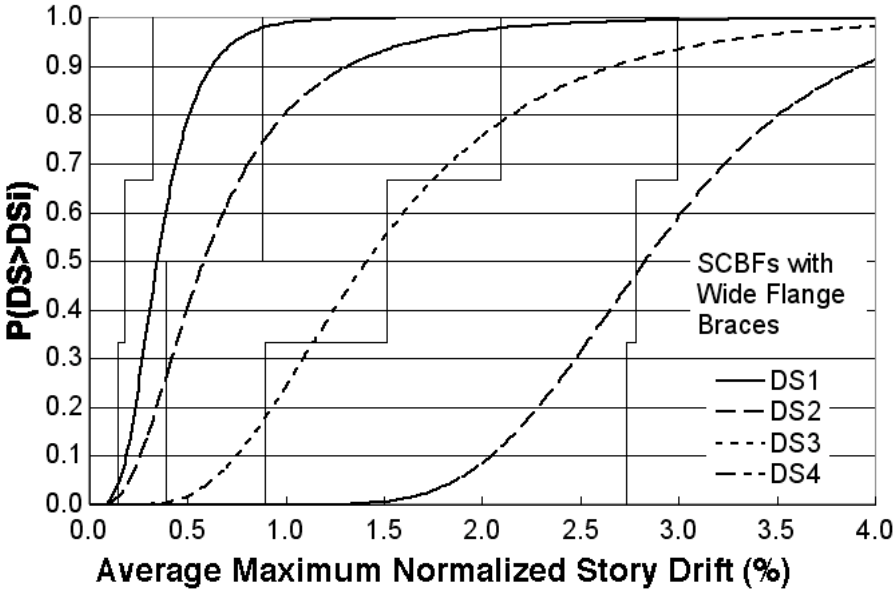

Figure 15. Fragility Curves for SCBFs with Wide Flange Braces

Table 8. Parameters for SCBF Fragility Curves With Wide Flange Braces

Damage State	M	β_r	β_u	θ
DS1	3	0.3879	0.25	0.346
DS2	3	0.5781	0.25	0.584
DS3	3	0.4271	0.25	1.415
DS4	3	0.0478	0.25	2.832

Nine system tests in Appendix D include double angle braces, and fragility curves also were developed for these systems. Figure 16 shows the fragility curves for these double braced frames, and Table 9 provides the statistical variables for these curves. While double angles are open sections and are less susceptible to the localization of damage noted with HSS rectangular tubes, the ductility achieved in these tests are significantly smaller than achieved with HSS tubes as shown by comparison of Figs. 12, 13, and 14 with Fig. 16. The tests used to develop Fig. 16 are not recent, and there is insufficient information to generate fragility curves for DS3 damage state. The age of these tests may be an issue of concern, in that there is considerable scatter in the data, and deformation capacity is significantly smaller than may be expected based upon individual brace tests. Most of these tests are also marginal when compared to current local slenderness limits. As a result, somewhat more generous fragility curves may be possible with an increased test database.

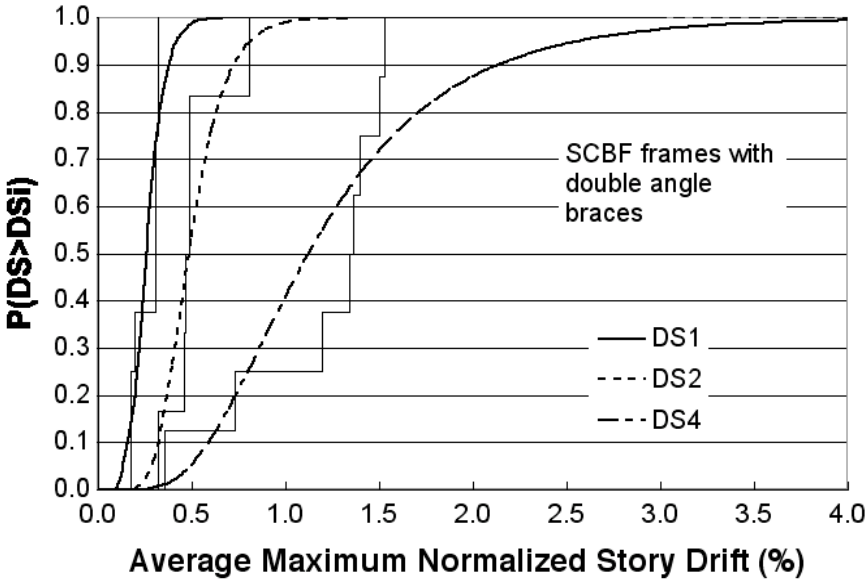

Figure 16. Fragility Curves for SCBFs with Double Angle Braces

Table 9. Parameters for SCBF Fragility Curves With Double Angle Braces

Damage State	M	β_r	β_u	θ
DS1	8	0.2827	0.1	0.256
DS2	6	0.2970	0.1	0.485
DS4	9	0.4897	0.1	1.124

S2-CBF-3c - SCBF DESIGN WITH CHEVRON BRACING CONFIGURATION

Only 4 of the 69 tests included in Appendix D have inverted V- or chevron bracing. Of those 4 specimens, only 2 are tested to deformations achieving the DS4 damage state. The other two specimens had chevron bracing in one story, and brace buckling occurred, but DS3 and DS4 damage occurred in other stories with different bracing configurations. As a result, there is insufficient data to support development of fragility curves for this bracing configuration. However, two tests were completed and provide reasonable documentation for DS1 and DS4 damage states. Neither of these tests provides the documentation needed to establish the DS2 and DS3 damage states. Two tests are too limited to permit development of a fragility curve, but the range of DS1 and DS4 damage is plotted in Fig. 17. These ranges are plotted on the DS1 and DS4 fragility curves for HSS rectangular tubes designed to current AISC SCBF provisions as illustrated in Fig. 12. This comparison is quite appropriate since the two chevron braced frames also HSS rectangular braces.

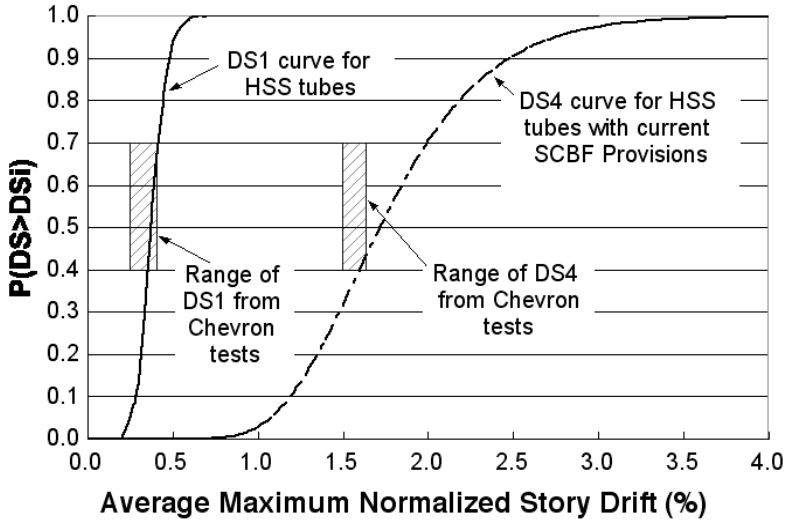

Figure 17. Range of DS1 and DS4 Damage in Chevron Braced Frames Relative to Other HSS Rectangular Braced Frames

While there is insufficient data to generate a fragility curve for specific case of chevron bracing, the comparison of Fig. 17 suggests that the fragility curves with this brace configuration are similar to those provided for HSS rectangular tube braces designed to meet current SCBF provisions in Fig. 12. This is interesting because the behavior exhibited by the two chevron braced frames are somewhat different from one another. The least ductile test frame had a strong beam as required to resist the unbalanced forces in the current AISC Seismic Design Provisions. The more ductile frame was designed to standards comparable to earlier SCBF provisions, and significant beam yielding occurred. Further, the brace in the weak beam system had greater local slenderness than the tubes in the other specimen, and thus the more slender tube would be expected to fail at smaller story drift. First, it is interesting that the chevron with weaker beam and more slender brace produced the greater ductility, and yet both systems had similar failure modes. This shows that some of the current SCBF design provisions have been developed with little experimental documentation of their effect on the performance of the frame. As a result, the performance achieved with these provisions may be less desirable than anticipated. Second, it is also interesting that both specimens fit within the lower band of the normal current HSS brace performance.

S2-CBF-3d - SCBF DESIGN WITH X-BRACE CONFIGURATION

Eleven tests results are available for X-braced frames as shown in Appendix D. However, only 5 of these test results are useful for developing fragility curves for engineering practice. Further, all 5 tests provide insight into the DS4 damage state, but the documentation of data is inadequate to define initiation of all damage states for all specimens. The other 6 specimens were early tests completed by Wakabayashi (1967), and they are of very small scale. These early tests by Wakabayashi are designed to obtain a basic understanding braced frame behavior, and they are inappropriate for determining realistic structural behavior. Figure 18 is the fragility curves developed based upon the 5 usable tests. Table 10 provides the statistical data that describes the fragility curves.

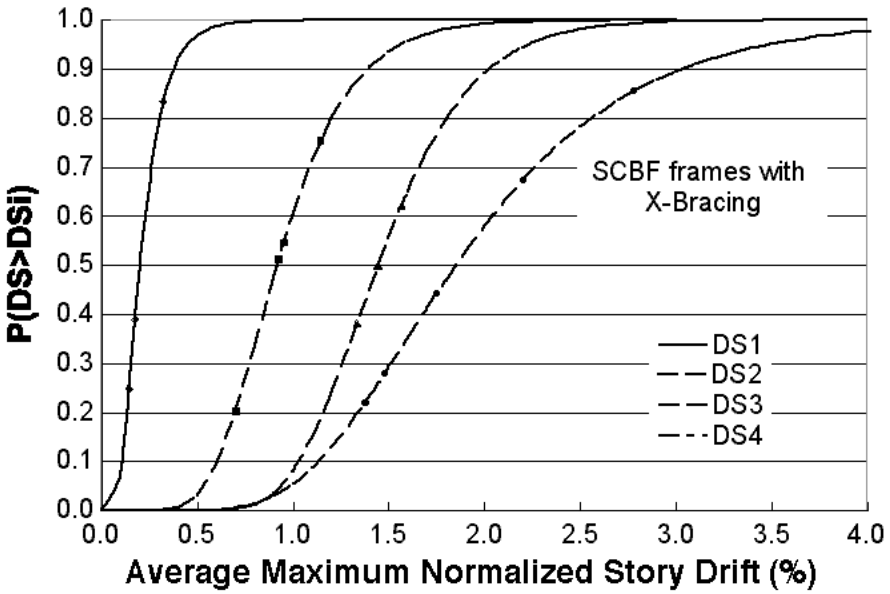

Figure 18. Fragility Curves for SCBFs with Double Angle Braces

Table 10. Parameters for SCBF Fragility Curves With X-Bracing

Damage State	M	β_r	β_u	θ
DS1	3	0.414	0.25	0.226
DS2	3	0.489	0.25	0.748
DS3	4	0.0803	0.25	1.446
DS4	6	0.265	0.25	1.854

S2-CBF-3e - SCBF DESIGN WITH MOMENT RESISTING BRACE CONNECTIONS

Thirteen of the 69 braced frame systems described in Appendix D have welded moment resisting brace connections. However, 12 of those tests were again part of the early Wakabayashi test series. These were again very small scale specimens. Small scale specimens have proportionally smaller local strains when a given story drift is applied, and hence the deformation associated with initiation of a given damage state (with the exception of DS1) is proportionally larger for these small scale specimens. Hence, their performance is not meaningful in evaluating the performance of full size structures. It is not possible to develop a rational fragility curve from a single data point, and so no fragility curves are presented for this case.

ACCURACY AND RELIABILTIY OF FRAGILITY CURVES

This chapter has presented fragility curves for various CBF systems and the 4 proposed damage states. The curves must be applied on a story by story basis using the average maximum normalized story drift for each story as the engineering demand parameter. Chapter 3 provides information on factors affecting CBF performance, and the inherent limitations in the accuracy and reliability of fragility curves in predicting CBF system performance. This section attempts to reiterate the importance of employing care and caution when using these fragility curves. It is recognized that different brace configurations are likely to have different damage levels at given frame deformations. However, there is very limited experimental data with the variations in brace configuration needed to develop fragility curves for these different configurations. There are a number of tests for the X-braced frames, but the tests themselves are less accurate simulations of frame behavior than most tests in the database. As a result, Fig. 17 and 18 are viewed as very approximate indicators of system behavior.

Figures 12, 13, and 14 are fragility curves for braced frame with rectangular HSS braces and various SCBF design alternatives. The data behind these fragility curves is quite good and the tests generally are good simulations of CBF systems. As a result, these curves are viewed high quality and generally good representations of system performance. However, comparison of Figs. 12, 13, and 14 show that relatively small changes in design may result in significant changes in system performance. As a result, it is important to assure that a given structure truly fits the category in question and to understand the effect of changes in the design on the system performance. Nevertheless, these figures are the best indicators of SCBF performance available with current data.

Figures 15 and 16 present fragility curves for CBFs with wide flange and double angle braces. Chapter 3 clearly shows that different brace cross-section will result in changes in seismic performance of the system. Comparison of Fig. 15 to Fig. 13 shows a significant increase in deformation capacity with the wide flange braces compared with rectangular HSS tube braces for the DS3 and DS4 damage states. Tests on individual braces strongly support this observation. Figure 15 is based upon a very small experimental database, however the quality of the data for these tests is very good. As a result, there is relatively high confidence in the fragility curves of Fig. 15, but the variance is quite large because of the limited number of test results. It is expected that additional test data would significantly reduce the variance but retain a similar mean for SCBF frames with wide flange braces. There are a larger number of tests for the double angle CBFs in Fig. 16. Comparison of Fig. 16 to Fig. 13 suggests that double angle braces sustain greater damage than rectangular HSS tubular braces. The quantity of data suggests that this observation may be correct. However, the specific data behind Fig. 16 is somewhat distorted by local failure modes and this fragility curve should be used with caution.

Finally, Figs. 10 and 11 present fragility curves for R=3 and OCBF designs. The general trends of these two curves as they compare to SCBF designs in Figs. 12 and 13 are thought to be valid and correct. However, there is no experimental data available to support Fig. 10, and very little data to support Fig. 11. Hence, while the general placement of these fragility curves are thought to be accurate, the specific curves are approximate and likely to change with additional test data.

USING THESE FRAGILITY CURVES

The fragility curves presented in this report are based upon the average maximum normalized story drift ($\Delta_{range,max}/2h$), and ideally these curves should be compared to the computed average maximum normalized story drift for each for to predict the expected performance of the braced frame at that story level. However, for most earthquake acceleration records, the peak story drift is not very different from the average maximum normalized story drift value. The computed peak story drift is always larger than the average maximum normalized story drift, and it is easier to compute. As a result, it is generally conservative and easier to use computed peak story drift for predicting the expected performance of the braced frame at each story level. However, some acceleration records (particularly some near fault records) cause very one sided dynamic response, which produce much larger story drifts in one direction than the other. For these records, it is overly conservative to use computed peak story drift, and the computed average maximum normalized story drift as defined in Eq. should be used. This can be compute by:

$$\Delta_{range,max} = \Delta_{tens,max} - \Delta_{comp,max} \quad \text{(Eq 1a)}$$

so that

$$\text{Average Maximum Normalized Drift} = \frac{\Delta_{range,max}}{2h}. \quad \text{(Eq 1b)}$$

CHAPTER 5 Closing Comments

This report has presented the available experimental data for the seismic performance of concentrically braced frames. The data includes 69 braced frame system tests described in some detail in Appendix D, and a much larger number of brace and gusset plate tests summarized in Appendix B and C. The data is used to develop fragility curves for a number of different brace cross-section shapes and brace configuration combinations. There are clear limitations with these curves, because of limitations of the test data and the fit of the test data to the desired structural system. Clearly a much larger body of experimental research is needed to properly define fragility curves for many of the desired applications.

Appendix A References

AISC (1997) "Seismic Provisions for Structural Steel Buildings," First Edition, American Institute of Steel Construction, Chicago, IL.

AISC (2005a) "Manual of Steel Construction, Load and Resistance Factor Design," 3rd Edition, American Institute of Steel Construction, Chicago, IL.

AISC (2005). "Seismic Provisions for Structural Steel Buildings," ANSI/AISC Standard 341-05, American Institute of Steel Construction, Chicago, IL.

Aslani, F., and Goel, S.C., (1989). "Experimental and Analytical Study of the Inelastic Behavior of Double Angle Bracing Members Under Severe Cyclic Loading," Research Report UMCE 89-5, Department of Civil Engineering, University of Michigan, Ann Arbor, MI.

Astaneh-Asl, A., (1989) " Simple Methods for Design of Steel Gusset Plates," Proceedings ASCE Structures Conference, San Francisco, CA.

Astaneh-Asl, A., Goel, S.C., and Hanson, R.D., (1982) "Cyclic Behavior of Double Angle Bracing Members with End Gusset Plates," Research Report UMEE 82R7, Department of Civil Engineering, University of Michigan, Ann Arbor, MI.

Balendra, T., Lim, E.L., and Liaw, C.Y. (1997) "Large-scale seismic testing of knee-brace-frame," ASCE, Journal of Structural Engineering, Vol. 123, No. 1, pgs 11-19.

Bjorhovde, R., and Chakrabarti, S.K., (1985) "Test of Full Size Gusset Plate Connections," ASCE, *Journal of Structural Engineering*, Vol 111, No. 3, pg 667-84.

Black, R.G., Wenger, W.A., and Popov, E.P. (1980) "Inelastic Buckling of Steel Struts Under Cyclic Load Reversals," EERC Report 80/40, College of Engineering, University of California, Berkeley, CA.

Brown, V.L.S., (1988) " Stability of Gusseted Connections in Steel Structures," A thesis submitted in partial fulfillment of Doctor of Philosophy in Civil Engineering, University of Delaware.

Cheng, J.J.R, Yam, M.C.H., and Hu, S.Z, (1994) "Elastic Buckling Strength of Gusset Plate Connections," Journal of Structural Engineering, Vol. 120, No. 2,

Clark, Kelly (2009 projected) "Experimental Performance of Multi-Story X-braced SCBF Systems," a thesis submitted in partial fulfillment of the Master of Science in Civil Engineering Degree, University of Washington.

Connor, J.J., Wada, A., Iwata, M., and Huang, Y.H., (1997) " Damage-Controlled Structuresl I: Preliminary Design Methodology for Seismically Active Regions," ASCE, Journal of Structural Engineering, Vol. 123, No. 4, pgs 423-31.

DiSarno, L., and Elnashai, A.S., (2009) "Bracing Systems for Seismic Retrofitting of Steel Frames," Elsevier, *Journal of Constructional Steel Research*, Vol 65, No 2, pgs 452-65.

Fell, B.V., Myers, A.T., Deierlein, G.G., and Kanvinde, A.M., (2006) "Testing and Simulation of Ultra-Low Cycle Fatigue and Fracture in Steel Braces," *Proceedings*, Paper 587, 8th US Conference on Earthquake Engineering, April 18-22, 2006, San Francisco, CA.

Filiatrault, A., and Tremblay, R., (1998) "Design of Tension-Only Concentrically Braced Steel Frames for Seismic Induced Impact Loading," Elsevier, *Engineering Structures*, Vol 20, No. 12, pgs 1087-96.

Foutch, D.A., Goel, S.C. and Roeder, C.W., (1987) Seismic testing of a full scale steel building - Part I, *Journal of Structural Division*, ASCE, No. ST11, Vol. 113, New York, pgs 2111-29.

Ghanaat, Y., and Clough, R.W. (1982) "Shaking Table Tests of a Tubular Steel Frame Model," EERC Report 82/02, College of Engineering, University of California, Berkeley, CA.

Ghanaat, Y. (1980) "Study of X-Braced Steel Frame Structures Under Earthquake Simulation, EERC Report 80/08, College of Engineering, University of California, Berkeley, CA.

Goel, S.C. (1992). "Earthquake Resistant Design of Ductile Braced Steel Structures," Stability and Ductility of Steel Structures Under Cyclic Loading, edited by Y. Fukumoto and G.C. Lee, CRC Press, Boca Raton, Florida.

Grondin, G.Y, Nast, T.E., and Cheng, J.J.R., (2000) " Strength and Stability of Corner Gusset Plates Under Cyclic Loading, Proceedings of Annual Technical Session and Meeting, Structural Stability Research Council.

Herman, D. (2006) “Further Improvements on and Understanding of SCBF Systems”, a thesis submitted in partial fulfillment of the requirements of the MSCE, University of Washington, 2006.

Hu, S.Z., and Cheng, J.J.R., (1987) "Compressive Behavior of Gusset Plate Connections," Structural Engineering Report No. 153, University of Alberta, Canada.

ICBO (1988). "Uniform Building Code," International Conference of Building Officials, Whittier, CA.

Ikeda, K., and Mahin, S., (1986) "Cyclic Response of Steel Braces," ASCE, Journal of Structural Engineering, Vol 112, No. 2, pgs 342-361.

Inoue, K., Sawaizumi, S., and Higashibata, Y., "Stiffening Requirements for Unbonded Braces Encased in Concrete Panels, ASCE, Journal of Structural Engineering, Vol 127, No.6, pgs 712-19.

Itani. A.M., and Dietrich, A.M., (1999). "Cyclic Behavior of Double Gusset Plate Connections, " Report CCEER 98-7, Center for Civil Engineering Research, University of Nevada, Reno, Nevada.

Johnson, S. (2005) “Improved Seismic Performance of Special Concentrically Braced Frames”, a thesis submitted in partial fulfillment of the requirements of the MSCE, University of Washington, 2005.

Kahn, L.F., and Hanson, R.D., (1976). "Inelastic Cycles of Axially Loaded Steel Members," Journal of Structural Division, ASCE, No. ST5, Vol. 102, pgs 947-59.

Kotulka, B.A., (2007) "Analysis for a Design Guide on Gusset Plates used in Special Concentrically Braced Frames, a thesis submitted in partial fulfillment of the requirements of the MSCE, University of Washington, 2007.

Lee, S., and Goel, S.C., (1987). "Seismic Behavior of Hollow and Concrete Filled Square Tubular Bracing Members," Research Report UMCE 87-11, Department of Civil Engineering, University of Michigan, Ann Arbor, MI.

Leon, R., Yang, C.S., Reinhorn, A., Schachter, M., Stojadinovic, B., Yang, T., Shing, B., and Wei, Z., "Results of Early Collaborative Research on Behavior of Braced Steel Frames with Innovative Bracing Schemes (Zipper Frames),"

Lehman, D.E., Roeder, C.W., Herman, D., Johnson, S., and Kotulka, B., (2008) "Improved Seismic Performance of Gusset Plate Connections," ASCE, *Journal of Structural Engineering*, Vol.134, No. 6, Reston, VA, pgs 890-901

Lumpkin, Eric (2009 projected) "The Seismic Response of a Three-Story Special Concentric Braced Frame with Emphasis on Middle Gusset Plate Performance and System Fragility," a thesis submitted in partial fulfillment of the Master of Science in Civil Engineering Degree, University of Washington

Popov, E.P. Takanashi, K., and Roeder, C.W. (1976) Structural Steel Bracing Systems, EERC Reprot 76-17, University of California, Berkeley, 1976

Porter, K., Hamburger, R., and Kennedy, R., "Practical Development and Application of Fragility Functions,"

Porter, K., Kennedy, R., and Bachman, R.E., (2006) "Developing Fragility Functions for Building Components for ATC-58," Applied Technology Council, Redwood City, CA.

Powell, Jacob (2009 projected) "," a thesis submitted in partial fulfillment of the Master of Science in Civil Engineering Degree, University of Washington

Rabinovitch, J.S., and Cheng, J.J.R. (1993) "Cyclic Behavior of Steel Gusset Plate Connections," Structural Engineering Report No. 191, University of Alberta, Canada.

Roeder, C.W., and Lehman, D.E., (2009a) Unpublished University of Washington Test Data on Braced Frame Connections, available on NEES Database.

Roeder, C.W., and Lehman, D.E., (2009b) "Performance and Behavior of Gusset Plate Connections,"AISC NASSC, Phoenix, Arizona, April 1-4, 2009.

Shibata, M., and Wakabayashi, M., (1984) "Hysteretic Behavior of K-Type Braced Frame," Proceedings of 8th World Conference on Earthquake Engineering, San Francisco, CA, Vol VI, pgs 201-8.

Shibata, M., Nakamura, T., Yoshida, N., Morino, S., Nonaka, T., and Wakabayashi, M. (1974) "Elastic-Plastic Behavior of Steel Braces Under Repeated Axial Loading," Proceedings, 5th World Conference on Earthquake Engineering, Rome, Italy, Vol. 1, pgs 845-47.

Swanson,J., Leon, R.D., and Smallridge, J., (2000). "Tests on Bolted Connections", Report SAC/BD-00/04, SAC Joint Venture, 555 University Ave, Suite 126, Sacramento, CA.

Thornton, W.A., (1991) "On the Analysis and Design of Bracing Connections," AISC, *Proceedings of National Steel Construction Conference*, Section 26, pgs 1-33.

Tremblay, R., and Filiatrault, A., (1996) "Seismic Impact Loading in Inelastic Tension-Only Concentrically Braced Steel Frames Myth or Reality," John Wiley, *Earthquake Engineering and Structural Dynamics*, Vol 25, pgs 1373-89.

Tremblay, R., Haddad, M., Martinez, G., Richard, J., and Moffatt, K. (2008) "Inelastic Cyclic Testing of Large Size Steel Bracing Members," 14th World Conference on Earthquake Engineering, October 12-17, 2008, Beijing, China.

Tremblay, R. (2002) "Inelastic Seismic Response of Steel Bracing Members," Elsevier, *Journal of Constructional Steel Research*, Vol. 58, pgs 665-701.

Tsai, K.C., (2003) Test results obtainable from the website, "http://cft-brbf.ncree.gov.tw/fs.html", for the National Center for Research in Earthquake Engineering, Taipei, Taiwan.

Uang, C.M, and Bertero, V.V. (1986) "Earthquake Simulation Tests and Associated Studies of a 0.3-Scale Model of a Six-Story Concentrically Braced Steel Structure," EERC Report 86/10, College of Engineering, University of California, Berkeley, CA.

Uriz, P., and Mahin, S., (2004) "Summary of Test Results for UC Berkeley Special Concentric Braced Frame Specimen No. 1. (SCBF-1)," summary report from Dept. of Civil Engineering, University of California, Berkeley, CA.

Wakabayashi, M. (1980) "Experimental Studies of Braced Steel Frame," Bulletin of the Disaster Prevention Research Institute, Kyoto University, 1980, v 29, pt 4.

Wakabayashi, M., and Tsuji, B., (1967) "Experimental Investigation on the Behavior of Frames with and without Bracing under Horizontal Loading," *Bulletin Disaster Prevention Research Institute,* Kyoto University, Japan, Vol 16, Part 2, No. 112, 1967.

Wakabayashi, M., Matsui, C., Minami, K, and Mitani, I. (1974) "Inelastic Behavior of Full-Scale Steel Frames with and without Bracing," *Bulletin Disaster Prevention Research Institute,* Kyoto University, Japan, Vol 24, Part 1, No. 216, 1974

Wakabayashi, M., Nakamura, T, and Yoshida, N. (1980) " Experimental Studies on the Elastic-Plastic Behavior of Braced Frames Under Repeated Horizontal Loading - Experiments of Braces Composed of Steel Circular Tubes, Angle-Shapes, Flat Bars or Round Bars," Bulletin of the Disaster Prevention Research Institute, Kyoto University, 1980, v 29, pt 4, p 99-127

Wakabayashi, M., Nakamura, T, and Yoshida, N. (1980) " Experimental Studies on the Elastic-Plastic Behavior of Braced Frames Under Repeated Horizontal Loading - 3. Experiments of One

Story-One Bay Braced Frames," Bulletin of the Disaster Prevention Research Institute, Kyoto University, 1980, v 29, pt 4, p 143-164.

Whittaker, A.S., Uang, C.M., and Bertero, V.V., (1987) "Earthquake Simulation Tests and Associated Studies of a 0.3-Scale Model of a Six-Story Eccentrically Braced Steel Structure," EERC Report 87/02, College of Engineering, University of California, Berkeley, CA.

Whittaker, A.S., Uang, C.M., and Bertero, V.V., (1988) "An Experimental Study of the Behavior of Dual Steel Systems," EERC Report 88/14, College of Engineering, University of California, Berkeley, CA.

Whitmore, R.E., (1950) "Experimental Investigation of Stresses in Gusset Plates," a thesis submitted in partial fulfillment of the Master of Science Degree at the University of Tennessee, Knoxville, Tennessee.

Yam, M.C.H., (1994) " Compressive Behavior and Strength of Steel Gusset Plate Connections," a thesis submitted in partial fulfillment of Doctor of Philosophy degree, University of Alberta, Canada.

Yam, M.C.H., and Cheng, J.J.R., (2002) "Behavior and Design of Gusset Plate Connections in Compression," *Journal of Constructional Steel Research*, Vol 58, No. 5-8, Elsevier, pgs 1143-59.

Yang, C.S., Leon, R.T., and DesRoches, R., (2008) "Design and Behavior of Zipper-Braced Frames, Elsevier, Engineering Structures, Vol. 30, pgs 1092-1100.

Zayas, V.A., Mahin, S.A., and Popov, E.P. (1980) "Cyclic Inelastic Behavior of Steel Offshore Structures," EERC Report 80/27, College of Engineering, University of California, Berkeley, CA.

Zayas, V.A., Popov, E.P, and Mahin, S.A. (1980) "Cyclic Inelastic Buckling of Tubular Steel Braces," EERC Report 80/16, College of Engineering, University of California, Berkeley, CA.

Appendix B

Summary of Test Data for Brace Tests

Researcher	Spec ID	Loading History	Failure Mode	Pcr/Py or Rn/Py by AISC	Meas. Pcr/Py for 1st Circle	Meas. Pcr/Py for 2nd Circle	Meas Pcr/Py for 10th Circle	Max Tensile Load/Py	Location & Quantity of Plastic Hinges
Astaneh-Asl (1982)[1]	AB1	Cyclic	Fracture of specimen at the first bolt hole located at specimen end	0.528	0.401	0.327	Failed at 8th Cycle		--
Astaneh-Asl (1982)[1]	AB2	Cyclic	Fracture of specimen at midspan	0.367	0.347	0.234	0.084		--
Astaneh-Asl (1982)[1]	AB3	Cyclic	Fracture of specimen at bolt hole located at midspan	0.657	0.576	0.458	Failed at 8th Cycle		--
Astaneh-Asl (1982)[1]	AB4	Cyclic	Fracture of specimen at the first bolt hole located at specimen end	0.291	0.337	0.280	0.110		--
Astaneh-Asl (1982)[1]	AB5	Cyclic	Fracture of specimen at midspan	0.657	0.695	0.575	0.458		--
Astaneh-Asl (1982)[1]	AB6	Cyclic	Fracture of specimen at the first bolt hole located at specimen end	0.291	0.477	0.239	0.140		--
Astaneh-Asl (1982)[1]	AB7	Cyclic	Fracture of specimen at midspan	0.659	0.968	0.781	0.169		
Astaneh-Asl (1982)[1]	AW8	Cyclic	--	0.427	0.656	0.341	0.230	1.15	
Astaneh-Asl (1982)[1]	AW9	Cyclic	--	0.176	0.196	0.147	0.081		
Astaneh-Asl (1982)[1]	AW11	Cyclic	Fracture of specimen at the conjunction of gusset	0.384	0.336	0.226	0.088		

Researcher	Spec ID	Loading History	Failure Mode	Pcr/Py or Rn/Py by AISC	Meas. Pcr/Py for 1st Circle	Meas. Pcr/Py for 2nd Circle	Meas Pcr/Py for 10th Circle	Max Tensile Load/Py	Location & Quantity of Plastic Hinges
Astaneh-Asl (1982)[1]	AW12	Cyclic	Stitch failure & single angle buckling	0.154	0.259	0.163	0.072	--	
Astaneh-Asl (1982)[1]	AW13	Cyclic	Severe local buckling of specimen at the end	0.384	0.371	0.265	0.174		
Astaneh-Asl (1982)[1]	AW15	Cyclic	--	0.183	0.214	0.186	0.096		
Astaneh-Asl (1982)[1]	AW18	Cyclic	--	0.150	0.264	0.170	0.074	--	
Aslani (1987) [4]	A1	Cyclic	Fracture in angle compression leg at the location of local buckling	0.403	0.444	0.268	0.134		
Aslani (1987) [4]	A2	Cyclic	Fracture in angle compression leg at the location of local buckling	0.403		0.291	0.093		
Aslani (1987) [4]	A3	Cyclic	Fracture in angle compression leg at the location of local buckling	0.498		0.371	0.206		
Aslani (1987) [4]	A4	Cyclic	Fracture in angle compression leg at the location of local buckling	0.498	0.667	0.444	Failed at 10^{th} Cycle	0.85	
Aslani (1987) [4]	A5	Cyclic	Fracture in angle compression leg at the location of local buckling	0.498	0.653	0.399	0.198	0.85	
Aslani (1987) [4]	C1	Cyclic	Fracture at a location next the plastic hinge						3 hinges at brace
Aslani (1987) [4]	C2, C3	Cyclic	Fracture at a mid span						3 hinges at brace
Aslani (1989) [5]	AB1	Cyclic	Fracture in angle compression leg at the location of local buckling	0.326	0.378	0.24	0.12		
Aslani (1989) [5]	AB2	Cyclic	Fracture in angle compression leg at the location of local buckling	0.350	0.400	0.265	0.14		

Researcher	Spec ID	Loading History	Failure Mode	Pcr/Py or Rn/Py by AISC	Meas. Pcr/Py for 1st Circle	Meas. Pcr/Py for 2nd Circle	Meas Pcr/Py for 10th Circle	Max Tensile Load/Py	Location & Quantity of Plastic Hinges
Aslani (1989) [5]	AB3	Cyclic	Fracture in angle compression leg at the location of local buckling	0.374		0.261	0.083		
Aslani (1989) [5]	AB4	Cyclic	Fracture in angle compression leg at the location of local buckling	0.401		0.332	0.184		
Aslani (1989) [5]	AB5	Cyclic	Fracture in angle compression leg at the location of local buckling	0.443	0.597	0.397	Failed at 10th Cycle		
Aslani (1989) [5]	AB6	Cyclic	Fracture in angle compression leg at the location of local buckling	0.451	0.600	0.366	0.182		
Aslani (1989) [5]	ABS7	Cyclic	Fracture of angle at the location of local buckling	0.524	0.428	0.296	Failed at 8th Cycle		
Aslani (1989) [5]	AB9	Cyclic	Fracture in angle compression leg at the location of local buckling	0.648	0.750	0.467	Failed at 10th Cycle		
Aslani (1989) [5]	AXH10	Cyclic	Sudden fracture of brace	0.617	0.646	0.467	0.267		
Aslani (1989) [5]	AXH11	Cyclic	Sudden fracture of brace	0.617	0.516	0.292	0.182		
Aslani (1989) [5]	AXH12	Cyclic	Fracture of brace	0.617	0.94	0.520	0.265		
Aslani (1989) [5]	AXH13	Cyclic	Early fracture of brace	0.617	0.605	0.413	Failed at 10th Cycle		
Aslani (1989) [5]	AXH14	Cyclic	Sudden fracture of brace	0.617	0.442	0.319	0.177		
Aslani	AXF15	Cyclic	Fracture of brace at the location	0.767	0.976	0.805	0.441		

Researcher	Spec ID	Loading History	Failure Mode	Pcr/Py or Rn/Py by AISC	Meas. Pcr/Py for 1st Circle	Meas. Pcr/Py for 2nd Circle	Meas Pcr/Py for 10th Circle	Max Tensile Load/Py	Location & Quantity of Plastic Hinges
(1989) [5]			of local buckling						
Aslani (1989) [5]	AXF16	Cyclic	Early fracture of brace at the end of connection	0.798	1.39	1.21	0.505		
Aslani (1989) [5]	AXF17	Cyclic	Fracture of brace at the end of connection	0.798	1.35	1.09	0.420		
Maison (1980) [6]	P1	Cyclic			27	10		40	
Maison (1980) [6]	P2	Cyclic			22			58	
Jain (1978) [7]	1	Cyclic	Buckling of brace		0.90*	0.52*		0.875*	
Jain (1978) [7]	2A	Cyclic	Buckling of brace		0.99*	0.59*		0.95*	
Jain (1978) [7]	2B	Cyclic	Fracture of brace at mid-span		0.8*			1.0*	
Jain (1978) [7]	3	Cyclic	Fracture of brace at the end of connection			0.92*		1.0*	
Jain (1978) [7]	4	Cyclic	Buckling of brace		1.0*	0.875*		0.90*	
Jain (1978) [7]	5	Cyclic	Fracture of brace at the end of connection			0.90*		1.0*	
Jain (1978) [7]	6	Cyclic			0.77*			1.0*	
Jain (1978) [7]	7A	Cyclic			0.85*	0.40*		0.99*	
Jain (1978) [7]	7B	Cyclic			0.37*			1.0*	
Jain (1978) [7]	8	Cyclic	Fracture of brace at the end of connection			0.69*		0.99*	
Jain (1978) [7]	9	Cyclic	Fracture of brace at the end of connection		0.98*	0.70*		0.94*	

Researcher	Spec ID	Loading History	Failure Mode	Pcr/Py or Rn/Py by AISC	Meas. Pcr/Py for 1st Circle	Meas. Pcr/Py for 2nd Circle	Meas Pcr/Py for 10th Circle	Max Tensile Load/Py	Location & Quantity of Plastic Hinges
Jain (1978) [7]	10	Cyclic	Fracture of brace at the end of connection		0.98*	0.69*		0.99*	
Jain (1978) [7]	11	Cyclic			0.38*	0.25*		1. *0	
Jain (1978) [7]	12A	Cyclic				0.28*		1.0*	
Jain (1978) [7]	12B	Cyclic			0.42*			1.0*	
Jain (1978) [7]	13	Cyclic			0.87*	0.49*		0.99*	
Jain (1978) [7]	14	Cyclic			0.85*	0.47*		0.99*	
Jain (1978) [7]	15	Cyclic			0.85*	0.48*		0.99*	
Jain (1978) [7]	16	Dynamic	Fracture of brace at mid-span		1.14*	0.53*	0.28*	0.94*	
Jain (1978) [7]	17	Dynamic	Fracture of brace at mid-span						
Jain (1978) [7]	18	Dynamic							
Jain (1978) [7]	19	Dynamic	Fracture of brace at the end of connection		1.08*	0.632*	0.347*	1.0*	
Jain (1978) [7]	20	Dynamic							
Jain (1978) [7]	21	Dynamic							
Jain (1978) [7]	1L	Cyclic							
Jain (1978) [7]	2L	Cyclic							
Jain	3L	Cyclic							

Researcher	Spec ID	Loading History	Failure Mode	Pcr/Py or Rn/Py by AISC	Meas. Pcr/Py for 1st Circle	Meas. Pcr/Py for 2nd Circle	Meas Pcr/Py for 10th Circle	Max Tensile Load/Py	Location & Quantity of Plastic Hinges
(1978) [7]									
Jain (1978) [7]	4L	Cyclic							
Jain (1978) [7]	5L	Cyclic		0.572	0.661	0.221	0.144	0.819	
Jain (1978) [7]	6L	Cyclic		0.33	0.363	0.132		0.747	
Jain (1978) [7]	7L	Cyclic		0.583	0.506	0.169	0.098	0.829	
Jain (1978) [7]	8L	Cyclic		0.567	0.247	0.098		0.646	
Gugerli (1982) [8]	WW1	Cyclic		0.604	0.65	0.25		1.05	
Gugerli (1982) [8]	WW3	Cyclic		0.865	1.0	0.50		1.00	
Gugerli (1982) [8]	WW4	Cyclic		0.668	0.70	0.25		1.00	
Gugerli (1982) [8]	WW5	Cyclic		0.649	0.65	0.23		1.00	
Gugerli (1982) [8]	WW6	Cyclic		0.863	0.85	0.50		1.00	
Gugerli (1982) [8]	TW2	Cyclic		0.752	0.66	0.39		1.00	
Gugerli (1982) [8]	TW3	Cyclic		0.476	0.43	0.23		0.90	
Gugerli (1982) [8]	TW4	Cyclic		0.890	0.85	0.50		0.90	
Gugerli (1982) [8]	TW6	Cyclic		0.745	0.74	0.27		0.98	
Itani (1999)	1	Cyclic lateral	Test terminated due to the significant amount of distortion						

Researcher	Spec ID	Loading History	Failure Mode	Pcr/Py or Rn/Py by AISC	Meas. Pcr/Py for 1st Circle	Meas. Pcr/Py for 2nd Circle	Meas Pcr/Py for 10th Circle	Max Tensile Load/Py	Location & Quantity of Plastic Hinges
[10]		load	occurring in connection and loading member						
Itani (1999) [10]	2	Constant axial+ cyclic lateral load	Test terminated due to the significant out-of- plane bending of gusset						
Itani (1999) [10]	3812	Cyclic axial load with 12 inches eccentricity	Fracture at the location of edge buckling					Pt/Py= 0.58 Mtc/Mp =1.65	
Itani (1999) [10]	3816	Cyclic axial load with 16 inches eccentricity	Fracture at the location of Whitmore section					Pt/Py=0.57 Mtc/Mp =2.16	
Itani (1999) [10]	3820	Cyclic axial load with 20 inches eccentricity	Test stop at 8th cycle, no crack found					Pt/Py=0.44 Mtc/Mp =2.10	
Itani (1999) [10]	1412	Cyclic axial load with 12 inches eccentricity	Fracture at the location of edge buckling					Pt/Py=0.64 Mtc/Mp =1.83	

Researcher	Spec ID	Loading History	Failure Mode	Pcr/Py or Rn/Py by AISC	Meas. Pcr/Py for 1st Circle	Meas. Pcr/Py for 2nd Circle	Meas Pcr/Py for 10th Circle	Max Tensile Load/Py	Location & Quantity of Plastic Hinges
Itani (1999) [10]	1416	Cyclic axial load with 16 inches eccentricity	Fracture at the location of Whitmore section					Pt/Py=0.64 Mtc/Mp =2.43	
Itani (1999) [10]	1420	Cyclic axial load with 20 inches eccentricity	Fracture at the location of Whitmore section					Pt/Py=0.38 Mtc/Mp =1.78	
Bjorhovde (1985) [11]	TG4	Monotonic tension	Not fail					320	
Bjorhovde (1985) [11]	TG5	Monotonic tension	Not fail					324	
Bjorhovde (1985) [11]	TG6	Monotonic tension	Not fail					399	
Wakabayashi (1977) [12]	SIM1	Monotonic		0.913	0.966				
Wakabayashi (1977) [12]	SIC1	Cyclic	Crack observed in 10^{th} cycle	0.911	1.03	0.82*	0.46*	1.08*	

Researcher	Spec ID	Loading History	Failure Mode	Pcr/Py or Rn/Py by AISC	Meas. Pcr/Py for 1st Circle	Meas. Pcr/Py for 2nd Circle	Meas Pcr/Py for 10th Circle	Max Tensile Load/Py	Location & Quantity of Plastic Hinges
Wakabayashi (1977) [12]	SIM2	Monotonic		0.722	0.68				
Wakabayashi (1977) [12]	SIC2	Cyclic	Crack observed in 13th cycle	0.689	0.70	0.45*	0.27*	1.05*	
Wakabayashi (1977) [12]	SIM3	Monotonic		0.464	0.516				
Wakabayashi (1977) [12]	SIC3	Cyclic	Not failed	0.462	0.530	0.35*	0.22*	1.13*	
Wakabayashi (1977) [12]	SOM1	Monotonic		0.912	1.007				
Wakabayashi (1977) [12]	SOC1	Cyclic	Not failed	0.908	0.990	0.82*	0.48*	1.05*	
Wakabayashi (1977) [12]	SOM2	Monotonic		0.689	0.652				
Wakabayashi (1977) [12]	SOC2	Cyclic	Not failed	0.691	0.723	0.45*	0.27*	1.02*	

Researcher	Spec ID	Loading History	Failure Mode	Pcr/Py or Rn/Py by AISC	Meas. Pcr/Py for 1st Circle	Meas. Pcr/Py for 2nd Circle	Meas Pcr/Py for 10th Circle	Max Tensile Load/Py	Location & Quantity of Plastic Hinges
Wakabayashi (1977) [12]	SOM3	Monotonic		0.459	0.479				
Wakabayashi (1977) [12]	SOC3	Cyclic	Not failed	0.464	0.471	0.26*	0.22*	1.18*	
Wakabayashi (1977) [12]	DIM1	Monotonic		0.97	0.969				
Wakabayashi (1977) [12]	DIC1	Cyclic	Crack observed in 8^{th} cycle	0.971	1.025	1.03*	--	1.02*	
Wakabayashi (1977) [12]	DIM2	Monotonic		0.89	0.927				
Wakabayashi (1977) [12]	DIC2	Cyclic	Crack observed in 6^{th} cycle	0.891	0.953	0.75*	0.42*	0.85*	
Wakabayashi (1977) [12]	DIM3	Monotonic		0.787	0.814				
Wakabayashi (1977) [12]	DIC3	Cyclic	Crack observed in 9^{th} cycle	0.785	0.908	0.50*	--	0.65*	

Researcher	Spec ID	Loading History	Failure Mode	Pcr/Py or Rn/Py by AISC	Meas. Pcr/Py for 1st Circle	Meas. Pcr/Py for 2nd Circle	Meas Pcr/Py for 10th Circle	Max Tensile Load/Py	Location & Quantity of Plastic Hinges
Wakabayashi (1977) [12]	DOM1	Monotonic		0.955	1.084				
Wakabayashi (1977) [12]	DOC1	Cyclic	Crack observed in 13th cycle	0.954	1.099	1.01*	0.62*	1.05*	
Wakabayashi (1977) [12]	DOM2	Monotonic		0.832	0.899				
Wakabayashi (1977) [12]	DOC2	Cyclic	Crack observed in 14th cycle	0.832	0.964	0.54*	0.4*5	0.77*	
Wakabayashi (1977) [12]	DOM3	Monotonic		0.686	0.846				
Wakabayashi (1977) [12]	DOC3	Cyclic	Not failed	0.687	0.791	0.48*	0.40*	0.65*	
Wakabayashi (1980) [13]	SPM1	Monotonic			0.859				
Wakabayashi (1980) [13]	SPC1	Cyclic	Crack observed in 2nd cycle		0.835	0.70*		0.97*	

Researcher	Spec ID	Loading History	Failure Mode	Pcr/Py or Rn/Py by AISC	Meas. Pcr/Py for 1st Circle	Meas. Pcr/Py for 2nd Circle	Meas Pcr/Py for 10th Circle	Max Tensile Load/Py	Location & Quantity of Plastic Hinges
Wakabayashi (1980) [13]	SPM3	Monotonic			0.378				
Wakabayashi (1980) [13]	SPC3	Cyclic	Fracture of brace at the end of connection		0.335	0.21*		0.95*	
Wakabayashi (1980) [13]	DPM1	Monotonic	Fracture of brace at the end of connection		0.945				
Wakabayashi (1980) [13]	DPC1	Cyclic	Fracture of brace at the end of connection		0.945	0.88*		0.90*	
Wakabayashi (1980) [13]	DPM2	Monotonic			0.798				
Wakabayashi (1980) [13]	DPM3	Monotonic	2 Cracks observed at the end of braces		0.601				
Wakabayashi (1980) [13]	DPC3	Cyclic	Cracks observed in 2^{nd} and 4^{th} cycle		0.601	0.52*		0.65*	
Wakabayashi (1980) [13]	SAM1	Monotonic			0.926				

Researcher	Spec ID	Loading History	Failure Mode	Pcr/Py or Rn/Py by AISC	Meas. Pcr/Py for 1st Circle	Meas. Pcr/Py for 2nd Circle	Meas Pcr/Py for 10th Circle	Max Tensile Load/Py	Location & Quantity of Plastic Hinges
Wakabayashi (1980) [13]	SAC1	Cyclic	Crack observed in 7^{th} cycle		0.964	0.66*		1.0*	
Wakabayashi (1980) [13]	SAM3	Monotonic			0.709				
Wakabayashi (1980) [13]	SAC3	Cyclic	Cracks observed in 3^{rd} and 7^{th} cycle		0.634	0.33*		0.95*	
Wakabayashi (1980) [13]	DAM1	Monotonic			0.918				
Wakabayashi (1980) [13]	DAC1	Cyclic	Cracks observed in 6^{th} and 7^{th} cycle		0.918	0.80*		0.80*	
Wakabayashi (1980) [13]	DAM2	Monotonic	Crack observed at the end of brace		0.91				
Wakabayashi (1980) [13]	DAC2	Cyclic	Cracks observed in 5^{th} cycle		0.91	0.57*		0.88*	
Wakabayashi (1980) [13]	DAM3	Monotonic	Crack observed at the end of brace		0.81				

Researcher	Spec ID	Loading History	Failure Mode	Pcr/Py or Rn/Py by AISC	Meas. Pcr/Py for 1st Circle	Meas. Pcr/Py for 2nd Circle	Meas Pcr/Py for 10th Circle	Max Tensile Load/Py	Location & Quantity of Plastic Hinges
Wakabayashi (1980) [13]	DAC3	Cyclic	Cracks observed in 1st and 3rd cycle		0.81	0.45*		0.60*	
Wakabayashi (1980) [13]	FTBM	Cyclic			0.15*	0.14*		1.25*	
Wakabayashi (1980) [13]	FTBC	Cyclic			0.15*	0.14*		1.25*	
Wakabayashi (1980) [13]	RB4M	Cyclic			0.5*			0.5*	
Wakabayashi (1980) [13]	RB4C	Cyclic			0.5*			0.5*	
Wakabayashi (1980) [14]	BFSI	Cyclic	Fracture of column at the connection to beam	0.706	0.72*	0.45*	0.33*	1.06*	
Wakabayashi (1980) [14]	BFSO	Cyclic	Fracture of column at the connection to beam	0.706	0.72	0.45*	0.33*	0.99*	
Wakabayashi	BFDI	Cyclic	Severe cracking of brace near the intersecting joint of braces	0.896	1.06	0.79*	0.59*	0.94*	

Researcher	Spec ID	Loading History	Failure Mode	Pcr/Py or Rn/Py by AISC	Meas. Pcr/Py for 1st Circle	Meas. Pcr/Py for 2nd Circle	Meas Pcr/Py for 10th Circle	Max Tensile Load/Py	Location & Quantity of Plastic Hinges
(1980) [14]									
Wakabayashi (1980) [14]	BFDO	Cyclic	Not failed before test stop at 15th cycle	0.837	0.90	0.54*	0.50*	0.94*	
Morino (1978) [15]	1	Monotonic	Test stopped after the buckling of brace		0.93*				
Morino (1978) [15]	2	Monotonic	Test stopped after the buckling of brace		0.92*				
Morino (1978) [15]	3	Monotonic	Test stopped after the buckling of brace		0.91*				
Morino (1978) [15]	4	Monotonic	Test stopped after the buckling of brace		0.88*				
Morino (1978) [15]	5	Monotonic	Test stopped after the buckling of brace		0.75*				
2042	SR14M	Monotonic		0.377	0.443				
2042	SR12M	Monotonic		0.489	0.614				
2042	SR10M	Monotonic		0.607	0.757				
2042	SR9M	Monotonic		0.663	0.803				
2042	SR8M	Monotonic		0.724	0.890				

Researcher	Spec ID	Loading History	Failure Mode	Pcr/Py or Rn/Py by AISC	Meas. Pcr/Py for 1st Circle	Meas. Pcr/Py for 2nd Circle	Meas Pcr/Py for 10th Circle	Max Tensile Load/Py	Location & Quantity of Plastic Hinges
2042	SR7M	Monotonic		0.781	0.919				
2042	SR6M	Monotonic		0.835	0.981				
2042	SR5M	Monotonic		0.882	0.963				
2042	SR4M	Monotonic		0.923	0.964				
2042	SR12C	Cyclic		0.487	0.732				
2042	SR10C	Cyclic		0.608	0.837				
2042	SR9C	Cyclic		0.665	1.108				
2042	SR8C	Cyclic		0.727	1.069				
2042	SR7C	Cyclic		0.786	1.097				
2042	SR6C	Cyclic		0.835	1.031				
2042	SR5C	Cyclic		0.882	1.010				
2042	SR4C	Cyclic		0.922	1.083				
2287	RMC40	Cyclic		0.906	0.980				
2287	RMC80	Cyclic		0.702	0.879				
2287	RMC120	Cyclic		0.465	0.534				
2287	RMC160	Cyclic		0.274	0.325				
2287	RME40	Cyclic		0.906	0.859				

Researcher	Spec ID	Loading History	Failure Mode	Pcr/Py or Rn/Py by AISC	Meas. Pcr/Py for 1st Circle	Meas. Pcr/Py for 2nd Circle	Meas Pcr/Py for 10th Circle	Max Tensile Load/Py	Location & Quantity of Plastic Hinges
2287	RME80	Cyclic		0.703	0.618				
2287	RME120	Cyclic		0.465	0.386				
2287	RRC40	Cyclic		0.906	1.049				
2287	RRC40R	Cyclic		0.907	0.884				
2287	RRC60	Cyclic		0.814	1.000				
2287	RRC80	Cyclic		0.697	0.924				
2287	RRC100	Cyclic		0.584	0.606				
2287	RRC100R	Cyclic		0.584	0.438				
2287	RRC120	Cyclic		0.464	0.626				
2287	RRC160	Cyclic		0.275	0.391				
2287	RRE40	Cyclic		0.907	0.891				
2287	RRE80	Cyclic		0.703	0.641				
2287	RRE120	Cyclic		0.465	0.434				
2288	C45-1	Cyclic		0.894	0.982				
2288	C45-2	Cyclic		0.894	0.985				
2288	C50-1	Cyclic		0.871	0.985				
2288	C50-2	Cyclic		0.871	0.985				

Researcher	Spec ID	Loading History	Failure Mode	Pcr/Py or Rn/Py by AISC	Meas. Pcr/Py for 1st Circle	Meas. Pcr/Py for 2nd Circle	Meas Pcr/Py for 10th Circle	Max Tensile Load/Py	Location & Quantity of Plastic Hinges
2288	C60-1	Cyclic		0.812	0.983				
2288	C60-2	Cyclic		0.820	0.985				
2288	C80	Cyclic		0.698	0.983				
2288	T80	Cyclic		0.702	0.986				
2288	C100	Cyclic		0.579	0.755				
2288	T100	Cyclic		0.574	0.740				
2295	RC400	Cyclic		0.899	0.965				
2295	RC401	Cyclic		0.949	0.986				
2295	RC402	Cyclic		0.965	0.977				
2295	RE400	Cyclic		0.899	0.963				
2295	RE401	Cyclic		0.948	0.979				
2295	RE402	Cyclic		0.965	0.981				
2295	RC800	Cyclic		0.682	0.882				
2295	RC801	Cyclic		0.825	0.939				
2295	RC802	Cyclic		0.880	0.955				
2295	RE800	Cyclic		0.682	0.882				
2295	RE801	Cyclic		0.825	0.937				
2295	RE802	Cyclic		0.881	0.951				
2295	RC1200	Cyclic		0.436	0.524				

Researcher	Spec ID	Loading History	Failure Mode	Pcr/Py or Rn/Py by AISC	Meas. Pcr/Py for 1st Circle	Meas. Pcr/Py for 2nd Circle	Meas Pcr/Py for 10th Circle	Max Tensile Load/Py	Location & Quantity of Plastic Hinges
2295	RC1201	Cyclic		0.660	0.868				
2295	RC1202	Cyclic		0.760	0.922				
2295	RE1200	Cyclic		0.437	0.519				
2295	RE1201	Cyclic		0.661	0.870				
2295	RE1202	Cyclic		0.758	0.917				
2295	RC1600	Cyclic		0.256	0.303				
2295	RC1601	Cyclic		0.484	0.598				
2295	RC1602	Cyclic		0.619	0.906				

Appendix C

Summary of Gusset Plate Connection Tests

Specimen ID	Brace Section	Length of Brace (in)	Gusset Plate Size (inxin)	Thickness (in)	Whimore width (in)	Failure Mode	Reference
1	2C8x11.5	20.5	15x15	0.251	9.196	Free edge buckling	Brown (1988)
2	2C4x7.25	17.5	15x15	0.196	8.66	Free edge buckling	Brown (1988)
3	2C8x11.5	20.5	15x15	0.198	9.196	Free edge buckling	Brown (1988)
4	2C8x11.5	20.5	15x15	0.379	9.196	No failure	Brown (1988)
5	2C8x11.5	20.5	15x15	0.248	9.196	Free edge buckling	Brown (1988)
6	2C8x11.5	20.5	15x15	0.21	9.196	Free edge buckling	Brown (1988)
7	2C8x11.5	20.5	15x15	0.202	9.196	Free edge buckling	Brown (1988)
8	2C4x7.25	17.5	15x15	0.188	8.66	Test stopped	Brown (1988)
9	2C4x7.25	17.5	15x15	0.192	8.66	Free edge buckling	Brown (1988)
10	2C4x7.25	17.5	15x15	0.197	8.66	Free edge buckling	Brown (1988)
11	2C8x11.5	20.5	15x15	0.25	9.196	Free edge buckling	Brown (1988)
12	2C8x11.5	20.5	15x15	0.377	9.196	Buckling of brace	Brown (1988)
13	2C8x11.5	20.5	15x15	0.248	9.196	Free edge buckling	Brown (1988)
14	2C4x7.25	17.5	15x15	0.248	8.66	Free edge buckling	Brown (1988)
15	2C8x11.5	20.5	15x15	0.25	9.196	Free edge buckling	Brown (1988)
16	2C4x7.25	17.5	15x15	0.25	8.66	Free edge buckling	Brown (1988)
17	2C8x11.5	20.5	15x15	0.194	9.196	Free edge buckling	Brown (1988)
18	2C4x7.25	17.5	15x15	0.251	8.66	Free edge buckling	Brown (1988)
19	2C8x11.5	20.5	15x15	0.378	9.196	Buckling of brace	Brown (1988)
20	2C4x7.25	17.5	15x15	0.376	8.66	Buckling of brace	Brown (1988)
21	2C8x11.5	20.5	15x15	0.378	9.196	Not failed	Brown (1988)
22	2C4x7.25	17.5	15x15	0.379	8.66	Braces buckled	Brown (1988)
23	2C4x7.25	17.5	15x15	0.378	8.66	Connection failed	Brown (1988)
24	2C4x7.25	17.5	15x15	0.376	8.66	Connection failed	Brown (1988)
FR C1	W250x58		33.5x21.6	0.263	22.36	Buckling of gusset	Cheng (1987,1994)

FR C2	W250x58		33.5x21.6	0.122	22.36	Buckling of gusset	Cheng (1987,1994)
FR C3	W250x58		33.5x27.6	0.263	22.36	Buckling of gusset	Cheng (1987,1994)
FR C4	W250x58		33.5x27.6	0.122	22.36	Buckling of gusset	Cheng (1987,1994)
FX C1	W250x58		33.5x21.6	0.263	22.36	Free edge buckling	Cheng (1987,1994)
FX C2	W250x58		33.5x21.6	0.122	22.36	Free edge buckling	Cheng (1987,1994)
FX C3	W250x58		33.5x27.6	0.263	22.36	Free edge buckling	Cheng (1987,1994)
FX C4	W250x58		33.5x27.6	0.122	22.36	Free edge buckling	Cheng (1987,1994)
FR E5	W250x58		33.5x21.6	0.263	22.36	Yielding of splice plate at the last row of bolts	Cheng (1987,1994)
FR E6	W250x58		33.5x27.6	0.263	22.36	Yielding of splice plate at the last row of bolts	Cheng (1987,1994)
FRS E5	W250x58		33.5x21.6	0.263	22.36	Yielding of splice plate at the last row of bolts	Cheng (1987,1994)
FRS E6	W250x58		33.5x27.6	0.263	22.36	Buckling of gusset	Cheng (1987,1994)
FXS E5	W250x58		33.5x21.6	0.263	22.36	Yielding of splice plate at the last row of bolts	Cheng (1987,1994)
FXS E6	W250x58		33.5x27.6	0.263	22.36	Buckling of gusset	Cheng (1987,1994)
GP1			19.7x15.8	0.524	12.22	Sway buckling of the gusset	Yam (1994)
GP2			19.7x15.8	0.386	12.22	Sway buckling of gusset	Yam (1994)
GP3			19.7x15.8	0.256	12.22	Sway buckling of gusset	Yam (1994)
GP1R			19.7x15.8	0.524	12.22	Free edge buckling	Yam (1994)

GP2R			19.7x15.8	0.386	12.22	Free edge buckling	Yam (1994)
GP3R			19.7x15.8	0.256	12.22	Free edge buckling	Yam (1994)
SP1			33.5x27.6	0.524	18.59	Sway buckling of gusset	Yam (1994)
SP2			33.5x27.6	0.386	18.59	Sway buckling of gusset	Yam (1994)
AP1			19.7x15.8	0.524	12.22	Sway buckling of gusset	Yam (1994)
AP2			19.7x15.8	0.386	12.22	Sway buckling of gusset	Yam (1994)
AP3			19.7x15.8	0.256	12.22	Sway buckling of gusset	Yam (1994)
MP1			19.7x15.8	0.524	12.22	Sway buckling of gusset	Yam (1994)
MP2			19.7x15.8	0.386	12.22	Sway buckling of gusset	Yam (1994)
MP3			19.7x15.8	0.256	12.22	Sway buckling of gusset	Yam (1994)
MP3A			19.7x15.8	0.256	12.22	Sway buckling of gusset	Yam (1994)
MP3B			19.7x15.8	0.256	12.22	Sway buckling of gusset	Yam (1994)
EP1			19.7x15.8	0.524	12.22	Yielding of splice plate	Yam (1994)
EP2			19.7x15.8	0.524	12.22	Yielding of splice plate	Yam (1994)
EP3			19.7x15.8	0.524	12.22	Yielding of splice plate	Yam (1994)
A-1	W250x67		21.6x17.7	0.367	15.40	Net section fracture of gusset	Rabinovitch (1993)
A-2	W250x67		21.6x17.7	0.243	15.40	Net section fracture of gusset	Rabinovitch (1993)
A-3	W250x67		21.6x17.7	0.367	15.40	Net section fracture of gusset	Rabinovitch (1993)
A-4	W250x67		21.6x17.7	0.243	15.40	Net section fracture of gusset	Rabinovitch (1993)
A-5	W250x67		21.6x17.7	0.367	15.40	Net section fracture of gusset	Rabinovitch (1993)
T-1	W250x49	43.3	17.7x21.6	0.374		Buckling of gusset plate	Grondin (2000)
T-2	W250x49	43.3	17.7x21.6	0.378		Buckling of gusset plate	Grondin (2000)
T-3	W250x49	206.7	17.7x21.6	0.373		Buckling of brace	Grondin

							(2000)
T-4	W250x49	206.7	17.7x21.6	0.375		Buckling of brace	Grondin (2000)
Brace Tests with Gusset Plate Failure							
AW10						Fracture of Gusset	Astaneh-Asl (1982)
AW14						Fracture of stitch & gusset	Astaneh-Asl (1982)
AW15						--	Astaneh-Asl (1982)
AW16						Fracture of gusset	Astaneh-Asl (1982)
CG1						Shear yielding of gusset pl	Astaneh-Asl (1992)
CG2						Block shear failure of gusset plate	Astaneh-Asl (1992)
CG3						Gusset plate buckling and block shear failure	Astaneh-Asl (1992)
ABS8						Fracture of gusset plate	Aslani (1989)
AW0						Fracture of gusset at base	El-Tayem (1985)
AW3						Fatigue fracture of gusset at the end of brace	El-Tayem (1985)
1						Buckling of gusset plate	Yamamoto (1988)
2						Buckling of gusset plate	Yamamoto (1988)
3						Buckling of gusset plate	Yamamoto (1988)
4						Buckling of gusset plate	Yamamoto

							(1988)
HZ						Crack at gusset pl weld	Yamada (1977)
HK						Crack at gusset pl weld	Yamada (1977)

Appendix D

Database of CBF Test Data

Title:	Summary of Test Results for UC Berkeley Special Concentric Braced Frame Specimen No. 1 (SCBF-1)
Authors:	Patxi Uriz, Stephen Mahin
Year:	2004

Test Setup

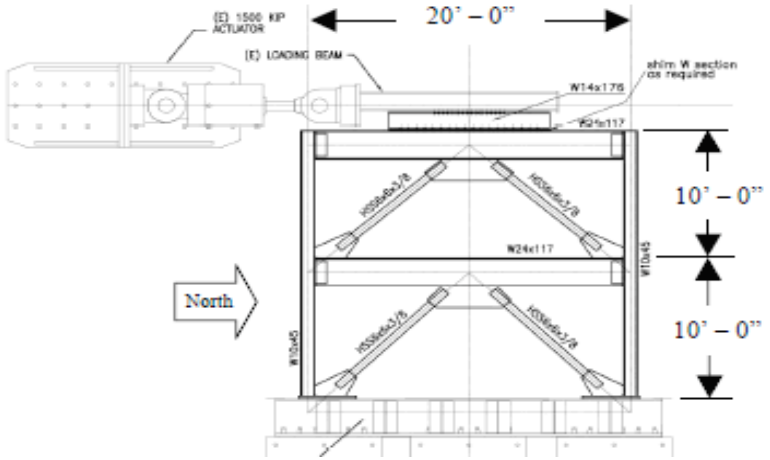

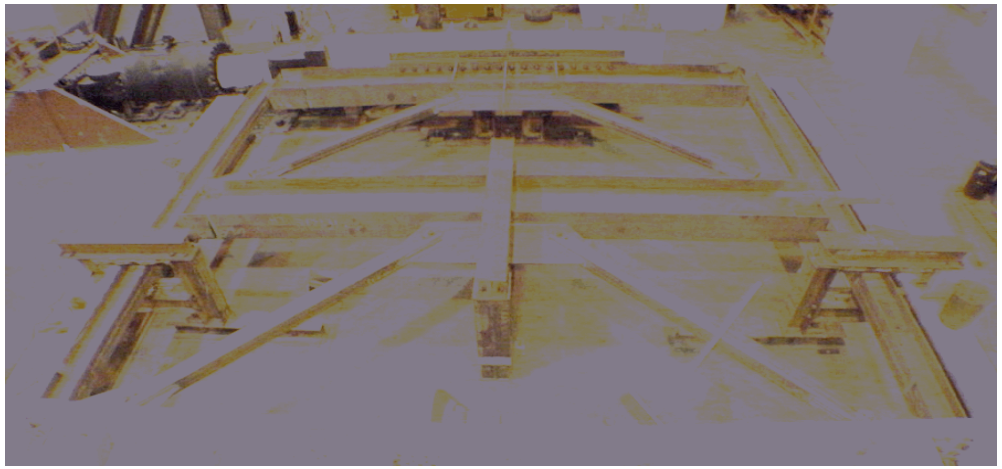

1st Floor Innerstory Drift Hysteresis

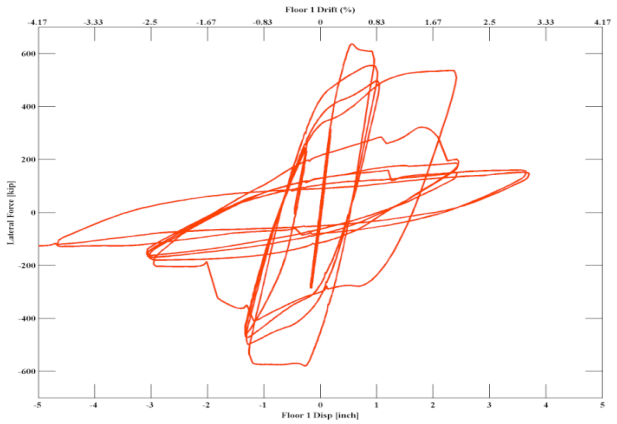

Range: -1.0% to 0.9% → 1.9% Total

Roof Drift Hysteresis

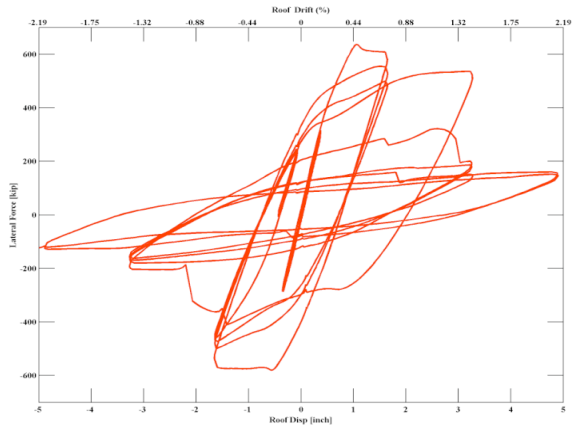

Range: -0.7% to 0.7% → 1.4% Total

Member Sizes

1st Story Beam	W24x117
2nd Story Beam	W24x117
1st Story Column	W10x45
2nd Story Column	W10x45
1st Story Braces	HSS6x6x3/8
2nd Story Braces	HSS6x6x3/8
Gusset Plate Thick. (in)	0.875

1st Story Inner-Story Drift	Damage Picture			
0% to 1.1%	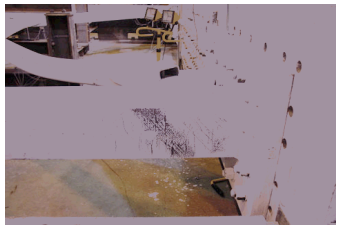		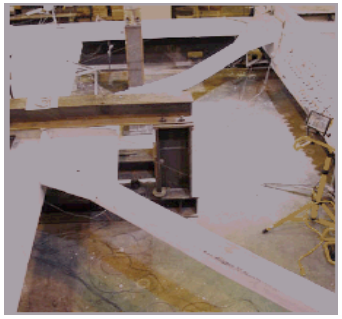	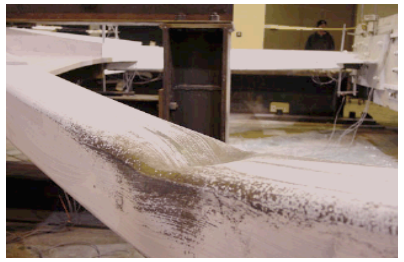
	Column Base Yielding	1st Story Gusset Buckling	1st Story North Brace Buckling	1st Story South Brace Buckling and Cupping
1.1% to 2.5%	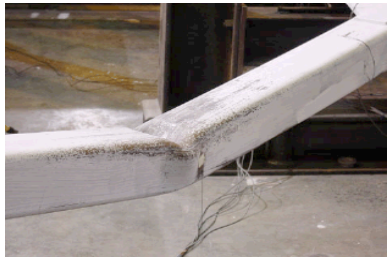	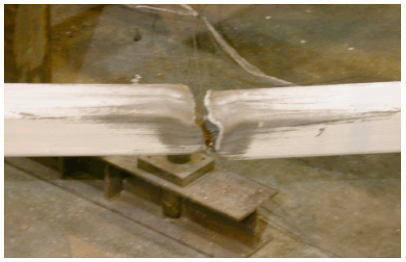	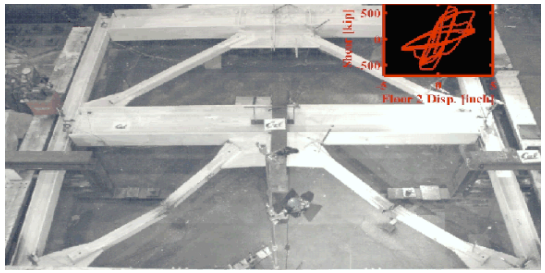	
	1st Story North Brace Severe Buckling	1st Story South Brace Fracture	Overall Damge (note concentrated damge in 1st story)	
	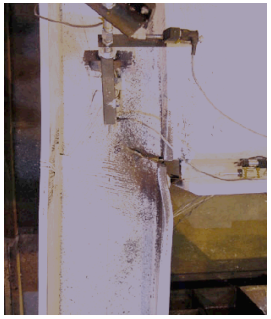			
	1st Story South Column Fracture	1st Story North Column Fracture	1st Story North Brace Prior to Fracture	

Note: There is little to no damage in the 2nd story

Title:	Experimental and Analytical Study of the Inelastic Behavior of Double Angle Bracing Members Under Severe Cyclic Loading
Authors:	Farhang Aslani, Subash Goel
Year:	1989

Specimen	Section	Stitch Spacing (in)	A (in^2)	F_y (ksi)	P_y (kip)	Δ_y (in)	Axial Range (Δ/Δ_y)	
							Tens.	Comp.
AB1	2L3.5x2.5x1/4	55	2.88	46.4	133.6	0.208	7	-10

Brace Layout

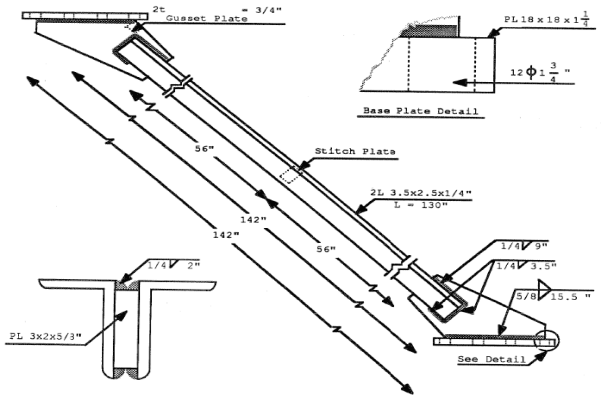

Gusset Dimensions

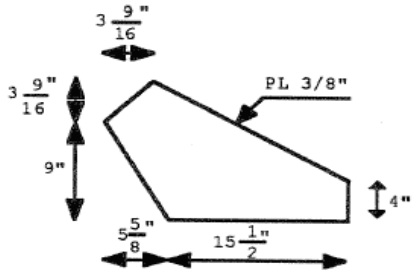

Axial Force - Axial Displacement Hysteresis

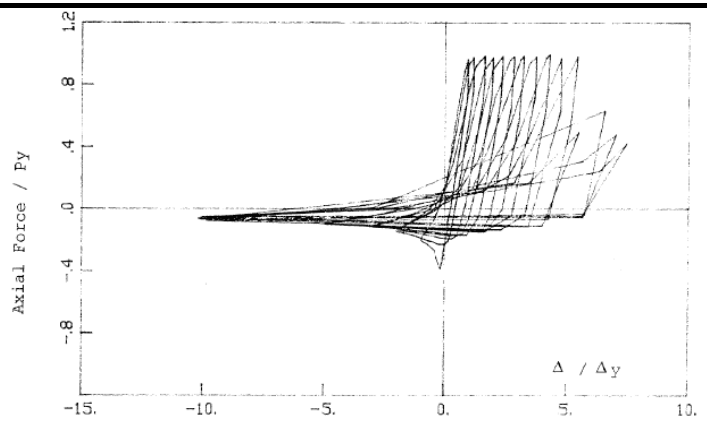

Drift Range (%)

Tens		Comp.		Total
1.12	to	-1.60	→	2.72

Noticable Damage

Damage	Drift (Δ/Δ_y)	Drift(%)
Initial Yield	1.1	0.18
Local Buckling	-2	-0.32
Initial Gap Closing	-1	-0.16
Complete Gap Closing	-1	-0.16
Complete Fracture	3	0.48

Damage Pictures

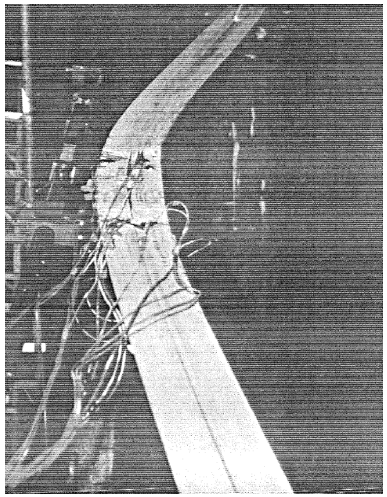

Buckling

Title:	Experimental and Analytical Study of the Inelastic Behavior of Double Angle Bracing Members Under Severe Cyclic Loading
Authors:	Farhang Aslani, Subash Goel
Year:	1989

Specimen	Section	Stitch Spacing (in)	A (in^2)	F_y (ksi)	P_y (kip)	Δ_y (in)	Axial Range (Δ/Δ_y)	
							Tens.	Comp.
AB2	2L3.5x2.5x1/4	37	2.88	47	135.4	0.211	8.5	-10

Brace Layout

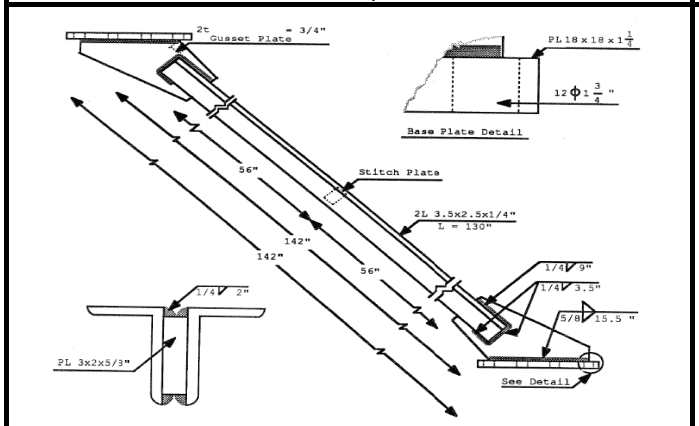

Gusset Dimensions

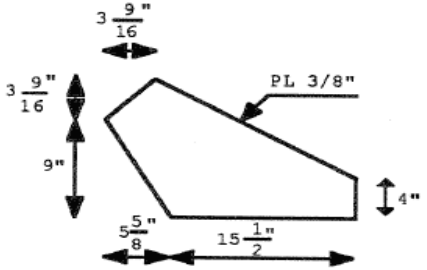

Axial Force - Axial Displacement Hysteresis

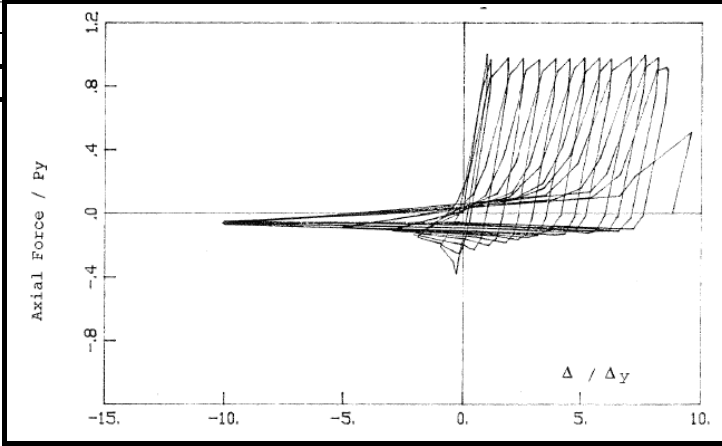

Drift Range (%)

Tens		Comp.		Total
1.38	to	-1.62	→	3.00

Noticable Damage

Damage	Drift (Δ/Δ_y)	Drift(%)
Initial Yield	1.1	0.18
Local Buckling	-3	-0.49
Initial Gap Closing	-1	-0.16
Complete Gap Closing	-2	-0.32
Complete Fracture	9.5	1.54

Damage Pictures

Buckling

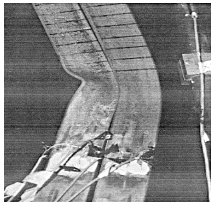

Local Buckling

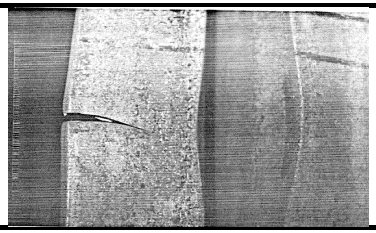

Initiation of Fracture

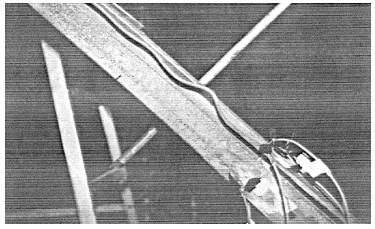

Reverse Plastic Hinge

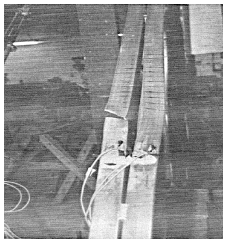

Rotation of Tension Brace

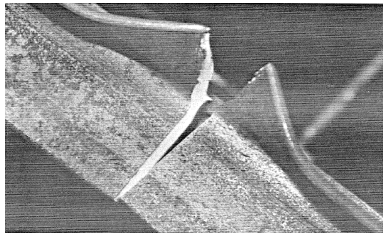

Complete Fracture

Title:	Experimental and Analytical Study of the Inelastic Behavior of Double Angle Bracing Members Under Severe Cyclic Loading
Authors:	Farhang Aslani, Subash Goel
Year:	1989

Specimen	Section	Stitch Spacing (in)	A (in^2)	F_y (ksi)	P_y (kip)	Δ_y (in)	Axial Range (Δ/Δ_y)	
							Tens.	Comp.
AB3	2L3.5x2.5x1/4	12	2.88	47	135.4	0.211	4.8	-10

Brace Layout

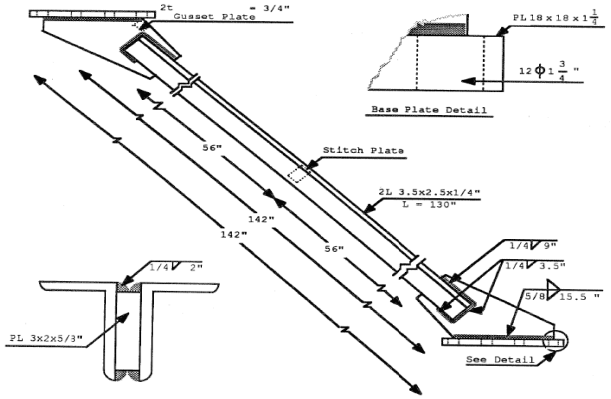

Gusset Dimensions

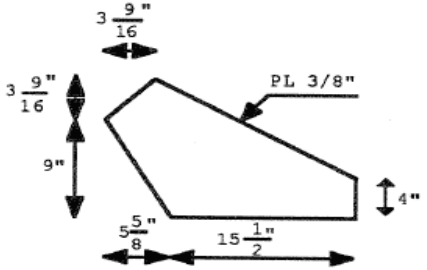

Axial Force - Axial Displacement Hysteresis

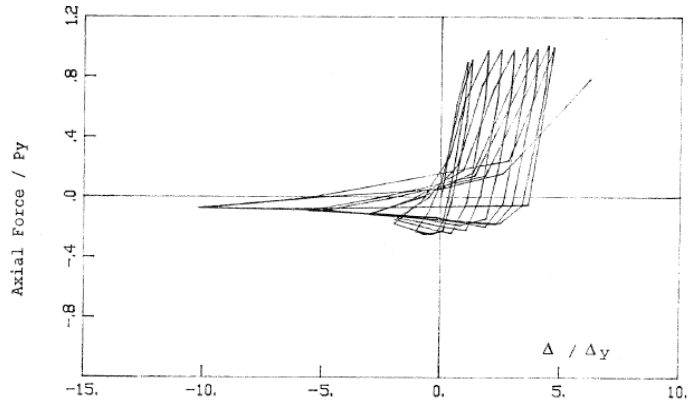

Drift Range (%)

Tens		Comp.		Total
0.78	to	-1.62	→	2.40

Noticable Damage

Damage	Drift (Δ/Δ_y)	Drift(%)
Initial Yield	1.2	0.19
Local Buckling	-3	-0.49
Initial Gap Closing	-3	-0.49
Complete Gap Closing	-6	-0.97
Complete Fracture	6	0.97

Damage Pictures

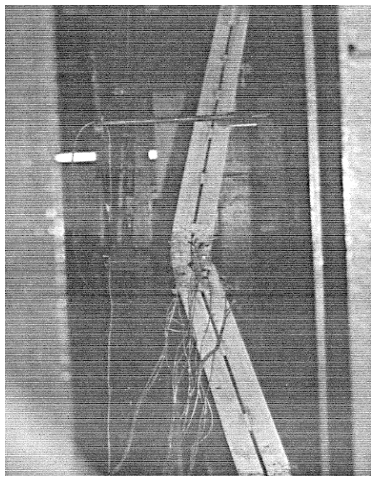

Buckling

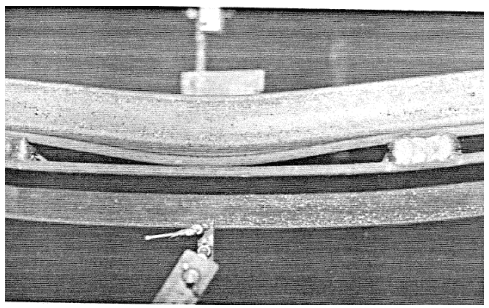

Complete Gap Closing

Title:	Experimental and Analytical Study of the Inelastic Behavior of Double Angle Bracing Members Under Severe Cyclic Loading
Authors:	Farhang Aslani, Subash Goel
Year:	1989

Specimen	Section	Stitch Spacing (in)	A (in^2)	F_y (ksi)	P_y (kip)	Δ_y (in)	Axial Range (Δ/Δ_y)	
							Tens.	Comp.
AB4	2L3.5x2.5x3/8	37	4.22	47	198.3	0.209	8.5	-11

Brace Layout

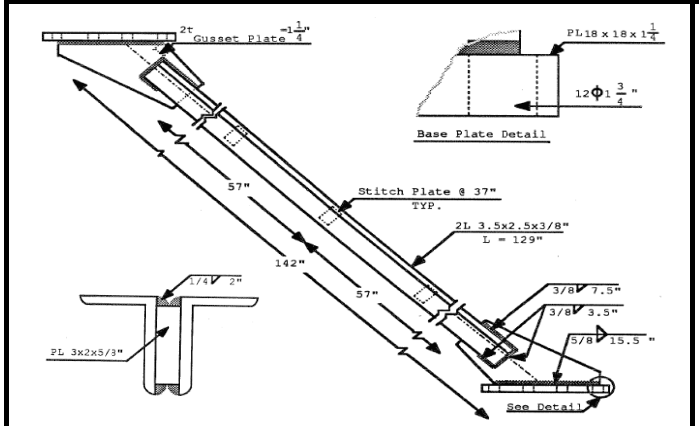

Gusset Dimensions

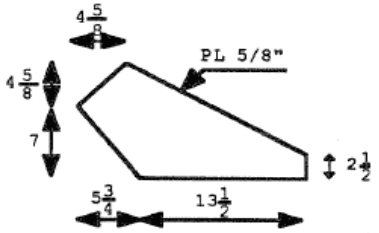

Axial Force - Axial Displacement Hysteresis

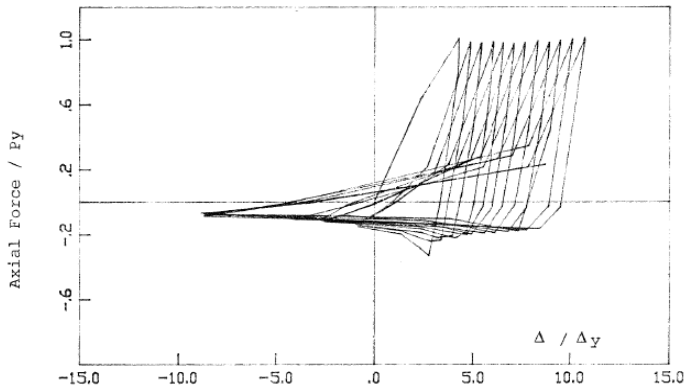

Drift Range (%)

Tens		Comp.		Total
1.38	to	-1.78	→	3.16

Noticable Damage

Damage	Drift (Δ/Δ_y)	Drift(%)
Initial Yield	2	0.32
Local Buckling	-5	-0.81
Initial Gap Closing	-1	-0.16
Complete Gap Closing	-3	-0.49
Complete Fracture	6.5	1.05

Damage Pictures

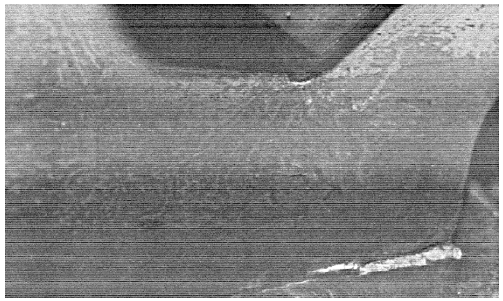

Small Gusset Plate Crack

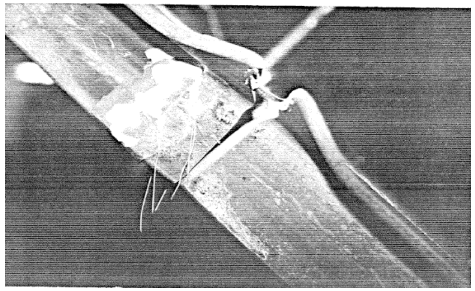

Local Buckling and Fracture

Title:	Experimental and Analytical Study of the Inelastic Behavior of Double Angle Bracing Members Under Severe Cyclic Loading
Authors:	Farhang Aslani, Subash Goel
Year:	1989

Specimen	Section	Stitch Spacing (in)	A (in^2)	F_y (ksi)	P_y (kip)	Δ_y (in)	Axial Range (Δ/Δ_y)	
							Tens.	Comp.
AB5	2L3.5x2.5x3/8	17	4.22	45	189.9	0.200	10.5	-7.5

Brace Layout

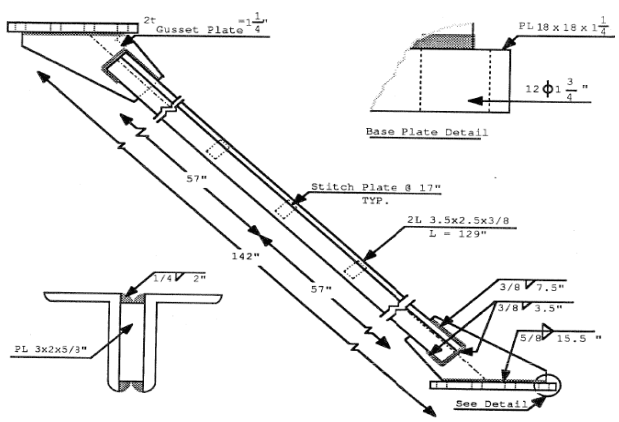

Gusset Dimensions

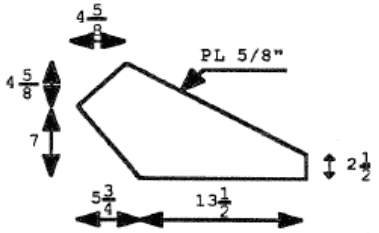

Axial Force - Axial Displacement Hysteresis

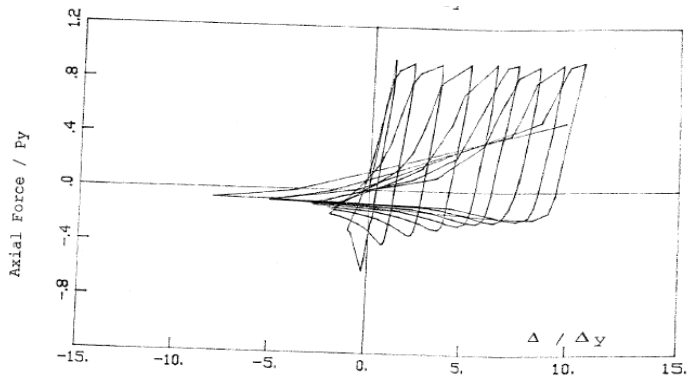

Drift Range (%)

Tens		Comp.		Total
1.63	to	-1.16	→	2.79

Noticable Damage

Damage	Drift (Δ/Δ_y)	Drift(%)
Initial Yield	2	0.31
Local Buckling	-3	-0.47
Initial Gap Closing	-2	-0.31
Complete Gap Closing	-2.5	-0.39
Complete Fracture	7	1.09

Damage Pictures

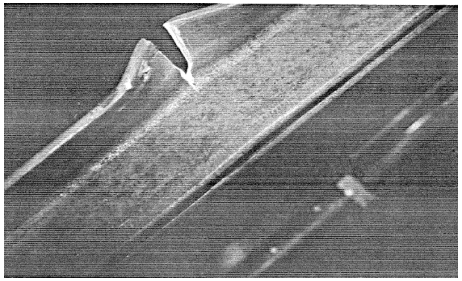

Initiation of Fracture

Title:	Experimental and Analytical Study of the Inelastic Behavior of Double Angle Bracing Members Under Severe Cyclic Loading
Authors:	Farhang Aslani, Subash Goel
Year:	1989

Specimen	Section	Stitch Spacing (in)	A (in^2)	F_y (ksi)	P_y (kip)	Δ_y (in)	Axial Range (Δ/Δ_y)	
							Tens.	Comp.
AB6	2L3.5x2.5x3/8	12	4.22	44.4	187.4	0.198	10.5	-9.5

Brace Layout

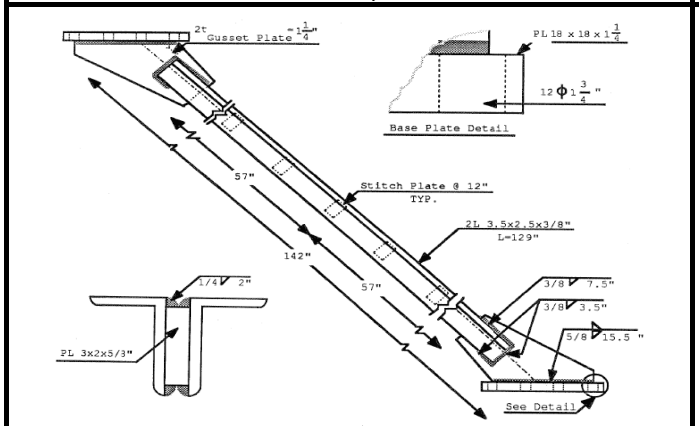

Gusset Dimensions

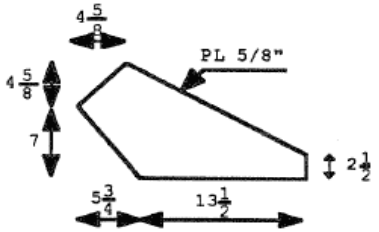

Axial Force - Axial Displacement Hysteresis

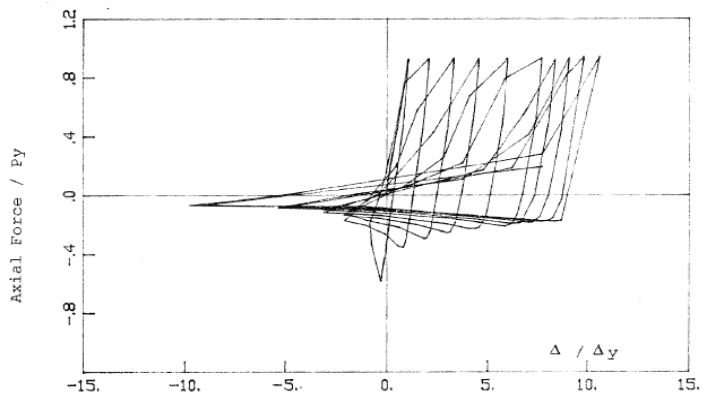

Drift Range (%)

Tens		Comp.		Total
1.61	to	-1.45	→	3.06

Noticable Damage

Damage	Drift (Δ/Δ_y)	Drift(%)
Initial Yield	2	0.31
Local Buckling	-3	-0.46
Initial Gap Closing	-2	-0.31
Complete Gap Closing	-3	-0.46
Complete Fracture	3	0.46

Damage Pictures

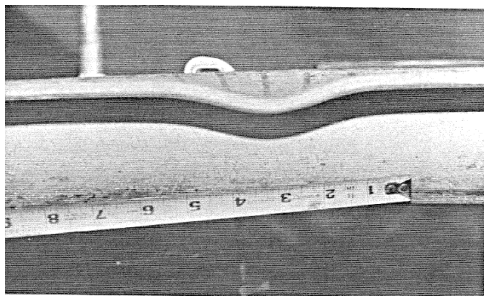

Initial Local Buckling

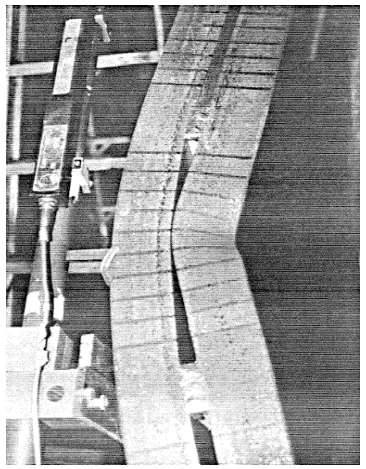

Complete Gap Closing

Title:	Experimental and Analytical Study of the Inelastic Behavior of Double Angle Bracing Members Under Severe Cyclic Loading
Authors:	Farhang Aslani, Subash Goel
Year:	1989

Specimen	Section	Stitch Spacing (in)	A (in^2)	F_y (ksi)	P_y (kip)	Δ_y (in)	Axial Range (Δ/Δ_y)	
							Tens.	Comp.
ABS7	2L3.5x2.5x1/4	55	2.88	47	135.4	0.211	4	-5

Brace Layout

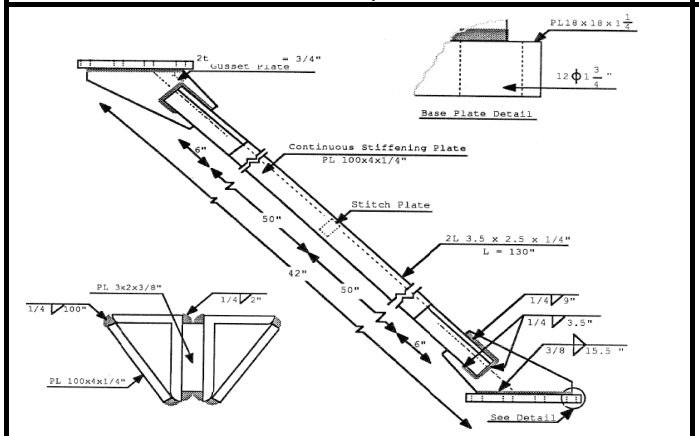

Gusset Dimensions

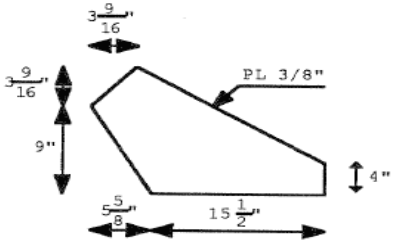

Axial Force - Axial Displacement Hysteresis

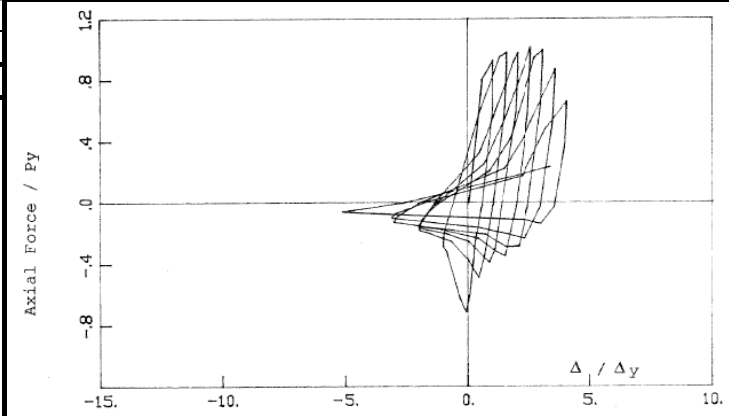

Drift Range (%)				
Tens		Comp.		Total
0.65	to	-0.81	→	1.46

Noticable Damage

Damage	Drift (Δ/Δ_y)	Drift(%)
Initial Yield	2	0.32
Local Buckling	-2	-0.32
Initial Gap Closing	-1	-0.16
Complete Gap Closing	-1	-0.16
Complete Fracture	3.5	0.57

Damage Pictures

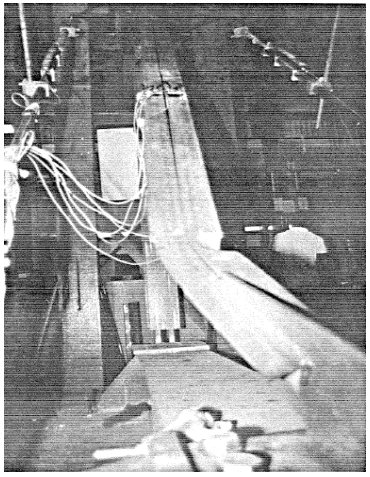

Buckling

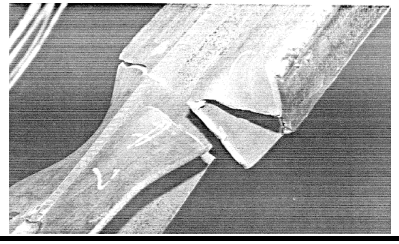

Complete Fracture

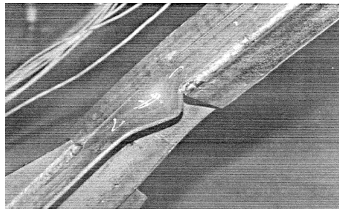

Middle Plastic Hinge

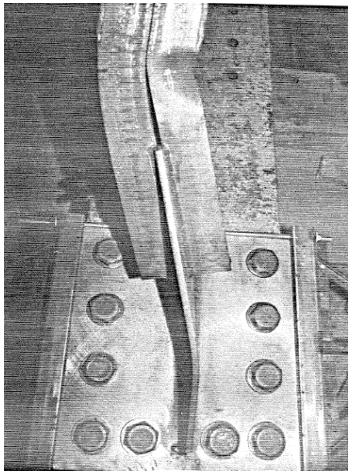

Lower Plastic Hinge

Title:	Experimental and Analytical Study of the Inelastic Behavior of Double Angle Bracing Members Under Severe Cyclic Loading
Authors:	Farhang Aslani, Subash Goel
Year:	1989

Specimen	Section	Stitch Spacing (in)	A (in^2)	F_y (ksi)	P_y (kip)	Δ_y (in)	Axial Range (Δ/Δ_y)	
							Tens.	Comp.
ABS8	2L3.5x2.5x1/4	55	2.88	47	135.4	0.211	1.2	-3.2

Brace Layout

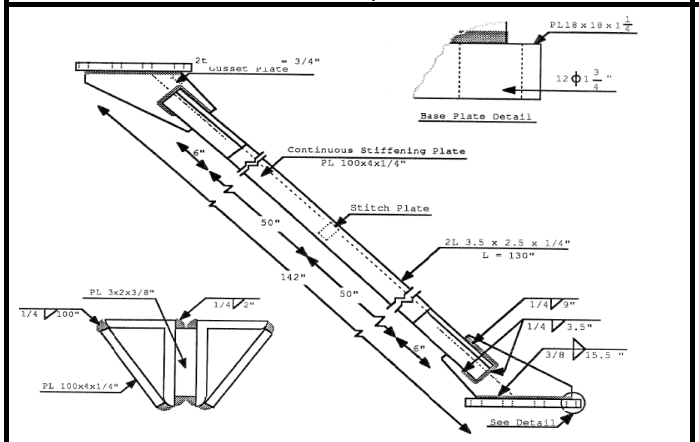

Gusset Dimensions

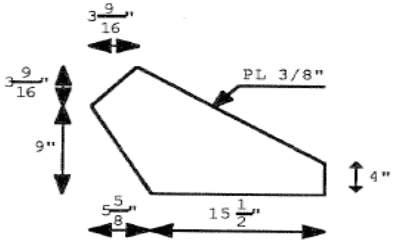

Axial Force - Axial Displacement Hysteresis

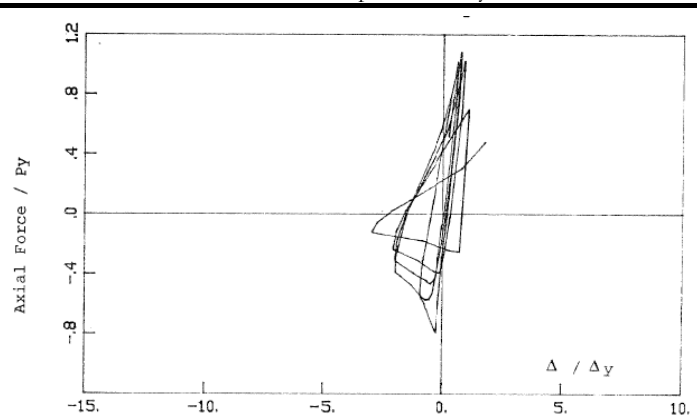

Drift Range (%)

Tens		Comp.		Total
0.19	to	-0.52	→	0.71

Noticable Damage

Damage	Drift (Δ/Δ_y)	Drift(%)
Initial Yield	-	-
Initial Brace Fracture	-2	-0.32
Initial Gap Closing	-1	-0.16
Complete Gap Closing	-1	-0.16
Gusset Fracture	-3.2	-0.52

Damage Pictures

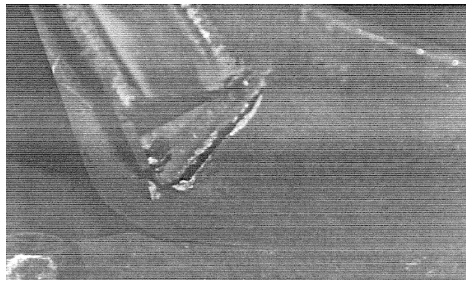

Gusset Fracture

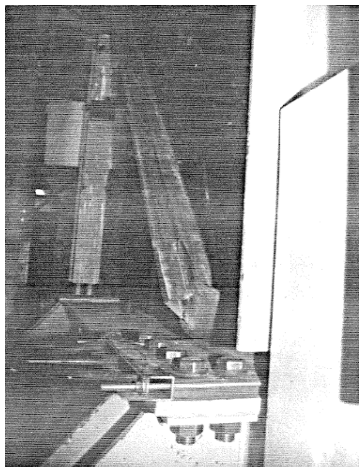

Buckling

Title:	Experimental and Analytical Study of the Inelastic Behavior of Double Angle Bracing Members Under Severe Cyclic Loading
Authors:	Farhang Aslani, Subash Goel
Year:	1989

Specimen	Section	Stitch Spacing (in)	A (in^2)	F_y (ksi)	P_y (kip)	Δ_y (in)	Axial Range (Δ/Δ_y)	
							Tens.	Comp.
AB9	2L3x3x3/8	12	4.22	44.4	187.4	0.198	11	-6.5

Brace Layout

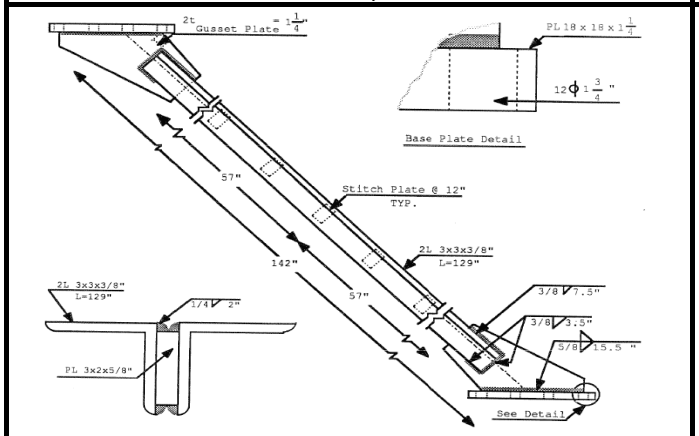

Gusset Dimensions

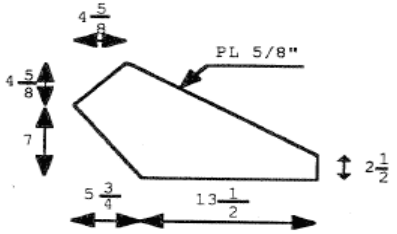

Axial Force - Axial Displacement Hysteresis

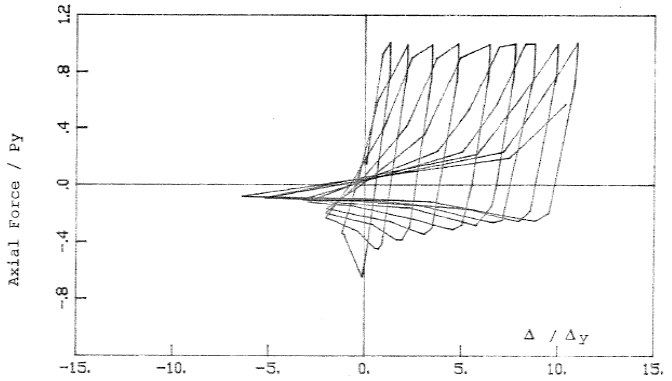

Drift Range (%)

Tens		Comp.		Total
1.68	to	-1.00	→	2.68

Noticable Damage

Damage	Drift (Δ/Δ_y)	Drift(%)
Initial Yield	2	0.31
Local Buckling	-2	-0.31
Initial Gap Closing	-3	-0.46
Complete Gap Closing	-3.5	-0.54
Complete Fracture	3.5	0.54

Damage Pictures

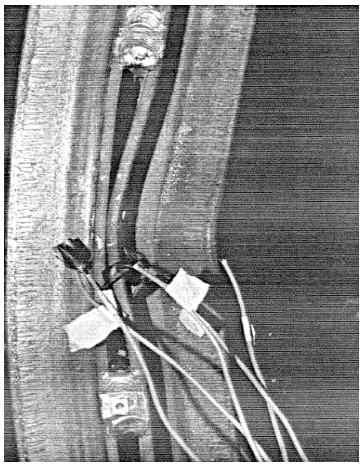

Gap Closing

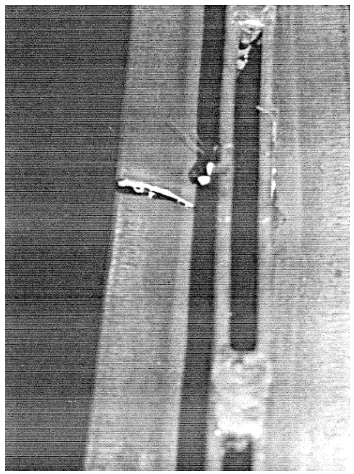

Complete Fracture

Title:	Experimental and Analytical Study of the Inelastic Behavior of Double Angle Bracing Members Under Severe Cyclic Loading
Authors:	Farhang Aslani, Subash Goel
Year:	1989

Specimen	Section	Stitch Spacing (in)	A (in^2)	F_y (ksi)	P_y (kip)	Δ_y (in)	Axial Range (Δ/Δ_y)	
							Tens.	Comp.
AXH10	2L3x3x3/8	12	4.22	45.8	193.3	0.204	15.5	-10

Brace Layout

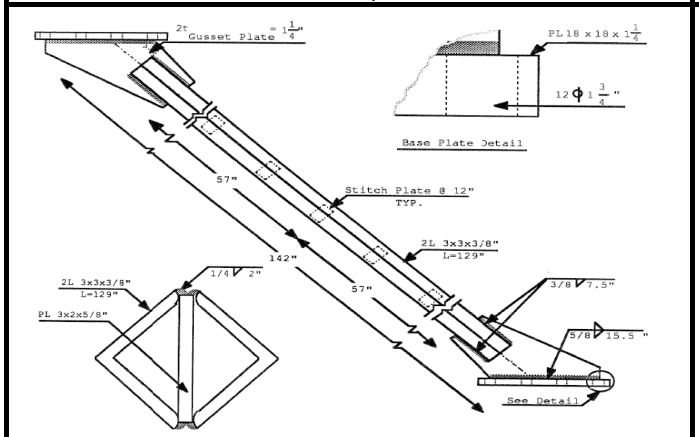

Gusset Dimensions

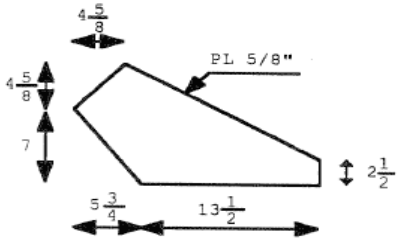

Axial Force - Axial Displacement Hysteresis

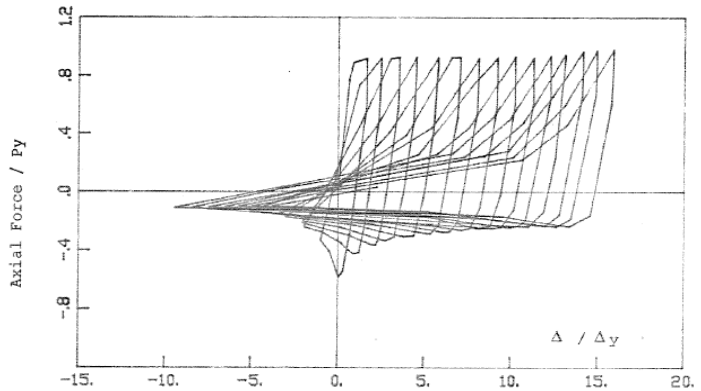

Drift Range (%)

Tens		Comp.		Total
2.45	to	-1.58	→	4.03

Noticable Damage

Damage	Drift (Δ/Δ_y)	Drift(%)
Initial Yield	2	0.32
Local Buckling	-9.5	-1.50
Initial Gap Closing	-3	-0.47
Complete Gap Closing	-5	-0.79
Complete Fracture	2	0.32

Damage Pictures

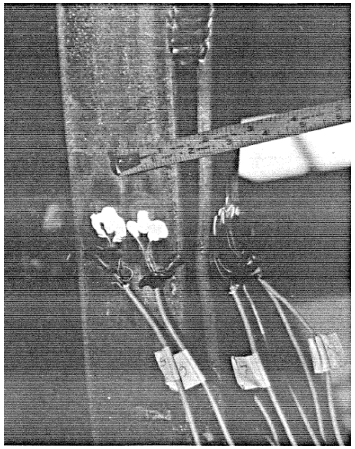

Gap Closing and Local Buckling

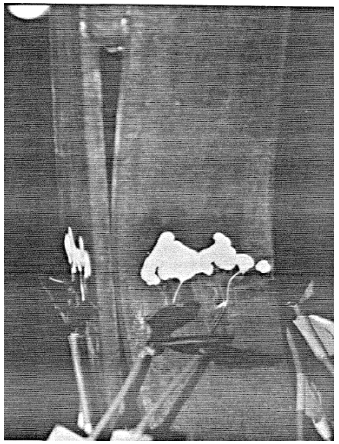

Complete Gap Closing

Title:	Experimental and Analytical Study of the Inelastic Behavior of Double Angle Bracing Members Under Severe Cyclic Loading
Authors:	Farhang Aslani, Subash Goel
Year:	1989

Specimen	Section	Stitch Spacing (in)	A (in^2)	F_y (ksi)	P_y (kip)	Δ_y (in)	Axial Range (Δ/Δ_y)	
							Tens.	Comp.
AXH11	2L3x3x3/8	6	4.22	45.9	193.7	0.204	16	-10

Brace Layout

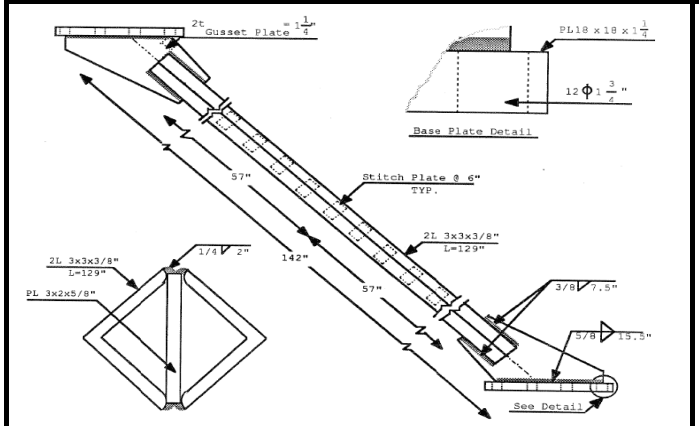

Gusset Dimensions

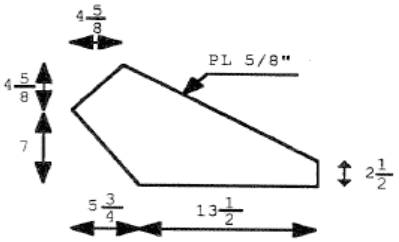

Axial Force - Axial Displacement Hysteresis

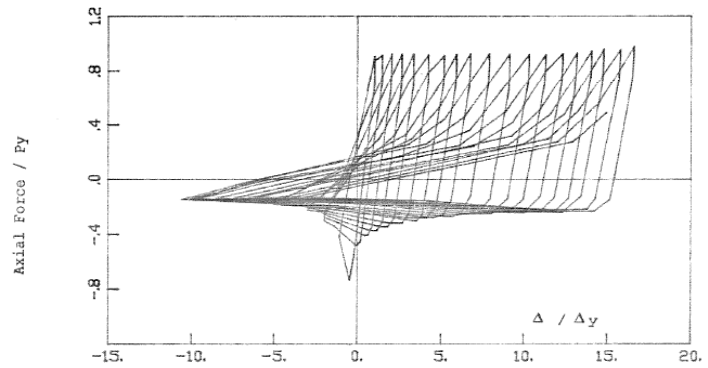

Drift Range (%)

Tens		Comp.		Total
2.53	to	-1.58	→	4.12

Noticable Damage

Damage	Drift (Δ/Δ_y)	Drift(%)
Initial Yield	2	0.32
Local Buckling	-10	-1.58
Initial Gap Closing	-	-
Complete Gap Closing	-	-
Complete Fracture	15	2.37

Damage Pictures

Local Buckling and Slight Gap Closing

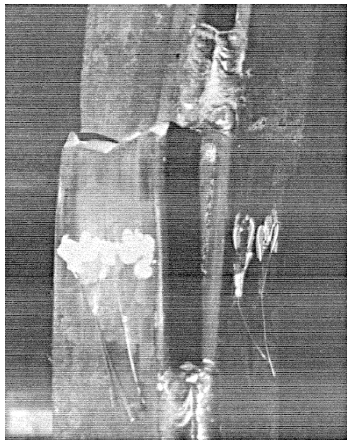

Complete Fracture

Title:	Experimental and Analytical Study of the Inelastic Behavior of Double Angle Bracing Members Under Severe Cyclic Loading
Authors:	Farhang Aslani, Subash Goel
Year:	1989

Specimen	Section	Stitch Spacing (in)	A (in^2)	F_y (ksi)	P_y (kip)	Δ_y (in)	Axial Range (Δ/Δ_y)	
							Tens.	Comp.
AXH12	2L3x3x3/8	0	4.22	47	198.3	0.209	19.5	-10

Brace Layout

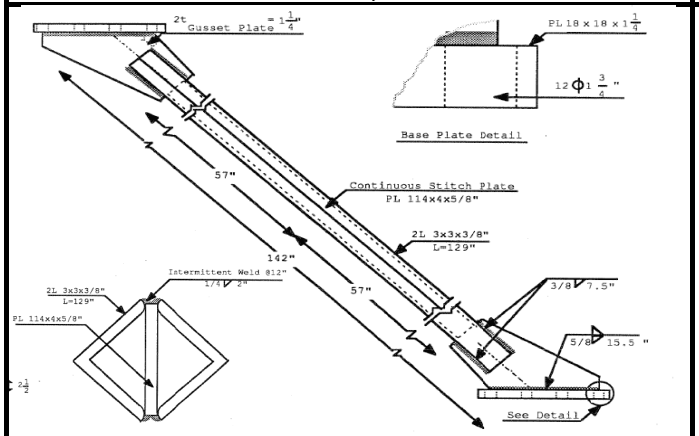

Gusset Dimensions

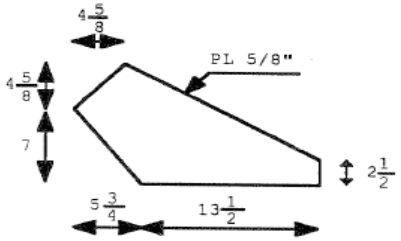

Axial Force - Axial Displacement Hysteresis

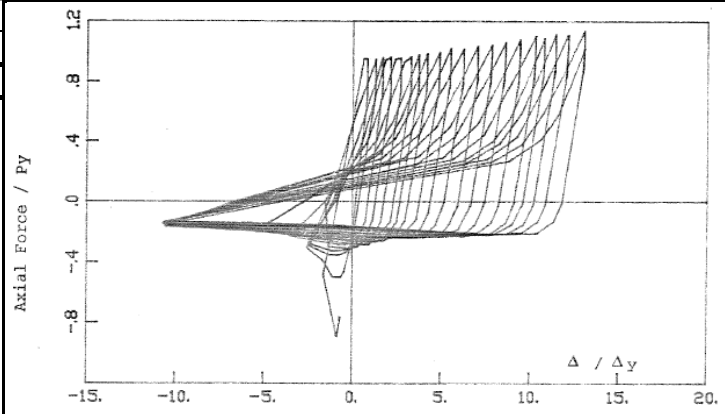

Drift Range (%)				
Tens		Comp.		Total
3.16	to	-1.62	→	4.78

Noticable Damage

Damage	Drift (Δ/Δ_y)	Drift(%)
Initial Yield	2	0.32
Local Buckling	-	-
Initial Gap Closing	-	-
Complete Gap Closing	-	-
Complete Fracture	10	1.62

Used a continuous weld to join braces

Damage Pictures

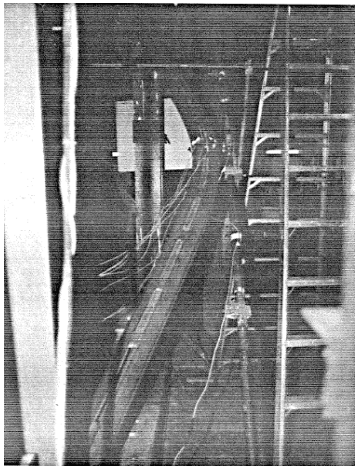

Buckling

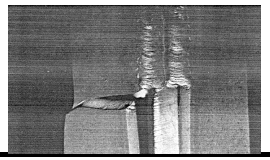

Complete Fracture

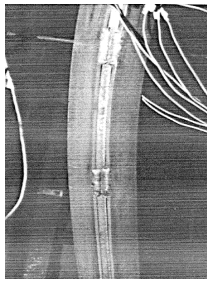

Buckling at -1.61%

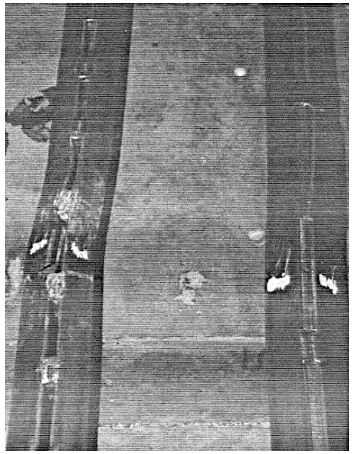

Comparison of AXH11 to AX12 After Failure

Title:	Experimental and Analytical Study of the Inelastic Behavior of Double Angle Bracing Members Under Severe Cyclic Loading
Authors:	Farhang Aslani, Subash Goel
Year:	1989

Specimen	Section	Stitch Spacing (in)	A (in^2)	F_y (ksi)	P_y (kip)	Δ_y (in)	Axial Range (Δ/Δ_y)	
							Tens.	Comp.
AXH13	2L3x3x3/8	37	4.22	43.7	184.4	0.194	9	-10

Brace Layout

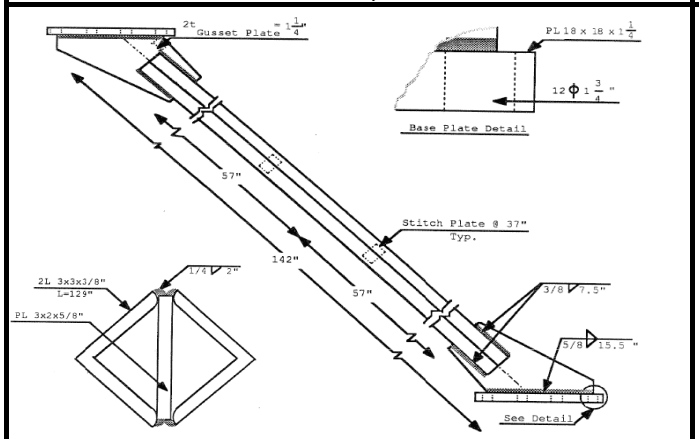

Gusset Dimensions

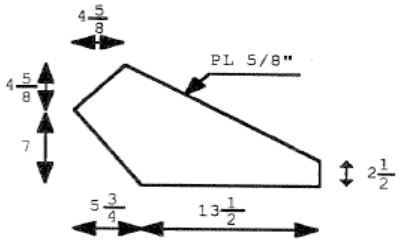

Axial Force - Axial Displacement Hysteresis

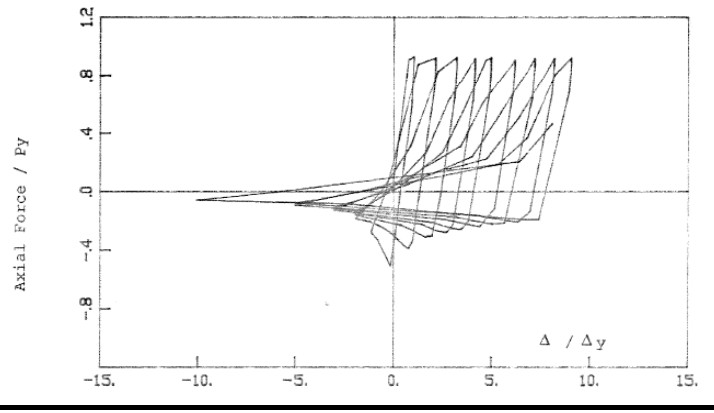

Drift Range (%)

Tens		Comp.		Total
1.36	to	-1.51	→	2.86

Noticable Damage

Damage	Drift (Δ/Δ_y)	Drift(%)
Initial Yield	2	0.30
Local Buckling	-3	-0.45
Initial Gap Closing	-2	-0.30
Complete Gap Closing	-2	-0.30
Complete Fracture	2.5	0.38

Damage Pictures

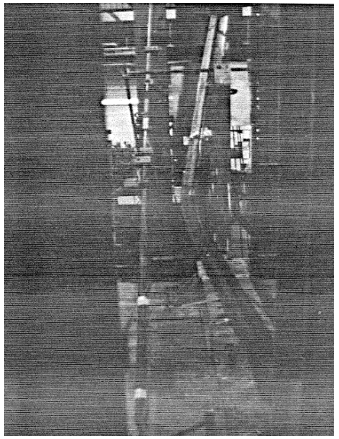

Buckling

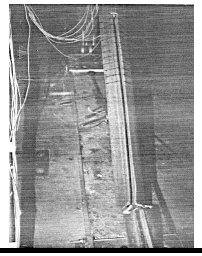

Fracture

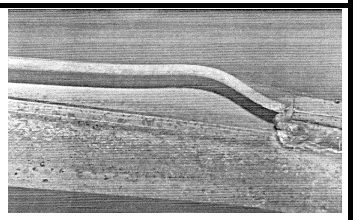

Excessive Gap Opening

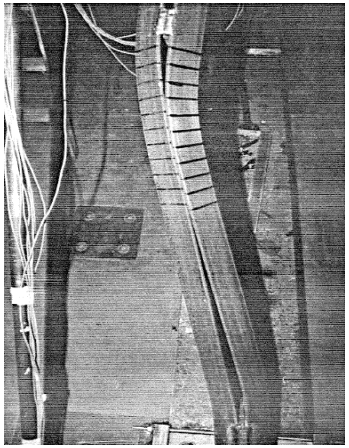

Individual Bending of Braces

Title:	Experimental and Analytical Study of the Inelastic Behavior of Double Angle Bracing Members Under Severe Cyclic Loading
Authors:	Farhang Aslani, Subash Goel
Year:	1989

Specimen	Section	Stitch Spacing (in)	A (in^2)	F_y (ksi)	P_y (kip)	Δ_y (in)	Axial Range (Δ/Δ_y)	
							Tens.	Comp.
AXH14	2L3x3x3/8	54	4.22	43.7	184.4	0.194	15.5	-10

Brace Layout

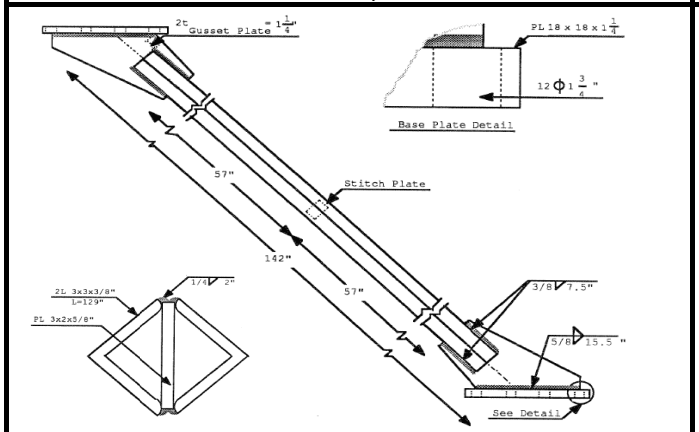

Gusset Dimensions

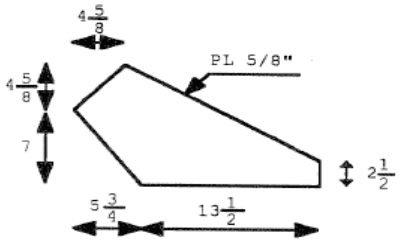

Axial Force - Axial Displacement Hysteresis

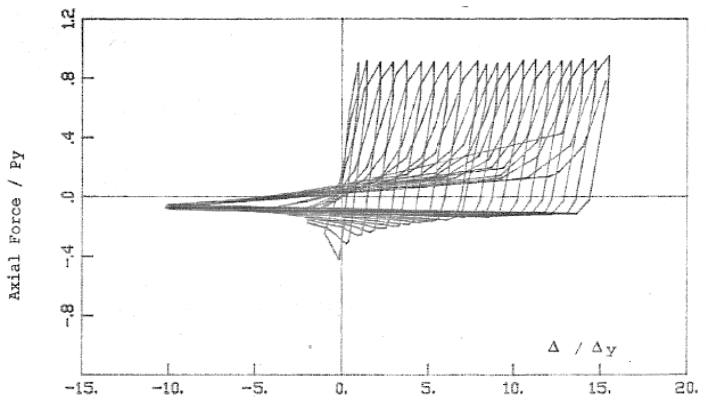

Drift Range (%)

Tens		Comp.		Total
2.34	to	-1.51	→	3.84

Noticable Damage

Damage	Drift (Δ/Δ_y)	Drift(%)
Initial Yield	2	0.30
Local Buckling	-5	-0.75
Initial Gap Closing	-2	-0.30
Complete Gap Closing	-2	-0.30
Complete Fracture	15.5	2.34

Damage Pictures

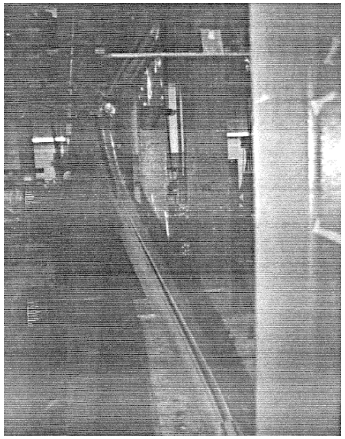

Buckling

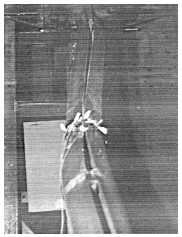

Complete Gap Closing

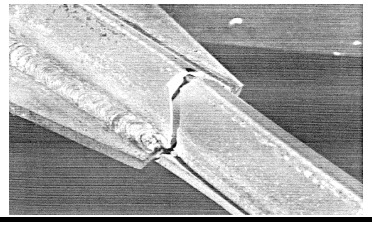

Net Section Fracture

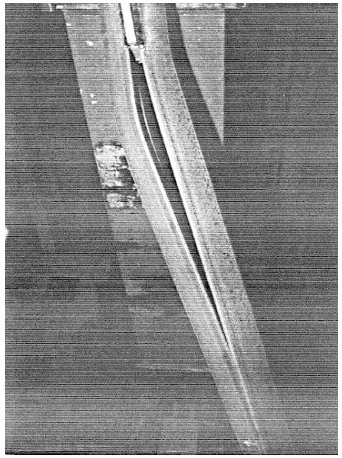

Individiual Plastic Hinges

Title:	Experimental and Analytical Study of the Inelastic Behavior of Double Angle Bracing Members Under Severe Cyclic Loading
Authors:	Farhang Aslani, Subash Goel
Year:	1989

Specimen	Section	Stitch Spacing (in)	A (in^2)	F_y (ksi)	P_y (kip)	Δ_y (in)	Axial Range (Δ/Δ_y)	
							Tens.	Comp.
AXH15	2L3x3x3/8	0	4.22	47.5	200.5	0.211	5	-10

Brace and Gusset Layout

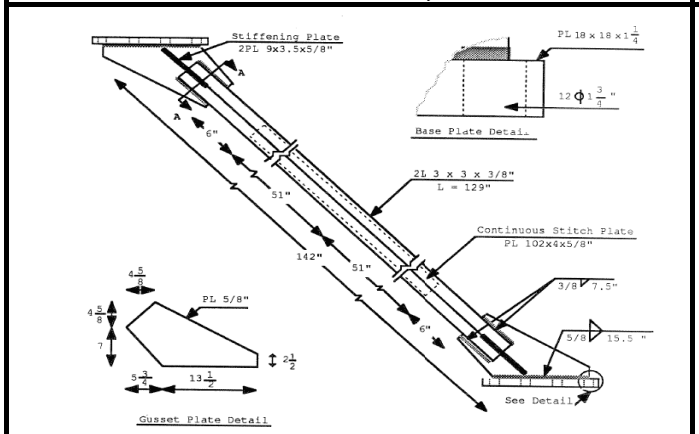

Connection Detail

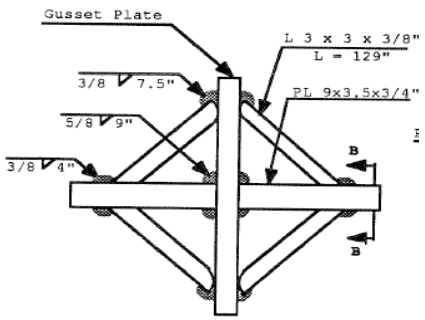

Axial Force - Axial Displacement Hysteresis

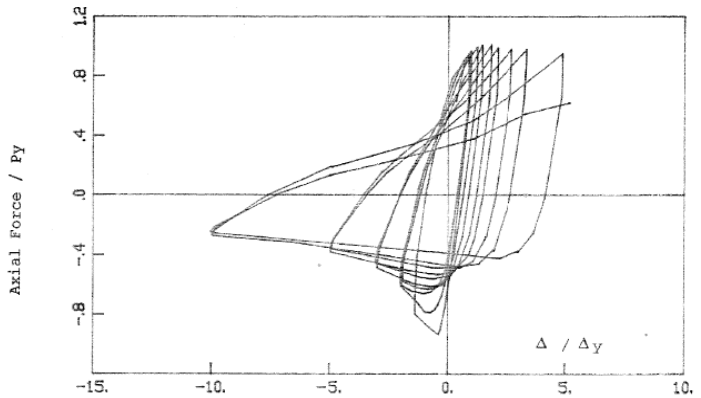

Drift Range (%)

Tens		Comp.		Total
0.82	to	-1.64	→	2.46

Noticable Damage

Damage	Drift (Δ/Δ_y)	Drift(%)
Initial Yield	2	0.33
Local Buckling	-10	-1.64
Initial Gap Closing	-	-
Complete Gap Closing	-	-
Complete Fracture	5.5	0.90

Used a continuous stitch plate

Damage Pictures

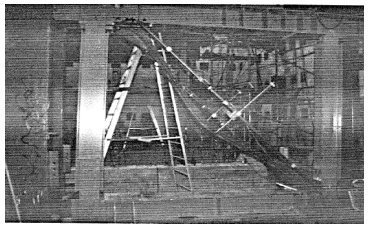

In-Plane Buckling

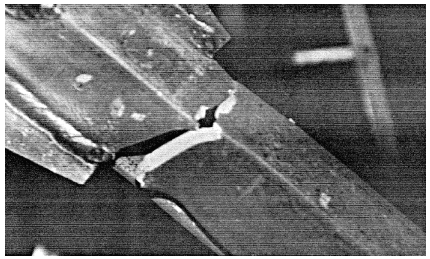

Net Section Fracture

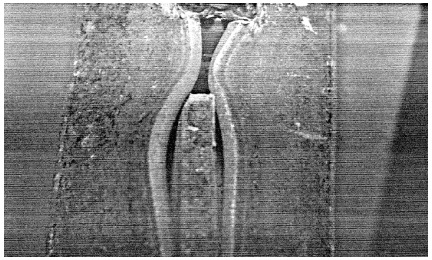

Local Buckling

Title:	Experimental and Analytical Study of the Inelastic Behavior of Double Angle Bracing Members Under Severe Cyclic Loading
Authors:	Farhang Aslani, Subash Goel
Year:	1989

Specimen	Section	Stitch Spacing (in)	A (in^2)	F_y (ksi)	P_y (kip)	Δ_y (in)	Axial Range (Δ/Δ_y)	
							Tens.	Comp.
AXH16	2L3x3x3/8	0	4.22	46.1	194.5	0.205	9	-10

Brace and Gusset Layout

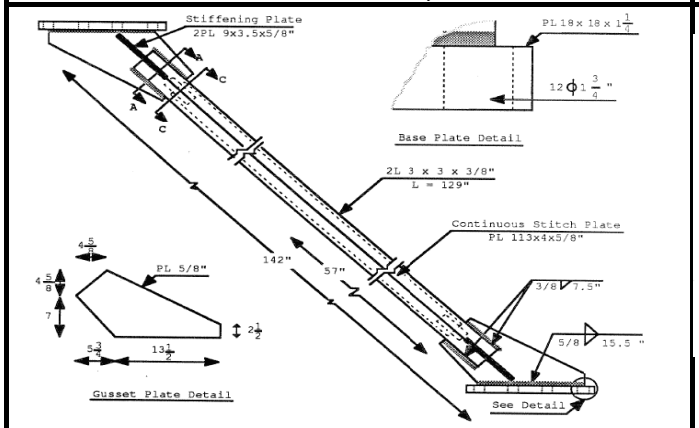

Connection Detail

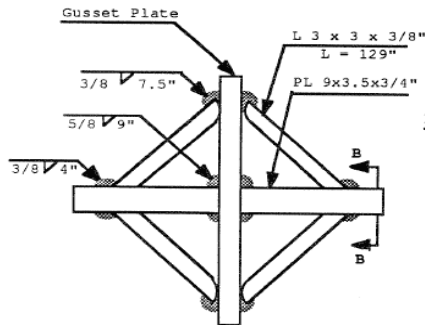

Axial Force - Axial Displacement Hysteresis

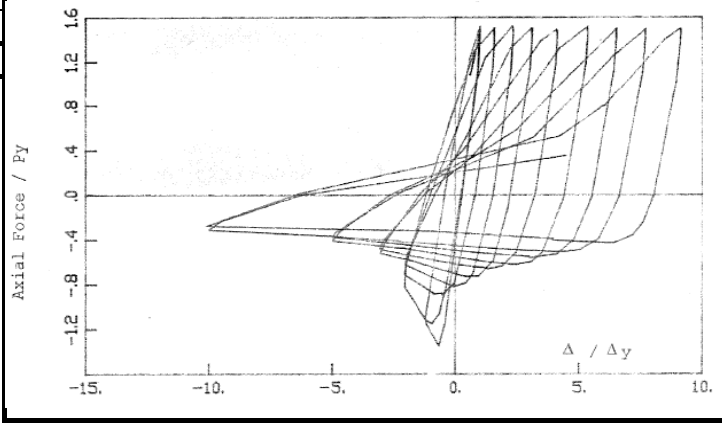

Drift Range (%)

Tens		Comp.		Total
1.43	to	-1.59	→	3.02

Noticable Damage

Damage	Drift (Δ/Δ_y)	Drift(%)
Initial Yield	2	0.32
Local Buckling	-10	-1.59
Initial Gap Closing	-	-
Complete Gap Closing	-	-
Complete Fracture	5	0.79

Used a continuous stitch plate

Damage Pictures

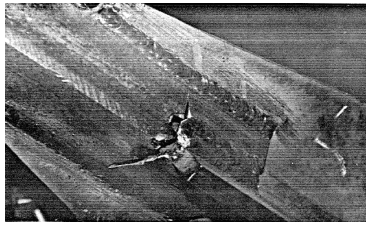

Crack at Brace on Gusset

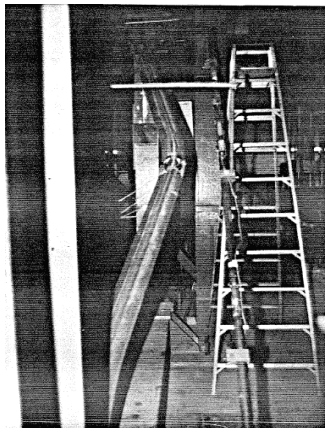

Buckling

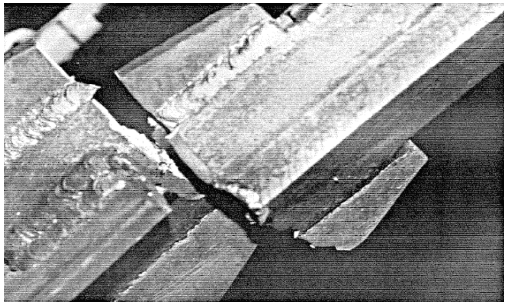

Fracture of Brace and Gusset

Title:	Experimental and Analytical Study of the Inelastic Behavior of Double Angle Bracing Members Under Severe Cyclic Loading
Authors:	Farhang Aslani, Subash Goel
Year:	1989

Specimen	Section	Stitch Spacing (in)	A (in^2)	F_y (ksi)	P_y (kip)	Δ_y (in)	Axial Range (Δ/Δ_y)	
							Tens.	Comp.
AXFS17	2L3x3x3/8	0	4.22	46.5	196.2	0.216	16	-10

Brace and Gusset Layout

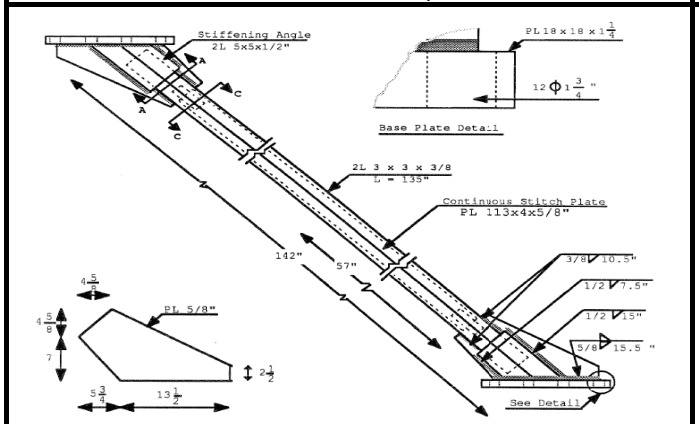

Connection Detail

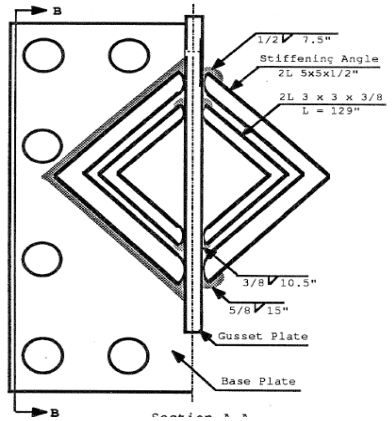

Axial Force - Axial Displacement Hysteresis

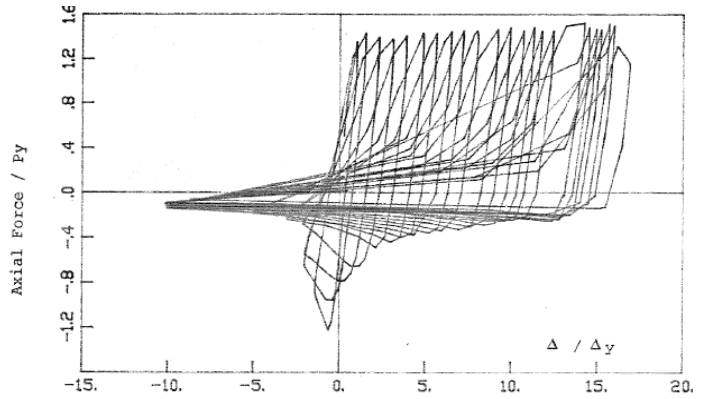

Drift Range (%)

Tens		Comp.		Total
2.57	to	-1.60	→	4.17

Noticable Damage

Damage	Drift (Δ/Δ_y)	Drift(%)
Initial Yield	2	0.32
Local Buckling	-2	-0.32
Fracture in SP Weld	-10	-1.60
Complete Gap Closing	-2	-0.32
Complete Fracture	-10	-1.60

Used a continuous stitch plate

Damage Pictures

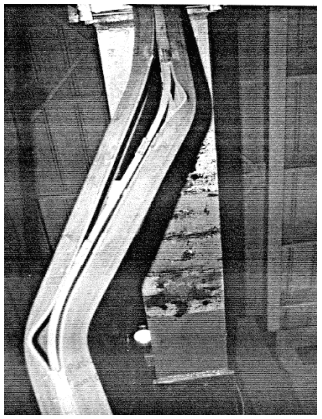

Failure of Stitch Plate

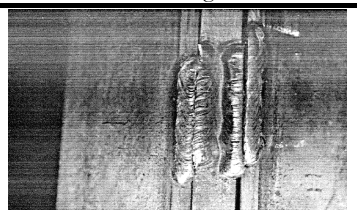

Fracture of Stitch Plate Weld

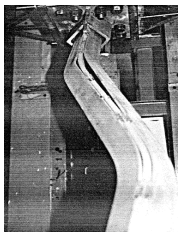

Excessive Gap Separation

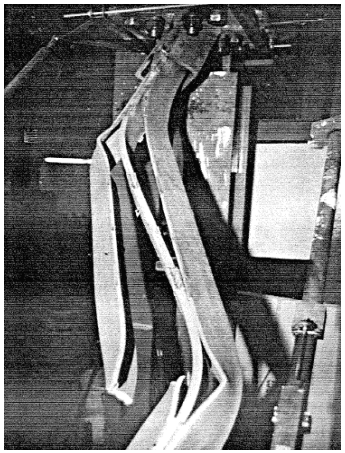

Fracture

Title:	Cyclic behavior of Angle X-Bracing With Welded Connections
Authors:	Adel A. El-Tayem, Subhash Goel
Year:	1985

Specimen	Brace Section	A (in^2)	F_y (ksi) (min)	P_y (kip)	L (brace) (in)	Δ_y (in)	Drift Range (Δ/Δ_y)	
							Tens.	Comp.
AW0	L2.5x2.5x1/4	1.19	41.5	49.4	137.0	0.196	7.75	-7.4

Brace Layout

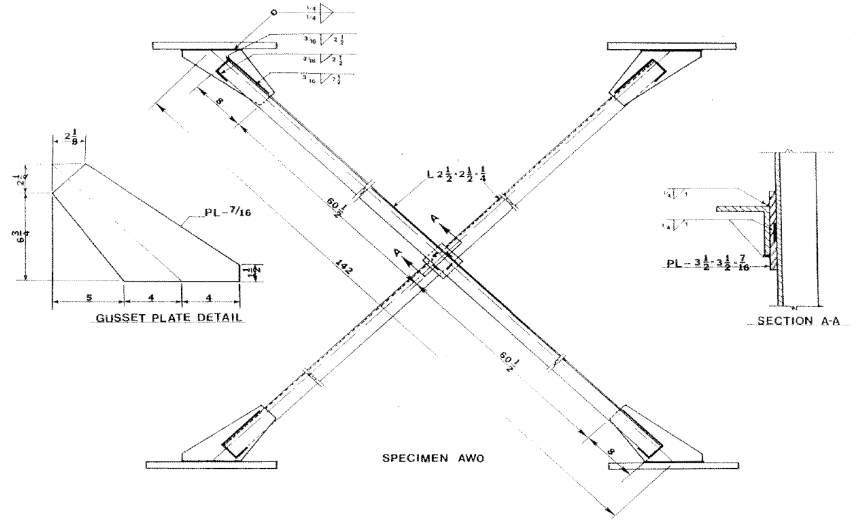

Noticable Damage

Damage	Drift (Δ/Δ_y)	Drift(%)
Initial Yielding	0.9	0.18
Local Buckling	3.6	0.70
Crack in Gusset Base Metal	-7.4	-1.44

F-D Hysteresis (Cycle 1-2)

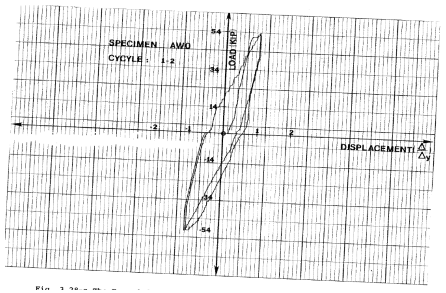

F-D Hysteresis (Cycle 3-10)

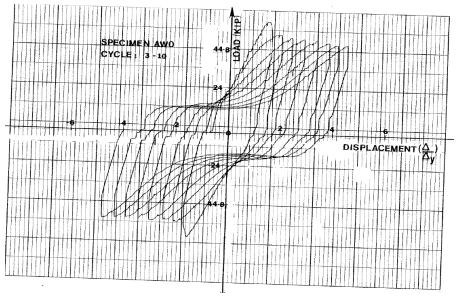

Damage Pictures

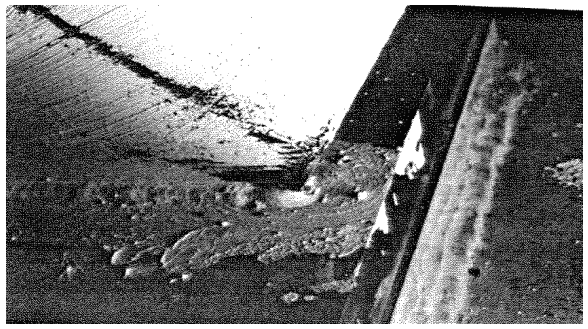

Crack in gusset plate base metal

F-D Hysteresis (Cycle 11-13)

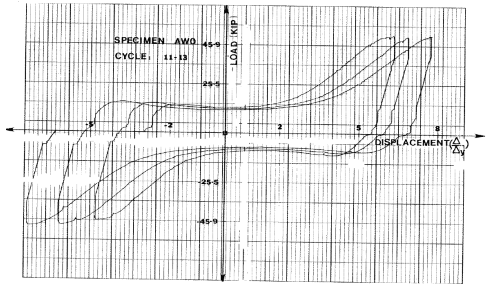

Drift Range

Tens		Comp.	Total
1.51	to	-1.44	2.96

Title:	Cyclic behavior of Angle X-Bracing With Welded Connections
Authors:	Adel A. El-Tayem, Subhash Goel
Year:	1985

Specimen	Brace	A (in^2)	F_y (ksi) (min)	P_y (kip)	L (brace) (in)	Δ_y (in)	Drift Range (Δ/Δ_y)	
							Tens.	Comp.
AW1	L4x4x1/4	1.94	41.8	81.1	129.3	0.186	14.4	-15.6

Brace Layout

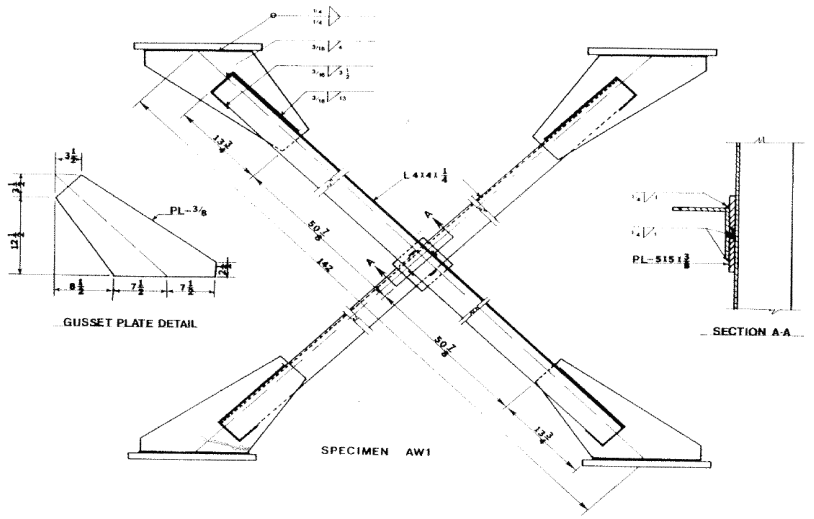

Noticable Damage

Damage	Drift (Δ/Δ_y)	Drift(%)
Initial Yielding	-	-
Local Buckling	5	0.93
Fracture of Intersection Joint Weld	-7.2	-1.34

Please note that the F-D Hysteresis loops are not available for cycles 10-30, instead the deformation history is presented below

F-D Hysteresis (Cycle 1-2)

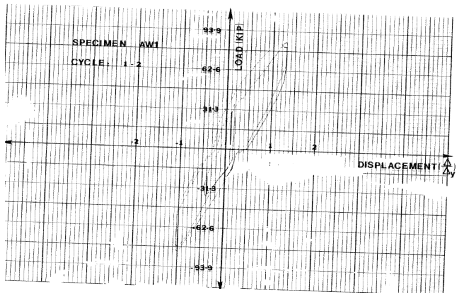

F-D Hysteresis (Cycle 3-5)

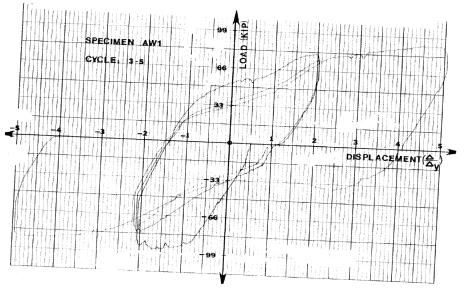

F-D Hysteresis (Cycle 6-9)

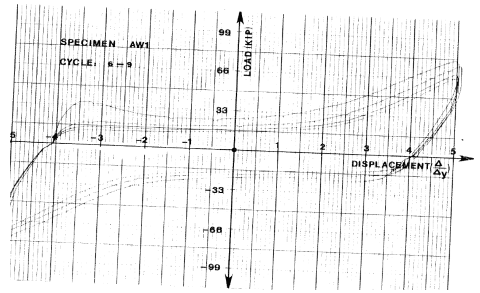

Damage Pictures

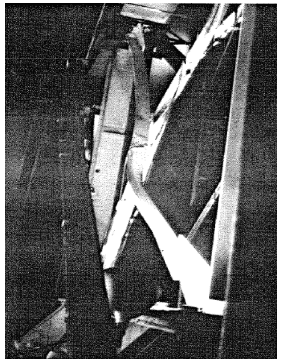

Biased Buckling

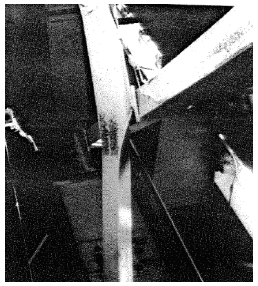

Intersection Joint Weld

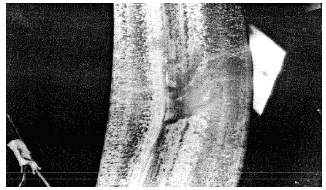

Initial Fracture

Cyclic Behavior

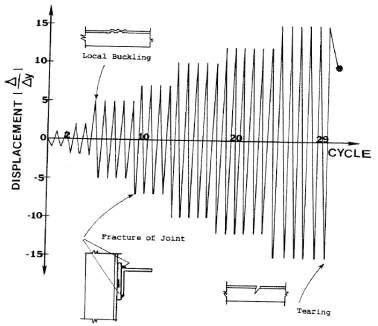

Drift Range

Tens		Comp.	Total
2.67	to	-2.89	5.57

Title:	Cyclic behavior of Angle X-Bracing With Welded Connections
Authors:	Adel A. El-Tayem, Subhash Goel
Year:	1985

Specimen	Brace	A (in^2)	F_y (ksi) (min)	P_y (kip)	L (brace) (in)	Δ_y (in)	Drift Range (Δ/Δ_y)	
							Tens.	Comp.
AW2	L4x4x3/8	2.86	36.2	103.5	128.8	0.161	12.5	-15

Brace Layout

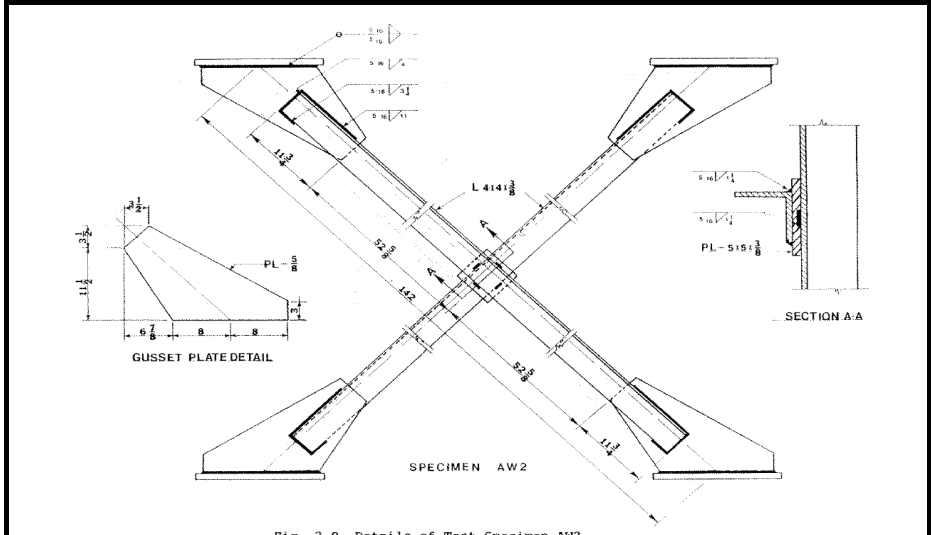

Fig. 2.9. Details of Test Specimen AW2

Noticable Damage

Damage	Drift (Δ/Δ_y)	Drift(%)
Initial Yielding	-	-
Local Buckling	-10	-1.60
Fracture of Intersection Joint Weld	9.8	1.57

Please note that the F-D Hysteresis loops are not available for cycles 10-27, instead the deformation history is presented below

F-D Hysteresis (Cycle 1-5)

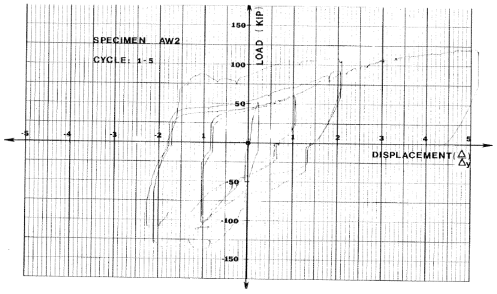

F-D Hysteresis (Cycle 6)

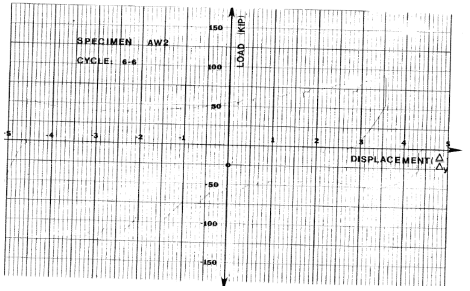

F-D Hysteresis (Cycle 8-9)

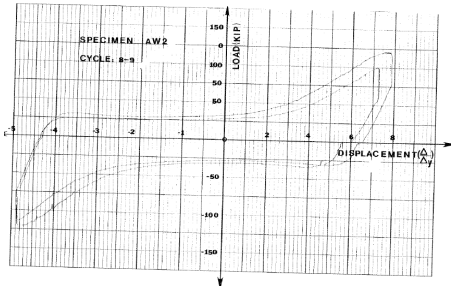

Damage Pictures

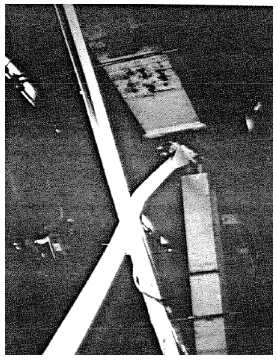

Biased Buckling

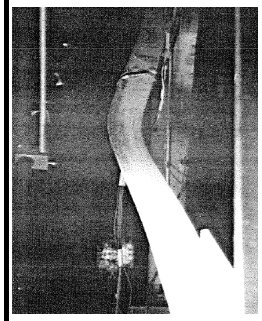

Buckled Shape

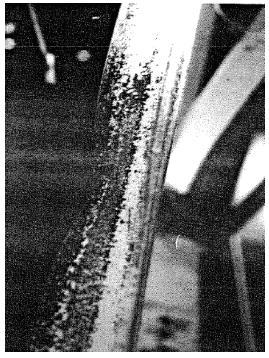

Local Buckling

Cyclic Behavior

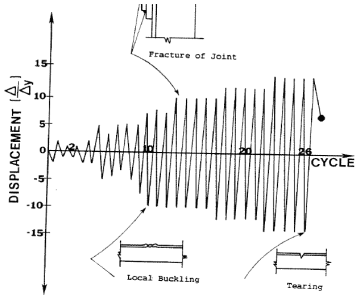

Drift Range

Tens		Comp.	Total
2.00	to	-2.40	4.40

Title:	Cyclic behavior of Angle X-Bracing With Welded Connections
Authors:	Adel A. El-Tayem, Subhash Goel
Year:	1985

Specimen	Brace	A (in^2)	F_y (ksi) (min)	P_y (kip)	L (brace) (in)	Δ_y (in)	Drift Range (Δ/Δ_y)	
							Tens.	Comp.
AW3	L2.5x2.5x5/16	1.46	38.3	55.9	134.0	0.177	9.2	-10.7

Brace Layout

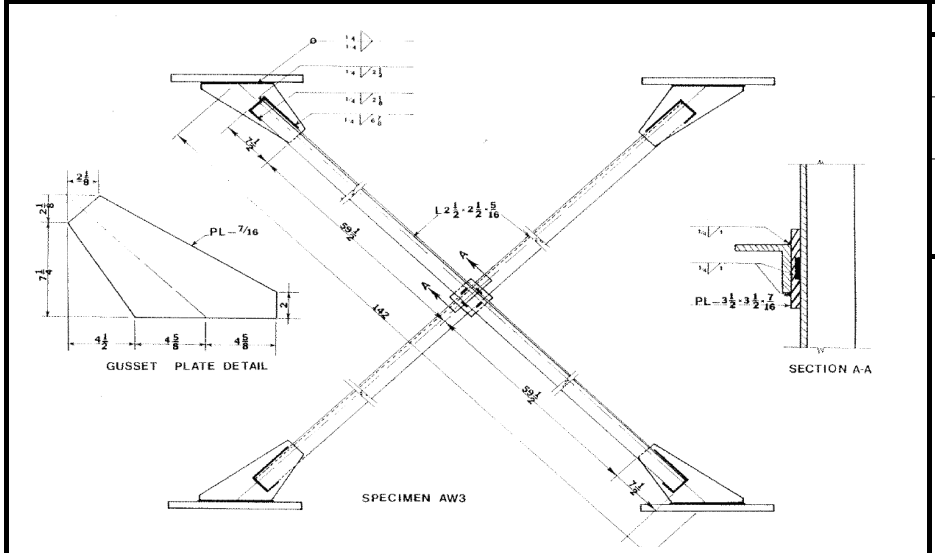

Noticable Damage

Damage	Drift (Δ/Δ_y)	Drift(%)
Initial Yielding	0.82	0.14
Local Buckling	6.5	1.15
Gusset Fatigue Fracture	-10.7	-1.89

F-D Hysteresis (Cycle 1-3)

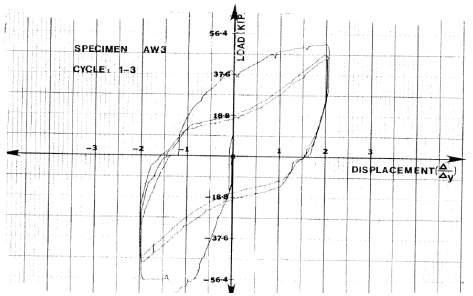

F-D Hysteresis (Cycle 4-8)

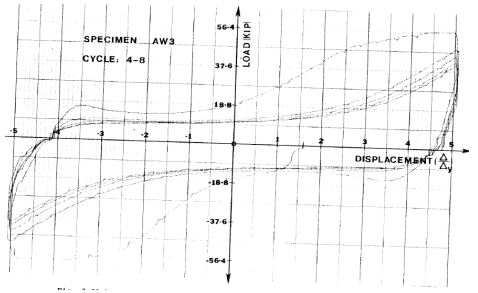

Damage Pictures

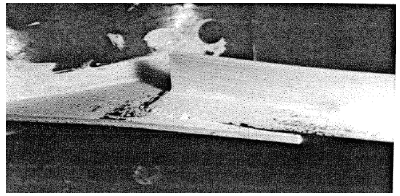

Gusset Hinging

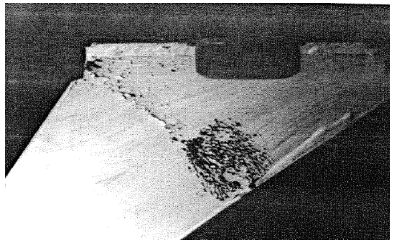

Initial Fatigue Fracture

Complete Gusset Fracture

F-D Hysteresis (Cycle 9-12)

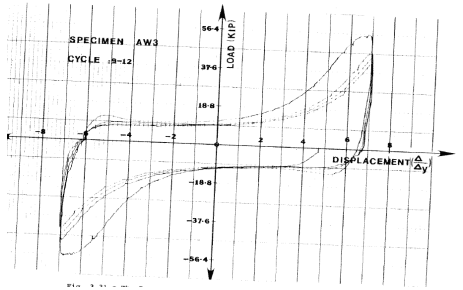

Drift Range

Tens		Comp.	Total
1.62	to	-1.89	3.51

Title:	Cyclic behavior of Angle X-Bracing With Welded Connections
Authors:	Adel A. El-Tayem, Subhash Goel
Year:	1985

Specimen	Brace	A (in^2)	F_y (ksi) (min)	P_y (kip)	L (brace) (in)	Δ_y (in)	Drift Range (Δ/Δ_y)	
							Tens.	Comp.
AW4	L2.5x2.5x3/16	0.902	43.4	39.1	136.0	0.204	6.4	-7.2

Brace Layout

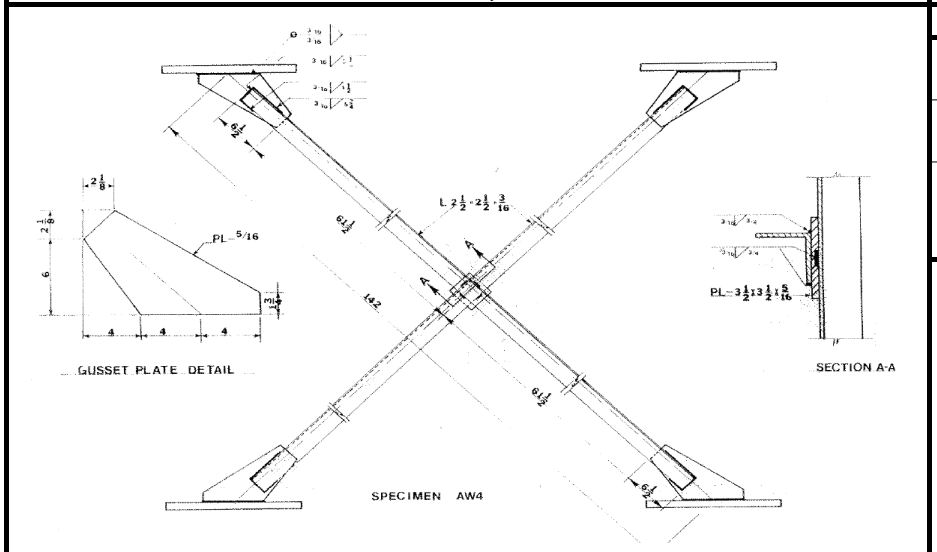

Noticable Damage

Damage	Drift (Δ/Δ_y)	Drift(%)
Initial Yielding	1.6	0.32
Local Buckling	4.7	0.95
Fracture of Brace Welds	-10.5	-2.13

F-D Hysteresis (Cycle 1-3)

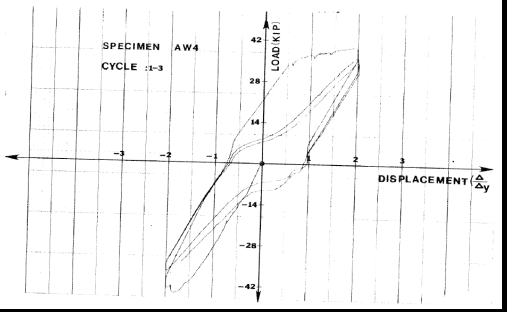

F-D Hysteresis (Cycle 4-8)

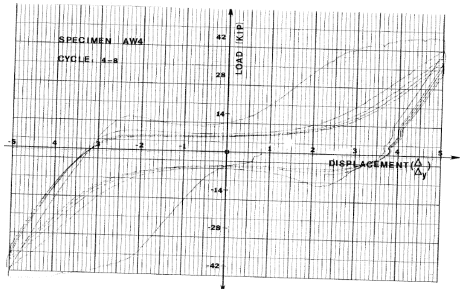

Damage Pictures

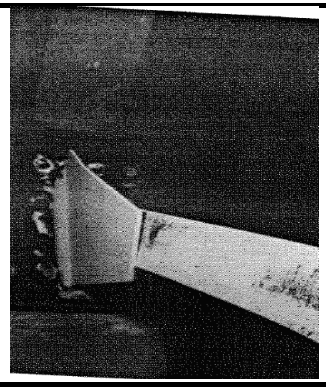

OOP Rotation of Gusset

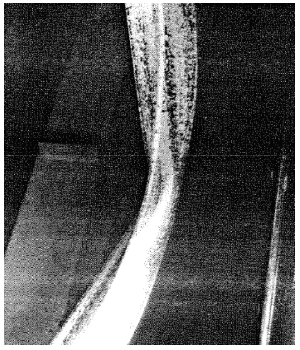

Local Buckling of Brace

Cyclic Behavior

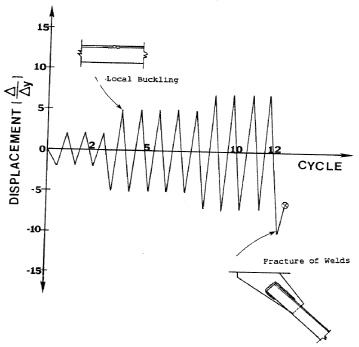

F-D Hysteresis (Cycle 9-12)

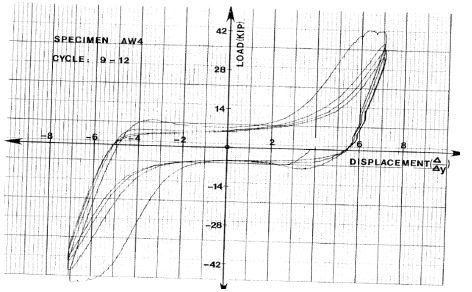

Drift Range

Tens		Comp.	Total
1.30	to	-1.46	2.76

Title:	Preliminary Report on Seismic Testing of a Full-Scale Six-Story Steel Building
Authors:	Douglas Foutch, Subash Goel,Charles Roeder
Year:	1986

Experiment Setup

Frame Plan

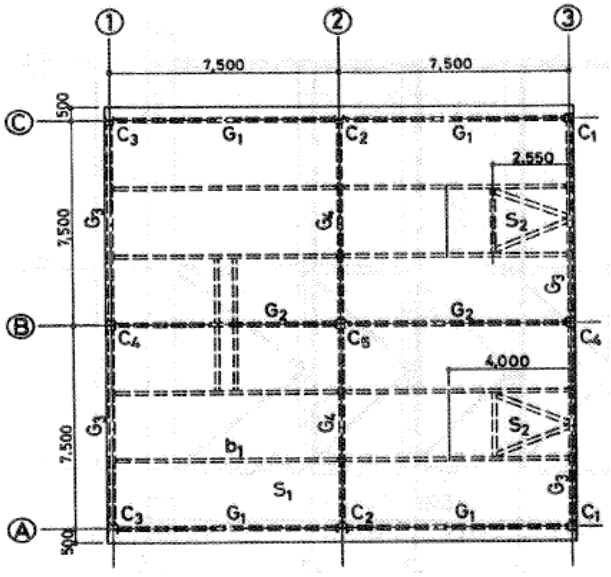

Frame Elevation

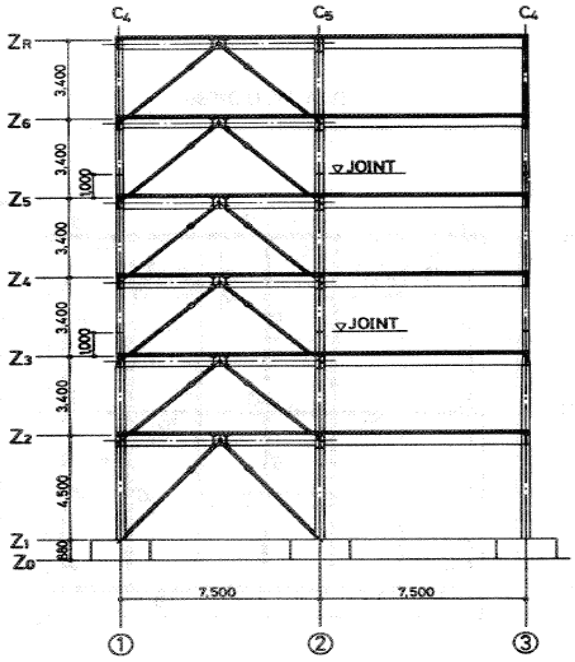

Member Sizes

	Columns					Floor Beam	Brace
Story	C1	C2	C3	C4	C5	b1	
6	W10x49	W10x33	W10x33	W10x33	W12x40	W16x31	ST4x4x3/16
5	W10x49	W10x33	W10x33	W10x33	W12x40	W16x31	ST4x4x3/16
4	W12x65	W12x53	W10x39	W10x60	W12x72	W16x31	ST5x5x1/4
3	W12x65	W12x53	W10x39	W10x60	W12x72	W16x31	ST6x6x1/4
2	W12x79	W12x65	W12x50	W12x79	W12x103	W16x31	ST6x6x1/4
1	W12x87	W12x87	W12x65	W12x106	W12x136	W16x31	ST6x6x1/4

	Girders			
Story	G1	G2	G3	G4
Roof	W16x31	W16x31	W18x35	W21x50
6F	W16x31	W16x31	W18x35	W21x50
5F	W16x31	W18x35	W18x35	W21x50
4F	W18x35	W18x35	W18x35	W21x50
3F	W18x35	W18x40	W18x35	W21x50

Miyagi-ken
Acceleration Record
Used for Experiment

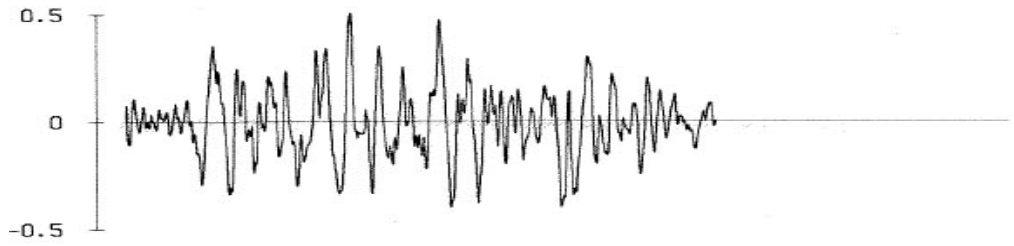

Moderate Shaking

1st Story Response

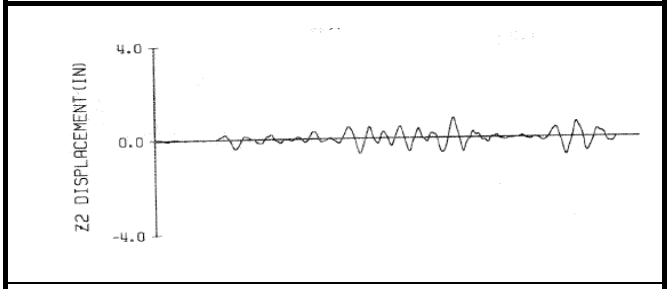

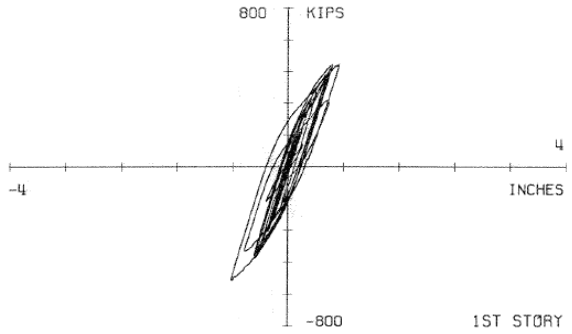

2nd Story Response

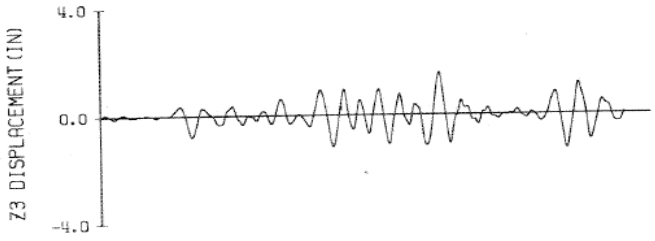

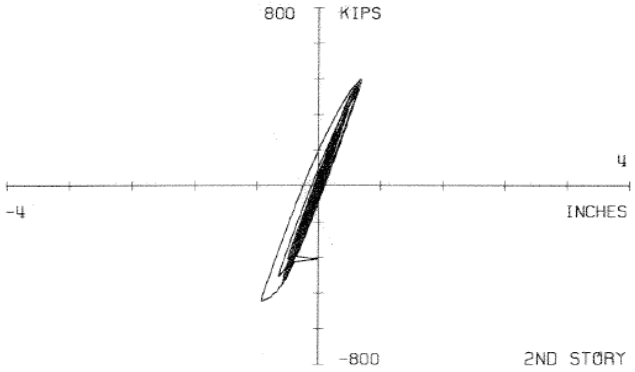

3rd Story Response

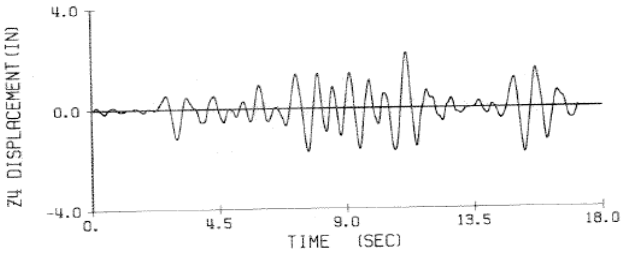

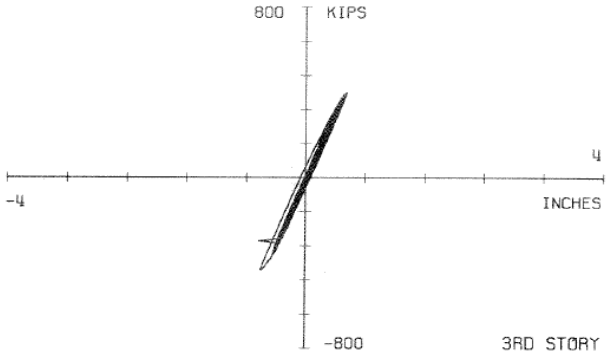

4th Story Response

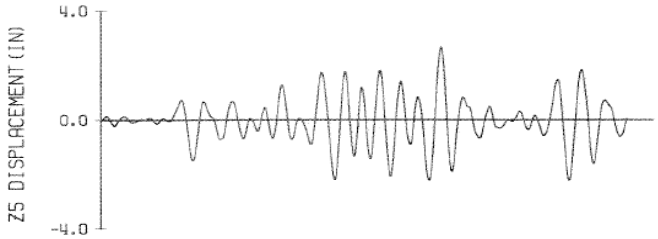

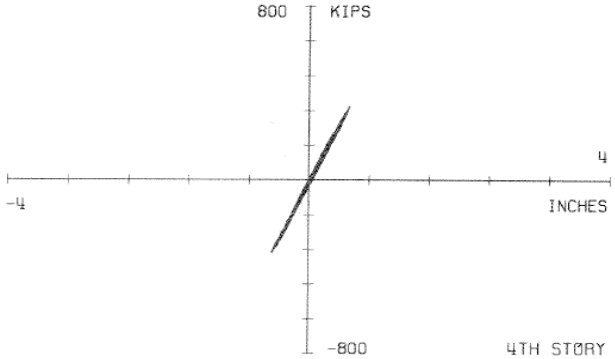

Moderate Shaking

5th Story Response	6th Story Response
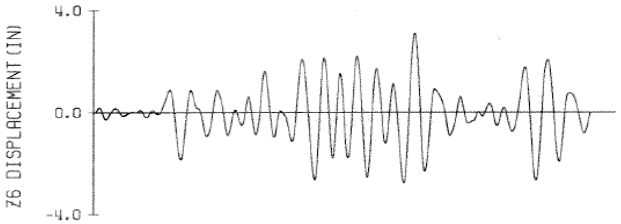	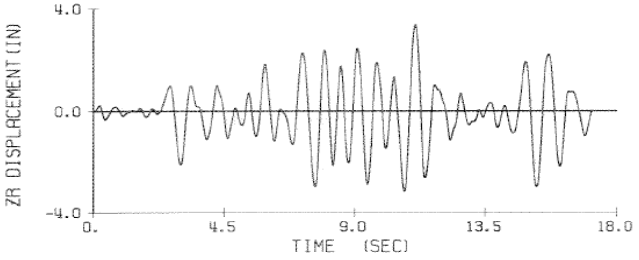
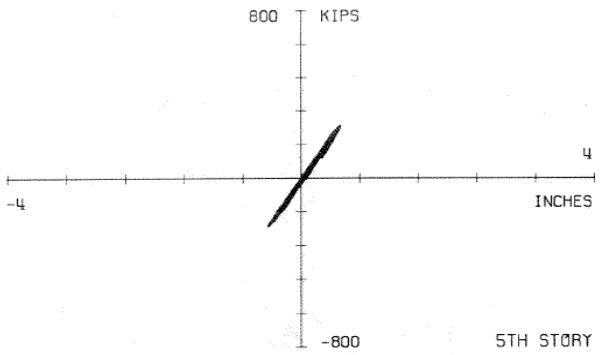	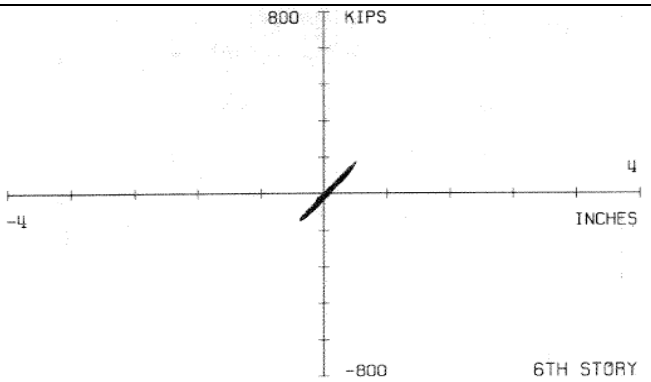

Moderate Shaking Damage Summary

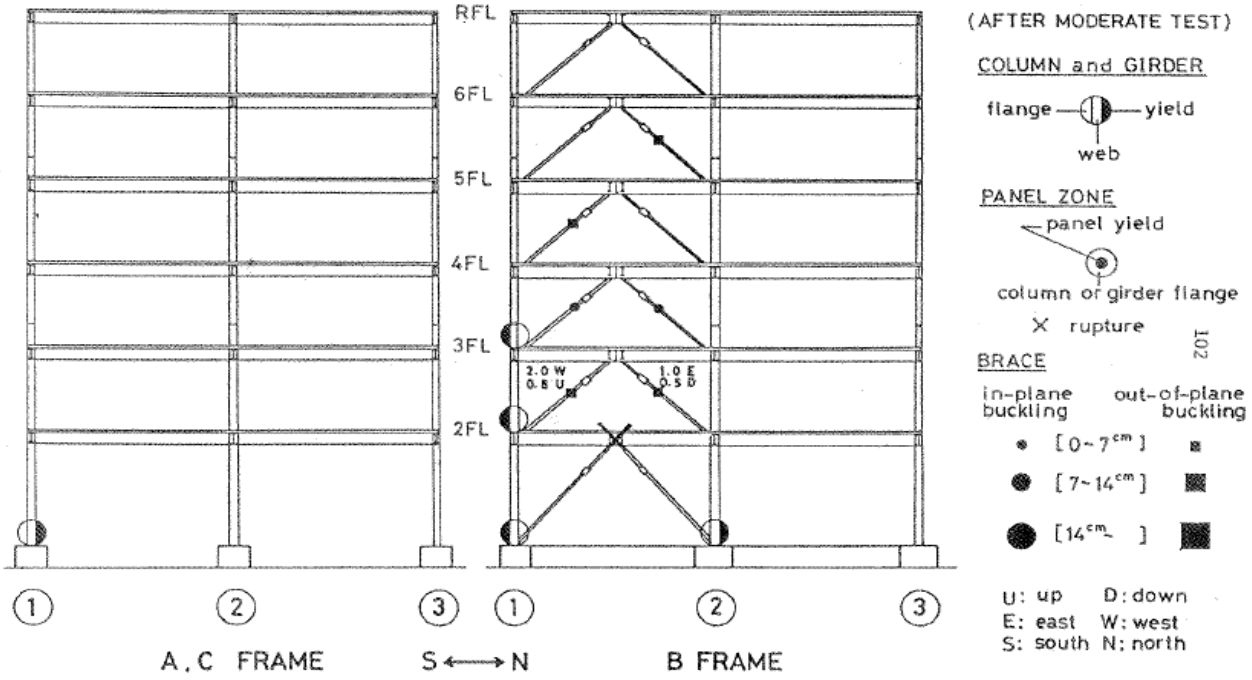

Severe Shaking

1st Story Response	2nd Story Response
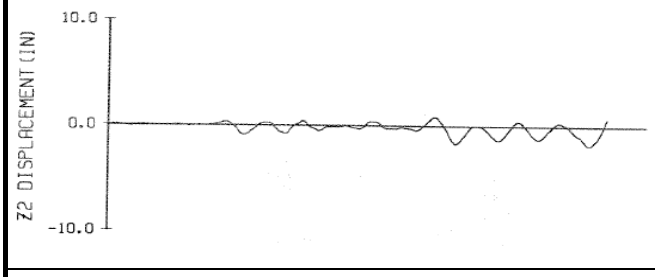	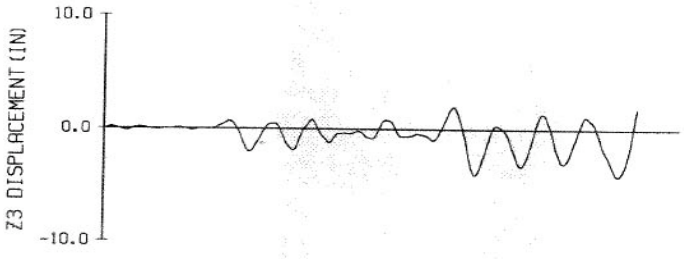
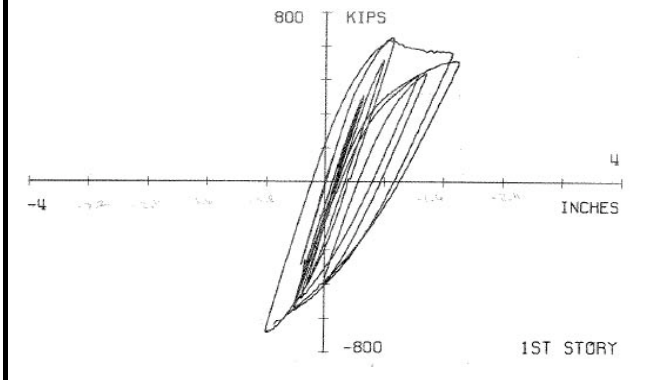	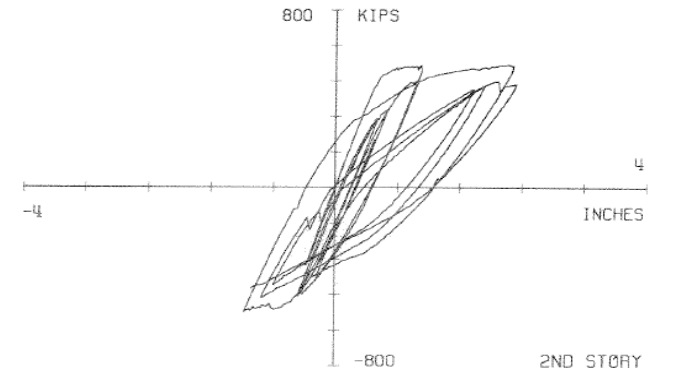
3rd Story Response	4th Story Response
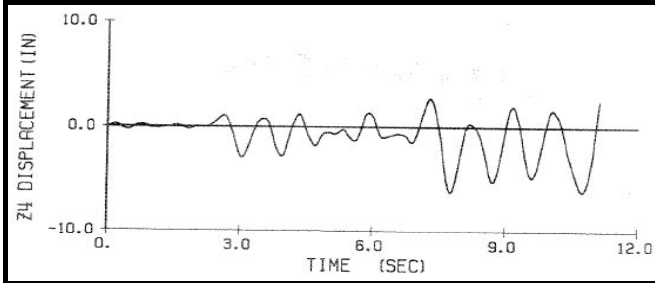	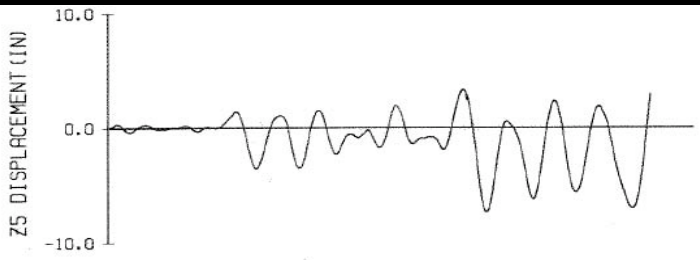
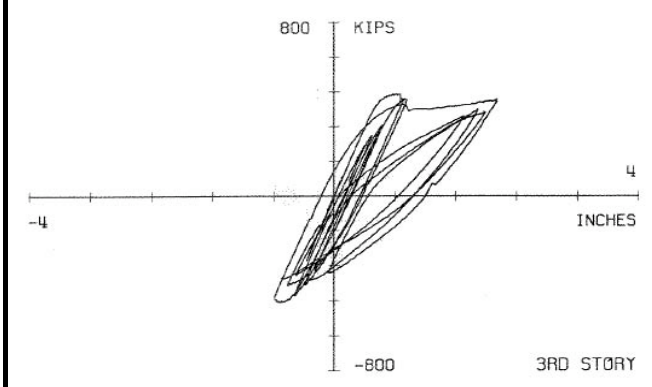	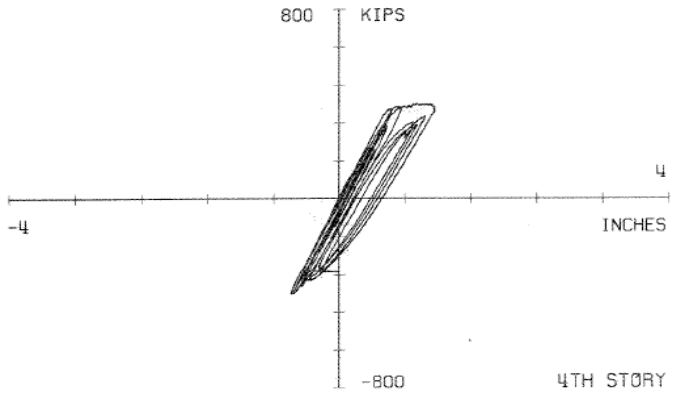

Severe Shaking

5th Story Response	6th Story Response
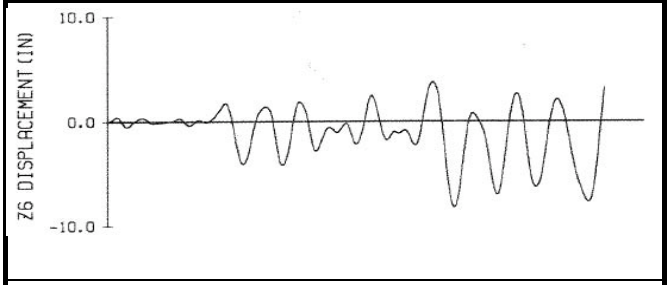	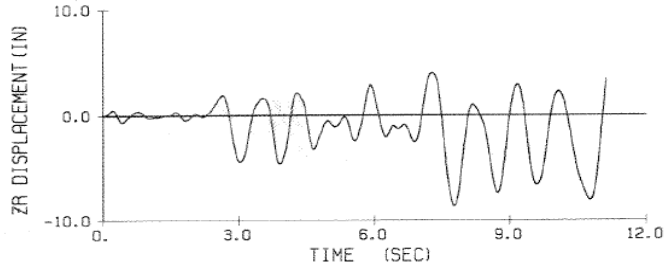
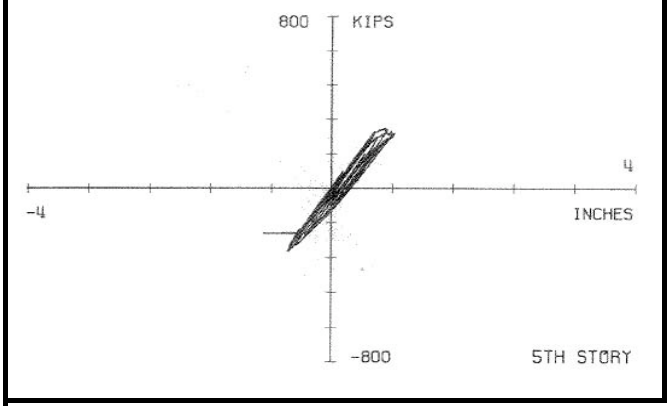	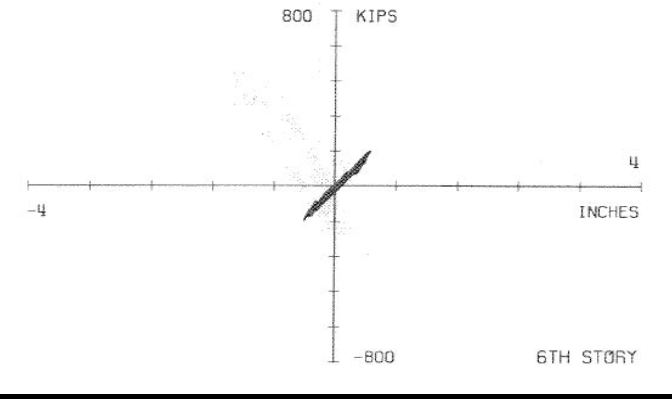

Severe Shaking Damage Summary

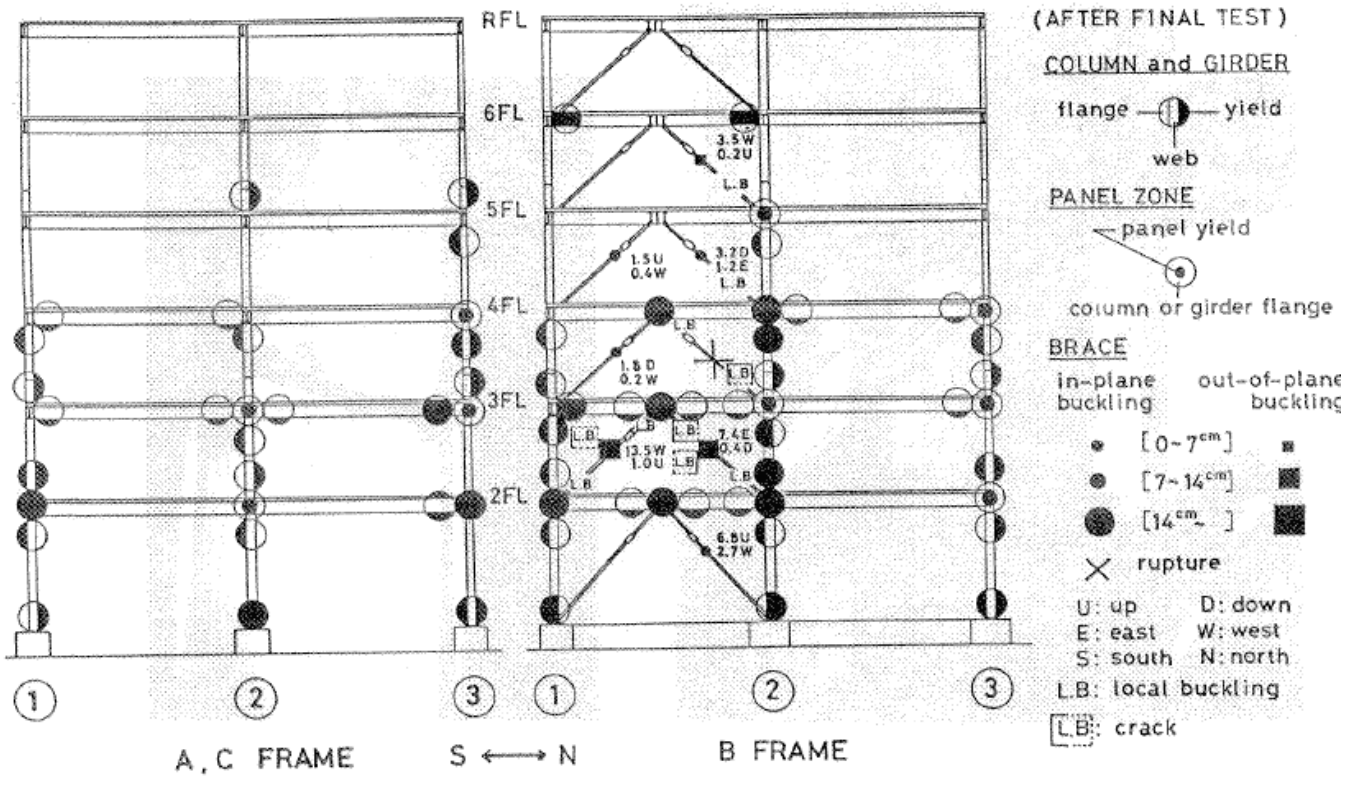

Damage Summary by Story Drift											
Moderate Shaking											
Story	Height	Drift	Drift	Beam Yielding		Column Yielding		Brace Buckling (cm)			Brace
	(in)	(in)	(%)	Web	Flange	Web	Flange	0 to 7	7 to 14	>14	Fracture
1	177.2	0.8	0.45								
2	133.9	0.75	0.56					2 -OOP			
3	133.9	0.6	0.45					2 -IP			
4	133.9	0.6	0.45					1 -OOP			
5	133.9	0.55	0.41					1 -OOP			
6	133.9	0.4	0.30								
Severe Shaking											
Story	Height	Drift	Drift	Beam Yielding		Column Yielding		Brace Buckling (cm)			Brace
	(in)	(in)	(%)	Web	Flange	Web	Flange	0 to 7	7 to 14	>14	Fracture
1	177.2	1.80	1.02					1-IP			
2	133.9	2.40	1.79						2-OOP		
3	133.9	2.20	1.64					1-IP			1
4	133.9	1.20	0.90					2-IP			
5	133.9	0.80	0.60					1-OOP			
6	133.9	0.50	0.37								

Title:	Part 2: Experimental Studies on the Elastic-Plastic Behavior of Braced Frames under Repeated Horizontal Loading												
Authors:	Minoru Wakabayshi, Takeshi Nakamura, Nozomu Yoshida												
Year:	1979												
Designation	Bracing	Config.	B (cm)	t (cm)	L (cm)	A (cm2)	Q_y (KN)	Δ_y (cm)	Initial Brace Buckling (%)	Initial Brace Local Buckling (%)	Initial Brace Cracking (%)	Brace Fracture (%)	Other
SPC 3	Circular Tube	Single Brace	4.29	0.345	296.9	4.28	127.20	0.884	0.13	-	1.11	1.46	-
	Force-Dirft Hysteresis							Test Layout			Damage Pictures		
	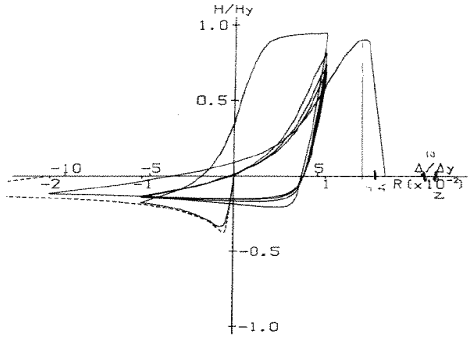							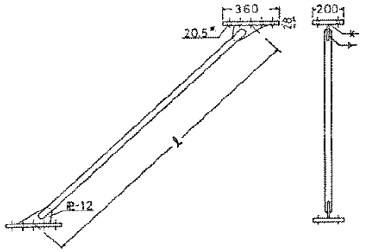					
	Drift Range	-2.00%	to	1.46%	→	3.46%	Total						
Designation	Bracing	Config.	B (cm)	t (cm)	L (cm)	A (cm2)	Q_y (KN)	Δ_y (cm)	Initial Brace Buckling (%)	Initial Brace Local Buckling (%)	Initial Brace Cracking (%)	Brace Fracture (%)	Other
DPC 1	Circular Tube	X-Bracing	4.3	0.346	98.3	4.30	127.86	0.293	0.22	-	-0.81	-3.88	-
	Force-Dirft Hysteresis							Test Layout			Damage Pictures		
	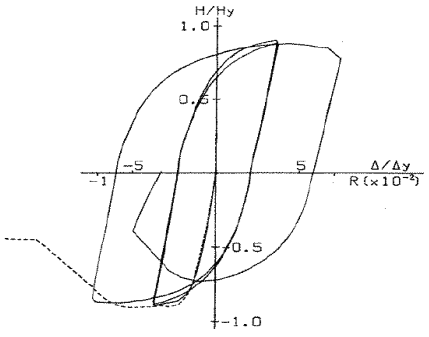							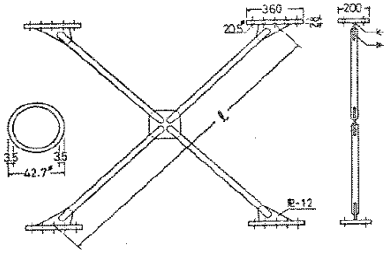			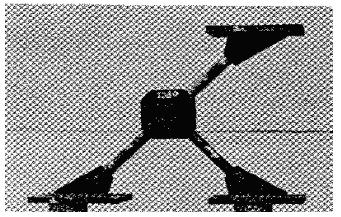		
	Drift Range	-1.00%	to	1.00%	→	2.00%	Total						

Title:	Part 2: Experimental Studies on the Elastic-Plastic Behavior of Braced Frames under Repeated Horizontal Loading												
Authors:	Minoru Wakabayshi, Takeshi Nakamura, Nozomu Yoshida												
Year:	1979												
Designation	Bracing	Config.	B (cm)	t (cm)	L (cm)	A (cm2)	Q_y (KN)	Δ_y (cm)	Initial Brace Buckling (%)	Initial Brace Local Buckling (%)	Initial Brace Cracking (%)	Brace Fracture (%)	Other
SAC 3	Double Angle	Single Brace	5.01	0.381	297.2	7.34	180.81	0.732	0.07	-0.08	1.01	-	-
	Force-Dirft Hysteresis							Test Layout			Damage Pictures		
	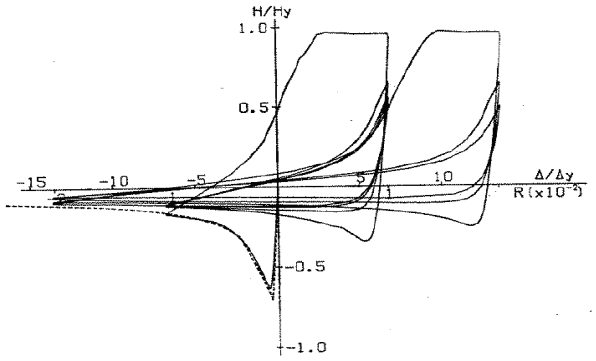							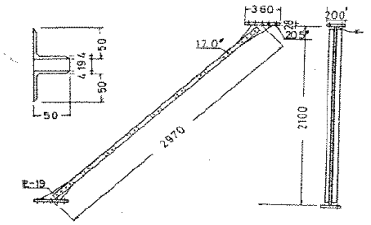			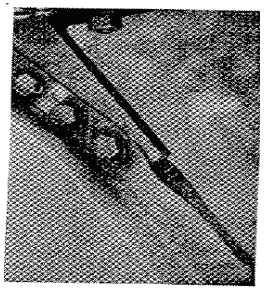		
	Drift Range	-3.42%	to	2.00%	→	5.42%	Total						
Designation	Bracing	Config.	B (cm)	t (cm)	L (cm)	A (cm2)	Q_y (KN)	Δ_y (cm)	Initial Brace Buckling (%)	Initial Brace Local Buckling (%)	Initial Brace Cracking (%)	Brace Fracture (%)	Other
DAC 2	Double Angle	X-Bracing	5	0.38	198.3	7.31	179.98	0.488	0.32	-0.33	1.1	2.25	-
	Force-Dirft Hysteresis							Test Layout			Damage Pictures		
	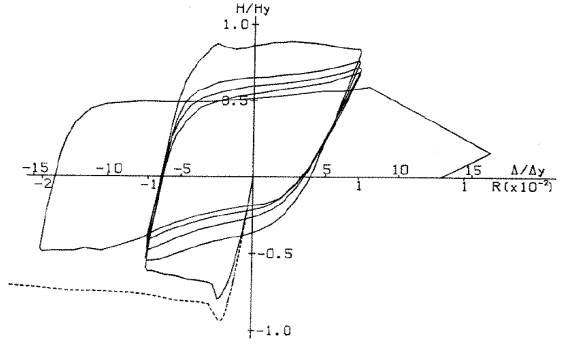							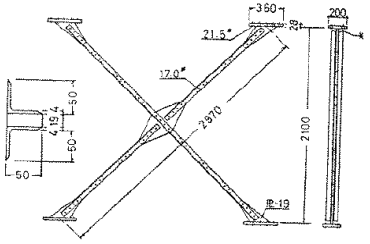					
	Drift Range	-2.00%	to	2.25%	→	4.25%	Total						

Title:	Part 1: Experimental Studies on the Elastic-Plastic Behavior of Braced Frames under Repeated Horizontal Loading											
Authors:	Minoru Wakabayshi, Takeshi Nakamura, Nozomu Yoshida											
Year:	1977											
Designation	Bracing	Config.	B (cm)	D (cm)	t_w (cm)	t_f (cm)	L (cm)	A (cm2)	Q_y (KN)	Δ_y (cm)	Initial Brace Local Buckling (%)	Initial Brace Cracking (%)
SIC 1	Wide Flange	Single Brace	5.00	5.01	0.626	0.597	98.47	8.51	170.54	0.197	-3.00	3.00
	Force-Dirft Hysteresis							Initial Brace Buckling (%)			0.29	
	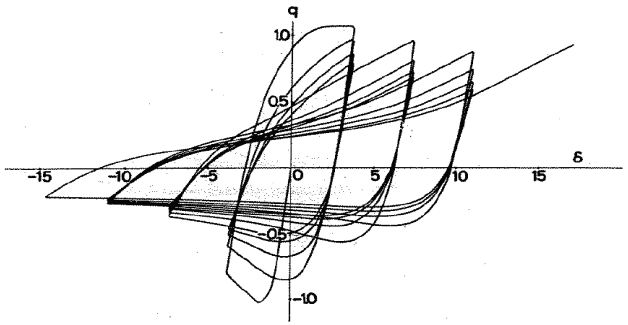							Test Layout				
								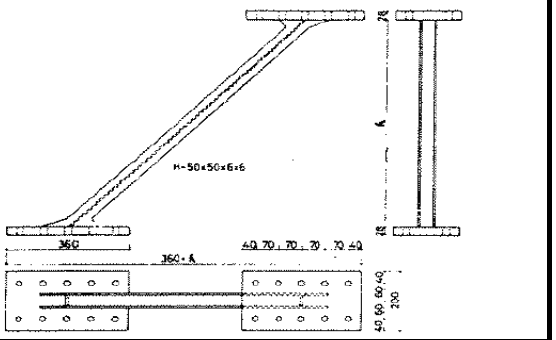				
	Drift Range	-4.25%	to	3.12%	→	7.37%	Total					
Designation	Bracing	Config.	B (cm)	D (cm)	t_w (cm)	t_f (cm)	L (cm)	A (cm2)	Q_y (KN)	Δ_y (cm)	Initial Brace Local Buckling (%)	Initial Brace Cracking (%)
DIC 1	Wide Flange	X-Bracing	4.99	5.07	0.61	0.599	98.82	8.49	340.28	0.198	-2.00	2.00
	Force-Dirft Hysteresis							Initial Brace Buckling (%)			0.25	
	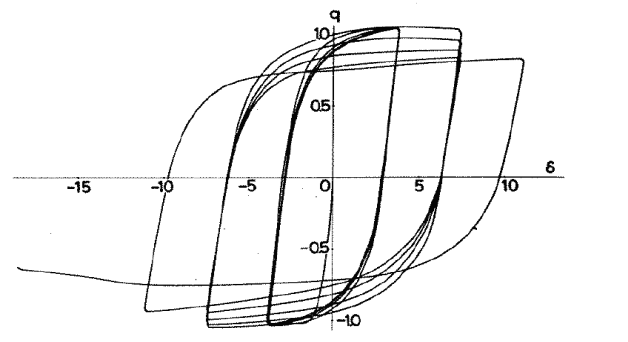							Test Layout				
								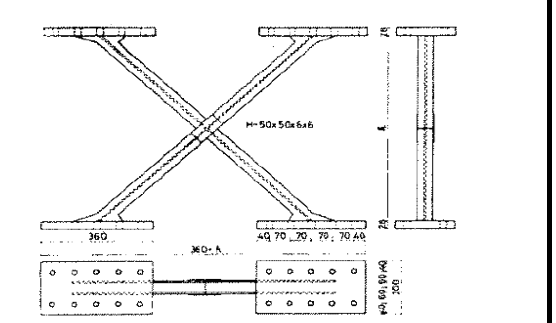				
	Drift Range	-3.12%	to	3.12%	→	6.24%	Total					

Title:	Part 1: Experimental Studies on the Elastic-Plastic Behavior of Braced Frames under Repeated Horizontal Loading
Authors:	Minoru Wakabayshi, Takeshi Nakamura, Nozomu Yoshida
Year:	1977

Designation	Bracing	Config.	B (cm)	D (cm)	t_w (cm)	t_f (cm)	L (cm)	A (cm2)	Q_y (KN)	Δ_y (cm)	Initial Brace Local Buckling (%)	Initial Brace Cracking (%)
DOC 1	Wide Flange	X-Bracing	5.01	4.97	0.596	0.601	99.2	8.24	330.26	0.199	-2.00	4.00

Force-Dirft Hysteresis

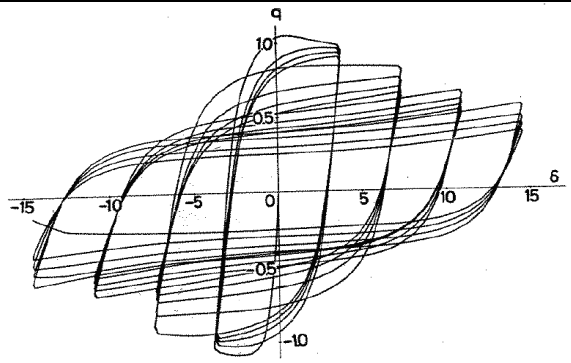

Drift Range -4.25% to 4.25% → 8.51% Total

Test Layout

Initial Brace Buckling (%) 0.20

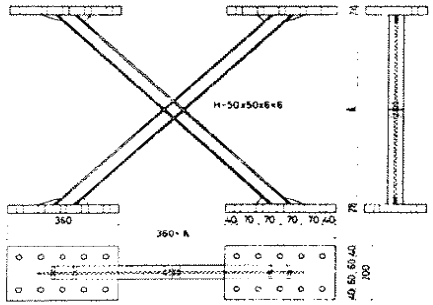

Designation	Bracing	Config.	B (cm)	D (cm)	t_w (cm)	t_f (cm)	L (cm)	A (cm2)	Q_y (KN)	Δ_y (cm)	Initial Brace Local Buckling (%)	Initial Brace Cracking (%)
DOC 2	Wide Flange	X-Bracing	5.02	4.93	0.611	0.61	197.8	8.34	334.27	0.397	-4.00	4.00

Force-Dirft Hysteresis

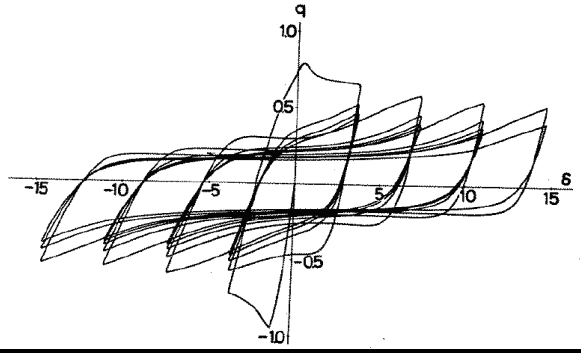

Drift Range -4.25% to 4.25% → 8.51% Total

Initial Brace Buckling (%) 0.42

Test Layout

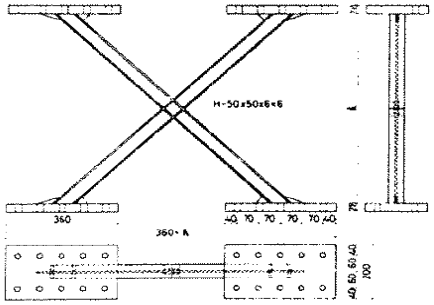

Title:	Part 1: Experimental Studies on the Elastic-Plastic Behavior of Braced Frames under Repeated Horizontal Loading											
Authors:	Minoru Wakabayshi, Takeshi Nakamura, Nozomu Yoshida											
Year:	1977											
Designation	Bracing	Config.	B (cm)	D (cm)	t_w (cm)	t_f (cm)	L (cm)	A (cm2)	Q_y (KN)	Δ_y (cm)	Initial Brace Local Buckling (%)	Initial Brace Cracking (%)
SIC 2	Wide Flange	Single Brace	5.05	5.04	0.602	0.598	197	8.37	335.47	0.395	-	3.00
	Force-Dirft Hysteresis							Initial Brace Buckling (%)			0.18	
	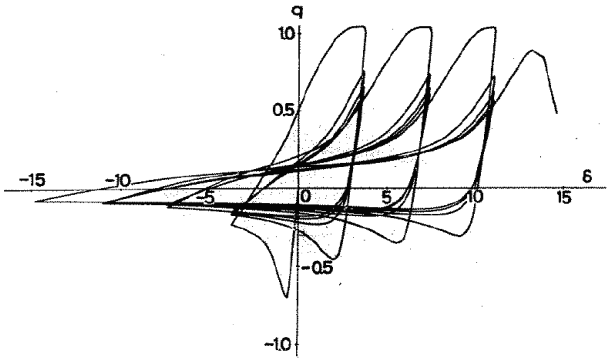							Test Layout				
								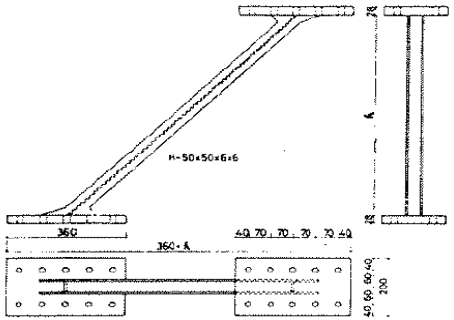			
	Drift Range	-4.25%	to	3.12%	→	7.37%	Total					
Designation	Bracing	Config.	B (cm)	D (cm)	t_w (cm)	t_f (cm)	L (cm)	A (cm2)	Q_y (KN)	Δ_y (cm)	Initial Brace Local Buckling (%)	Initial Brace Cracking (%)
SIC 3	Wide Flange	Single Brace	4.97	4.99	0.602	0.583	297.2	8.19	291.91	0.530	-	-
	Force-Dirft Hysteresis							Initial Brace Buckling (%)			0.07	
	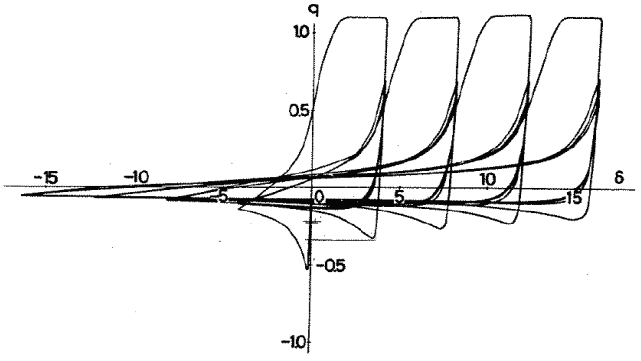							Test Layout				
								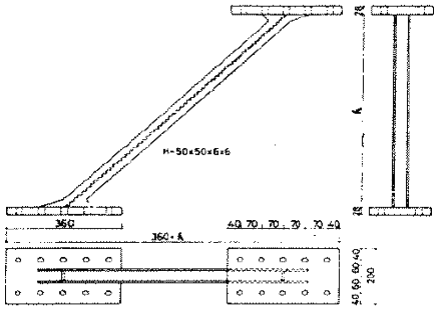			
	Drift Range	-4.10%	to	4.03%	→	8.13%	Total					

Title:	Part 1: Experimental Studies on the Elastic-Plastic Behavior of Braced Frames under Repeated Horizontal Loading
Authors:	Minoru Wakabayshi, Takeshi Nakamura, Nozomu Yoshida
Year:	1977

Designation	Bracing	Config.	B (cm)	D (cm)	t_w (cm)	t_f (cm)	L (cm)	A (cm2)	Q_y (KN)	Δ_y (cm)	Initial Brace Local Buckling (%)	Initial Brace Cracking (%)
SOC 1	Wide Flange	Single Brace	4.93	4.92	0.631	0.592	98.93	8.39	336.28	0.198	-2.00	-

Force-Dirft Hysteresis	Initial Brace Buckling (%)	0.37

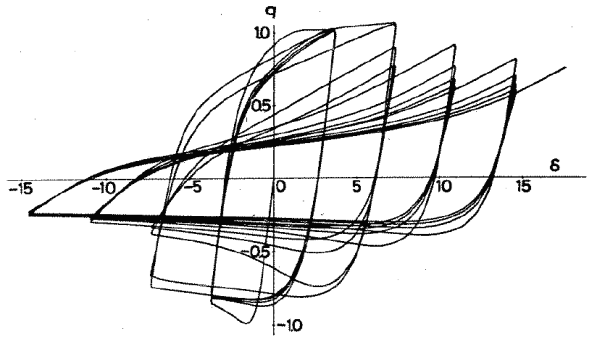

Test Layout

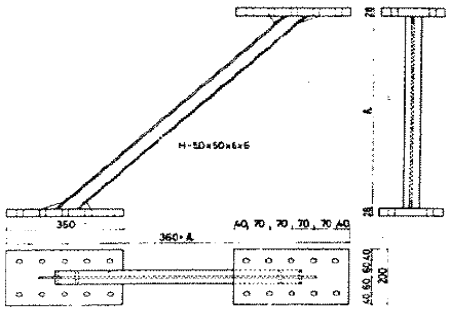

Drift Range -4.11% to 4.11% → 8.22% Total

Designation	Bracing	Config.	B (cm)	D (cm)	t_w (cm)	t_f (cm)	L (cm)	A (cm2)	Q_y (KN)	Δ_y (cm)	Initial Brace Local Buckling (%)	Initial Brace Cracking (%)
SOC 2	Wide Flange	Single Brace	5.04	4.94	0.614	0.603	197	8.43	337.88	0.395	-	-

Force-Dirft Hysteresis	Initial Brace Buckling (%)	0.18

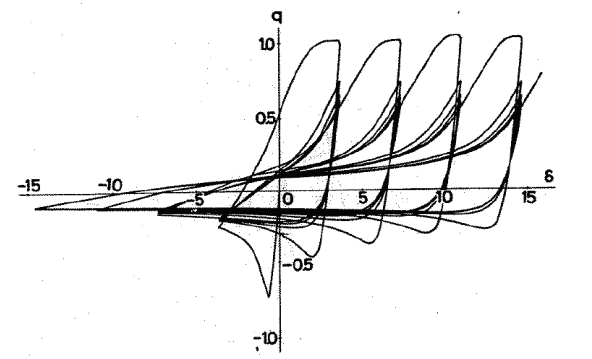

Test Layout

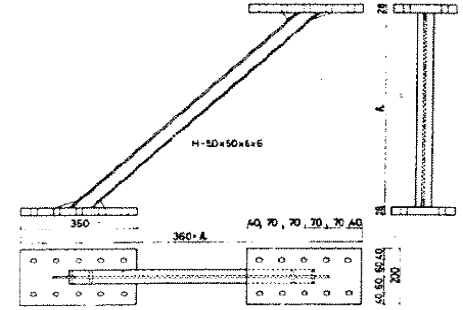

Drift Range -4.11% to 4.11% → 8.22% Total

Title:	Part 1: Experimental Studies on the Elastic-Plastic Behavior of Braced Frames under Repeated Horizontal Loading											
Authors:	Minoru Wakabayshi, Takeshi Nakamura, Nozomu Yoshida											
Year:	1977											
Designation	Bracing	Config.	B (cm)	D (cm)	t_w (cm)	t_f (cm)	L (cm)	A (cm2)	Q_y (KN)	Δ_y (cm)	Initial Brace Local Buckling (%)	Initial Brace Cracking (%)
SOC 3	Wide Flange	Single Brace	5.00	5.01	0.597	0.596	296.8	8.24	293.69	0.529	-	-
	Force-Dirft Hysteresis							Initial Brace Buckling (%)			0.05	
	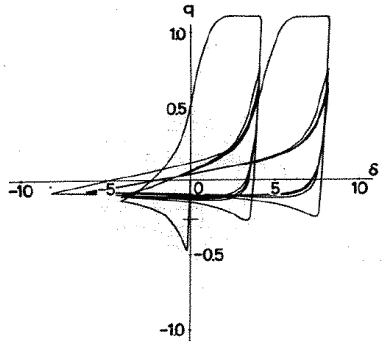							Test Layout 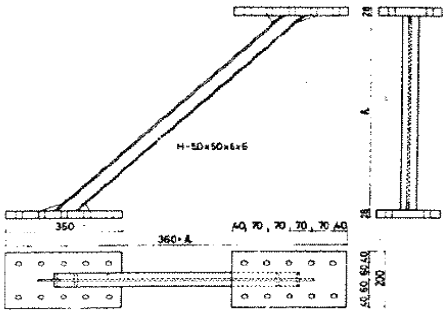				
	Drift Range	-2.02%	to	2.02%	→	4.03%	Total					
Designation	Bracing	Config.	B (cm)	D (cm)	t_w (cm)	t_f (cm)	L (cm)	A (cm2)	Q_y (KN)	Δ_y (cm)	Initial Brace Local Buckling (%)	Initial Brace Cracking (%)
DIC 2	Wide Flange	X-Bracing	4.99	4.95	0.604	0.594	197.9	8.34	334.27	0.397	-	2.00
	Force-Dirft Hysteresis							Initial Brace Buckling (%)			0.28	
	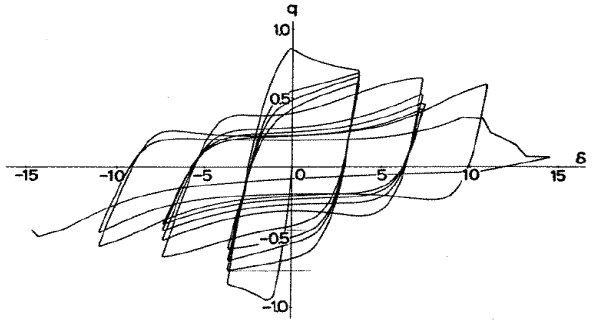							Test Layout 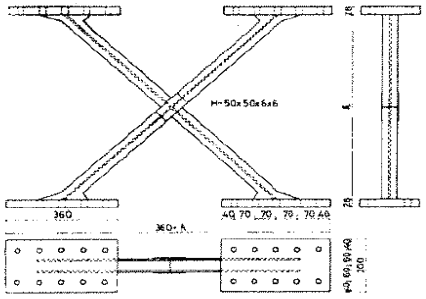				
	Drift Range	-3.12%	to	3.12%	→	6.24%	Total					

Title:	Part 1: Experimental Studies on the Elastic-Plastic Behavior of Braced Frames under Repeated Horizontal Loading											
Authors:	Minoru Wakabayshi, Takeshi Nakamura, Nozomu Yoshida											
Year:	1977											
Designation	Bracing	Config.	B (cm)	D (cm)	t_w (cm)	t_f (cm)	L (cm)	A (cm2)	Q_y (KN)	Δ_y (cm)	Initial Brace Local Buckling (%)	Initial Brace Cracking (%)
DIC 3	Wide Flange	X-Bracing	4.97	5.01	0.604	0.585	296.8	8.23	293.34	0.529	-	3.00
	Force-Dirft Hysteresis							Initial Brace Buckling (%)			0.26	
	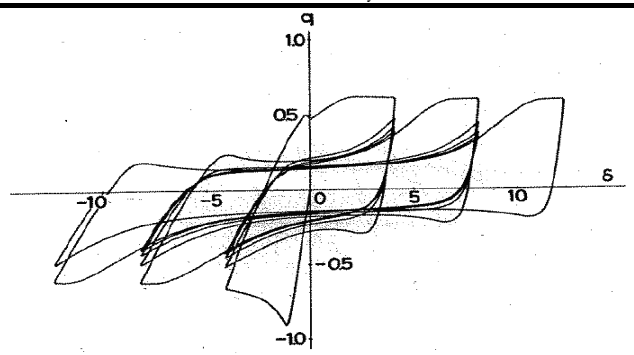							Test Layout				
								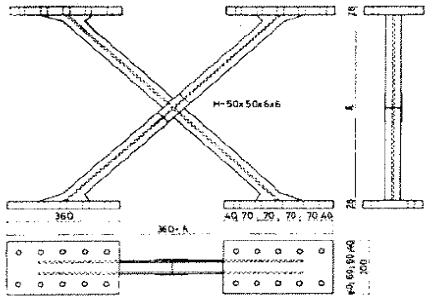				
	Drift Range	-3.15%	to	3.15%	→	6.30%	Total					
Designation	Bracing	Config.	B (cm)	D (cm)	t_w (cm)	t_f (cm)	L (cm)	A (cm2)	Q_y (KN)	Δ_y (cm)	Initial Brace Local Buckling (%)	Initial Brace Cracking (%)
DOC 3	Wide Flange	X-Bracing	4.99	5	0.598	0.58	297.3	8.17	291.20	0.530	-	-
	Force-Dirft Hysteresis							Initial Brace Buckling (%)			0.36	
	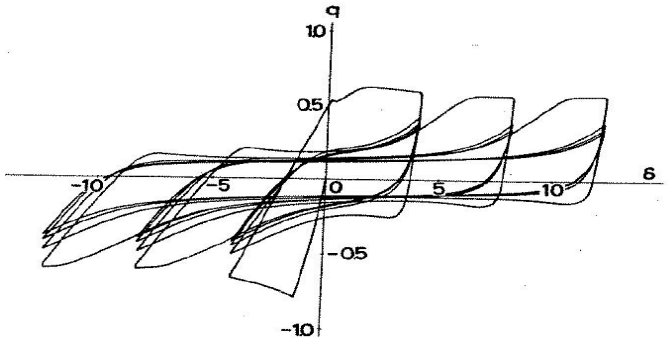							Test Layout				
								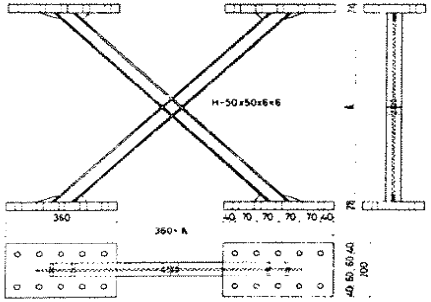				
	Drift Range	-3.15%	to	3.15%	→	6.30%	Total					

HSS03 - University of Washington - 12/13/04 - 3/8" Gusset Plate

Framing Layout

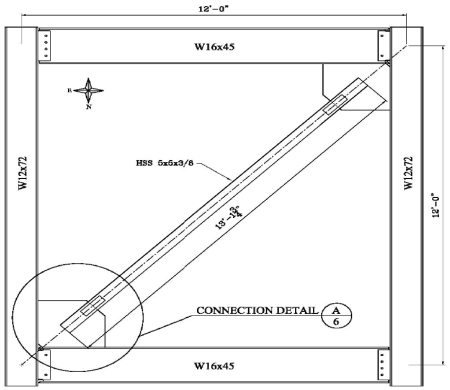

Gusset Plate Detail

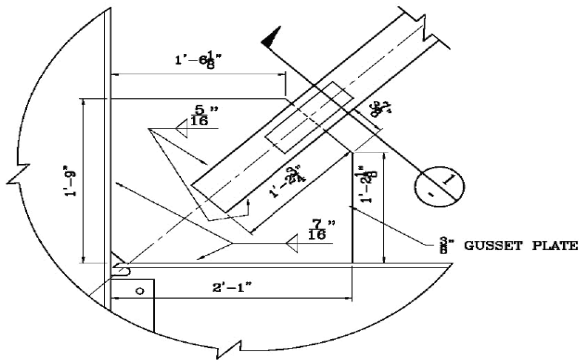

Force-Drift Hysteresis

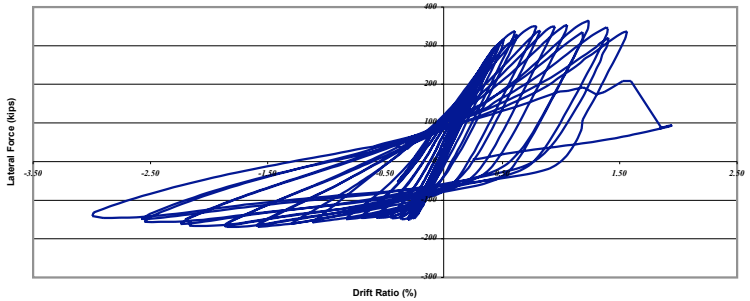

Range: -3.00% to 1.95% → 4.95% Total

Brace	Gusset Plate	Beams	Columns
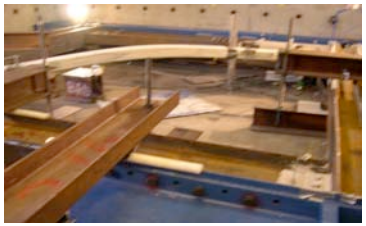			
DS2- Buckling at -1.30%	DS2- Yielding at 0.434%	DS3- Yielding at -2.24%	DS3- Yielding at 1.05%
		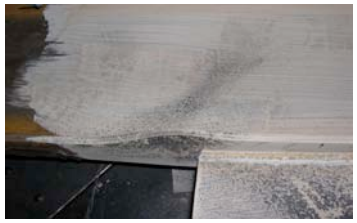	
DS3- Buckling at -1.87%	DS3- Yielding at -2.24%	DS3- Yielding, DS4- Buckling at -2.58%	DS3- Yielding and Buckling at -2.58%
			
DS4- Buckling at -2.58%			DS4- Yielding and Buckling at 1.95%

HSS01- University of Washington - 10/15/04 - 1/2" Gusset Plate, Designed per UFM, 2t linear clearance

Framing Layout

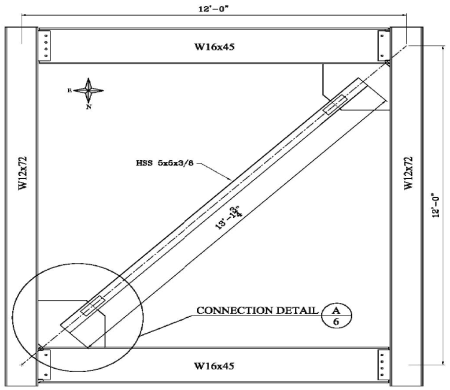

Gusset Plate Detail

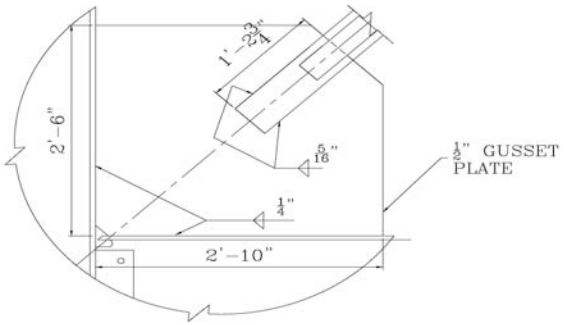

Force-Drift Hysteresis

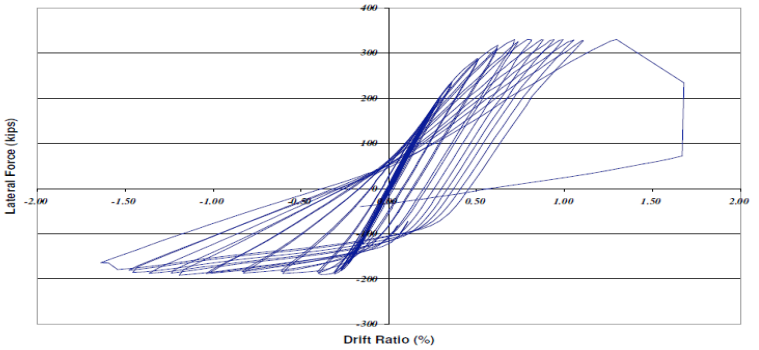

Range: -1.64% to 1.11% → 2.75% Total

Brace	Gusset Plate	Beams	Columns
	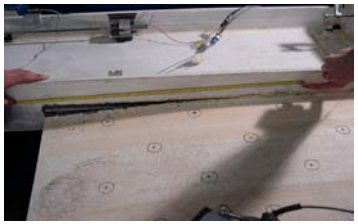	No Yielding on Beams	No Yielding on Columns
	DS3-Weld Fracture at -1.54%		
			
	DS4-Complete Weld Fracture at 1.11%		

HSS08 - University of Washington - 9/18/05 - 3t Elliptical Clearance

Framing Layout

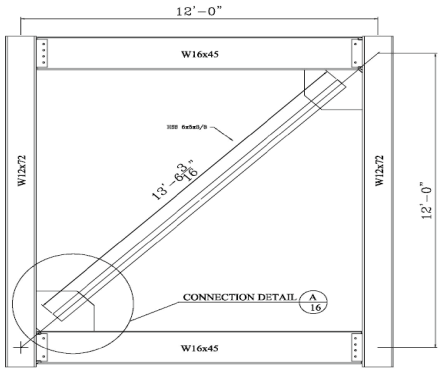

Gusset Plate Detail

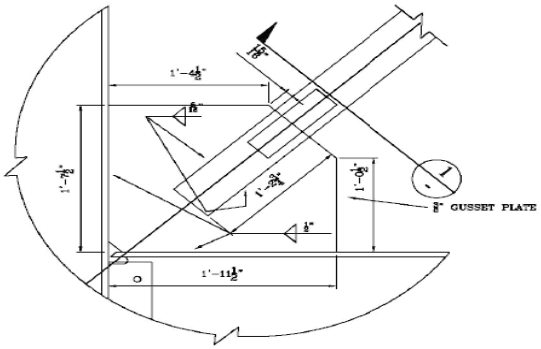

Force-Drift Hysteresis

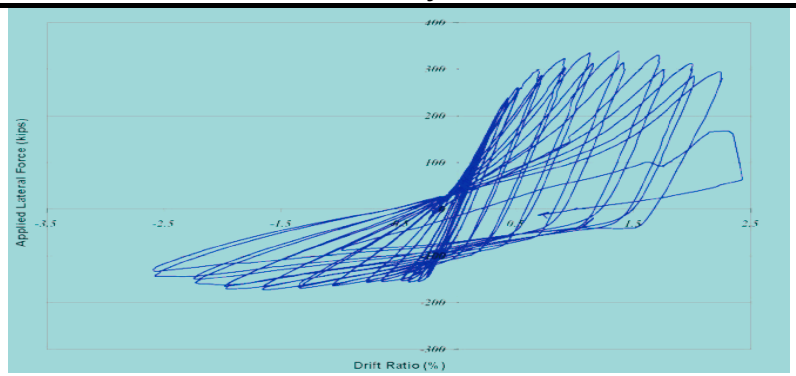

Range: -2.60% to 2.01% → 4.61% Total

Brace	Gusset Plate	Beams	Columns
	Yielding Could not be determined		
DS2- Buckling at -0.65%		DS2- Yielding at 1.15%	DS2- Yielding at -1.35%
			
DS3- Buckling at -1.66%	Tearing at -2.25%	DS3- Yielding at -2.25%	DS3- Yielding at -2.60%
			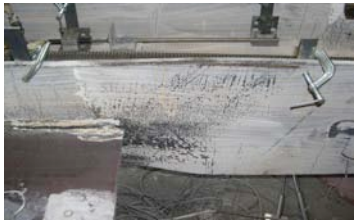
DS4- Buckling at -2.60%	Tearing at -2.60%	DS4- Yielding at Buckling at 2.01%	DS3- Yielding and Buckling at 2.01%

HSS09 - University of Washington - 11/17/05 - 1/2" Gusset Plate with CJP Welds and 6t Elliptical Clearance

Framing Layout

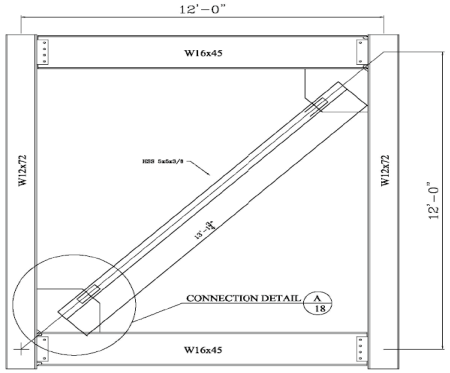

Gusset Plate Detail

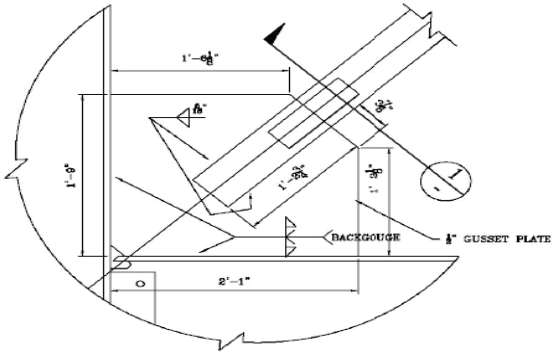

Force-Drift Hysteresis

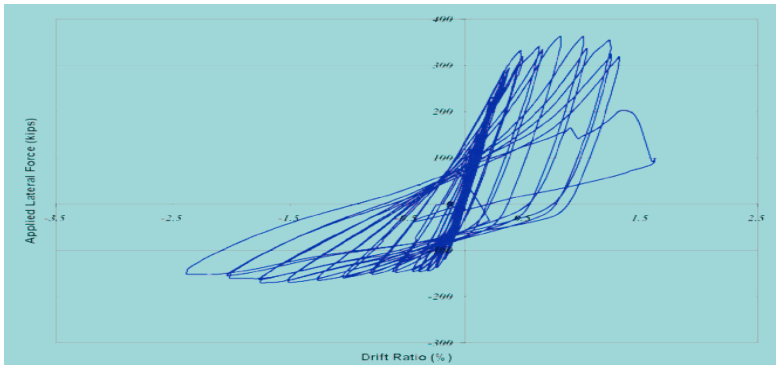

Range: -2.38% to 1.32% → 3.7% Total

Brace	Gusset Plate	Beams	Columns
	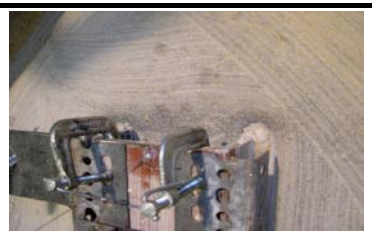		
DS2- Buckling at -0.81%	DS2- Yielding at -1.04%	DS2- Yielding at 0.82%	DS2- Yielding at 0.49%
			
DS3- Buckling at -1.27%	DS2- Yielding at -2.38%	DS3- Yielding at Buckling at 1.05%	DS3- Yielding at 1.25%
		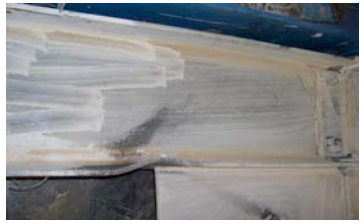	
DS4- Buckling at -2.38%		DS4- Buckling at -2.38%	DS4- Buckling at -2.38%

HSS23 - University of Washington - 11/2/07 - WF Brace

Framing Layout

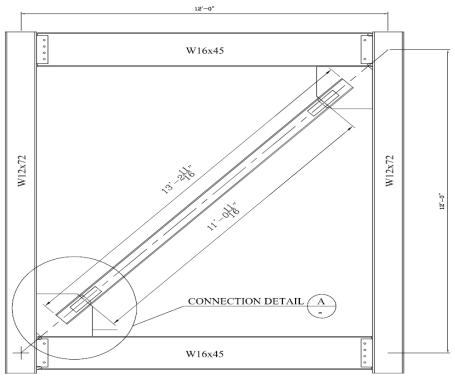

Gusset Plate Detail

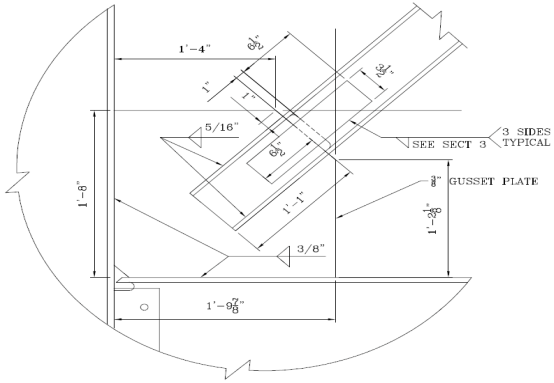

Force-Drift Hysteresis

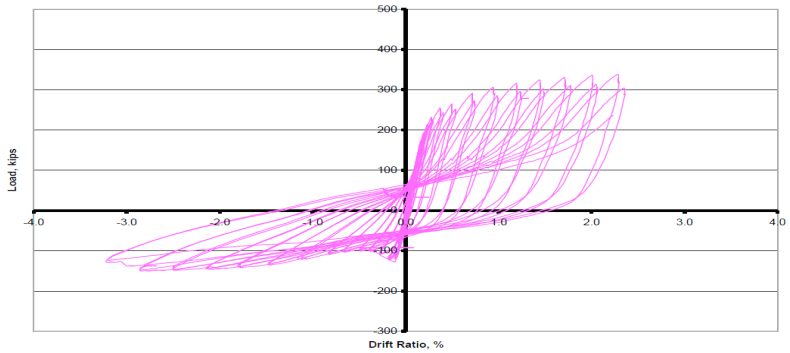

Range: -3.21% to 2.35% → 5.56% Total

Brace	Gusset Plate	Beams	Columns
			
DS2- Buckling at -0.83%	DS2- Yielding at -0.67%	DS2- Yielding at 1.23%	DS3- Yielding at -2.15%
			
DS3- Buckling at -1.80%	DS4- Yielding and Buckling at -3.21%	DS3- Yielding at 2.35%	DS3- Buckling at -2.86%
			
DS4- Buckling at -3.21%	DS4- Tearing at 2.32%		DS3- Yielding at -3.21%

HSS24 - University of Washington - 5/20/08 - Unwelded Beam Web to Column Connection

Framing Layout

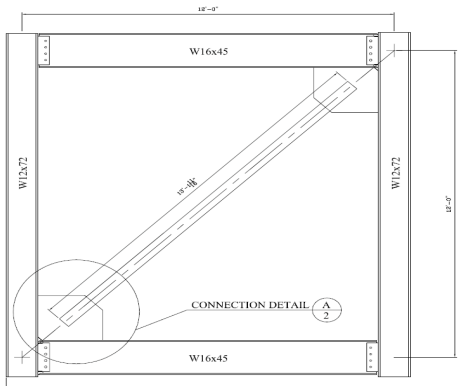

Gusset Plate Detail

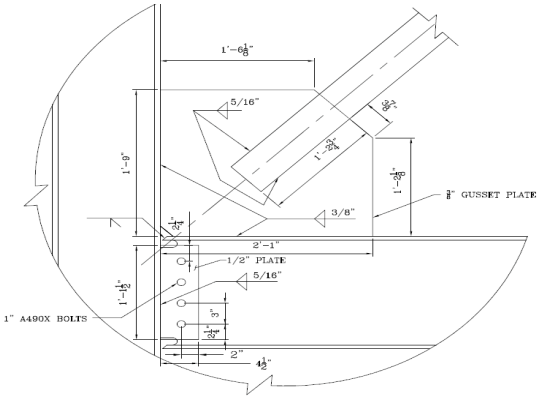

Force-Drift Hysteresis

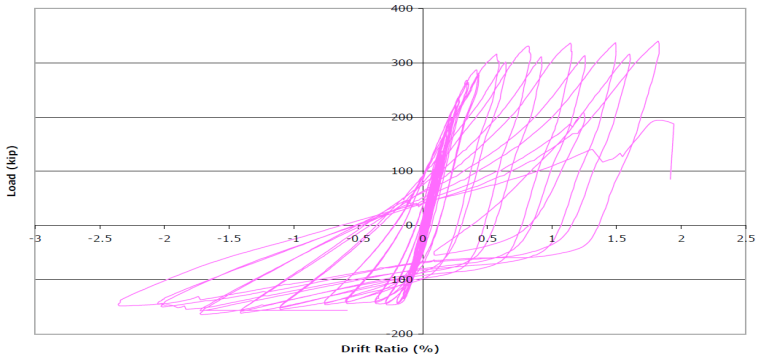

Range: -2.50% to 1.94% → 4.44% Total

Brace

DS2- Buckling at -0.79%

DS3- Buckling at -1.50%

DS4- Buckling at -2.50%

Gusset Plate

DS2- Yielding at -0.79%

DS3- Yielding at -1.95%

DS2- Tearing at 1.94%

Beams

DS2- Yielding at 1.59%

Columns

DS2- Yielding at -1.17%

DS3- Yielding at -2.50%

HSS25 - University of Washington - 6/5/08 - 7/8" Gusset With No Net Section Reinforcing and a Big Beam

Framing Layout

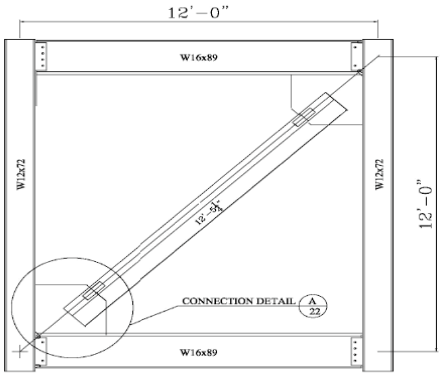

Gusset Plate Detail

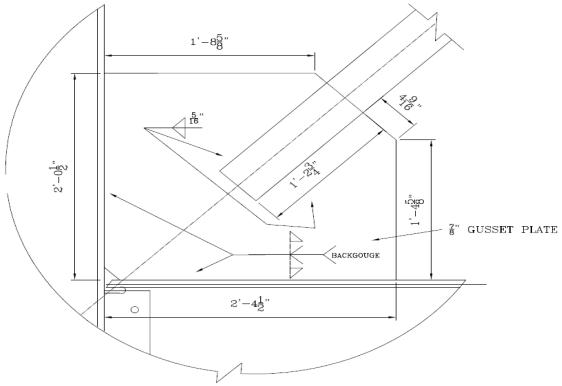

Force-Drift Hysteresis

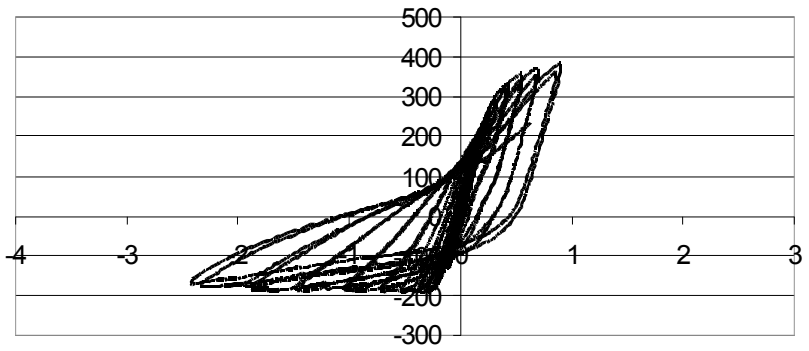

Range: -2.41% to 0.89% → 3.30% Total

Brace

DS2- Buckling at -0.73%

DS3- Buckling at -2.41%

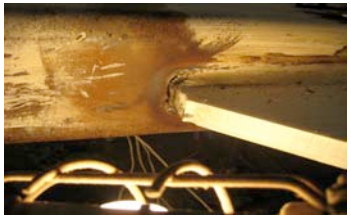

DS3- Net Section Tearing at 0.89%

Gusset Plate

DS2- Yielding at -0.73%

DS3- Yielding at -2.41%

Beams

None

Columns

DS2- Yielding at -1.50%

DS3- Yielding at -1.94%

DS4- Buckling at -2.41%

HSS26 - 7/8" Gusset With No Net Section Reinforcing and a Big Beam, Near Fault Loading Protocol

Framing Layout

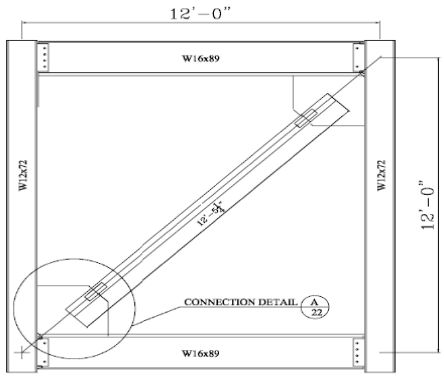

Gusset Plate Detail

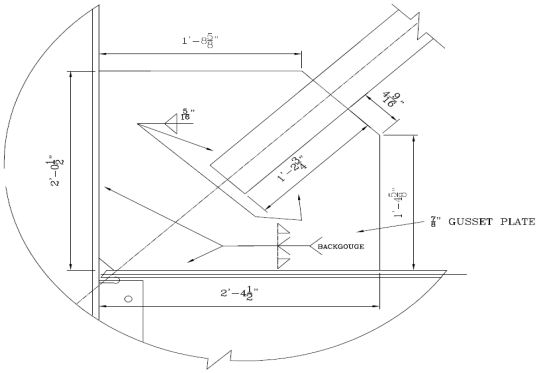

Force-Drift Hysteresis

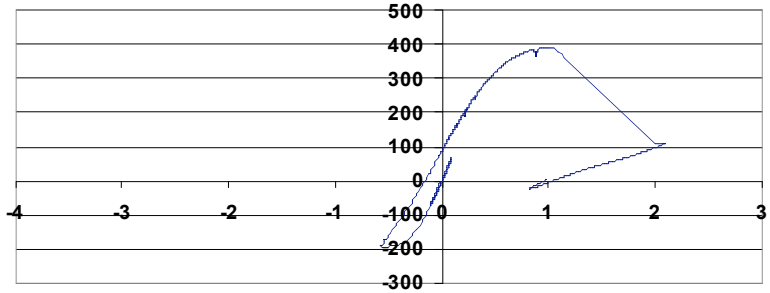

Range: -0.57% to 1.15% → 1.72 Total

Brace	Gusset Plate	Beams	Columns
	No Yielding	No Yielding	
Net Section Fracture- 1.15%			Yielding at 1.15%
			
Net Section Fracture- 1.15%			Yielding and Buckling at 1.15%

HSS27 - 3/8" Gusset With No Net Section Reinforcing and a Big Beam, Near Fault Loading Protocol

Framing Layout

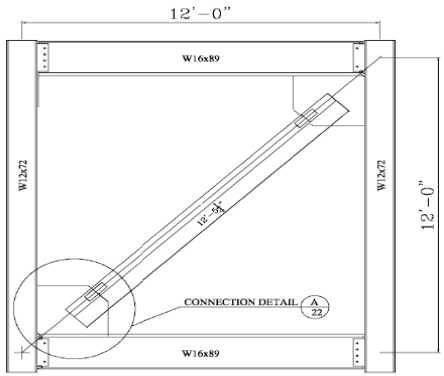

Gusset Plate Detail

Force-Drift Hysteresis

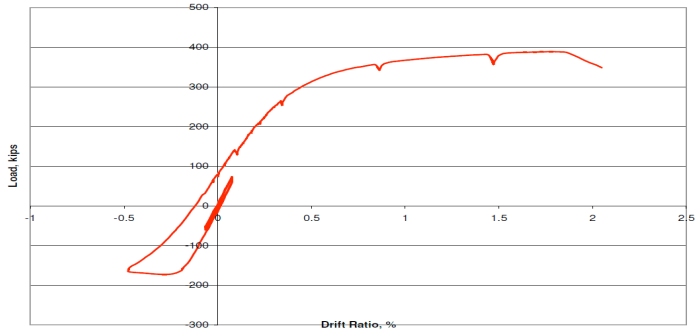

Range: -0.48% to 2.05% → 2.53 Total

Brace

Net Section Fracture at 2.05%

Net Section Fracture at 2.05%

Gusset Plate

Yielding at 2.05%

Beams

Columns

HSS05 - University of Washington - 4/29/05 - 3/8" Gusset Plate with Small Welds

Framing Layout

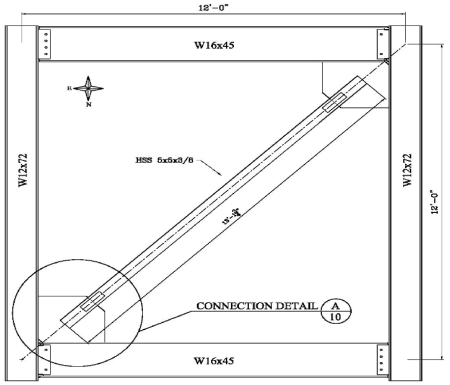

Gusset Plate Detail

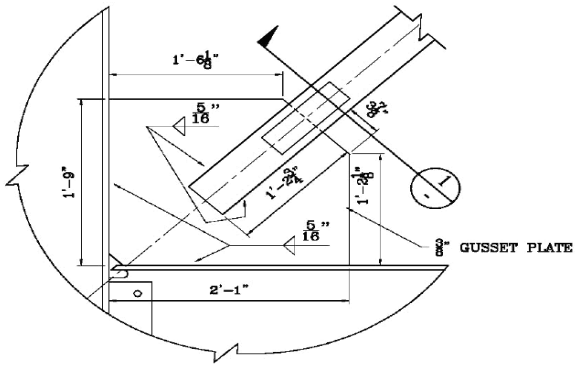

Force-Drift Hysteresis

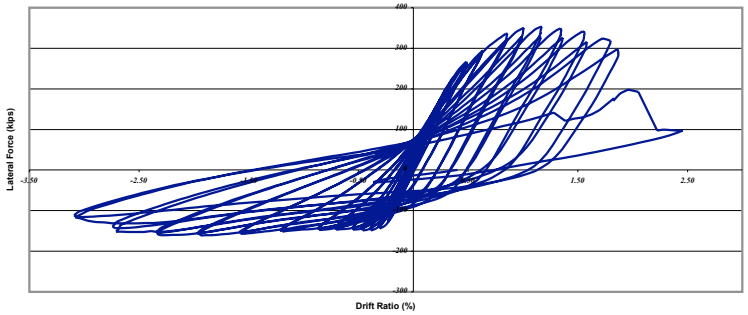

Range: -3.09% to 2.45% → 5.54% Total

Brace	Gusset Plate	Beams	Columns
	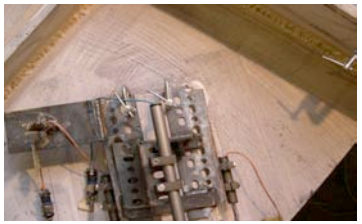		
DS2- Buckling at -0.72%	DS2- Yielding at 1.00%	DS2- Yielding at 1.00%	DS2- Yielding at 1.00%
			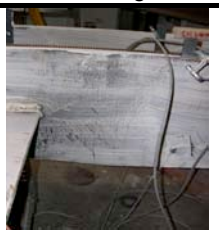
DS3- Buckling at -1.97%	DS3- Yielding at -2.74%	DS3- Yielding and Buckling at 1.87%	DS3- Yielding at 1.58%
			
DS4- Buckling at -3.09%	DS3-Yielding, DS4- Tearing at -3.09%		DS3- Yielding, DS4- Buckling at -3.09%

HSS06 - University of Washington - 6/14/05 - Reinforced Gusset Plate Weld

Framing Layout

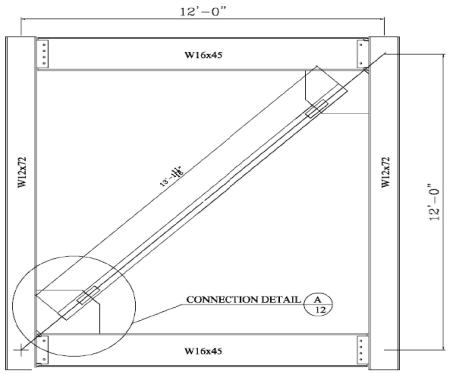

Gusset Plate Detail

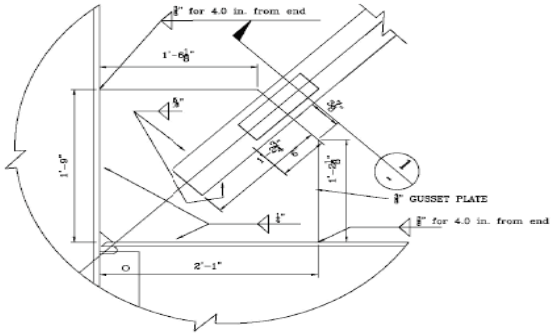

Force-Drift Hysteresis

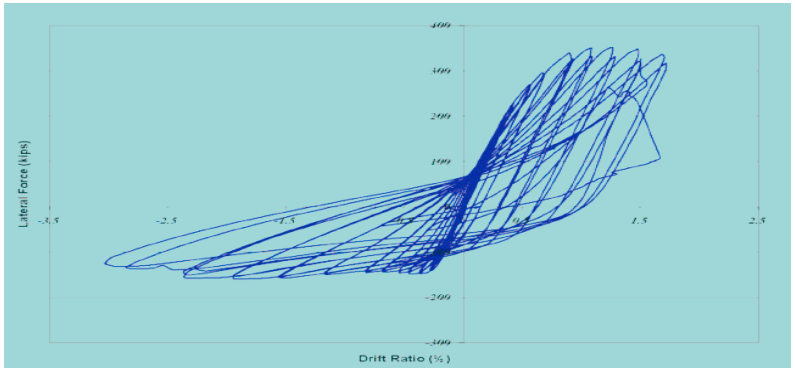

Range: -3.03% to 1.72% → 4.75% Total

Brace	Gusset Plate	Beams	Columns
	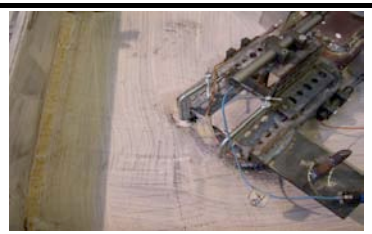		
DS2- Buckling at -0.83%	DS2- Yielding at 1.29%	DS2- Yielding at 1.50%	DS2- Yielding at -1.57%
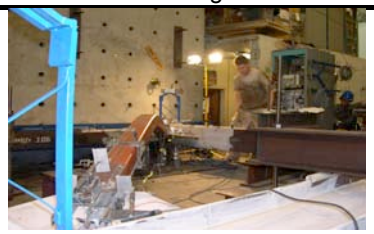			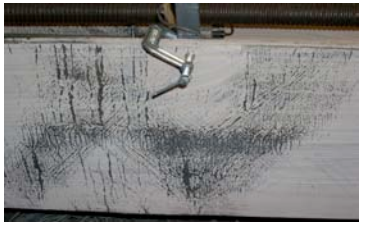
DS3- Buckling at -1.95%	DS2- Yielding at -3.03%		DS4- Yielding at 1.72%
			
DS4- Buckling at -3.03%	DS3- Tearing at 1.72%		DS4- Yielding and Buckling at -3.03%

HSS07 - University of Washington - 7/8/05 -7/8" Gusset Plate

Framing Layout	Gusset Plate Detail	Force-Drift Hysteresis
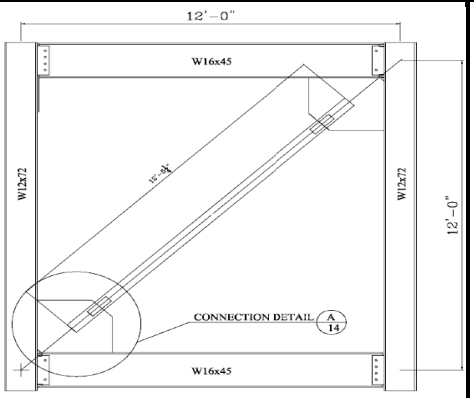	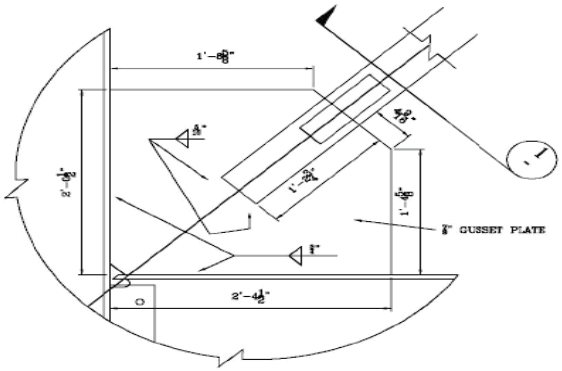	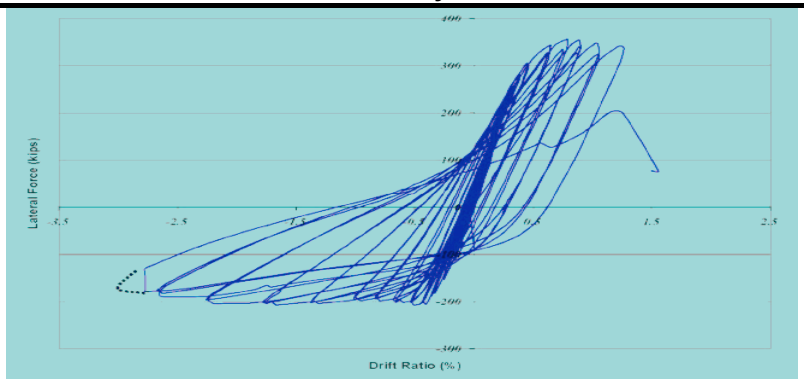
		Range: -2.78% to 1.26% → 4.04% Total

Brace	Gusset Plate	Beams	Columns
			
DS2- Buckling at -0.83%	DS2- Yielding at -0.83%	DS2- Yielding at 0.90%	DS2- Yielding at -0.83%
			
DS3- Buckling at -1.78%	DS2- Tearing at -2.78%	DS3- Yielding at -2.67%	DS3- Yielding at 0.90%
			
DS4- Buckling at -2.78%	DS3- Yielding at -2.78%	DS4- Yielding and Buckling at 1.56%	DS3- Yielding and Buckling at 1.56%

HSS02- University of Washington - 11/03/04 - 1/2" Gusset Plate, 6t Elliptical Clearance

Framing Layout

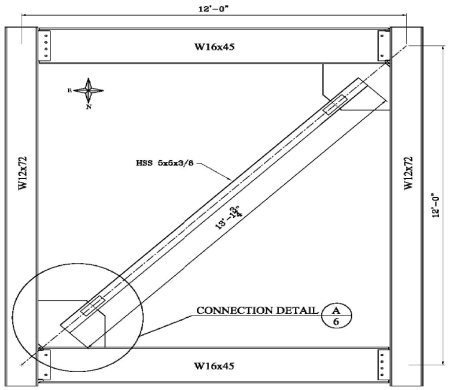

Gusset Plate Detail

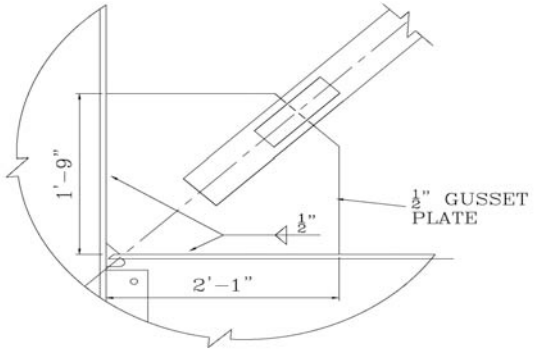

Force-Drift Hysteresis

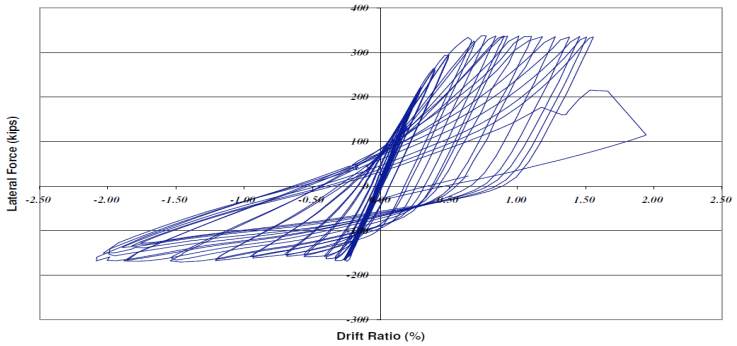

Range: -2.05% to 1.98% → 4.03% Total

Brace	Gusset Plate	Beams	Columns
			
DS3-Buckling at -2.05%	DS2-Yielding at 1.98%	DS2-Yielding at 0.40%	DS2-Yielding at 0.69%
			
		DS3-Yielding at 1.98%	DS3-Yielding at 1.31%
			
			DS3-Yielding at 1.98%

HSS20 - University of Washington - 4/11/07 - Bolted End Plate Connection

Framing Layout

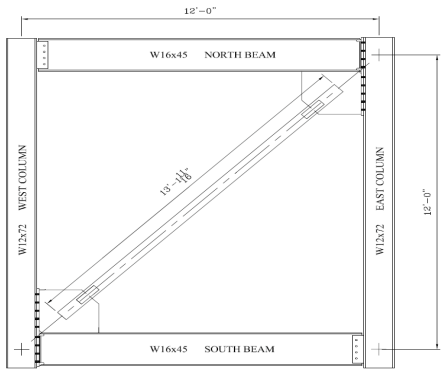

Gusset Plate Detail

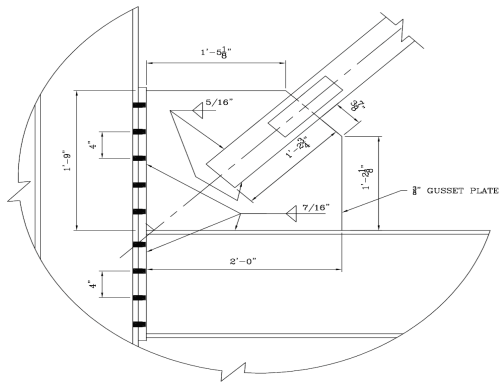

Force-Drift Hysteresis

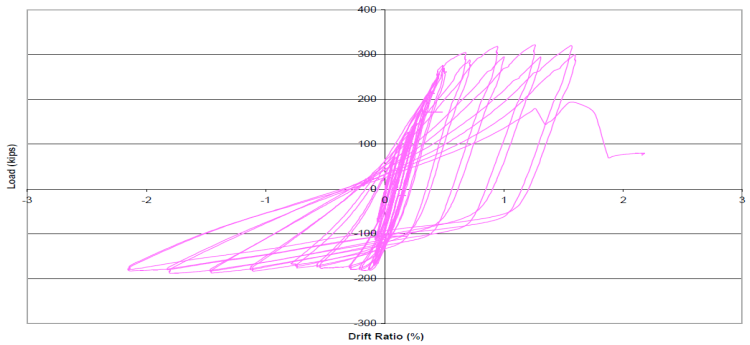

Range: -2.28% to 1.69% → 3.97% Total

Brace	Gusset Plate	Beams	Columns
	No Pictures for HSS20		

HSS21 - University of Washington - 6/15/07 - Bolted End Plate Connection

Framing Layout

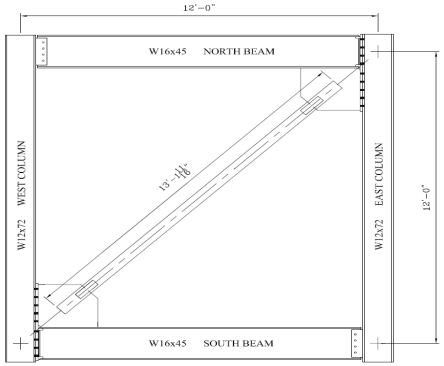

Gusset Plate Detail

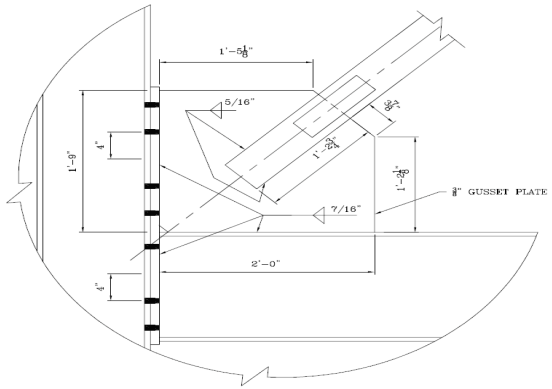

Force-Drift Hysteresis

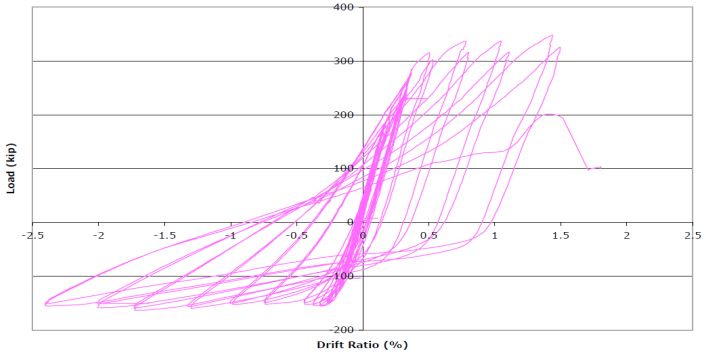

Range: -2.55% to 1.60% → 4.15% Total

Brace

DS2- Buckling at -1.06%

Gusset Plate

DS2- Yielding at -0.47%

DS3- Yielding at 0.86%

DS4- Yielding at -2.55%

Beams

DS2- Yielding at 1.19%

Columns

DS2- Yielding at -0.86%

DS2- Yielding at -2.13%

DS3- Yielding at -2.55%

HSS22 - University of Washington - 8/1/07 - Bolted Beam to Column Connection with 3/8" Tapered Plate

Framing Layout

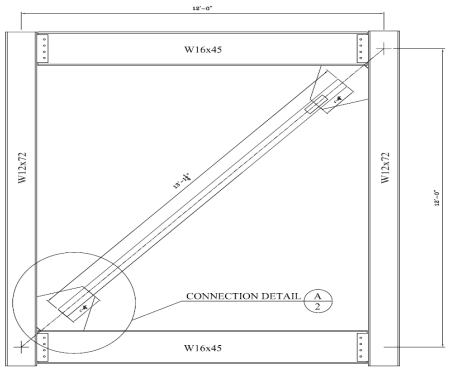

Gusset Plate Detail

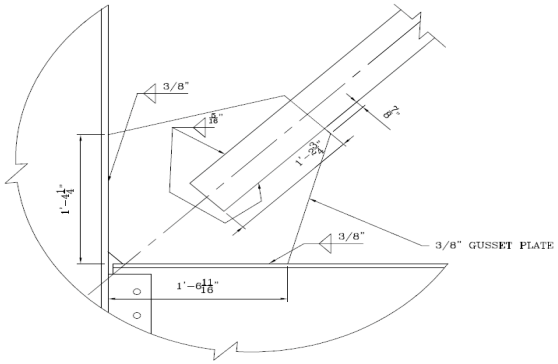

Force-Drift Hysteresis

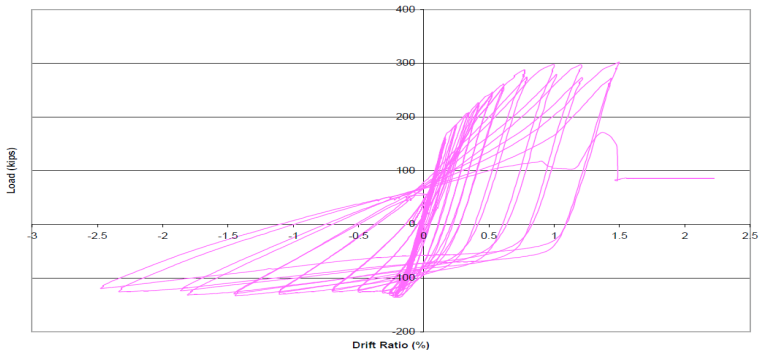

Range: -2.48% to 1.50% → 3.98% Total

Brace

DS2- Buckling at -1.11%

DS3- Buckling at -1.86%

Gusset Plate

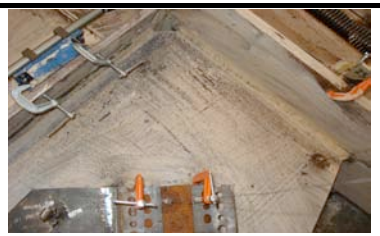

DS2- Yielding at -1.11%

DS3- Yielding at 1.50%

DS3- Tearing at 1.50%

Beams

None

Columns

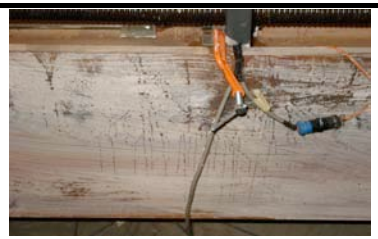

DS2- Yielding at -2.48%

HSS10 - University of Washington - 1/20/06 - 1/2" Tapered Gusset Plates

Framing Layout

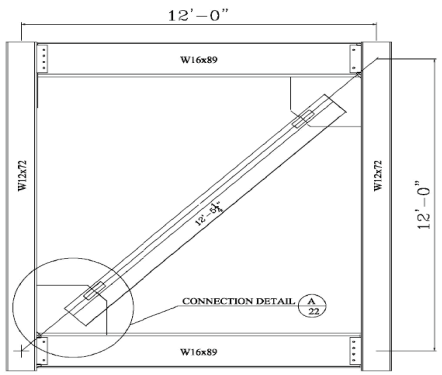

Gusset Plate Detail

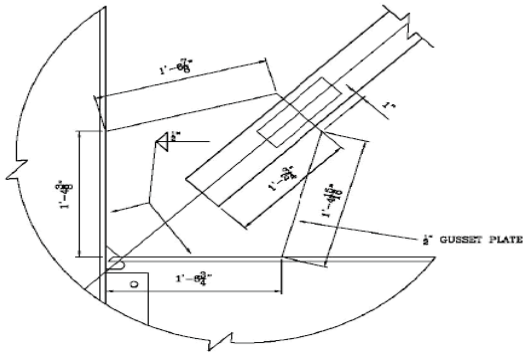

Force-Drift Hysteresis

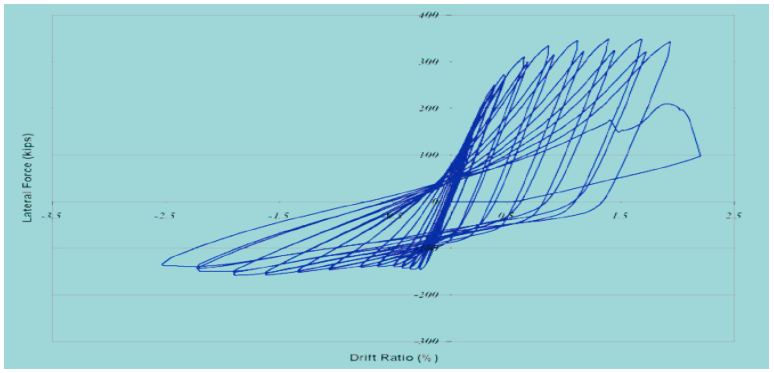

Range: -2.54% to 1.93% → 4.47% Total

Brace	Gusset Plate	Beams	Columns
		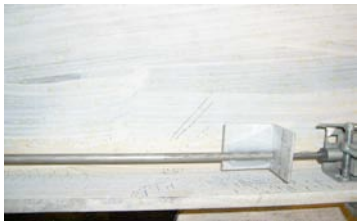	
DS2- Buckling at -0.64%	DS2- Yielding at -1.91%	DS2- Yielding at -1.91%	DS2- Yielding at 1.17%
			
DS3- Buckling at-1.35%	DS2- Yielding at -2.54%	DS3- Yielding at -2.23%	DS3- Yielding at 1.95%
			
DS4- Buckling at -2.54%	DS3- Tearing at -2.54%	DS4- Yielding and Buckling at 1.95%	DS3- Buckling at 1.95%

HSS11 - University of Washington - 1/20/06 - Big Beam with 7/8" Gusset Plate

Framing Layout	Gusset Plate Detail	Force-Drift Hysteresis
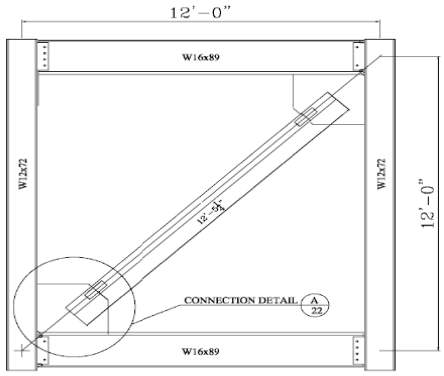	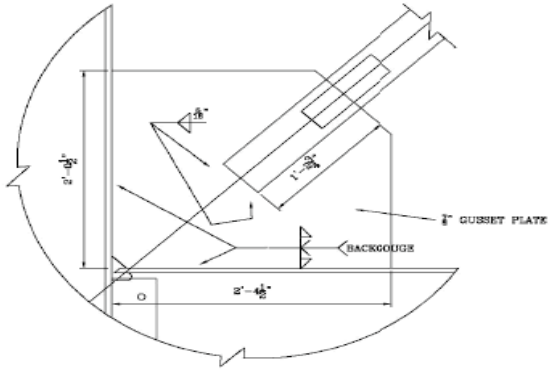	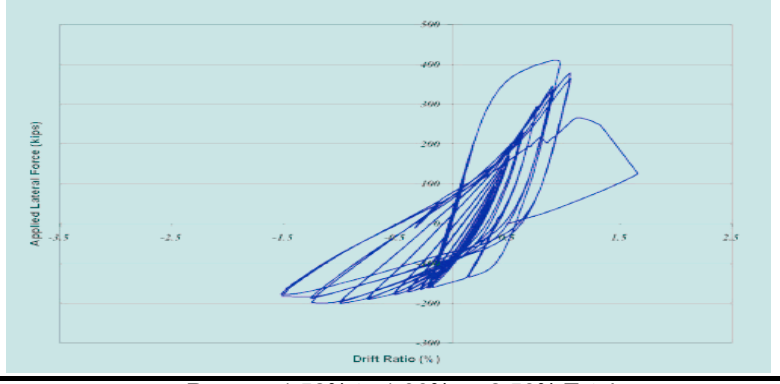
		Range: -1.52% to 1.06% → 2.58% Total

Brace	Gusset Plate	Beams	Columns
		No Yielding	
DS2- Buckling at -0.20%	DS2- Yielding at -0.198%		DS3- Yielding at 0.51%
			
DS3-Buckling at -1.0%	DS2- Tearing at -1.52%		DS3- Yielding at -1.25%
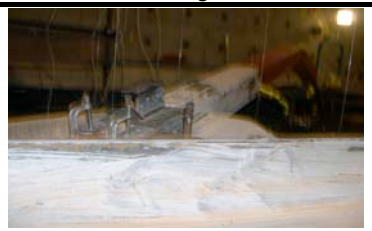			
DS4- Buckling at -1.52%	DS3- Yielding at -1.52%		DS4- Buckling at -1.52%

HSS12 - University of Washington - 5/11/06 - Reference Specimen with CJP Welds

Framing Layout

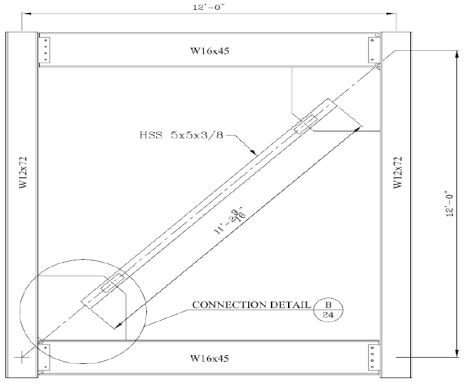

Gusset Plate Detail

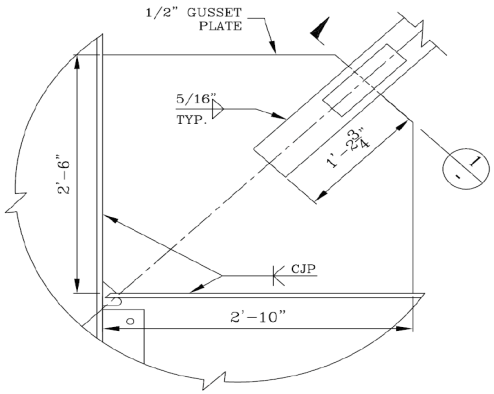

Force-Drift Hysteresis

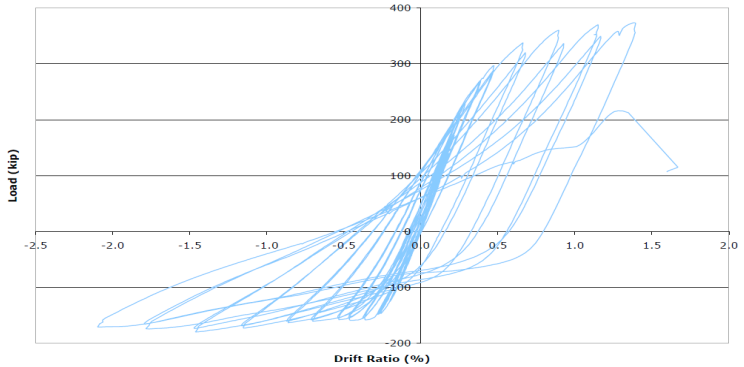

Range: -2.1% to 1.40% → 3.50% Total

Brace	Gusset Plate	Beams	Columns
			
DS2-Buckling at -0.71%	DS1-Yielding at 1.17%	DS2-Yielding at -1.47%	DS2-Yielding at 0.68%
			
DS3-Buckling at -1.47%		DS3-Yielding at 1.40%	DS3-Yielding at 0.93%
			
DS4-Buckling at -2.10%			DS3-Yielding and Buckling at 1.40%

HSS13 - University of Washington - 6/27/06 - Tapered Gusset with CJP Welds

Framing Layout

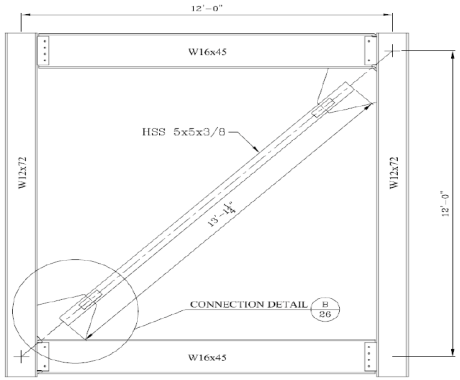

Gusset Plate Detail

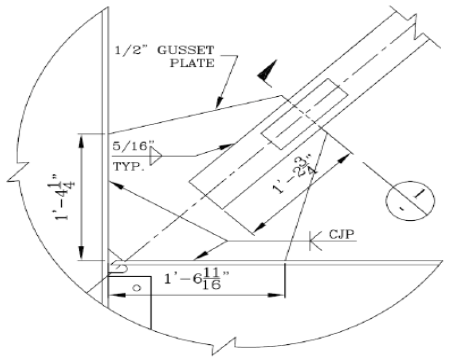

Force-Drift Hysteresis

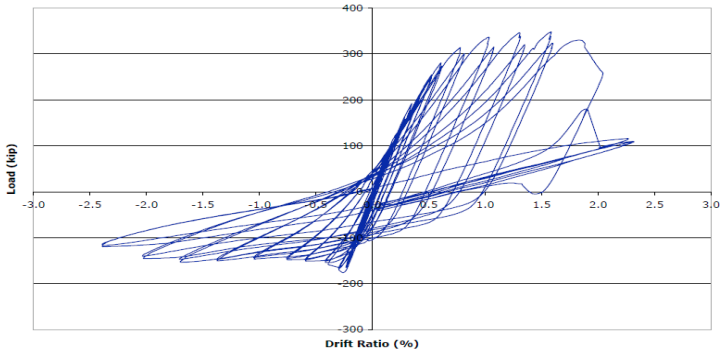

Range: -2.03% to 2.05% → 4.08% Total

Brace	Gusset Plate	Beams	Columns
			
DS2-Buckling at -0.60%	DS2-Yielding at -1.05%	DS2-Yielding at 1.08%	DS2-Yielding at 1.35%
			
DS3-Buckling at -1.38%	DS3-Yielding at -2.03%	DS3-Yielding at -2.03%	DS3-Yielding at 2.05%
			
DS3-Buckling at -2.03%		DS3-Yielding and Buckling at 2.05%	DS3-Yielding at 2.05%

HSS14 - University of Washington - 8/04/06 - Unreinforced Net Section

Framing Layout

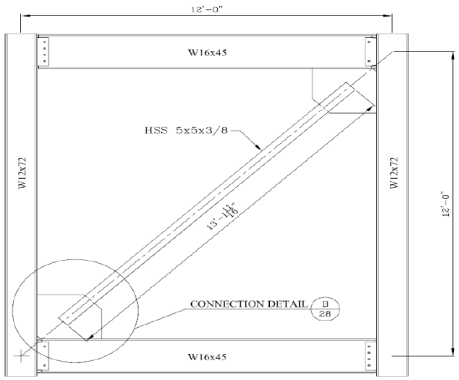

Gusset Plate Detail

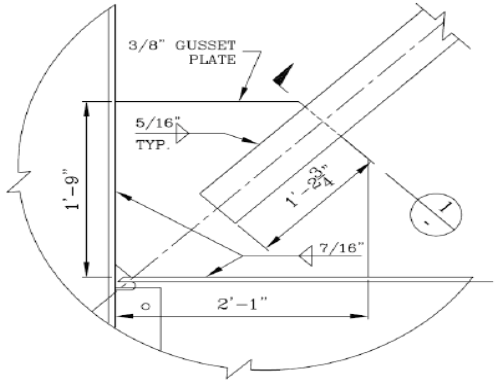

Force-Drift Hysteresis

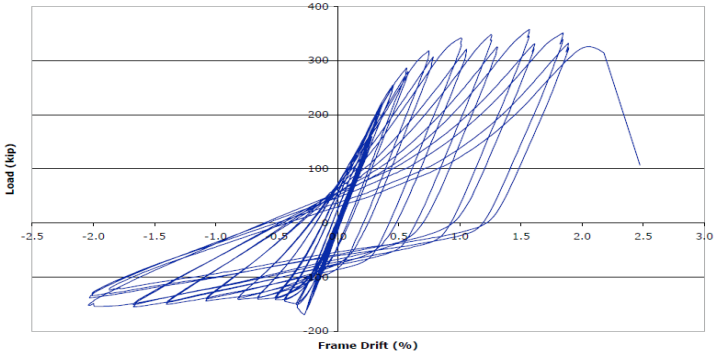

Range: -2.04% to 1.89% → 3.93% Total

Brace	Gusset Plate	Beams	Columns
Brace Buckling Down			
	DS2-Yielding at 1.89%	DS2-Yielding at -1.40%	DS2- Yielding at 1.31%
Brace Buckled Down	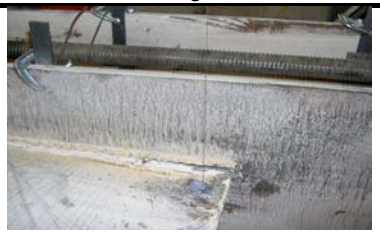		
	DS3-Tearing-1.89%	DS3-Yielding and Buckling at1.89%	DS3- Yielding at 1.89%
			
DS4- Fracture at 1.87%		DS3- Yielding at 1.89%	DS3- Yielding at 1.89%

HSS15 - University of Washington - 8/29/06 - Reduced Splice Length

Framing Layout

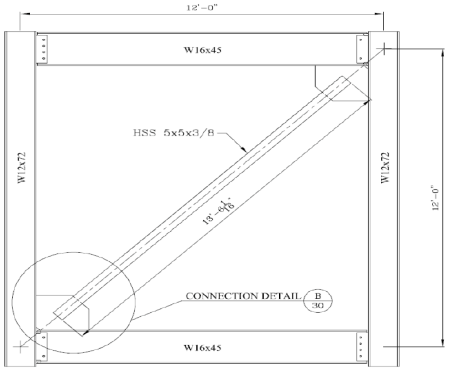

Gusset Plate Detail

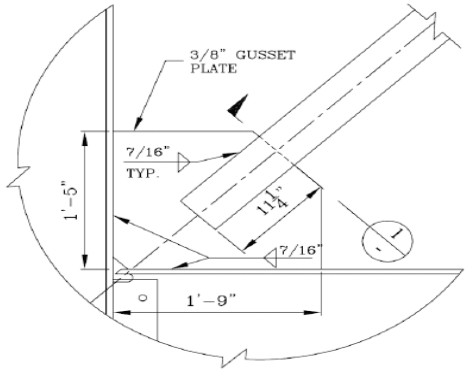

Force-Drift Hysteresis

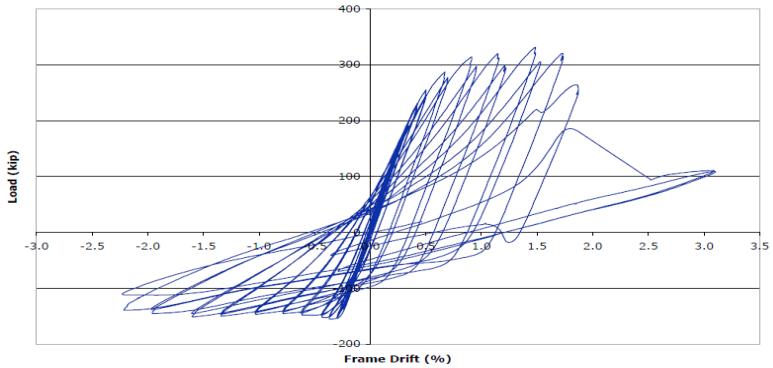

Range: -2.22% to 1.87% → 4.09% Total

Brace	Gusset Plate	Beams	Columns
			
DS2- Buckling at -0.63%	DS2-Yielding at -0.63%	DS2- Yielding at -1.35%	DS2- Yielding at 1.22%
			
DS3- Buckling at -1.35%	DS2- Tearing at -2.22%	DS3-Yielding at -2.22%	DS3- Yielding at 1.74%
	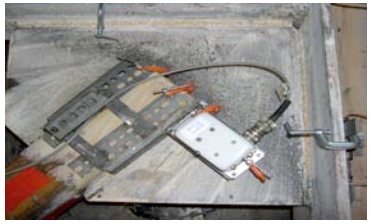		
DS3- Buckling at -1.61%	DS3- Yielding at -2.22%		

HSS17 - University of Washington - 11/14/06 - 3/8" Tapered Gusset Plate

Framing Layout

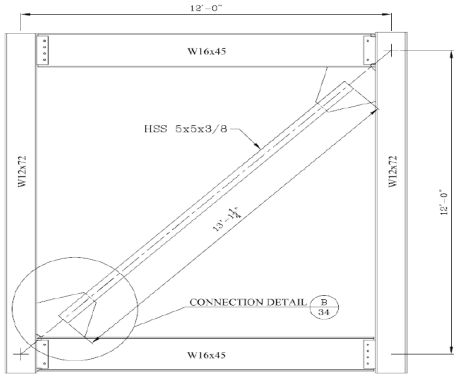

Gusset Plate Detail

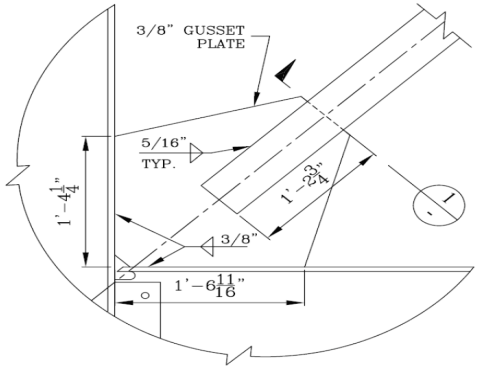

Force-Drift Hysteresis

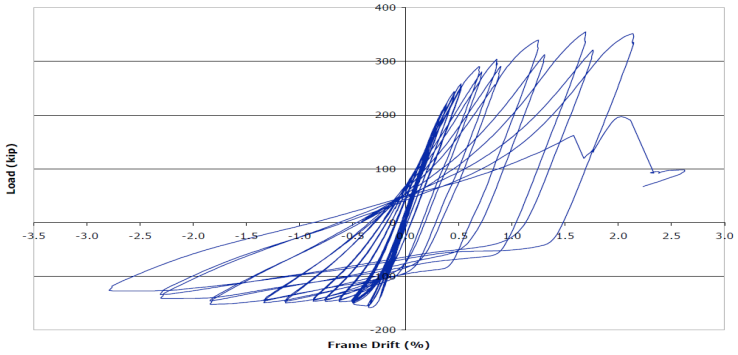

Range: -2.79% to 2.15% → 4.94% Total

Brace	Gusset Plate	Beams	Columns
			
DS2- Buckling at -0.63%	DS3- Yielding at -1.84%	DS2- Yielding at 1.31%	DS2 - Yielding at -1.84%
			
DS3- Buckling at -1.34%	DS4- Yielding at 2.15%	DS3- Yielding at 2.15%	DS3- Yielding at -2.79%
			
DS4- Buckling at -2.79%	DS4- Tearing at 2.15%		DS3- Yielding at -2.79%

HSS18 - University of Washington - 1/11/07 - Bolted Beam to Column Connection

Framing Layout

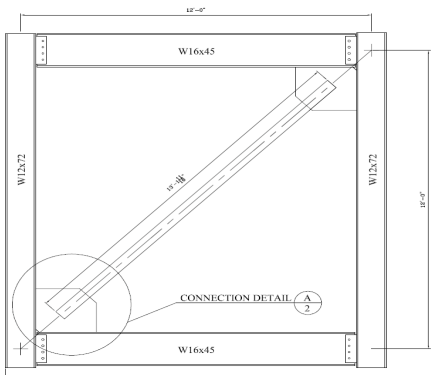

Gusset Plate Detail

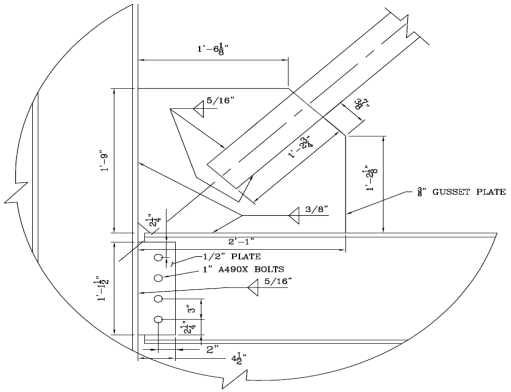

Force-Drift Hysteresis

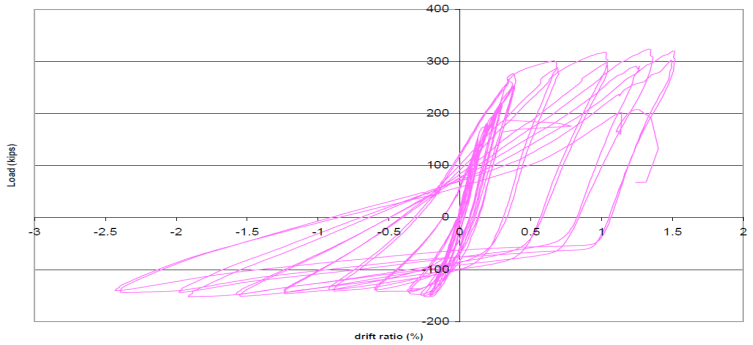

Range: -2.59% to 1.60% → 4.19% Total

Brace	Gusset Plate	Beams	Columns
			
DS2- Bucking at -0.64%	DS2- Yielding at -0.64%	DS2- Yielding at -2.59%	DS2-Yielding at -1.32%
			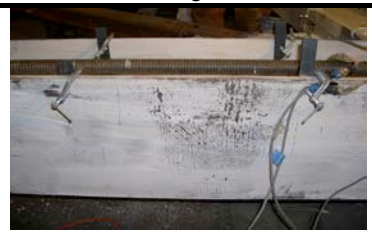
DS3- Buckling at -1.67%	DS3- Yielding at -1.67%		DS2- Yielding at -2.59%
			
DS4- Buckling at -2.59	DS4- Yieldng and Bucling at -2.59%		

HSS04 - University of Washington - 3/15/05 - Short Splice Length

Framing Layout

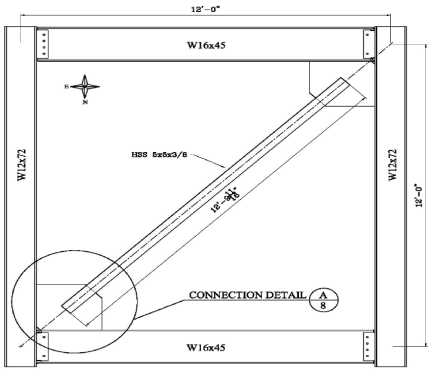

Gusset Plate Detail

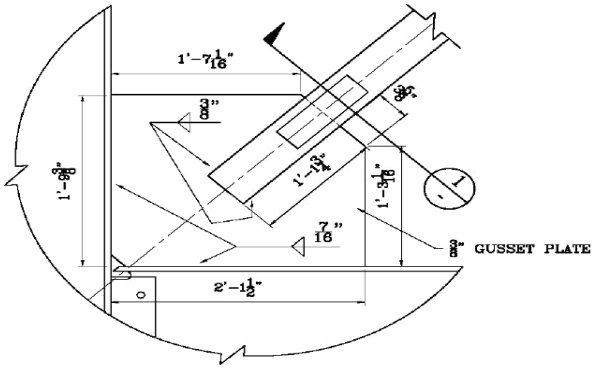

Force-Drift Hysteresis

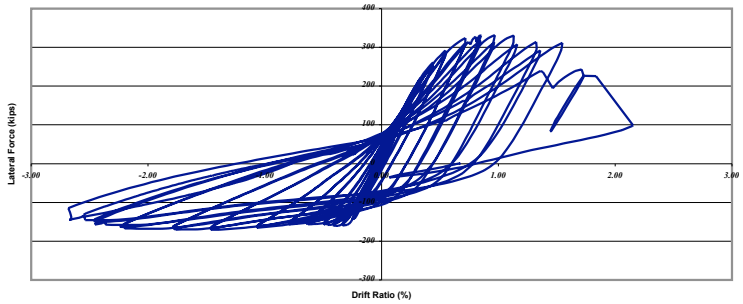

Range: -2.68% to 2.15% → 4.83% Total

Brace	Gusset Plate	Beams	Columns
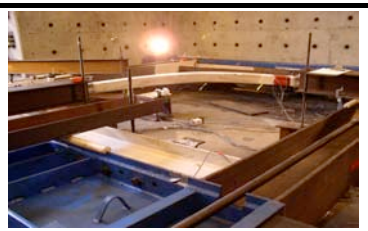			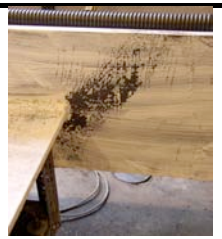
DS2- Buckling at -1.07%	DS2- Yielding at 0.41%	DS2- Yielding at 1.16%	DS3- Yielding at 0.85%
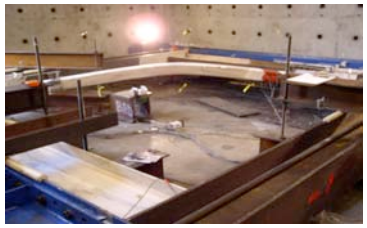			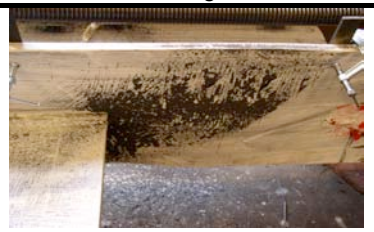
DS3- Buckling at -1.79%	DS3- Yielding at -2.68%		DS4- Yielding at -2.46%
			
DS4- Buckling at -2.46%			DS4- Yielding and Buckling at 2.15%

TCBF2-1 - UW, NCREE - 1/17/09 - Three Story SCBF Test, HSS Braces, 8t Elliptical Clearance on Corner Gussets

Test Frame

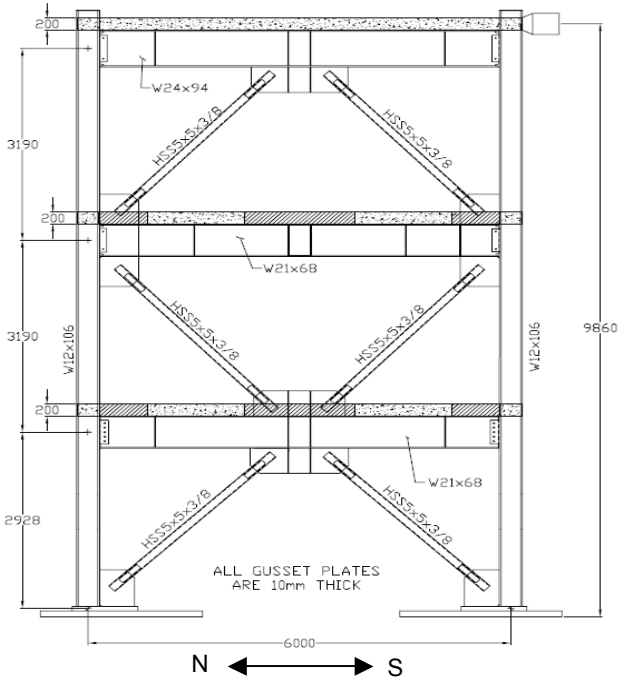

Total Frame Force-Drift Hysteresis

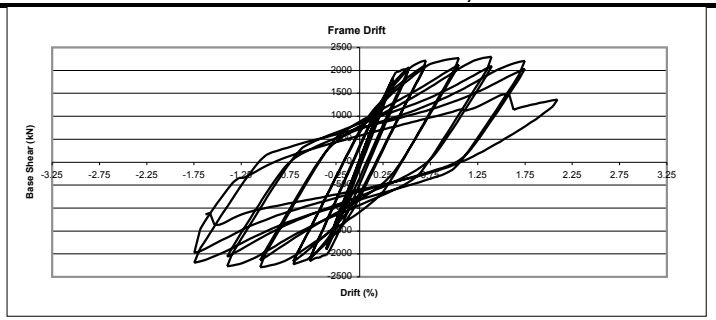

Range: -1.67% to 2.00% → 3.67% Total

1st Floor Force-Drift Hysteresis

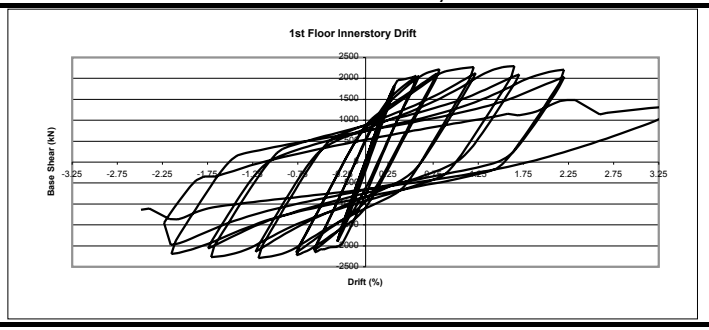

Range: -1.98 to 2.06% → 4.04% Total

3rd Floor Force-Drift Hysteresis

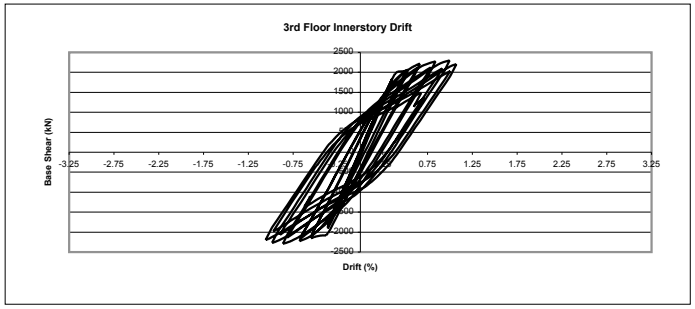

Range: -1.04 to 1.06% → 2.10% Total

2nd Floor Force-Drift Hysteresis

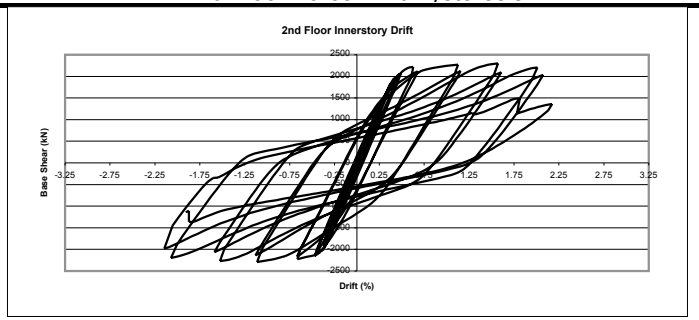

Range: -2.15 to 2.17% → 4.32% Total

Damage Pictures			
Braces	Misc.	Gusset Plates	
	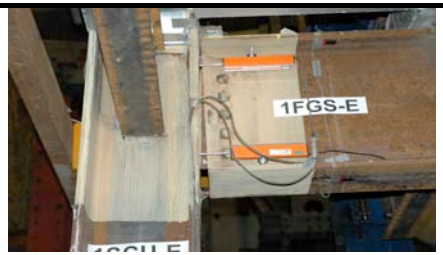		
1N at 1.67%	1S Shear Tab Rotation at 2.0%	1LNG Yielding at 2.0%	2UNG Yielding at 2.0%
			
3N at 1.67%	3N CJP Connection Yielding at 2.0%	1UMG Rotation at 2.0%	
			
2S at 2.0%	2N Beam at Stiffner Yielding at 2.0%	2LMG Rotation at 2.0%	
			
1S at 2.0%	1N Column Yielding at 2.0%	2LMG Yielding at 2.0%	

TCBF1-3 - UW, NCREE - 4/1/08 - Two Story, X-Braced Frame with 2t Linear Clearance, Tapered Gussets and HSS Braces

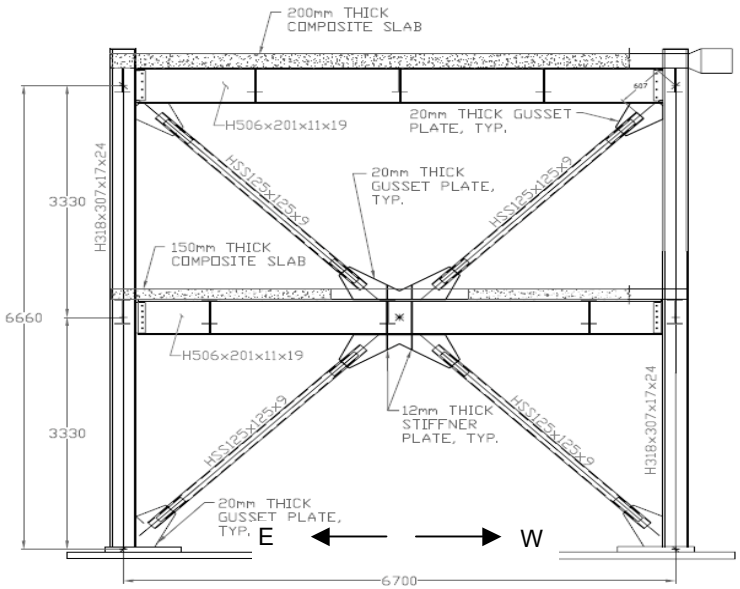

Total Frame Force-Drift Hysteresis

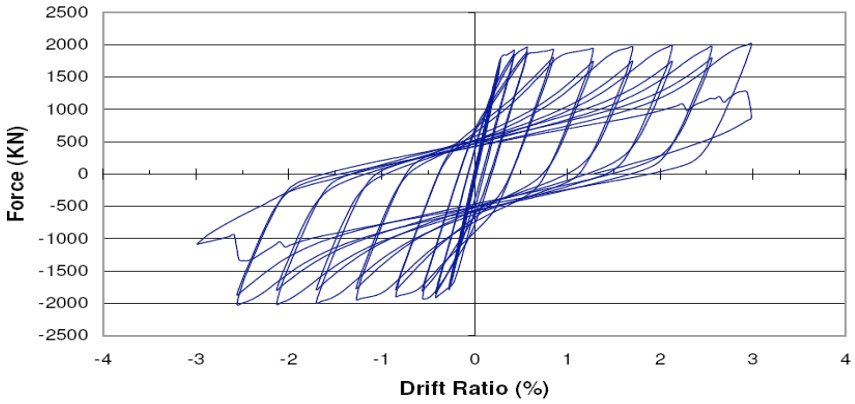

Range: -2.56% to 2.99% → 5.55% Total

Lower Level Force-Drift Hysteresis

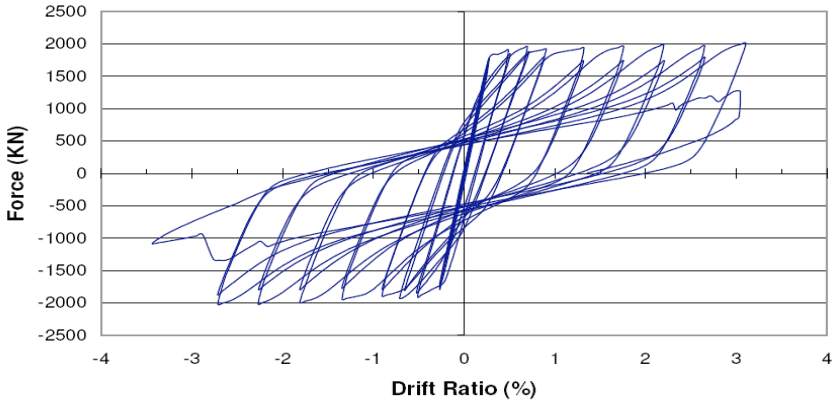

Range: -2.72% to 3.10% → 5.82% Total

Upper Level Force-Drift Hysteresis

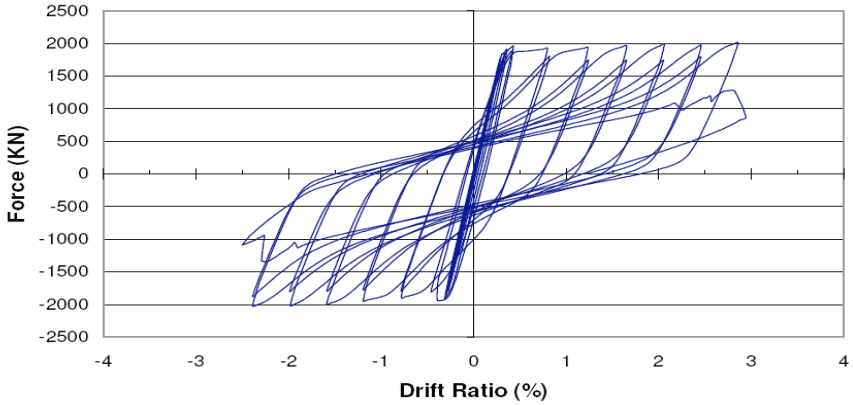

Range: -2.39% to 2.86% → 5.25% Total

Damage Pictures			
Brace Buckling	Weld Tearing	Gusset Plate Yielding	
	Weld Tearing was too slight to photograph		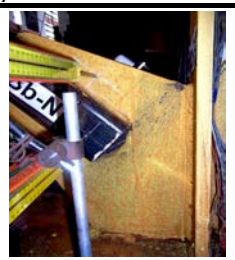
LWB at 0.56 FD and 0.71% SD		DS3- LWG at 2.99% FD and 3.10% SD	DS2- LWG at 0.56% FD and 0.71% SD
			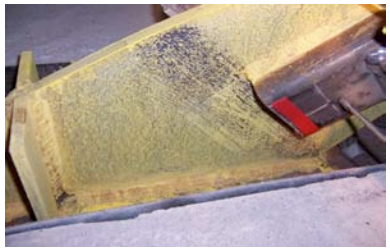
UEB at 1.27% FD and 1.19% SD		DS3- LMG at 2.99% FD and 3.10% SD	DS2- UEMG at 1.27% FD and 1.19% SD
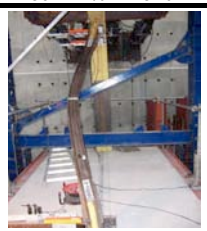			
UWB at 1.71% FD and 1.65% SD		DS3- UEG at 2.99% FD and 2.89% SD	DS2- UEG at 1.70% FD and 1.59% SD
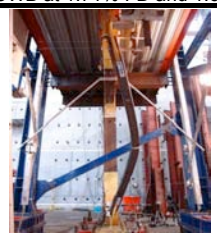			
LWB at 2.13% FD and 2.06% SD			DS2- LWMG at 1.70% FD and 1.81% SD

TCBF1-2 - UW, NCREE - 11/19/07 - Two Story, X-Braced Frame with 8t Elliptical Clearance and WF Braces

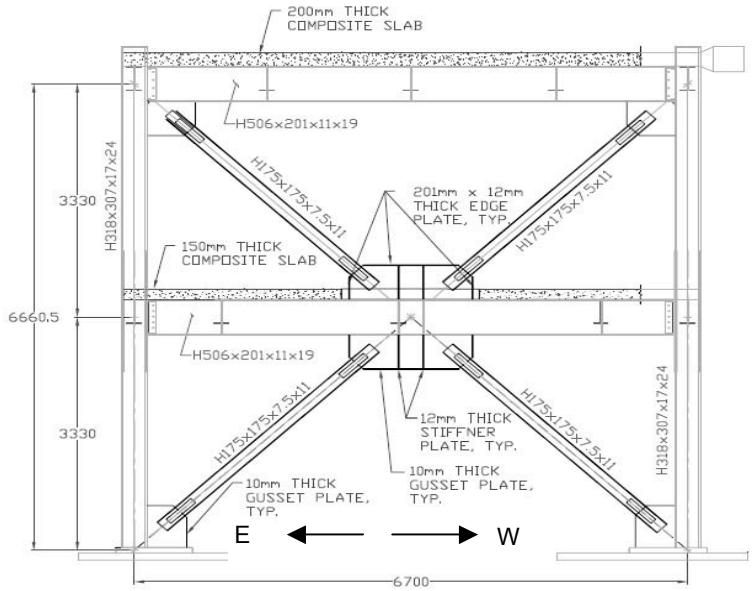

Total Frame Force-Drift Hysteresis

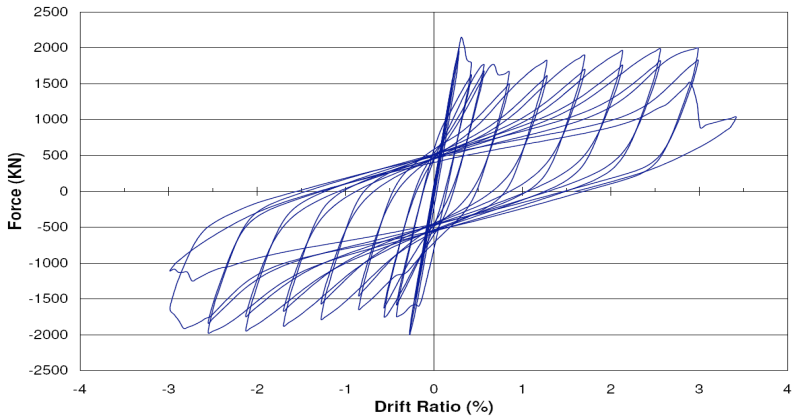

Range: -2.98% to 2.99% → 5.97% Total

Lower Level Force-Drift Hysteresis

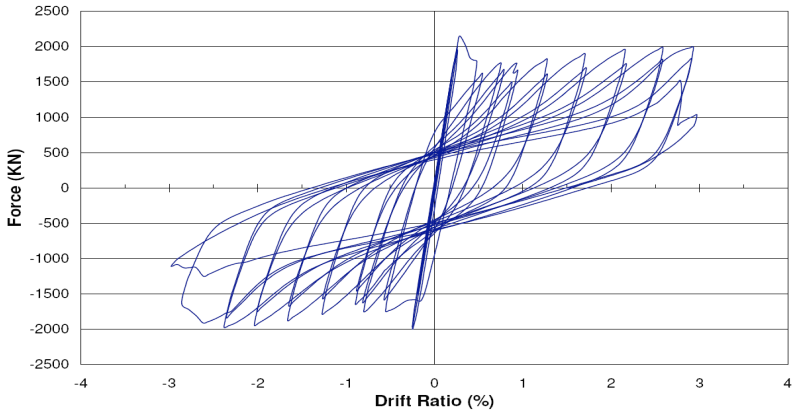

Range: -2.86% to 2.93% → 5.79% Total

Upper Level Force-Drift Hysteresis

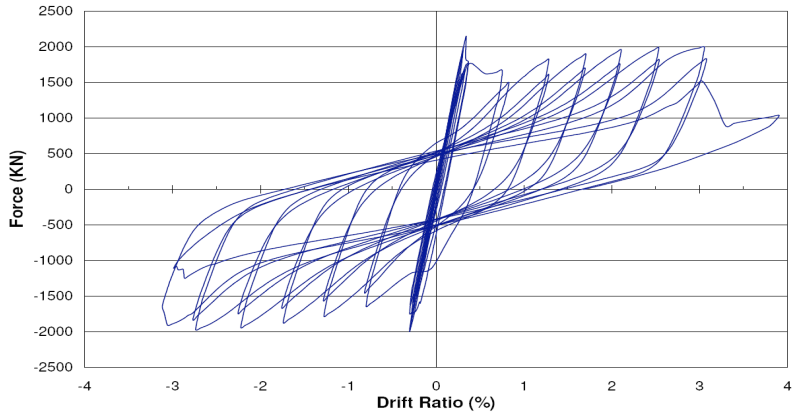

Range: -3.11% to 3.05% → 6.16% Total

Damage Pictures			
Brace Buckling	Weld Tearing	Gusset Plate Yielding	
			
LWB at 0.56% FD and 0.81% SD	DS3- UEG at 2.13% FD and 2.26% SD	DS2- UWMG at 2.13% FD and 2.11% SD	DS2- LEG at 0.56% FD and 0.79% SD
			
UEB at 0.85% FD and 0.81% SD	DS4- UEG at 2.98% FD and 3.05% SD		DS2- LWG at 2.13% FD and 2.04% SD
			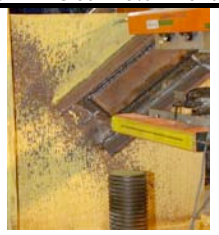
UWB at 1.70% FD and 1.71% SD	DS4- UWG at 2.98% FD and 3.05% SD		DS3- LEG at 2.98% FD and 2.98% SD
			
UEB at 2.13% FD and 2.26% SD			DS3- UWG at 2.98% FD and 3.05% SD

TCBF1-1 - UW, NCREE - 11/1/07 - Two Story, X-Braced Frame with 8t Elliptical Clearance and HSS Braces

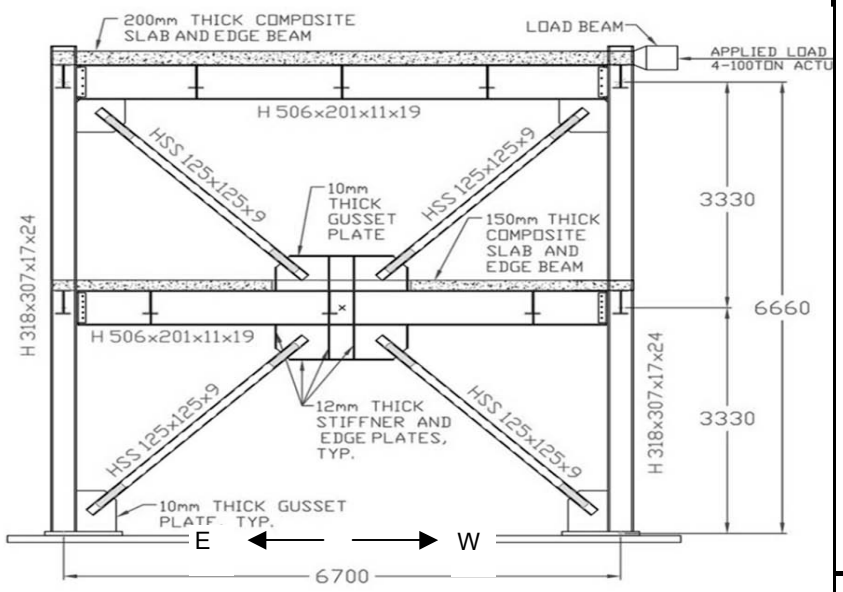

Total Frame Force-Drift Hysteresis

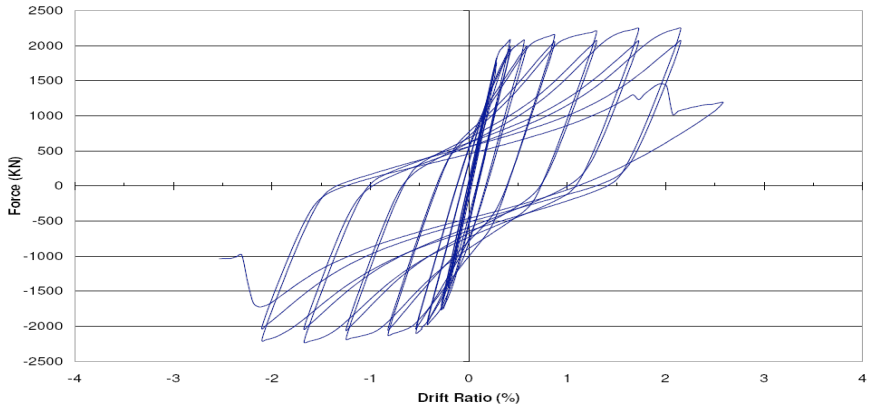

Range: -2.13% to 2.13% → 4.26% Total

Lower Level Force-Drift Hysteresis

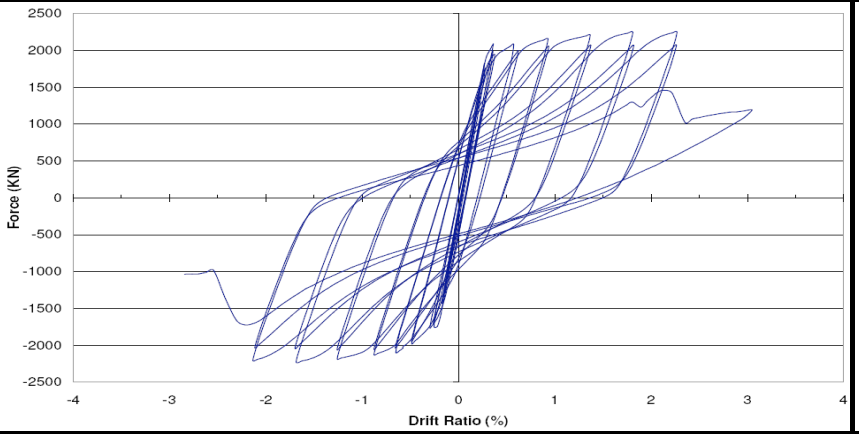

Range: -2.15% to 2.22% → 4.37% Total

Upper Level Force-Drift Hysteresis

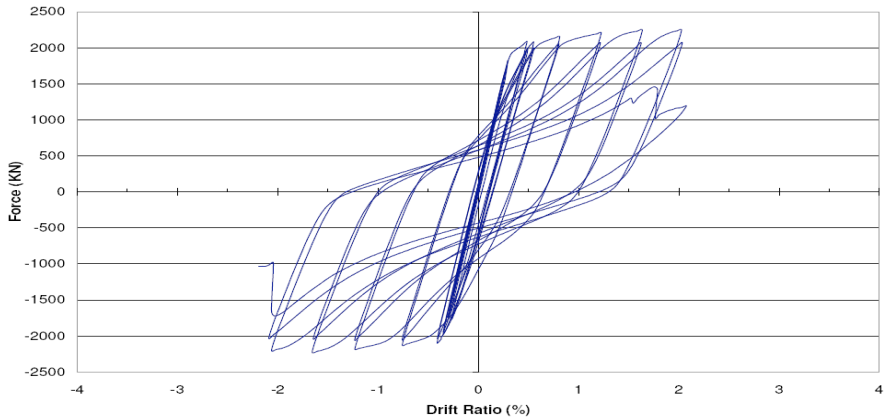

Range: -2.11% to 2.02% → 4.13% Total

Damage Pictures			
Brace Buckling	Weld Tearing	Gusset Plate Yielding	
			
UWB at 0.42% FD and 0.49% SD	DS2- LEG at 1.70% FD and 1.74% SD	DS3- LWG at 2.13% FD and 2.22% SD	DS2- UWMG at 0.56% FD and 0.55% SD
	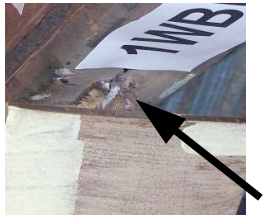		
UEB At 0.85% FD and 0.78% SD	DS2 -LWMG at 1.70% FD and 1.74% SD	DS3- LEG at 2.13% FD and 2.22% SD	DS2- UEMG at 0.85% FD and 0.78% SD
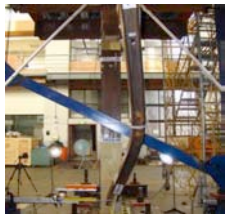	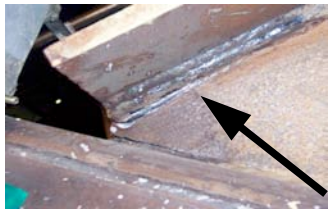		
LWB at 1.70% FD and 1.78% SD	DS2- UEMG at 2.13% FD and 2.02% SD	DS3- UWG at 2.13% FD and 2.02% SD	DS3- UWG at 1.70% FD and 1.67% SD
			
UEB At 2.13% FD and 2.11% SD		DS3- UEG at 2.13% FD and 2.02% SD	DS3- UEG at 1.70% FD and 1.67 SD

TCBF2-1 - UW, NCREE - 1/17/09 - Three Story SCBF, HSS Braces, 8t Elliptical Clear. on Corner Gussets, 6t Linear offset from Beam on Middle Gussets

Test Frame

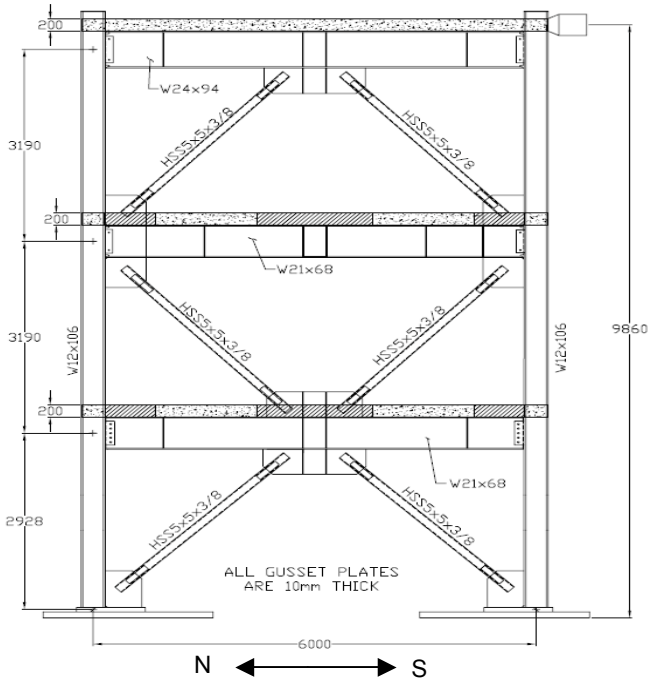

Total Frame Force-Drift Hysteresis

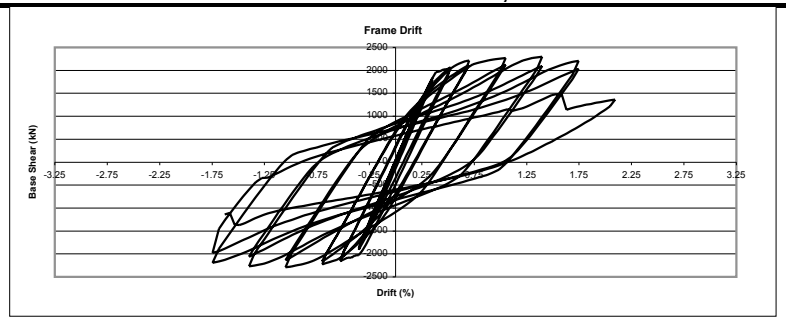

Range: -1.74% to 2.08% → 3.82% Total

1st Floor Force-Drift Hysteresis

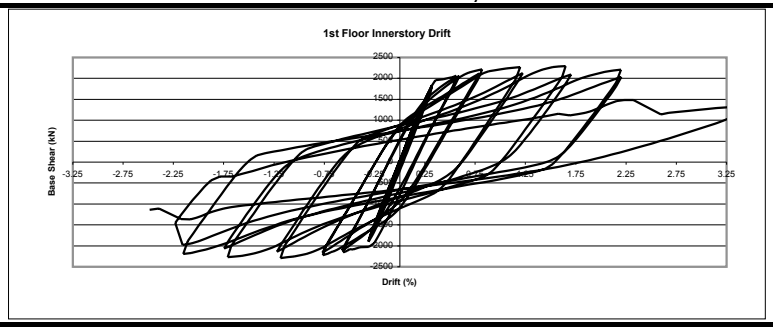

Range: -2.20 to 2.08% → 4.28% Total

3rd Floor Force-Drift Hysteresis

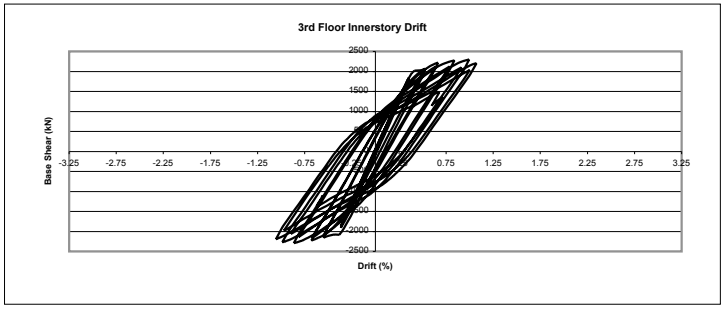

Range: -1.06 to 1.07% → 2.13% Total

2nd Floor Force-Drift Hysteresis

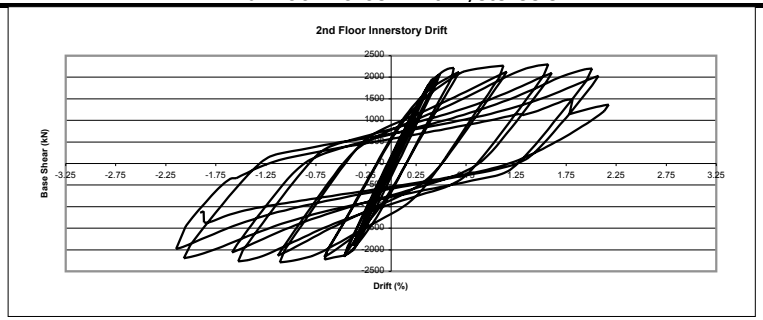

Range: -2.15 to 2.17% → 4.32% Total

Damage Pictures			
Braces		Gusset Plates	
			
DS4- 1NB at 2.08% FD and 2.30% SD	DS2- 2SB at 1.05% FD and 1.13% SD	DS2- 1LNG Yield. At 1.63% SD and 1.39% FD	DS2- 2USG Tear. At 2.08% FD and 2.30% SD
			
DS4-1NB at 1.74% FD and 2.17% SD	DS3- 2SB at 2.08 FD and 2.18% SD	DS2- 1LNG Yield. At 1.69% SD and 1.39% FD	2UNG Rotation at 1.39% FD and 1.53% SD
			
DS4- 1S Fr. at 2.08% FD and 2.18% SD	DS2- 3NB at 1.74% FD and 1.07% SD	DS2- 2UNG Yield at 1.74% FD and 2.07% FD	2LMG Rotation at 2.08% FD and 2.18% SD
			
DS4- 1N Tear at 2.08% FD and 2.20% SD			

TCBF2-2 - UW, NCREE - 3/28/09 - Three Story SCBF WF Braces, 8t Elliptical Clear. on Corner Gussets, 6t Linear offset from Beam on Middle Gussets

Test Frame

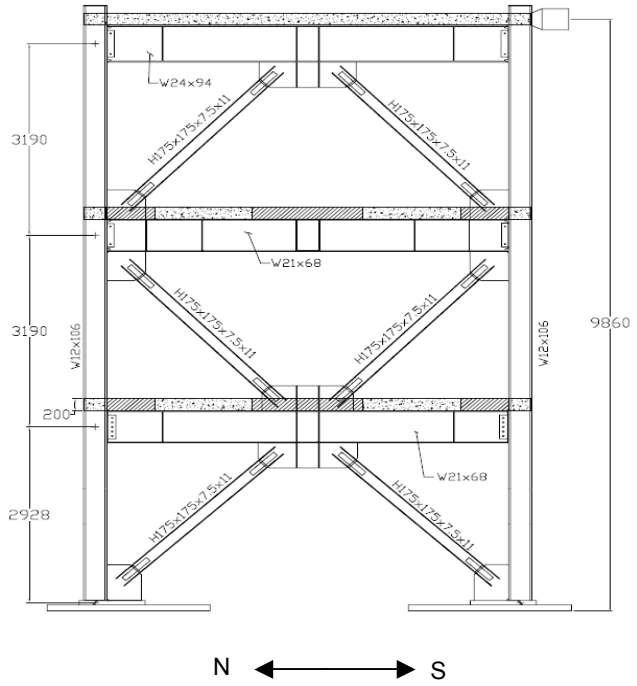

Total Frame Force-Drift Hysteresis

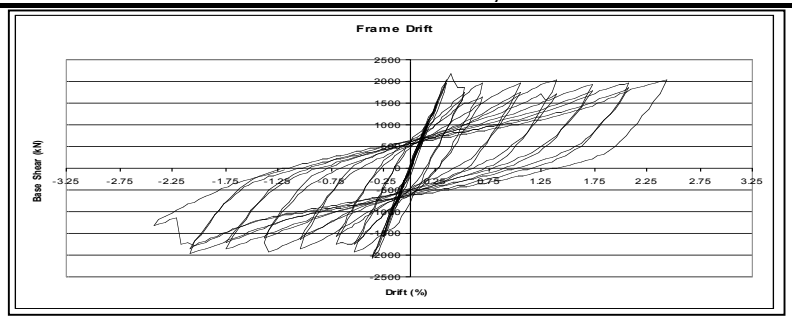

Range: -2.43% to 2.43% → 4.86% Total

1st Floor Force-Drift Hysteresis

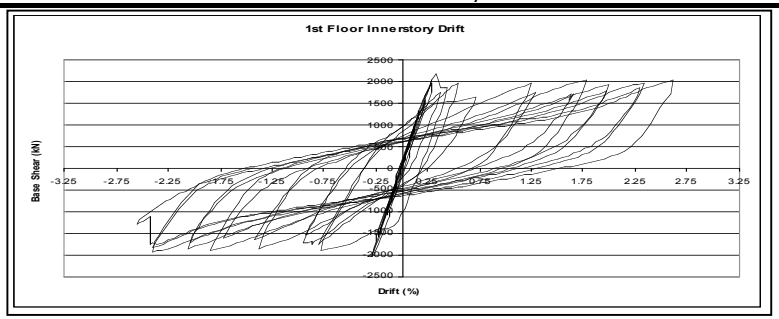

Range: -2.56 to 2.62% → 5.18% Total

3rd Floor Force-Drift Hysteresis

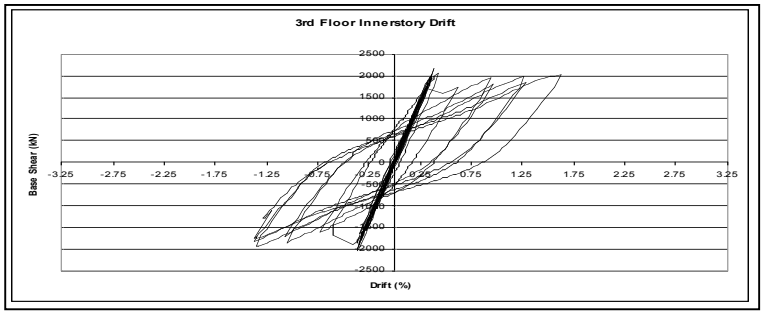

Range: -1.37 to 1.62% → 2.99% Total

2nd Floor Force-Drift Hysteresis

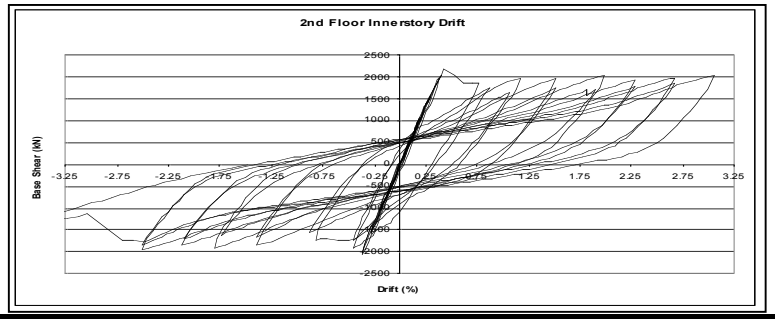

Range: -2.69 to 3.05% → 5.74% Total

Damage Pictures			
Braces		Gusset Plates	
			
DS2- 1NB at 1.04% FD and 1.25% SD	DS2- 2NB at 1.39% FD and 1.81% SD	DS2- 1LNG Yield. at 0.69% FD and 0.54% SD	2MG Rotation at 2.08% FD and 2.68% FD
			
DS2- 1NB at 1.73% FD and 1.99% SD	DS3- 2SB at 2.43% FD and 2.62% SD	DS3- 2UNG Yield at 1.39% FD and 1.90% SD	DS2- 2UNG Tear at 1.73% FD and 2.11% SD
			
DS3- 1NB at 2.43% FD and 2.62% SD	DS2- 3NB at 2.43% FD and 1.62% SD	DS3- 1LNG Yield. At 2.43% FD and 2.62% SD	DS3- 2UNG Tear at 2.43% FD and 3.05% SD
			
DS1- 2NB at 0.69% FD and -0.83%	DS3- 1NB at 2.08% FD and 2.33% SD	DS3- 2UNG Yield at 2.43% FD and 3.05% SD	